Charles University

Faculty of Science

Study program: Immunology

Mgr. Petra Weberová

IL-2/anti-IL-2 mAb immunocomplexes and polymer-modified IL-2 as potent immunomodulators

IL-2/anti-IL-2 mAb imunokomplexy a polymerně modifikovaný IL-2 jako účinné imunomodulátory

Doctoral thesis

Supervisor: RNDr. Marek Kovář, Ph.D.

Prague, 2024

Author's declaration

I declare that this thesis has been composed entirely by myself and that all information sources and literature have been properly cited. This thesis has not been submitted, in whole or in part, in any previous application for a degree. Artificial intelligence (ChatGPT 4.0) was used as a grammar editor of the text.

Prohlášení autorky

Prohlašuji, že jsem závěrečnou práci zpracovala samostatně a že jsem uvedla všechny použité informační zdroje a literaturu. Tato práce ani žádná její část nebyla předložena k získání jiného nebo stejného akademického titulu. Umělá inteligence (ChatGPT 4.0) byla využita k revizi anglické gramatiky textu.

V Praze 25.5. 2024

Mgr. Petra Weberová

Acknowledgment

First, I would like to thank my supervisor, Dr. Marek Kovář, for his guidance, support, and insightful feedback throughout my PhD studies. I am also deeply grateful to all the collaborators who contributed to the publications that form part of my dissertation. I extend my appreciation to the members of the Laboratory of Tumor Immunology, who fostered a friendly and creative environment in the group. Lastly, I would like to thank my family for their unwavering support.

Abstract

Interleukin-2 (IL-2) is recognized as a crucial cytokine for the proliferation, survival, and expression of effector functions in activated T and NK cells. However, IL-2 is involved not only in promoting effector T and NK cell functions but also in maintaining immune homeostasis, as it is an essential cytokine for the survival, proliferation, and suppressive activity of T regulatory (Treg) cells. This dual functionality makes IL-2 a potential immunotherapeutic drug for both cancer and autoimmune disease treatment, exploiting the differential expression of IL-2 receptor (IL-2R) subunits between Treg and effector cells. However, the therapeutic use of IL-2 is limited by its short half-life and significant dose-dependent adverse effects. To address these challenges, recent innovations such as IL-2/anti-IL-2 monoclonal antibody (mAb) immunocomplexes (IL-2co), IL-2 muteins with a modified affinity for some IL-2R subunit(s), and polymer-modified IL-2 have been developed. These advancements aim to refine the therapeutic profile of IL-2, enhancing its selectivity, efficacy, and safety.

In this thesis, I present several original studies in which we explored both current and new approaches to modify IL-2. Through molecular engineering and protein chemistry, we developed various novel IL-2 formulations: a protein chimera called immunocytokine (IC) where IL-2 is covalently linked to the light chain of the S4B6 mAb via a flexible $(Gly_4Ser)_3$ spacer (scIL-2/S4B6), an IL-2-poly(N-(2-hydroxypropyl)methacrylamide) (HPMA) conjugate, and an engineered IL-2-JES6 fusion protein called JY3 IC. These IL-2 variants were assessed *in vitro* and *in vivo* for their biological activity and therapeutic efficacy in models of autoimmune disease and vaccination.

The scIL-2/S4B6 demonstrated increased stimulatory activity for activated CD8$^+$ T cells compared to traditional IL-2co *in vivo*, without the stoichiometric limitations or the potential dissociation into free IL-2 and anti-IL-2 mAb associated with the use of IL-2co. The IL-2-poly(HPMA) conjugate demonstrated a dramatically improved pharmacokinetic profile compared to free IL-2 and enhanced activity in expanding recently activated and memory CD8$^+$ T, NK, NKT, and Treg cells. This conjugate also effectively potentiated the T cell response following peptide-based vaccination. The JY3 IC selectively stimulated Treg expansion and offered superior disease control in a mouse colitis model, illustrating its potential over noncovalently associated IL-2co. Mechanistic insights revealed differential IL-2R subunit interactions with IL-2 bound to either S4B6 or JES6-1A12 anti-IL-2 mAbs, influencing the balance between predominant stimulation of CD122^{high} effector T and NK cells or CD25^{high} Treg cells. However, safety concerns were highlighted by an increased sensitivity to LPS-induced shock mediated by CD25-biased IL-2co, emphasizing the need for careful evaluation of modified IL-2 therapies.

The engineered IL-2-based immunotherapeutics developed during this research offer significant advantages over unmodified IL-2 in terms of efficacy and safety, paving the way for more effective immunotherapeutic strategies. This work contributes novel insights into the design of cytokine-based therapies and underscores the importance of carefully selected receptor-targeting strategies in modulating immune responses for therapeutic benefit. The findings from this thesis have important implications for the treatment of cancer and autoimmune diseases, potentially extending to other therapeutic areas where the modulation of the immune system and its responses are critical issues.

Abstrakt

Interleukin-2 (IL-2) je klíčový cytokin pro proliferaci, přežití a expresi efektorových funkcí aktivovaných T a NK buněk. Zároveň je nezbytný pro udržení imunitní homeostáze, protože je esenciální pro přežití, proliferaci a supresorovou aktivitu T regulačních (Treg) buněk. Tyto vlastnosti činí z IL-2 významné imunoterapeutikum pro léčbu rakoviny a autoimunitních chorob, jelikož rozdílná exprese podjednotek IL-2 receptoru (IL-2R) mezi efektorovými a Treg buňkami umožňuje cílení biologické aktivity IL-2. Terapeutické využití IL-2 je však omezeno jeho krátkým poločasem v cirkulaci a závažnými vedlejšími účinky, které se vyskytují při použití vysokých dávek potřebných k dosažení účinnosti. Inovativní způsoby, jak zlepšit terapeutický profil IL-2 a zvýšit jeho selektivitu, účinnost a bezpečnost, zahrnují imunokomplexy IL-2/anti-IL-2 monoklonálních protilátek (mAb) (IL-2co), IL-2 muteiny s modifikovanou afinitou k některým podjednotkám IL-2R a polymerem modifikovaný IL-2.

V této disertační práci představuji několik původních studií, ve kterých jsme zkoumali současné i nové přístupy v modifikaci IL-2. Pomocí molekulárního inženýrství a proteinové chemie jsme vyvinuli tyto nové formy IL-2: proteinovou chiméru - imunocytokin (IC), kde je IL-2 kovalentně vázán na lehký řetězec S4B6 mAb prostřednictvím flexibilní $(Gly_4Ser)_3$ spojky (scIL-2/S4B6); konjugát IL-2-poly(N-(2-hydroxypropyl)methakrylamid) (HPMA) a modifikovaný fúzní protein IL-2-JES6, nazvaný JY3 IC. Tyto nové varianty IL-2 byly hodnoceny *in vitro* a *in vivo* pro jejich biologickou aktivitu a terapeutickou účinnost v modelech autoimunitních chorob a vakcinace.

Ve srovnání s tradičními IL-2co vykazoval scIL-2/S4B6 IC zvýšenou stimulační aktivitu pro aktivované CD8$^+$ T buňky *in vivo*, aniž by byly přítomny problémy spojené s použitím asociovaných IL-2co, jako jsou stechiometrická omezení (přebytek IL-2 nebo anti-IL-2 mAb) nebo možná disociace na volný IL-2 a anti-IL-2 mAb. Konjugát IL-2-poly(HPMA) měl oproti nemodifikovanému IL-2 výrazně vylepšený farmakokinetický profil a zvýšenou biologickou aktivitu pro čerstvě aktivované i paměťové CD8$^+$ T lymfocyty, NK, NKT a Treg buňky. Tento konjugát navíc efektivně zvyšoval T buněčnou odpověď po vakcinaci peptidem. JY3 IC selektivně stimuloval expanzi Treg buněk, což se projevilo vyšší terapeutickou účinností, než jakou disponovaly IL-2co, v modelu myší kolitidy. Mechanistické studie odhalily rozdílné interakce podjednotek IL-2R s IL-2 navázaným buď na S4B6, nebo JES6-1A12 anti-IL-2 mAb; to ovlivňuje rovnováhu mezi převládající stimulací CD122^{high} efektorových T a NK buněk nebo CD25^{high} Treg buněk. U CD25-biased IL-2co se nám podařilo odhalit, že zvyšují citlivost k LPS-mediovanému šoku, což znesnadňuje jejich klinické využití a dále zdůrazňuje potřebu pečlivého hodnocení terapií využívajících modifikovaný IL-2.

IL-2 imunoterapeutika vyvinutá během tohoto výzkumu nabízejí významné výhody oproti nemodifikovanému IL-2 z hlediska účinnosti a bezpečnosti, čímž se otevírá cesta pro efektivnější imunoterapeutické strategie. Tato práce přináší nové poznatky do návrhu cytokinových terapií a zdůrazňuje význam pečlivě vybraných receptor-cílených strategií v modulaci imunitních odpovědí pro terapeutický přínos. Zjištění z této práce mají důležité důsledky pro léčbu nádorových onemocnění a autoimunitních chorob, potenciálně přenositelné do dalších terapeutických oblastí, kde je kritická modulace imunitního systému a jeho odpovědí.

Table of contents

List of abbreviations

5-HTP	5-hydroxytryptophan
ACT	Adoptive cell therapy
ADCC	Antibody-dependent cellular cytotoxicity
AhR	Aryl hydrocarbon receptor
AICD	Activation-induced cell death
AIH	Autoimmune hepatitis
AKT	Protein kinase B
AP1	Activator protein 1
APC	Antigen-presenting cell
ARE	AU-rich element
Bcl	B cell lymphoma
BCR/ABL	Fusion gene, a marker of chronic myeloid leukemia
BCT	Biochemotherapy
Blimp1	B-lymphocyte-induced maturation protein 1
BrdU	Bromodeoxyuridine
BTLA	B- and T-lymphocyte attenuator
CAR	Chimeric antigen receptor
CARMA1	Caspase recruitment domain-containing membrane-associated guanylate kinase protein-1
CCR5	C-C chemokine receptor type 5
CD	Cluster of differentiation
CEA	Carcinoembryonic antigen
CFSE	Carboxyfluorescein succinimidyl ester (dye)
CTLA-4	Cytotoxic T-lymphocyte associated antigen-4
CTV	Cell trace violet dye
CVD	Cisplatin, Vinblastine, Dacarbazine
DC	Dendritic cell
EAE	Experimental autoimmune encephalomyelitis
EDTA	Ethylenediamine tetraacetic acid
EGF	Epidermal growth factor
EGFR	Epidermal growth factor receptor
ELISA	Enzyme-linked immunosorbent assay
ERK1/2	Extracellular signal-regulated kinase 1/2
FcRn	Neonatal fragment crystallizable (Fc) receptor
FDA	Food and drug administration
FLS	Fibroblast-like synoviocytes
Foxp3	Forkhead box p3 transcription factor

FBS	Fetal bovine serum
GALT	Gut-associated lymphoid tissue
GD2	Disialoganglioside GD2
GITR	Glucocorticoid-induced TNFR-related protein
gp100	Glycoprotein 100
GvHD	Graft versus host disease
GZMB	Granzyme B
HD	High-dose
HEPES	4-(2-hydroxyethyl)-1-piperazineethanesulfonic acid
HIF-1α	Hypoxia-inducible factor 1 alpha
hIL-2	Human IL-2
HPMA	N-(2-hydroxypropyl)methacrylamide
IC	Immunocytokine
ICAM-1	Intercellular adhesion molecule 1
ICOS	Inducible costimulator
IFN	Interferon
Ig	Immunoglobulin
IKK	Inhibitor of nuclear factor-κB kinase complex
IL-	Interleukin
ILC	Innate lymphoid cell
IL-2co	IL-2/anti-IL-2 mAb complexes
IL-2R	Interleukin 2 receptor
JAK	Janus kinase
Kd	Dissociation constant
KLRK1	Killer cell lectin-like receptor K1
LAG-3	Lymphocyte-activation gene 3
LAK	Lymphokine-activated killer cell
LCMV	Lymphocytic choriomeningitis mammarenavirus
LD	Low-dose
LPS	Lipopolysaccharide
MACS	Magnetic-activated cell sorting
MAGE	Melanoma-associated antigen
MAP kinase	Mitogen-activated protein kinase
MART-1	Melanoma antigen recognized by T cells 1
MCP-1	Monocyte chemoattractant protein-1
MHC	Major histocompatibility complex
mIL-2	Murine IL-2
MP	Memory phenotype
MS	Multiple sclerosis

mTOR	Mammalian target of rapamycin
mTORC1	Mammalian target of rapamycin complex 1
Myc	Myelocytomatosis oncogene
MyD88	Myeloid differentiation primary response 88
NF90	Nuclear factor 90
NFκB	Nuclear factor kappa-light-chain-enhancer of activated B cells
NK	Natural killer
NKT	Natural killer T cell
NFAT	Nuclear factor of activated T cells
NKG2D	Natural killer group 2D receptor
NFκB	Nuclear factor kappa B
NMA	Non-myeloablative chemotherapy
NOD2	Nucleotide-binding oligomerization domain containing 2
NSCLC	Non-small cell lung cancer
NY-ESO-1	New York esophageal squamous cell carcinoma-1
p56lck	Lymphocyte-specific protein tyrosine kinase
p70S6K	Ribosomal protein S6 kinase beta-1
PBS	Phosphate-buffered saline
PD-1	Programmed cell death protein 1
PEG-IL-2	Pegylated IL-2
PIM1	Pim-1 proto-oncogene
PI3K	Phosphoinositide 3-kinase
PIM	Proviral integration site for Moloney murine leukemia virus
PK	Protein kinase
PMA	Phorbol 12-myristate 13-acetate
PP	Peyer's patches
PPT2	Protein phosphatase 2
PTEN	Phosphatase and tensin homolog deleted on chromosome 10
RA	Rheumatoid arthritis
Raf	Rapidly accelerated fibrosarcoma protein
RasGRP1	Ras guanyl-releasing protein 1
RBC	Red blood cell
RCC	Renal cell carcinoma
rhIL-2	Recombinant human IL-2
RORγt	Retinoic acid-related orphan receptor γ
RunX1	RUNX family transcription factor 1
SABR	Stereotactic ablative radiotherapy
sCD25	Soluble CD25
SLE	Systemic lupus erythematosus

SLEC	Short-lived effector cells
SOCS	Suppressor of cytokine signaling
STAT	Signal transducer and activator of transcription
T1D	Type 1 diabetes
TAA	Tumor-associated antigen
TBI	Total body irradiation
TBX21 (T-bet)	T-box transcription factor 21
TCF-1	T cell factor 1
T_{CM}	Central memory T cell
Tconv	Conventional T cells
TCR	T cell receptor
Teff	Effector T cells
Tex	Exhausted T cells
Tfh	Follicular helper T cells
Tfr	T-follicular regulatory cell
TGF-β	Transforming growth factor β
Th	Helper T cell
TIGIT	T cell immunoreceptor with Ig and ITIM domains
TIL	Tumor-infiltrating lymphocyte
Tim-3	T cell immunoglobulin and mucin-domain containing-3
TKI	Tyrosine kinase inhibitor
TME	Tumor microenvironment
TNF	Tumor necrosis factor
TOX	Thymocyte selection-associated high mobility group box protein
Treg	Regulatory T cells
TST	Tumor-specific T cell
UC	Ulcerative colitis
XBP1	X-box binding protein 1
XSCID	X-linked severe combined immunodeficiency

I.   Introduction

Interleukin-2 (IL-2) is a key cytokine in the immune system, playing a central role in T cell proliferation, differentiation, and survival. Beyond T cells, IL-2 influences a variety of immune cells, connecting antigen recognition to a broad spectrum of cytokine-mediated effects, including cellular proliferation, differentiation, and functional modulation. Understanding the mechanisms behind IL-2 production and signaling is essential, as they play critical roles in immune homeostasis, autoimmunity, and the efficacy of immunotherapies. The chapters that follow describe the complexity of IL-2 production, exploring the diverse cellular sources involved in its synthesis and the signaling pathways that regulate it. A comprehensive analysis of the IL-2 receptor (IL-2R) will be presented, elucidating the biological effects of IL-2 on various cell populations. Finally, the focus will shift to IL-2 immunotherapy, examining its applications and potential in clinical settings.

I.1   The biology of IL-2

I.1.1   T cell receptor signaling and IL-2 production

IL-2 is an O-glycosylated, four-α-helix-bundle cytokine (Figure 1) primarily produced by CD4$^+$ T lymphocytes, including naïve, memory, and helper T (Th)1, following antigenic stimulation. Additionally, activated CD8$^+$ T cells [1], B cells [2], and, to a lesser extent, other innate immune cells such as natural killer (NK) cells, NKT cells [3, 4], and group-3 innate lymphoid cells (ILCs) in the small intestine and lungs [5, 6] produce IL-2. Under specific conditions, activated dendritic cells (DCs; CD8α$^+$, CD8α$^-$ DCs), Langerhans cells [7-9], and murine mast cells [10], as well as human monocyte-derived and plasmacytoid DCs [11], may be a source of small amounts of IL-2. The ability to produce IL-2 distinguishes effector T cells from regulatory T (Treg) cells, as direct repression of *IL2* by Foxp3 interacting with Runx1 and NFAT prevents Treg cells from producing IL-2 [12, 13].
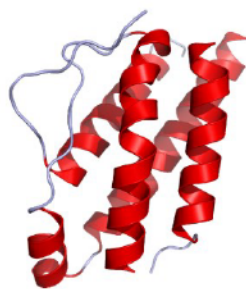
Figure 1. Crystal structure of IL-2. Published in the Protein Data Bank (PDB: 1M47).

Under resting conditions, CD4$^+$ T cells are the primary source of constant but low levels of IL-2. Upon activation, their IL-2 production rapidly increases. Low IL-2 secretion by activated DCs has been shown to provide an early IL-2 source [9, 14], thereby supporting T-cell stimulation. In parallel, activated T cells, including CD4$^+$ and CD8$^+$ T cells, start secreting

large amounts of IL-2 for their own (autocrine) use and to stimulate in a paracrine fashion neighboring IL-2 receptor-harboring cells [15, 16].

The induction of IL-2 production is tightly regulated at transcriptional and posttranscriptional levels, primarily dependent on the activation of NF-κB and NFAT transcription activators. In naïve T lymphocytes, the engagement of the T cell receptor (TCR) and co-stimulatory molecule CD28 within an immunological synapse triggers the formation of multi-molecular signalosomes at both TCR and CD28. This leads to the generation of proximal signaling, followed by the activation of multiple distal signaling cascades, such as Ca^{2+}–calcineurin–NFAT, PKCθ–IKK–NFκβ, RasGRP1–Ras–ERK1/2-AP1, and PI3K-AKT–mTOR, with the help of secondary messengers, enzymes, and various adaptor proteins (Figure 2).
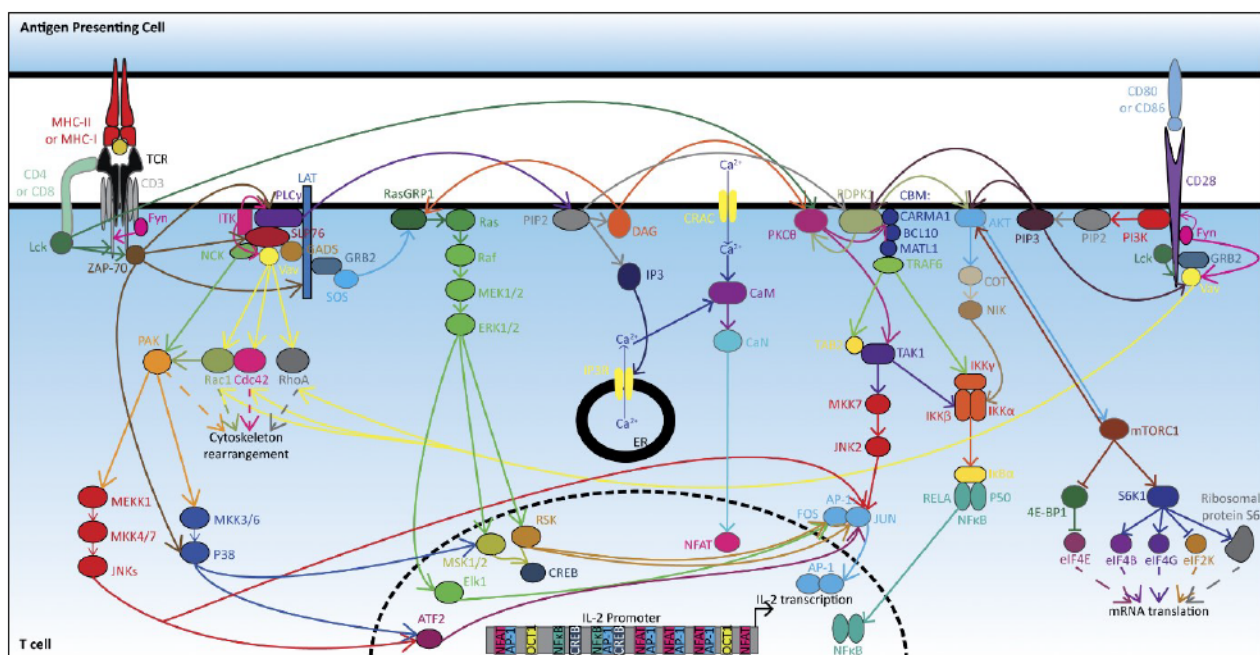
Figure 2. Signaling cascades following stimulation of the TCR and CD28, leading to IL-2 transcription. For details see the reference [17] in J Exp Med.

These signaling cascades finally bring out the diverse phenotypic effects, as they control many aspects of T cell biology [18]. AP-1, NFκB, and NFAT transcription factors, in cooperation with constitutive factors, promote the expression of the *IL2* gene [19]. *IL2* transcription occurs within 30 min after stimulation but is transient, declining to background levels within 24–48 h. Additionally, post-transcriptional regulatory mechanisms further restrict IL-2 mRNA availability, which usually peaks 4–8 h after stimulation [20]. The turnover of IL-2 mRNAs is mostly controlled by proteins interacting with an AU-rich cis-element (ARE) in their 3′-untranslated region. Among these trans-acting factors are nuclear factor 90 (NF90) and tristetraprolin. NF90 is activated by protein kinase (PK) B (best known as AKT) upon CD28 co-stimulation or by PK C upon restimulation with PMA, subsequently translocating from the nucleus to the cytosol, where it binds to ARE and stabilizes IL-2 mRNA, thus allowing its

translation [21]. In contrast, tristetraprolin, expressed in T lymphocytes following activation, plays a crucial role in the rapid decay of IL-2 mRNAs, as its interaction with ARE promotes its degradation [22, 23]. Additionally, IL-2 transcription is repressed in activated T cells by T-bet and Blimp-1 [24-26]. Naïve T cells lack the expression of Blimp-1, which is upregulated by antigen- and IL-2-dependent signaling [27, 28]. Blimp-1 expression is particularly high in chronically activated T cells, characterized by their inability to produce IL-2 [29]. Thus, Blimp-1-mediated IL-2 repression represents a negative feedback loop to limit IL-2 receptor (IL-2R) signaling and may represent a failsafe mechanism to limit IL-2-dependent responses in situations where antigen, the primary inductive signal for IL-2 and IL-2R, is not eliminated, potentially avoiding catastrophic expansion of the antigen-reactive T cells. Altogether, these transcriptional and post-transcriptional mechanisms collectively regulate the magnitude and duration of IL-2 production by activated T cells.

Mouse and human IL-2 display significant cross-species activity, although there are important differences. Human IL-2 (hIL-2) comprises 133 amino acids and has a molecular weight of approximately 15.5 kDa, while mouse IL-2 (mIL-2) consists of 149 amino acids and weighs about 16 kDa. Despite sharing only 56-57% sequence homology, hIL-2 effectively stimulates the murine IL-2R. However, mIL-2 shows a limited ability to bind to the human IL-2R [30]. This discrepancy is primarily due to differences in the N-terminal region of mIL-2, which contains a poly-glutamine stretch, resulting in strain-specific heterogeneity [31].

I.1.2 IL-2 signaling

I.1.2.1 Structure of the IL-2 receptor

Once secreted, IL-2 influences neighboring cells through autocrine and paracrine signaling by binding to its receptor, IL-2R. This receptor is a hetero-complex composed of up to three subunits: α (CD25), β (CD132), and the common γ-chain (γ_c, CD132). IL-2R subunits β and γ_c can independently bind IL-2, though with low affinity (Kd: $\sim 10^{-8}$–10^{-7} M). Only the intermediate-affinity dimeric $\beta\gamma_c$ IL-2R (Kd: $\sim 10^{-9}$ M) and the high-affinity trimeric $\alpha\beta\gamma_c$ IL-2R (Kd: $\sim 10^{-11}$ M) mediate signal transduction (Figure 3) [32].

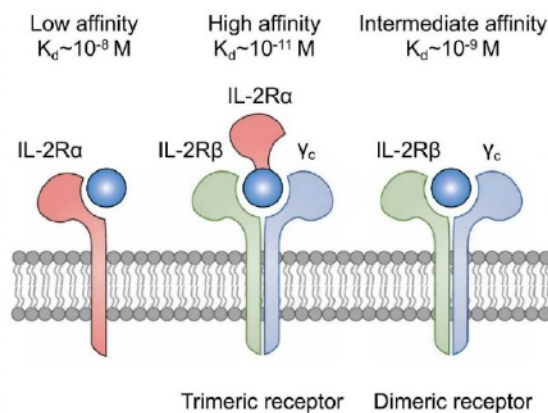**Figure 3.** Three subunits of IL-2R. High-affinity IL-2R$\alpha\beta\gamma_c$, intermediate affinity IL-2R$\beta\gamma_c$, and low-affinity IL-2Rα, with receptor composition and K_d's. Adapted from Cytokine Growth Factor Rev [33].

The γ_c subunit, also known as CD132 (58–64 kDa), is vital for ligand binding and signaling induced by γ_c cytokines. CD132, commonly found on most hematopoietic cells, acts as a receptor subunit for cytokines IL-2, IL-4, IL-7, IL-9, IL-15, and IL-21, which are collectively known as the γ_c family of cytokines. Members of the γ_c cytokine family, including IL-2, play distinct and nonredundant roles in the adaptive immune system, especially in the development and differentiation of T lymphocytes. Deficiency in the γ_c gene causes X-linked severe combined immunodeficiency (XSCID), highlighting its importance [34]. Thus, γ_c expression is essential for lymphocytes and is especially critical for T cells in both humans and mice. Alternative splicing generates soluble γ_c chains; however, in the case of IL-2R, all members produce soluble forms [35, 36]. A common feature shared among these soluble receptors is that they retain affinity for their cognate cytokine ligands. Consequently, these secreted proteins can either compete with membrane cytokine receptors for ligand binding or sequester the cognate cytokine, thereby limiting its bioavailability [37].

The β subunit (CD122; 67–75 kDa) has a large intracellular domain (286 residues) crucial for signal transduction. CD122 is constitutively expressed at various levels on T and NK(T) lymphocytes, where it, together with CD132, plays an essential role in orchestrating their development and differentiation [38-40]. While upregulated on naïve T cells after antigen activation, CD122 is most highly expressed on memory CD8$^+$ T and NK cells, emphasizing its importance in acute and memory immune responses [39].

The α subunit (CD25; 55 kDa), sometimes called low-affinity IL-2R, is detected on early thymocytes, absent on naïve/memory T cells (particularly in mice, but detectable on a minor fraction of human naïve/memory T cells), transiently expressed on activated/effector T lymphocytes, and constitutively expressed on Tregs [41, 42]. Antigens, mitogenic lectins, or antibodies to the TCR trigger its expression. These signals also result in the secretion of IL-2, which in turn can increase and prolong IL-2Rα expression, thus establishing a positive feedback loop for high-affinity receptor expression [43]. Treg cells rely on high and constitutive IL-2Rα expression to respond to very low IL-2 concentrations that are constantly available *in vivo*. In the absence of IL-2Rα, mature Treg cells are absent, and mice die within 8-20 weeks of age unless IL-2Rα-competent T regulatory cells are provided [44, 45]. The relatively high levels of the high-affinity IL-2R on Treg cells are consistent with chronic autoantigen stimulation and IL-2-dependent signals. Physiologically, the initial phase of an immune response functions to activate Treg cells. Within hours of T-cell priming, IL-2-dependent STAT5 phosphorylation occurs primarily in Foxp3$^+$ Treg cells. In contrast, the antigen-specific T cells receive STAT5 signals only after repeated antigen exposure or memory differentiation [46]. In addition to its prominent expression by Treg cells and activated T cells, CD25 is expressed at low levels by DCs and Langerhans cells in mice and by human DCs [47-50]. The highly inducible IL-2Rα was initially characterized by its ability to promote high-affinity binding of IL-2 to the IL-2Rβγ_c [51-53]. Research has suggested that IL-2Rα also helps to prolong IL-2 signaling, possibly through mechanisms involving cell-surface reservoirs or receptor recycling [54-57]. These properties may be relevant during the early stages of infection when lymphocytes express high levels of IL-2Rα [58, 59]. However, these findings are primarily based on experimental data and may involve model systems that don't completely mirror *in vivo* conditions. Soluble IL-2Rα (sCD25) may also play an important role in regulating immune responses [60-65] as soluble IL-2Rα has been detected in the serum of patients with systemic lupus erythematosus

(SLE) [66-69], multiple sclerosis (MS) [70, 71], type I diabetes (T1D) [71] and various neoplasms [72]. Although the exact role played by sCD25 is still unclear, recent work suggests that sCD25 prevents IL-2 signaling by competing with membrane-bound CD25 for circulating IL-2, and exacerbates experimental autoimmune encephalitis (EAE) by allowing aberrant Th17 responses [73].

The intermediate-affinity IL-2Rβγ$_c$ is almost undetectable on naïve CD4^{+} T cells, but this receptor is present at low but significant levels on naïve CD8^{+} T cells and memory CD4^{+} T cells and at high levels on antigen-experienced (memory) CD8^{+} T cells and NK cells. Cells expressing high levels of the dimeric IL-2R are sensitive to exogenously administered IL-2, but these cells are presumably unresponsive to the low physiological steady-state levels of IL-2 found *in vivo* [74].

Upon TCR stimulation, T cells transiently upregulate CD25 [58, 75, 76], thus expressing now high-affinity trimeric IL-2Rαβγ$_c$. Besides recently activated T cells, high levels of trimeric IL-2Rs (precisely, high CD25 levels plus intermediate levels of dimeric IL-2Rβγ$_c$) are constitutively found on thymus-derived ("natural") CD4^{+} Foxp3^{+} Treg cells [77], whereas type 2 innate lymphoid cells (ILC) have been reported to carry low to very low levels of trimeric IL-2R (Figure 4) [78].
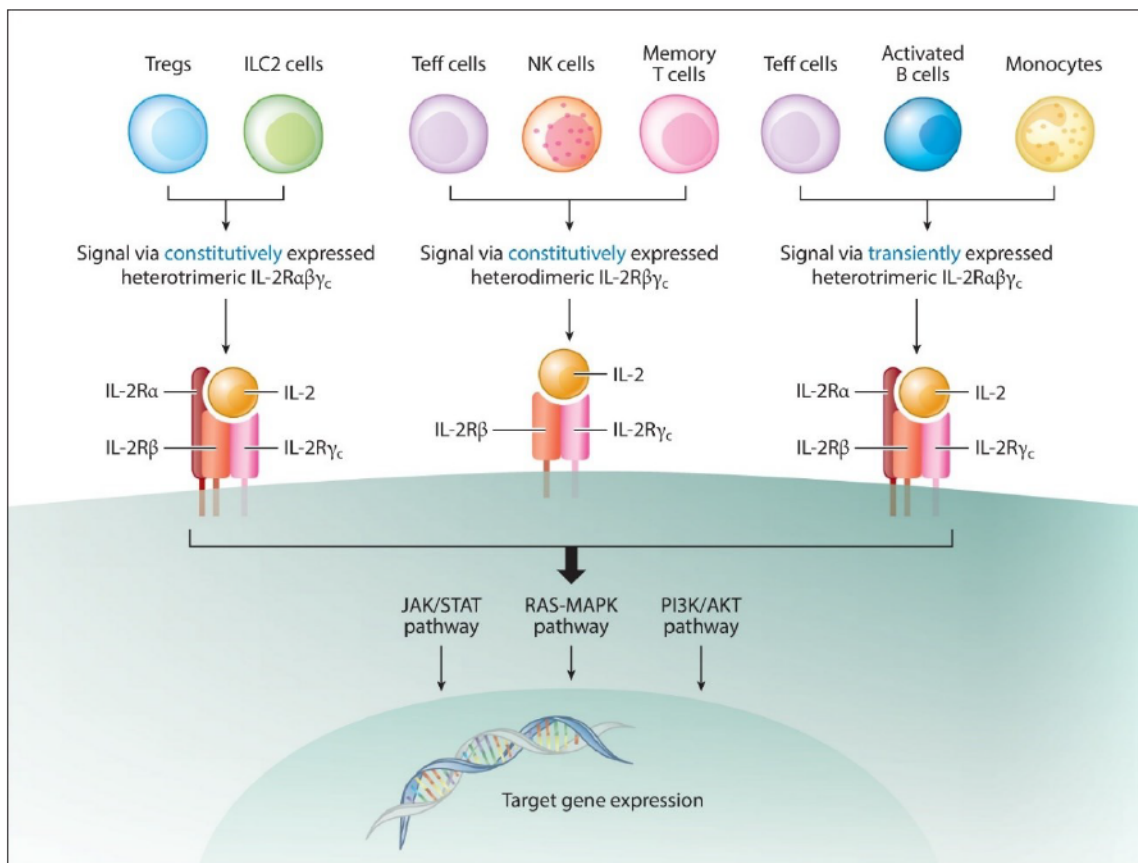

Figure 4. IL-2 signaling is mediated by different IL-2R configurations, which are expressed by various immune cells. Adapted from Annu Rev Med [79].

Within the myeloid compartment, monocytes typically display the intermediate-affinity IL-2Rβγc receptor, while DC subtypes can express all three IL-2R subunits [80-82], which allows IL-2-mediated intrinsic regulation of themselves or, importantly, allows them to *trans*-present the CD25/IL-2 complex to naïve T cells [15]. In such a way activated DCs express CD25 on their surface to trap and present T cell- or DC-derived IL-2 in *trans* to adjacent antigen-specific naïve T lymphocytes and NK cells that express IL-2Rβγc [83, 84]. This *trans*-presentation of IL-2 (Figure 5) has been shown to facilitate initial high-affinity IL-2 signaling during early immune response, before the responding T cells start to express CD25 [9, 85], and is consistent with the data showing that T cells [86, 87] and DCs [14, 85, 88] directionally secrete IL-2 towards the T cell-DC interface. In this scenario, the local concentration of IL-2 within the particular microenvironment of the DC-T cell contact may facilitate CD25/IL-2 binding by DCs and *trans*-presentation to CD4+ T cells, despite the rapid on/off dissociation rates and the low affinity of CD25 for IL-2. In agreement with this model, selective blockade of CD25 on DCs by daclizumab, a humanized anti-CD25 mAb, prevents T cell expansion by activated DCs [85]. It is possible that secretion of IL-2 by DCs in the synaptic cleft may provide an efficient and previously unexpected additional signal for T-cells, including T effector cells and Tregs [9].
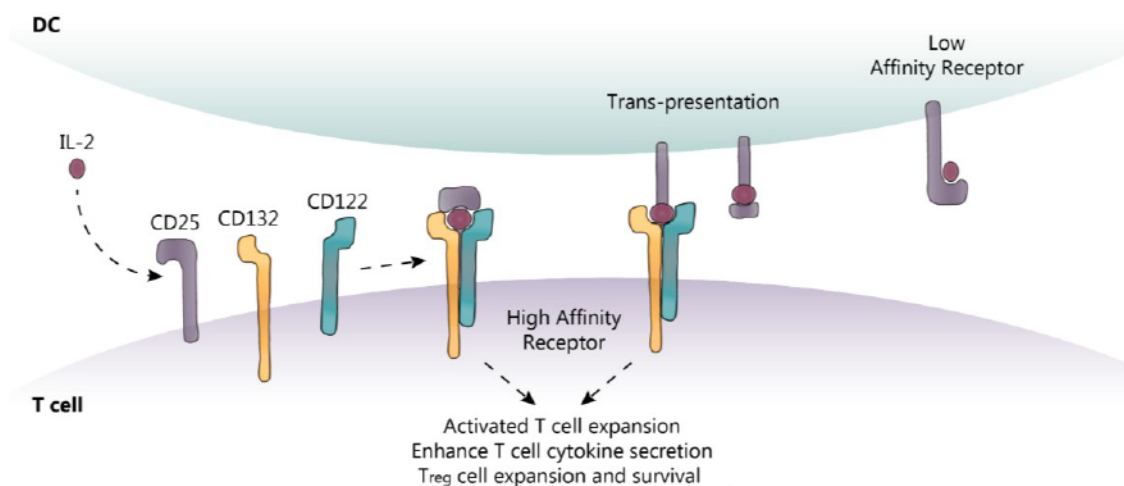
Figure 5. *Trans*-presentation of IL-2 by a DC that expresses IL-2Rα to a T cell that expresses IL-2Rβγc. Also, a *cis* presentation is shown. Adapted from Biomedicines [89].

Moreover, various nonhematopoietic cell types may harbor either (i) dimeric IL-2Rβγc, as this applies to intestinal epithelial cells [90, 91], dermal fibroblasts, or fibroblast-like synoviocytes [92]; or (ii) the high-affinity IL-2Rαβγc, as reported for endothelial cells [93, 94], vascular smooth muscle cells [95], proximal tubular epithelial cells [96], or gingival fibroblasts [97, 98]. These CD25+ cells probably contribute to the control of IL-2 homeostasis in peripheral organs. Notably, IL-2R expression is documented in most hematological malignancies and also in some non-lymphoid cancer cells, including malignant melanoma and carcinomas of the kidney, head and neck, cervix, esophagus, and lung [72, 99].

I.1.2.2 IL-2-induced signal transduction

The three IL-2R subunits are neither pre-formed as stable heterotrimers nor randomly associated with the cell membrane but rather localize selectively within lipid rafts [100, 101]. This colocalization facilitates IL-2R-dependent oligomerization and signaling. Crystallographic studies of IL-2 bound to the IL-2R provide molecular evidence supporting a model where IL-2 drives the assembly of the high-affinity trimeric IL-2R (Figure 6). Initially, IL-2 is captured by IL-2Rα through a large hydrophobic binding surface surrounded by a polar periphery, resulting in a relatively weak interaction (Kd: ~ 10^{-8} M) with rapid on-off binding kinetics (~30 s). This IL-2Rα/IL-2 binary complex induces a conformational change in IL-2, increasing its affinity for the IL-2Rβ subunit and promoting the association between IL-2 and IL-2Rβ through a distinct polar interaction. Notably, the extracellular domain of IL-2Rα does not interact with IL-2Rβ; instead, the binary complex of IL-2Rα/IL-2 appears to present IL-2 to IL-2Rβ in *cis*. The ternary IL-2Rα/IL-2Rβ/IL-2 complex then recruits γ$_c$ through a weak interaction with IL-2 and a stronger interaction with IL-2Rβ to produce a stable quaternary high-affinity IL-2R/IL-2 complex. This quaternary complex has a fast IL-2 on-rate but a slow off-rate, resulting in essentially irreversible IL-2 binding [102-104]. Following IL-2 binding, receptor-mediated endocytosis of the quaternary IL-2R/IL-2 complex limits IL-2 signal transduction and the biological response to the IL-2. The complex is rapidly internalized (t$_{1/2}$ of 10-20 min), and IL-2, CD122, and CD132 are subsequently degraded [105-108], while CD25 can be recycled to the cell surface [104, 108, 109].
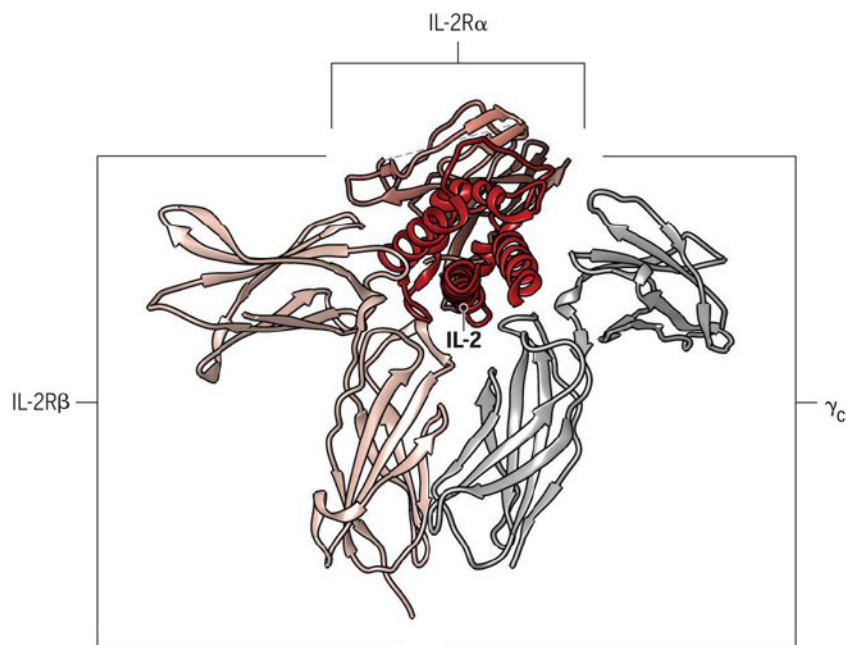

Figure 6. Structure of the high-affinity IL-2R/IL-2 complex. A ribbon diagram depicting the crystal structure of IL-2 with its trimeric receptor shows how the cytokine interacts with each of the three chains of the receptor. Adapted from Sci Immunol [110].

IL-2-induced heterodimerization of the IL-2Rβ and IL-2Rγc subunits brings their cytoplasmic tails into close proximity, which activates Janus tyrosine kinase (JAK) 3 associated with γc, followed by JAK1 activation associated with IL-2Rβ [32, 111-115]. Subsequent multiple tyrosine phosphorylation of the IL-2Rβ chain provides a docking site for effector molecules, recruiting various signal-transducing molecules to the cytoplasmic tail of the β-chain, including STAT5, STAT3, the Shc-adaptor protein, Syk, and p56lck [52]. This leads to the activation of three main signaling pathways: the JAK/STAT pathway, the PI3K/AKT pathway, and the Ras/Raf/MAP kinase pathway (Figure 7). Activation of mTOR, p70S6K, AKT, and ERK1/2 modulates the activity and *de novo* expression of numerous downstream regulators involved in protein synthesis, autophagy, cell metabolism, survival, proliferation, and differentiation [15, 51, 53, 116-120]. Concurrently, activated STAT5 determines the fate of the cell by transactivating numerous target genes. While these three signaling cascades are stimulated in effector T cells, it is important to note that the STAT5 pathway is predominantly triggered in Tregs, as they fail to activate the PI3K-Akt pathway due to high expression of PTEN [121-123].
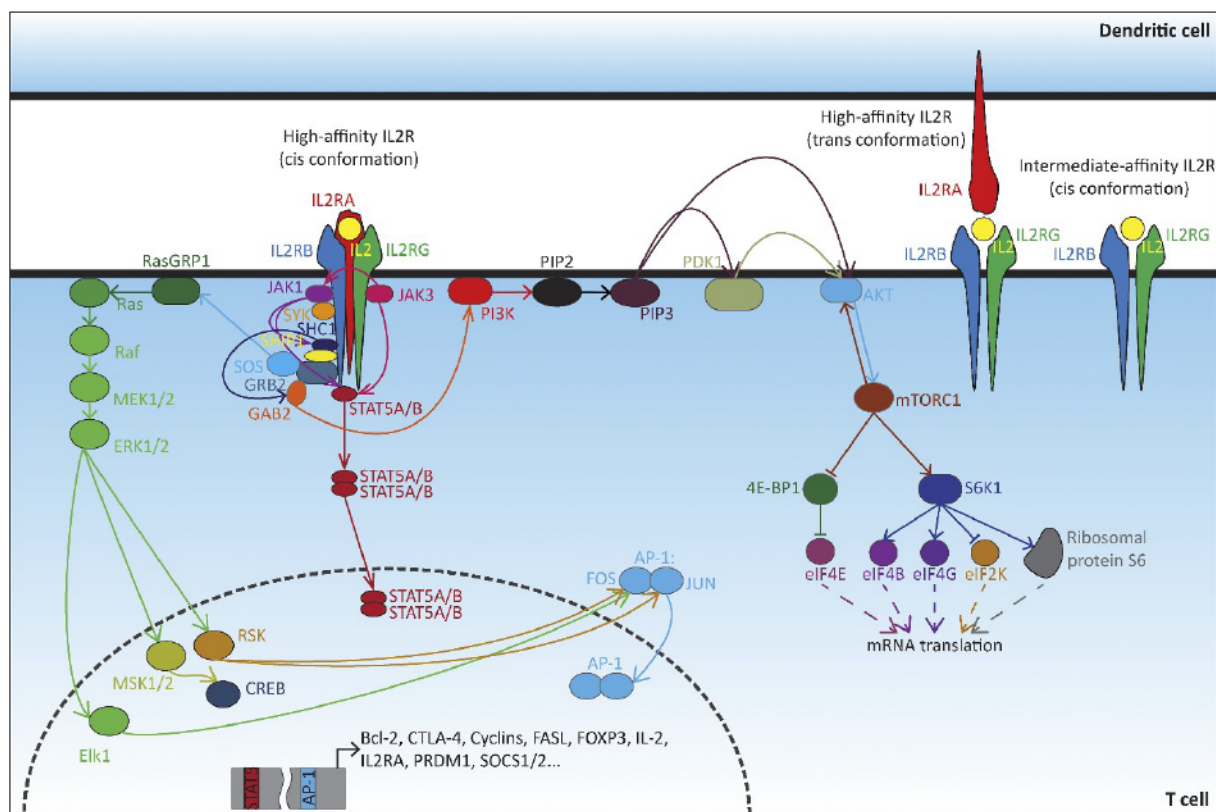

Figure 7. IL-2R signaling and modulation of T cell activity. For details, see the reference [17] in J Exp Med.

In T lymphocytes, the STAT5 signaling pathway may induce the expression of a variety of genes depending on the T cell subset. These genes encode for various cytokine receptors including IL-4Rα and IL-2Rβ (positive feedback); IL-4Rα or IL-12Rβ; diverse proteins

involved in cell proliferation and survival (e.g., PIM1, Myc, cyclins, and Bcl-2); effector molecules such as granzyme B, CD178 (best known as Fas ligand); cytokines like IFN-γ, TNF-α, or IL-4; immune cell function regulators like the SOCS1/2 or the transcription factor Foxp3. Moreover, IL-2-activated STAT5 represses the expression of specific genes such as *IL17A* and *BCL6* [124-129].

Interestingly, γ_c cytokines IL-2 and IL-15 are closely related, as they both signal through the IL-2Rβγ_c complex and activate the JAK/STAT, Ras/MAPK, and PI3K/Akt signaling pathways. This leads to both common and contrasting roles of IL-2 and IL-15 in T cell function [15, 52, 130, 131]. IL-2 and IL-15 share several functions, such as stimulating the proliferation of various T cell subsets (e.g., activated CD4^{+}, CD8^{+}, and γδ subsets of T cells) [132, 133]. Both cytokines facilitate the induction of cytolytic activity of T cells, and they induce the proliferation and immunoglobulin synthesis by B cells stimulated by anti-IgM or CD40 ligand [134]. They also promote the generation, proliferation, and activation of NK cells. Despite these shared functions, IL-2 and IL-15 have distinct differences, particularly in the homeostasis of adaptive immune responses (Table 1).

Properties	IL-2	IL-15
Gene structure and location	Four exons, chromosome 4q26	Eight exons, chromosome 4q31
Main site of synthesis	Activated CD4^{+} and CD8^{+} cells	Activated DCs and monocytes
Mechanism of regulation of expression	Transcriptional regulation and stabilization of mRNA	Mainly post-transcriptional, during translation, and intracellular trafficking
Mechanism of action	Secreted cytokine	Membrane-bound cytokine; induces signaling in the context of cell-cell contact in *trans*
Receptor	*Cis* presentation to IL2Rα, IL-2/IL-15Rβγ_c co-expressed on activated T and B cells, *trans*-presentation of IL-2Rα/IL-2 on the surface of DCs to T cells expressing IL-2/IL-15Rβγ_c	IL-15Rα/IL-15 on the surface of DCs and monocytes *trans*-presented to NK cells and CD8^{+} memory T cells expressing IL-2/IL-15Rβγ_c
Unique function	Maintenance of Tregs and elimination of self-reactive T cells mediated by AICD to yield self-tolerance	Maintenance of NK cells and CD8^{+}CD44^{hi} memory T cells to provide a long-term immune response to pathogens
Features of mice deficient in gene-encoding cytokine or its private receptor α-chain	Marked enlargement of peripheral lymphoid organs, polyclonal expansion of T and B cells associated with autoimmune disorders	Marked reduction in number of NK, NKT gamma/delta and CD8^{+}CD44^{hi} memory T cells

Table 1. Comparison of IL-2 and IL-15. Adapted from Cancer Immunol Res. [118].

IL-2 and IL-15 also bind their private α chains (IL-2Rα and IL-15Rα, respectively), which are structurally related and may have arisen evolutionarily from gene duplication [135, 136]. While IL-2 is predominantly a secreted cytokine that binds to high-affinity heterotrimeric receptors, IL-15 is a membrane-associated molecule that signals at an immunological synapse between antigen-presenting cells and CD8^{+} T or NK cells in *trans* (Figure 8). IL-2 or IL-15 availability and expression of IL-2Rα and IL-15Rα ensure the binding of the appropriate cytokine and therefore the specificity of the immune response [32, 136, 137].
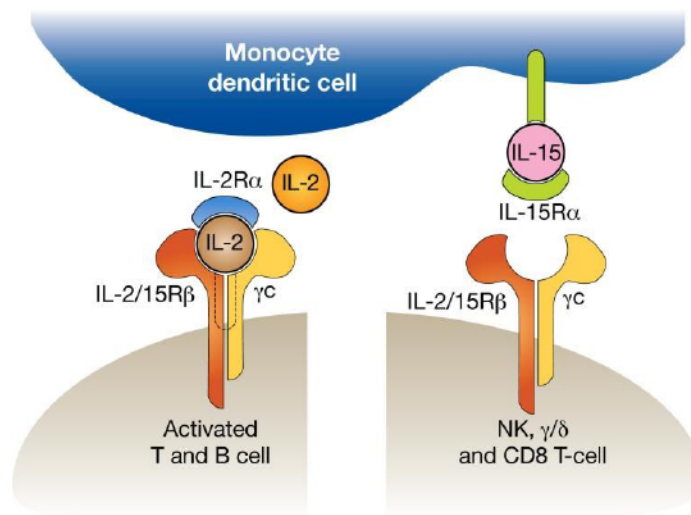
Figure 8. Mode of interaction of IL-2 and IL-15 with their receptors. IL-2 and IL-15 share the IL-2/IL-15Rβ and γ_c chains. Furthermore, the high-affinity forms of IL-2R and IL-15R contain a third cytokine-specific receptor α subunit, IL-2Rα or IL15-Rα. Adapted from Cancer Immunol Res. [118].

I.1.3 The role of IL-2 in the immune system homeostasis and activation

Originally identified as a T cell growth factor [138], IL-2 plays a critical role in immune response regulation and the maintenance of peripheral self-tolerance through its immunostimulatory and immunoregulatory functions. This activity depends on the type of target cell equipped with distinct IL-2R subunits, as well as the kinetics and amount of IL-2 produced. In essence, IL-2 is pivotal for activating and subsequently amplifying the T-cell response following antigenic stimulation. However, prolonged IL-2 signaling eventually leads to activation-induced cell death (AICD) [139]. Moreover, IL-2 is vital for maintaining self-tolerance by promoting Treg cell development and homeostasis while limiting Th17 cell polarization. Additionally, IL-2 affects a range of cellular targets, including nonhematopoietic and innate immune cells, as detailed later.

I.1.3.1 IL-2 optimizes CD8^{+} T-cell responses

IL-2 plays a pivotal role in influencing CD8^{+} T cell response at every stage - this includes primary expansion, contraction, memory generation, and secondary expansion. It

regulates various aspects such as proliferation, survival, effector function, exhaustion, memory formation, and the metabolic fitness of CD8^{+} T cells [140, 141]. While the initial expansion phase can occur independently of IL-2 *in vivo* [58, 109], the presence of IL-2 significantly enhances clonal expansion. Notably, autocrine IL-2 is crucial for the secondary expansion of CD8^{+} memory T cells [142].

The strength of TCR signaling is a key driver of memory CD8^{+} T cell functional characteristics and fitness. The extent to which naïve CD8^{+} T cells integrate TCR signals during priming dictates their dependence on IL-2 for developing into fully functional memory cells. These cells are characterized by their ability to rapidly reactivate (calcium signaling, cell cycling) and expand during an antigen rechallenge. They also exhibit enhanced stemness characteristics [143].

However, the strength and duration of IL-2 signaling during a primary immune response direct naïve CD8^{+} T cells toward differentiating into either short-lived effector (SLEC) or long-lived memory T cells [58, 141, 144, 145]. Suboptimal IL-2 signaling during priming leads to reduced primary expansion and severely impaired secondary expansion. Conversely, prolonged and strong IL-2 signaling results in the generation of short-lived, terminally differentiated effector CD8^{+} T cells, which express high levels of effector molecules like IFN-γ and granzyme B but produce low amounts of IL-2 [58, 141, 144, 146]. This differentiation process is mediated by the transcriptional repressor Blimp-1, which promotes the SLEC and terminal effector fate while directly repressing IL-2 transcription [27, 147].

Despite the potential to develop protective immunity without IL-2, optimal primary T-cell responses are significantly shaped by IL-2R signaling. During acute infections, high sustained levels of IL-2 rapidly up-regulate CD25, leading to an IL-2-driven expression of the death receptor Fas and its ligand FasL in cytotoxic effector cells. This process triggers AICD following pathogen clearance [141].

Moreover, the formation of functional, long-lived memory CD8^{+} T cells necessitates brief, yet potent, IL-2 signaling during antigen presentation by licensed DCs. Treg cells modulate CD8^{+} T cell responses by restricting both IL-2 production and consumption. This modulation helps to prioritize the priming of high-affinity over low-affinity polyclonal CD8^{+} T cells, reduces the generation of short-lived effector CD8^{+} T cells, and favors the formation of memory T cells [58, 148, 149]. In contrast, depriving effector T cells of IL-2 by Treg cells is fully dispensable for the suppression of IL-2R-sufficient CD4^{+} T cells, even though IL-2R signaling is required [150].

I.1.3.2 IL-2 signals control CD4^{+} T cell subsets

Similar to CD8^{+} T cells, the strength of TCR signaling critically determines the fate of naïve CD4^{+} T cells, guiding their differentiation towards various T helper cell types, including helper Th [151], follicular helper (Tfh) [152], and T follicular regulatory (Tfr) CD4^{+} T cells [153]. IL-2 signaling plays a crucial role in orchestrating these CD4^{+} T cell fates [154, 155], where strong IL-2 signals lead antigen-specific CD4^{+} T cells to become short-lived terminally differentiated effector T cells. In contrast, lower IL-2 signals promote their differentiation into T_{FH} or central memory T (T_{CM}) cells.

I.1.3.2.1 IL-2 influences CD4$^+$ T helper cell polarization

As helper cells, CD4$^+$ T cells carry out a variety of functions by differentiating into specialized subpopulations upon antigen stimulation and cytokine signaling. These functional subpopulations include Th1, Th2, Th17, Tfh, and Treg cells.

IL-2 signaling specifically affects the differentiation of effector CD4$^+$ T cells into Th1 or Th2 cells, as depicted in Figure 9. Th1 lymphocytes, which are critical for cellular immune responses against intracellular pathogens and cancer cells, undergo polarization through IL-2-mediated induction of IL-12 receptor β (IL-12Rβ) expression in activated CD4$^+$ T cells. This process, in conjunction with IL-12 from antigen-presenting cells (APCs), stimulates the expression of the transcription factor T-Box21 (TBX21, commonly known as T-bet), promoting Th1 differentiation and type 1 cytokine production, such as IFN-γ [156]. This regulatory mechanism involves IL-2-induced activation of STAT5a and STAT5b, which bind to the loci of *IL12RB2* and *TBX21* genes. Additionally, IL-2 enhances Myc and HIF-1α expression, which drives a transcriptional program supporting increased glycolysis in CD4$^+$ T cells [157]. Enhanced mTORC1 signaling by IL-2 further supports this metabolic shift, fostering Th1 cell differentiation [158].
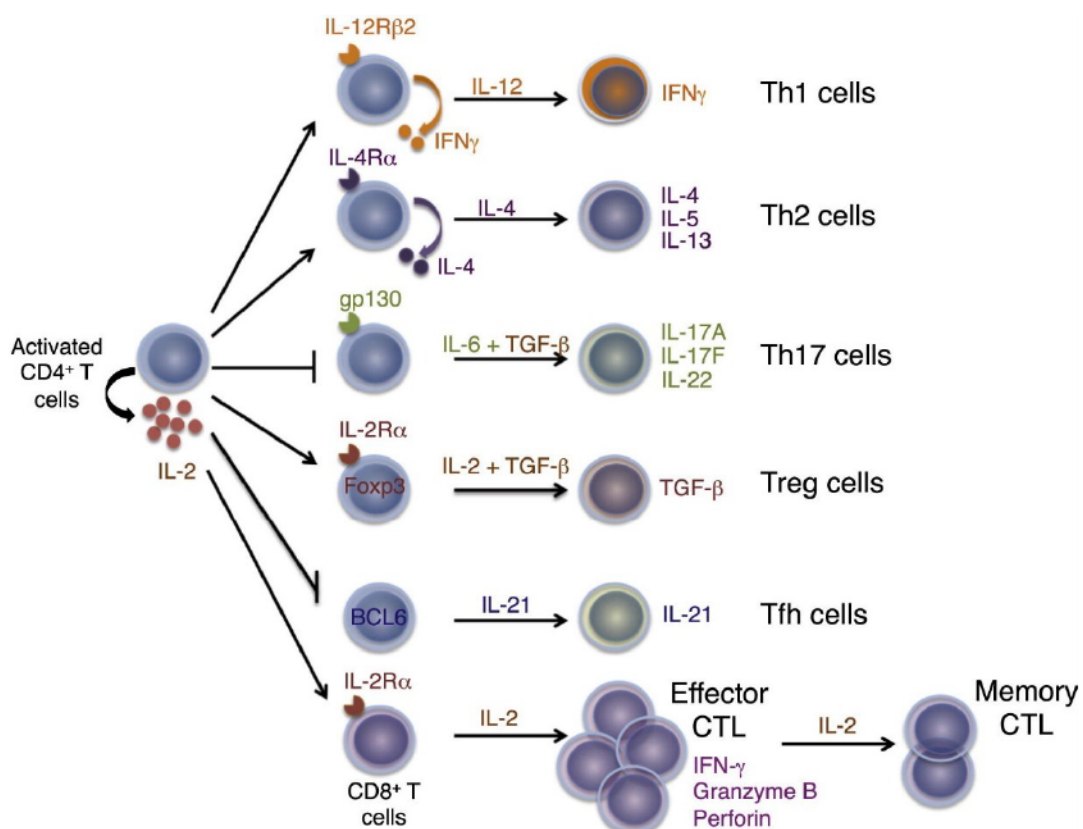
Figure 9. IL-2 is important for effector T-cell differentiation. Shown is IL-2-mediated induction of IL-12Rβ2 to promote Th1 cell differentiation, of IL-4Rα to promote Th2 cell differentiation, and of IL-2Rα to promote Treg cell differentiation. Conversely, IL-2 represses the expression of gp130 (and IL-6Rα) while inducing T-bet (not shown) to repress Th17 cell differentiation. IL-2 is also a repressor of Tfh differentiation based on its repression of Bcl-6 expression. Finally, IL-2 promotes the differentiation, expansion, and cytolytic activity of CD8$^+$ T cells. Adapted from Immunity [120].

Conversely, Th2 lymphocytes, key to humoral immunity against extracellular pathogens and allergic inflammation, are characterized by high expression of the transcription factor GATA3 and significant production of IL-4, IL-5, and IL-13 [159]. STAT5 also plays a crucial role in IL-2-driven differentiation and tissue memory formation in Th2 cells. IL-2-induced STAT5 activation upregulates the transcription of the IL-4Rα subunit, essential for initiating Th2 polarization in naïve CD4$^+$ T cells (Figure 9) [15]. Furthermore, STAT5A enhances the accessibility of the *IL4* gene locus, promoting its transcription followed by Th2 cell polarization [160]. IL-2 also affects the accessibility of the *IL3* gene locus in Th2 cells [161, 162], and is vital for the development of lung-resident, antigen-specific memory Th2 cells that mediate type 2 immune responses eventually leading to asthma and other pulmonary inflammations [163].

Interestingly, germinal center Tfh cells produce a high amount of IL-2, which, in turn, suppresses the differentiation of Tfh cells (Figure 9) [164]. Under normal conditions, Tregs and DCs can consume substantial amounts of IL-2, reducing its bioavailability around B cell follicles, and thereby creating a supportive environment for Tfh cell development [65]. Tfh cells can intrinsically diminish their responsiveness to high IL-2 levels through IL-6-induced STAT3 expression, which competes with IL-2-induced STAT5 signaling [164, 165].

I.1.3.2.2 IL-2 is crucial for the homeostasis of Treg cells

Treg cells, characterized by the expression of the transcription factor Foxp3, are integral in dampening immune responses to both self and foreign antigens, thereby maintaining immune tolerance [77]. IL-2 is vital for the homeostasis of Treg cells. This is evidenced by the observation that mice congenitally deficient in IL-2, CD25, or CD122 develop systemic autoimmunity [109] similarly to Foxp3-deficient mice. Treg cells are notable for their high surface expression of CD25, but they are unable to produce IL-2. Consequently, they depend on extrinsic sources of IL-2, produced either by mature single-positive CD4$^+$ T cells in the thymus or by naïve CD4$^+$ and CD8$^+$ T cells in the peripheral immune system (Figure 10) [166-168]. Due to their high CD25 expression, Treg cells consume IL-2, reducing its systemic concentration and helping to regulate immune balance. Without sufficient IL-2, the number of Treg cells decreases, and effector T cell numbers increase, leading to an enhanced susceptibility to autoimmune and inflammatory disorders.

IL-2, along with the transcription factor STAT5 - a key downstream target of JAK kinases linked to IL-2R - is essential for inducing Foxp3 expression and facilitating the differentiation of naturally occurring Treg cells in the thymus [45, 169-171]. Exposure to normal background levels of IL-2 is critical for the survival and homeostasis of these naturally occurring Treg cells [16, 166, 172]. Additionally, IL-2 signals enhance CD25 expression on Treg cells and bolster their suppressive functions by maintaining elevated levels of Foxp3 expression [166, 173].

Furthermore, there is strong evidence indicating that peripheral conventional T cells can develop into, or convert to, Foxp3$^+$ induced Treg cells, particularly in mucosal tissues such as the gut and lungs [174]. These induced Treg cells are also highly reliant on IL-2 for their generation (in synergy with TGF-β), as well as for their survival and continuous expression of Foxp3 [175, 176]. Notably, in the gastrointestinal tract, IL-2 is critically required to sustain these induced Treg cells, thus ensuring immunological homeostasis and maintaining oral tolerance to dietary antigens. ILC3s in the small intestine are the primary producers of IL-2,

triggered selectively by IL-1β from macrophages that sense microbiota through MYD88- and NOD2-dependent pathways [5, 177].
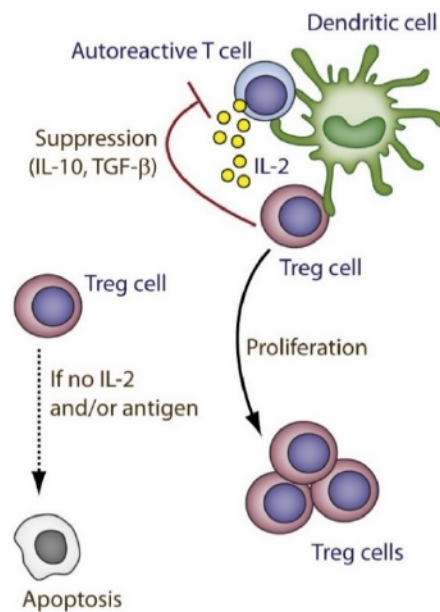
Figure 10. Model of peripheral Treg cell homeostasis. Focusing Treg and autoreactive T cells through recognition of autoantigens on DCs places them in close proximity for the Treg cells to receive an IL-2-dependent signal. This interaction promotes homeostatic proliferation and survival of Treg cells and enhances aspects of their functional program. Treg cells that fail to receive TCR and/or IL-2 signaling for an extended period of time undergo apoptosis. Thus, Treg cells adapt and are selectively maintained by the presence of self-antigens and IL-2, partly dependent on the autoreactive T cells they suppress. Adapted from Immunity [16].

I.1.3.2.3 IL-2 controls the reciprocal balance between Th17 cells and Foxp3⁺ Treg cells

Th17 cells are characterized by their production of IL-17 and the expression of the transcription factor retinoic acid receptor-related orphan receptor-γt (RORγt). These cells are found on mucosal surfaces, particularly in the lungs and gut, where they promote the activation of pro-inflammatory danger signals. These signals are crucial for recruiting neutrophils and enhancing the expression of anti-microbial factors [178]. IL-2 plays a suppressive role in Th17 differentiation by inhibiting their transcriptional programs through STAT5-mediated pathways, which include the augmentation of T-bet expression (Figure 9) [156].

Furthermore, IL-2 signals are vital for maintaining the reciprocal balance between Th17 cells and Foxp3⁺ Treg cells. In scenarios where IL-2 signaling is absent, there is a notable decline in Treg numbers, coupled with an increase of the Th17 cells. This imbalance leads to an elevated susceptibility to autoimmune and inflammatory disorders [179]. Interestingly, once Th17 cell-polarizing conditions are established, Treg cells can promote Th17 cell survival and function (notably IL-17 and IL-22 production), possibly by IL-2 consumption [180, 181].

I.1.3.3 IL-2 regulates innate immune cells

IL-2 produced early by bacterially activated DCs plays a fundamental role in activating NK cell-mediated immunity, enhancing both the proliferation and cytotoxicity of NK cells [182-184]. Additionally, IL-2 stimulates the functional maturation and activation of monocyte-derived DCs [81] and can support ongoing T cell activation by prompting plasmacytoid DCs to release other cytokines, such as TNF-α and IL-4 [185]. IL-2, either alone or in combination with other cytokines like TNF-α or IFN-γ, can increase macrophage cytotoxicity. Recent clinical studies indicate that IL-2 administration can substantially expand the type 1 DC population, which confers enhanced anti-tumor response [186].

Furthermore, IL-2 appears to play a role in coordinating fibroblast and monocyte responses in connective tissues, typically following activation by T lymphocytes [97, 98]. In the inflamed synovium, IL-2 from activated T cells prompts fibroblast-like synoviocytes (FLSs) to secrete MCP-1, thereby recruiting macrophages into the synovium and perpetuating inflammation [53]. In pulmonary ILC2s, IL-2 is crucial not only for promoting cell survival and proliferation but also acts as a cofactor in the production of type 2 cytokines such as IL-5 and IL-13[6].

I.1.3.4 Other cell targets of IL-2

IL-2 promotes B cell proliferation, facilitates their maturation into plasma cells, and enhances their capacity for immunoglobulin production [187-189]. Beyond its effects on lymphocytes, IL-2's influence extends to non-immune cells. For example, the expression of IL-2 receptors on intestinal epithelial cells establishes a dynamic pathway crucial for interactions between intestinal epithelial cells and lymphocytes, underpinning the functionality of the mucosal immune system [90, 91]. Additionally, IL-2 supports the survival and/or proliferation of vascular smooth muscle cells *in vivo*, highlighting its diverse roles in both immune and non-immune cell functions [95, 190].

I.2 Clinical applications of IL-2

IL-2 plays an important role in immunotherapy due to its unique dual ability to potently stimulate both T and NK cells on one side and Treg cells on the other. This dual functionality offers versatile strategies for treating a wide range of immune-related disorders. The therapeutic efficacy of IL-2 is critically dependent on maintaining a delicate balance between these contrasting immune cell subsets, a concept that is central to the design of targeted IL-2-based immunotherapies.

In the context of autoimmune diseases, immunosuppressive low-dose IL-2 therapies are tailored to selectively promote the expansion of CD25$^+$ Tregs over effector T (Teff) and NK cells. This selective expansion exploits the differential expression patterns of IL-2R subunits across these populations, a strategy depicted in Figure 11. Conversely, in cancer treatment, immunostimulatory high-dose IL-2 therapies aim to enhance the activity of CD122$^+$ effector T and NK cells. Such enhancement is crucial for mounting an effective anti-tumor response, harnessing the body's immune system to combat malignancies effectively.
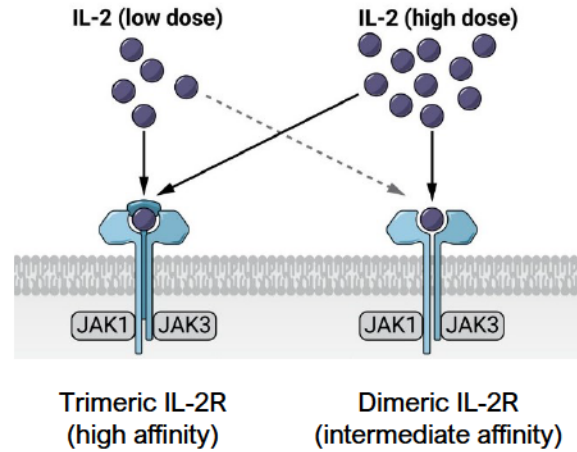
Figure 11. IL-2 dose is the key factor responsible for its dominant effect on the immune system. Low doses of IL-2 preferentially expand Treg cells. In addition to these cells, high doses of IL-2 also stimulate CD122+ Teff and NK cells to promote antitumor responses. Adapted from Sci Transl Med [191].

I.2.1   Cancer therapy

I.2.1.1   High-dose IL-2 monotherapy

The utilization of IL-2 in cancer treatment was motivated by its potential to enhance the anti-tumor immune response, a concept that has been extensively explored in clinical settings since the first trials in the 1980s. The clinical application of high-dose (HD) IL-2 has demonstrated notable successes [192], particularly in renal cell carcinoma (RCC) and metastatic melanoma, where 5-10% of patients achieved complete and durable responses [193-197]. This success led to the approval of recombinant human IL-2 (rhIL-2; Aldesleukin) by the FDA as the first immunotherapy for metastatic RCC in 1992 and for melanoma in 1998 [198, 199], further sparking extensive research into the use of HD IL-2 for treating metastatic cancer, either through HD bolus regimens or continuous infusions [194, 200, 201]. Patients with metastatic melanoma or RCC were uniquely responsive to IL-2 administration, and except for patients with advanced non-Hodgkin's lymphomas, only rare responses were seen in patients with other tumor types [202].

However, the administration of IL-2 poses significant challenges, requiring careful consideration of dose and schedule to balance efficacy and toxicity. The short half-life of IL-2, ranging between 10 and 85 minutes [203, 204] is one principal limitation of this therapy. Consequently, maintaining effective therapeutic levels requires frequent dosing, complicating treatment schedules, and patient compliance. Traditionally, IL-2 has been administered at high doses (~ 2 million Units/kg/day) to maximize its immunostimulatory effects, typically involving several cycles of treatment consisting of intravenous infusions twice daily for up to five days, followed by a rest period [205]. This intense regimen aims to induce rapid and potent immune activation; however, it necessitates careful selection of patients and their close monitoring within specialized centers, where the treatment-related mortality rate remains below 1% [206-210]. The most severe adverse effects stem from the massive cytokine release triggered by IL-2 [211] and from the off-target effects of IL-2 on endothelial cells [93, 94, 212, 213]. These collectively lead to a capillary leak syndrome characterized by hypotension,

pulmonary edema, and multi-organ dysfunction, known as vascular leak syndrome (VLS) [214]. Other common toxicities include fever, chills, and fatigue, which are generally manageable but can significantly impact the patient's quality of life.

Moreover, HD IL-2 therapy promotes the expansion of Treg cells, which constantly express high CD25 levels, necessary for high-affinity IL-2 binding and utilization of low IL-2 concentrations [118, 215-217]. Their expansion can paradoxically dampen the immune responses it aims to enhance, as evidenced by the increased frequency of Foxp3$^+$ Treg cells observed in patients treated with HD rhIL-2 [218-220]. Due to these factors, IL-2 monotherapy is no longer considered the optimal standard treatment for metastatic RCC or melanoma.

I.2.1.2 Combination of IL-2 with other therapeutic approaches for the treatment of cancer

I.2.1.2.1 IL-2 combined with cell-based therapies

Recent clinical efforts have focused on enhancing the efficacy of IL-2 therapy by combining it with other anticancer immunotherapies. Initial strategies included combining HD IL-2 with a lymphokine-activated killer (LAK) cell adoptive transfer, capitalizing on IL-2's role to stimulate T and NK cells. However, these combinations only achieved a clinical response rate of 20-35%, predominantly yielding transient responses in solid tumors [221-225]. A pivotal randomized trial involving 181 patients with metastatic melanoma or renal cancer compared IL-2 monotherapy against a combination with LAK cells, revealing that the antitumor effects were primarily attributable to IL-2 alone. Subsequently, LAK cells were excluded from future studies [226].

With the further development of cancer immunotherapy, highly personalized adoptive cell therapy (ACT) has emerged as an important therapeutic strategy against cancer [227]. A key advancement in ACT was the discovery that tumor-infiltrating lymphocytes (TILs) from resected metastatic melanoma could develop specific immune responses against autologous tumors when cultured with IL-2 [228, 229]. This insight facilitated the large-scale growth of TILs [230, 231], culminating in the successful regression of established metastatic melanoma [232]. Compared with other cancer immunotherapies which rely on the host's intrinsic antitumor lymphocytes, ACT holds the advantages of sufficient quantities, modifiable functions, and durable responses [233]. Numerous phase II trials reported promising outcomes, with about a 50% clinical response rate and a 13% complete regression rate in metastatic melanoma [234, 235]. Melanomas exhibit an average of ~300 exomic mutations, making them more responsive to IL-2 and TIL therapy than most other solid tumors, which typically have 5 times less or even fewer mutations [236]. This mutation abundance increases the likelihood that a processed peptide will strongly bind to a matching MHC molecule for tumor recognition by T cells. Attempts to improve the antitumor effects of TIL therapy using highly selected CD8$^+$ clones reactive to melanocyte differentiation antigens did not yield significant results in melanoma, indicating that polyclonal TIL reactivity and possibly also CD4$^+$ T cells are necessary for tumor rejection [237, 238].

Further mouse model studies elucidated the mechanisms behind successful ACT therapy [239]. Lymphodepletion prior to cell transfer, achieved through chemotherapy or total body irradiation (TBI), significantly enhances treatment efficacy by eliminating cells that compete

with transferred T cells for cytokines such as IL-2, IL-7, and IL-15. This strategy not only improves the persistence of donor lymphocytes but also boosts antitumor effects [240-246]. Host lymphocyte depletion also improves rhIL-2 availability for donor T cells. Elevated IL-7 and IL-15 levels after lymphodepletion further enhance antitumor effects [247-253]. Other mechanisms include reduced tumor burden, increased antigen-presenting cells, and release of lipopolysaccharide (LPS) from the host microflora [239, 246, 254-258]. The National Cancer Institute Surgery Branch saw response rates in metastatic melanoma patients rise from 15% with IL-2 alone to 34% with ACT/TILs, 49% with ACT/TILs after lymphodepleting chemotherapy [259], and 72% after maximum lymphodepletion including TBI (Figure 12) [251]. Despite these advancements, studies indicate a plateau in the benefits of increasing lymphodepletion, suggesting an optimal level that maximizes antitumor responses [260]. Due to study challenges, changing patient populations, and evolving protocols, the optimal lymphodepletion level for TIL therapy remains unclear. While IL-2-based TIL therapy is promising, the differentiated phenotype of IL-2-expanded TILs can limit their persistence and survival *in vivo*, compromising treatment benefits. Researchers are investigating other cytokines like IL-7, IL-15, and IL-21 for TIL expansion to improve TIL quality [261].
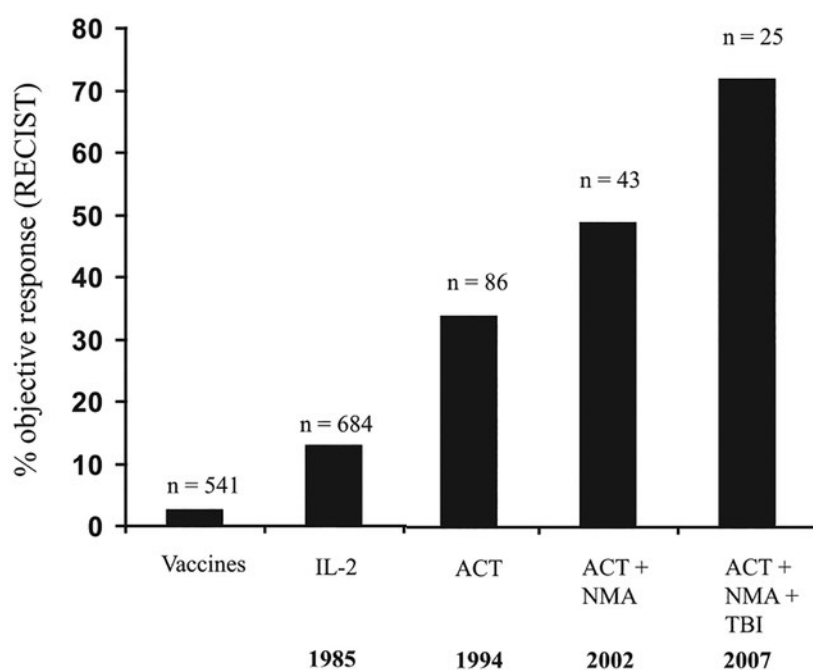
Figure 12. Objective response rates (using Response Evaluation Criteria in Solid Tumors) using various forms of cancer immunotherapy for patients with metastatic melanoma treated in the Surgery Branch at the National Cancer Institute. The years of these reports are shown on the bottom line of the figure. NMA - nonmyeloablative chemotherapy consisting of cyclophosphamide and fludarabine before cell transfer.

Beyond melanoma, the genetic engineering of lymphocytes has broadened the applicability of adoptive cell therapy. By inserting genes for tumor-specific TCRs or chimeric antigen receptors (CARs) into autologous lymphocytes cultured with IL-2, researchers have

expanded the range of treatable cancers [227, 234, 262-275]. IL-2 is crucial for *in vitro* expanding CAR-T cells to clinically relevant numbers, enhancing their growth and cytotoxic activity. Clinical trials targeting antigens like CEA, MART-1, gp100, NY-ESO-1, MAGE-A3, and MAGE-A4 [276-283] have highlighted the diverse roles of IL-2 in these settings, although the optimal conditions and cytokine support for CAR-T cell therapy continue to be refined.

I.2.1.2.2 IL-2 combined with chemotherapeutic agents

In the past two decades, researchers have extensively explored biochemotherapy (BCT), which combines IL-2 with chemotherapeutic agents, particularly for treating patients with metastatic melanoma [284]. A review of various inpatient regimens suggests a response rate of approximately 50%, with 10% to 20% achieving complete responses and a median survival time of 11-12 months. Despite these initially promising results in antitumor activity, BCT regimens have not demonstrated statistically significant benefits in overall survival across multiple randomized phase III trials.

Specifically, seven phase III trials have evaluated different BCT combinations [285-291], with varied outcomes. Notably, only one single-institution study, which explored the sequential administration of cisplatin, vinblastine, and dacarbazine (CVD) followed by IL-2 and IFN-α, reported an increase in overall survival; however, the statistical significance was marginal. Furthermore, two meta-analyses, which together assessed 18 trials involving over 2,600 patients, compared BCT (including regimens with IFN-α, IL-2, or both) against chemotherapy alone. These analyses reported higher response rates for BCT but found no survival advantage [292, 293].

While BCT has led to slightly higher response rates and longer median progression-free survival compared to CVD alone, it has not improved overall survival or resulted in durable responses. Given the additional toxicity and complexity associated with BCT regimens, they are not currently recommended for patients with metastatic melanoma. There is a pressing need to explore new combinations of IL-2 with other chemotherapeutic agents to potentially identify more effective treatment options.

I.2.1.2.3 IL-2 combined with targeted therapy

The advent of targeted therapy has revolutionized the treatment of cancer, notably following the identification of BCR-ABL in leukemia and EGFR mutations in non-small-cell lung cancer (NSCLC). Despite these advances, not all patients benefit from targeted therapies, and many who initially respond eventually develop resistance to these inhibitors [294-296]. In cases of advanced NSCLC, a disturbed balance in the IL-2/IL-2R system, characterized by decreased IL-2 levels and increased concentrations of sCD25, has been associated with a poor prognosis [297].

IL-2 has shown potential in restoring lymphocyte immune function against lung cancer, suggesting that it could counteract some of the deficiencies seen in NSCLC patients [298]. Furthermore, EGFR tyrosine kinase inhibitors (TKIs), which block EGF-stimulated EGFR autophosphorylation in tumor cells, have been found to modulate networks of pro-inflammatory cytokines, thereby activating lymphocytic responses. This interaction suggests a possible

synergistic effect between EGFR pathway inhibition and immune system modulation, which could enhance tumor reduction [299, 300].

In a phase II clinical trial [301], 70 patients with advanced NSCLC were assigned to receive either gefitinib (an EGFR inhibitor) alone or in combination with IL-2. The combination group exhibited significantly higher overall response rates and an extended median overall survival, while IL-2-related adverse events remained tolerable, and the treatment maintained a favorable safety profile. Separately, a retrospective analysis evaluated the safety and efficacy of HD IL-2 following TKI therapy in metastatic renal cell carcinoma [302], revealing clinical benefits from this combination. These findings underscore the potential of IL-2 to boost the efficacy of targeted inhibitors. More comprehensive research is required to ascertain the effectiveness of combining IL-2 with various targeted inhibitors, which could lead to more refined and effective cancer treatment protocols.

I.2.1.2.4 IL-2 combined with peptide vaccines

IL-2 synergizes with cancer vaccines to enhance anti-tumor immunity, theoretically offering a potent treatment strategy for malignancies [303]. When administered with vaccines such as recombinant viruses, DNA, or peptide antigens, IL-2 can amplify the immune response against tumors. In a pivotal phase II study, metastatic melanoma patients treated with HD IL-2 and the gp100 peptide vaccine exhibited a significantly higher response rate than those receiving IL-2 alone [304]. This finding was further corroborated by a subsequent phase III trial, which reinforced the efficacy of the combination. In this trial, advanced melanoma patients were randomly assigned to receive HD IL-2 alone or in combination with the gp100 vaccine formulated with incomplete Freund's adjuvant (Montanide ISA-51). The combination group demonstrated significantly improved overall clinical response, progression-free survival, and overall survival compared to the IL-2 monotherapy group [305]. These studies underscore the potential of IL-2 to enhance vaccine effectiveness in melanoma and demonstrate the promise of rationally combining immunotherapeutic agents for treating metastatic cancer.

I.2.2 IL-2 combined with immune checkpoint inhibitors for the treatment of cancer and chronic infections

Optimal immune responses require an antigen-specific signal generated by the TCR triggering, together with a second co-stimulatory signal. An array of different co-stimulatory and co-inhibitory receptors exists on T cells. Co-stimulatory receptors, which include CD28, inducible T-cell co-stimulator (ICOS), OX40, 4-1BB, and glucocorticoid-induced TNFR-related protein (GITR), provide critical positive second signals that promote and sustain T-cell responses. However, there are also co-inhibitory receptors on T cells providing negative signals. These include cytotoxic T-cell antigen 4 (CTLA-4), programmed death-1 (PD-1), B- and T-lymphocyte attenuator (BTLA), T-cell immunoglobulin and mucin domain-containing molecule-3 (TIM-3), T cell immunoreceptor with Ig and ITIM domains (TIGIT), and lymphocyte activation gene 3 (LAG-3), which all downregulate immune responses [306]. The balance between stimulatory and inhibitory signals is crucial to maximizing protective immune responses while maintaining immunological tolerance and preventing autoimmunity. However,

tumors can exploit these coinhibitory pathways ("checkpoints"), to establish an immunosuppressive microenvironment, hindering their eradication [307-309].

CD28 is a cell surface receptor for the proteins CD80 (B7-1) and CD86 (B7-2), and its ligation provides co-stimulatory signals essential for T cell activation and survival. Although CTLA-4 functions at the cell surface, it is predominantly localized within intracellular vesicles. During T cell activation via the TCR and CD28, CTLA-4 is immediately transported to the immunologic synapse [310]; and the intensity of TCR signaling correlates with the amount of CTLA-4 transported [311]. Similar to CD28, CTLA-4 binds to B7-1 and B7-2 but with significantly higher affinity (~ 10 times), allowing it to outcompete CD28 for these ligands. This interaction leads to the dislocation of PK C-θ and CARMA1 scaffolding protein [312], modulating the threshold of signals necessary for T cell cytokine production and proliferation, thereby inhibiting T cell activation [312-314]. Furthermore, CTLA-4 ligation inhibits cell cycle progression and the activity of transcription factors NF-κB, NF-AT, and AP-1 [315, 316].

Unlike effector T cells, Treg cells express CTLA-4 constitutively, which is important for their suppressive functions [317]. One proposed mechanism of Treg cell-mediated control of T cell responses involves the downregulation of B7 ligands on APCs, reducing CD28 co-stimulation and thereby modulating effector T cell activity [318, 319]. Recent studies have also demonstrated that enhanced CTLA-4 signaling promotes the generation of $CD4^+CD25^+FoxP3^+$ and $CD4^+CD25^-TGF^-\beta1^+$ Tregs [320]. These coinhibitory signals play critical roles in limiting the strength and duration of immune responses, curbing immune-mediated tissue damage, regulating inflammation resolution, and maintaining tolerance to prevent autoimmunity [321].

This understanding has guided the clinical targeting of CTLA-4, culminating in the FDA approval of Ipilimumab in 2011 for the treatment of advanced melanoma [322]. Although initial animal studies suggested potential benefits from combining CTLA-4 blockade with IL-2 therapy [323], subsequent clinical evaluations have not shown significant advantages over CTLA-4 blockade monotherapy [324, 325].

PD-1 is a cell-surface receptor on T cells and other immune cells, which delivers inhibitory signals upon ligation with PD-L1/2, impacting T cell survival, proliferation, cytokine production, and cytotoxic functions [326]. This balance is crucial for managing T cell activation, tolerance, and immunopathology [327, 328]. PD-1 expression is indicative of "exhausted" T cells, a state often seen in T cells that have repeatedly (or for a prolonged time) encountered antigen or reduced $CD4^+$ T cell help [329]. Such exhaustion, occurring in chronic infections and cancer, leads to T cell dysfunction and suboptimal control of infections and tumors [330-334]. PD-L1, the ligand for PD1, is notably expressed in several cancers [309], and its engagement with PD-1 on effector T cells inhibits their anti-tumor activity [335, 336], making PD-1 a prime target in the new generation of immune checkpoint therapy. The FDA approvals of Nivolumab and Pembrolizumab for malignant melanoma [337, 338] further underscore the critical role of PD-1 blockade.

Research has shown that up to half of the $CD8^+$ TILs co-express PD-1 and CTLA-4, with these double-positive cells exhibiting significant functional exhaustion. Dual blockade of these checkpoints has been shown to enhance T cell functions in cancer settings, as the effects are not redundant [339-344]. However, studies indicate that PD-1 blockade often exhibits greater anticancer activity and fewer immune-related adverse events compared to anti-CTLA-

4 therapies such as Ipilimumab [337], which are associated with severe adverse effects like colitis [345, 346].

With increasing interest in immune checkpoint inhibitors, IL-2 immunotherapy has regained attention for its complementary mode of action. The strategy involves removing the PD-1 inhibitory brake while simultaneously providing a positive signal for T cells through IL-2R. While checkpoint inhibitors demonstrate limited efficacy in non-immunogenic and poorly immune cell-infiltrated tumors, IL-2 might lower the threshold of required immunogenicity for these tumors, making them more amenable to checkpoint inhibitor treatment through direct stimulation [186]. Several ongoing clinical trials are exploring the combination of PD-1 blockade and IL-2 for various cancers [17, 79].

Moreover, combining IL-2 with PD-1 blockade has shown promise in animal models of chronic infection as it potently boosts virus-specific CD8$^+$ T cell responses and reduces viral loads despite increased Treg cell counts [347]. This approach was highly effective in reinvigorating exhausted T cells (Tex) during chronic infection [348]. Such synergistic effects likely arise because IL-2 modifies the differentiation trajectory of these cells. Hashimoto *et al.* [348] demonstrated that in contrast to anti-PD-1 mAb monotherapy, PD-1 blockade combined with IL-2 substantially alters the differentiation program of the PD-1$^+$TCF1$^+$ stem-like CD8$^+$ T cells, resulting in the generation of transcriptionally and epigenetically distinct and highly functional effector CD8$^+$ T cells that resemble those seen after an acute viral infection. The generation of these qualitatively superior CD8$^+$ T cells ("better effectors") that mediate viral control underlies the synergy between PD-1 blockade and IL-2 in chronic infection. Emerging from the stem-like CD8$^+$ T cells after such combination therapy, these virus-specific "better effectors" expressed increased levels of the high-affinity IL-2R, a feature not observed with PD-1 blockade alone in chronic viral infection [348]. Moreover, PD-1$^+$TCF1$^+$ stem-like CD8$^+$ T cells, also referred to as precursors of exhausted CD8$^+$ T cells, are not fate-locked into the exhaustion program and their differentiation trajectory can be changed by IL-2 signal. These findings highlight the potential of combining IL-2 with PD-1 inhibitors to enhance T cell responses and provide new treatment strategies for chronic infections and cancer, although further research is necessary to fully understand the synergy between IL-2 and various checkpoint inhibitors.

I.2.3 Low-dose IL-2 for the treatment of autoimmune diseases

Autoimmune diseases are characterized by the breakdown of immune tolerance and excessive immune activity, often associated with defects in Treg cells contributing to these pathophysiological mechanisms. Mice deficient in components of the IL-2/IL-2R pathway and Foxp3-deficient mice develop excessive T-cell proliferation and autoimmunity [349], underscoring the crucial role of IL-2 in Treg cell maintenance and function. Notably, IL-2 maintains and increases Foxp3 expression in Tregs and expands the number of Foxp3$^+$ Tregs in both mice and humans [350].

Based on the selective stimulation of Treg cells with low levels of IL-2, which does not activate CD4$^+$ or CD8$^+$ T cells, and their major role in maintaining immune tolerance and suppressing inflammation [77], reestablishing Treg cell functions through the efficacy of low-dose (LD) IL-2 administration has been proven effective. Initial studies demonstrated that LD

IL-2 therapy reversed and prevented experimental T1D in mice [172, 351-354]. Furthermore, LD IL-2 achieved disease control in mouse models of autoimmune diseases like Alzheimer's disease [355], particularly with chronic administration or when used in combination with glucocorticoids for graft-versus-host disease (GvHD) [356], Trypanosoma cruzi infection, and rapamycin in skin transplantation [357].

The encouraging results from preclinical models led to clinical trials for chronic GvHD and vasculitis related to hepatitis C infection [77, 358-365]. Further trials explored its potential in treating T1D [366-368] and alopecia areata [369]. All these trials have confirmed the safety and efficacy of LD IL-2, with doses below 3 million IU/day being well tolerated and effective. Notably, in all tested conditions, LD IL-2 increased circulating Tregs, leading to clinical improvement.

In SLE, controlled clinical trials have demonstrated that LD IL-2 therapy not only expands Tregs [370, 371] but also inhibits the generation of autoreactive Tfh and Th17 cells, thereby reducing disease severity [370, 372]. Other clinical studies have demonstrated similar efficacy and safety in treating SLE [358, 373-375]. Moreover, LD IL-2 therapy has effectively altered the ratio between Tfh and Tfr cells in SLE patients, with the frequency of Tfr cells markedly increased in patients' periphery compared to the baseline level and those treated with placebo [376]. Tfr cells are essential in regulating germinal center reaction, where excessive self-reactive antibodies are selected and matured in autoimmunity. Therapeutic use of LD IL-2 thus provided a promising approach to improve autoantibody-induced disorders by restoring abnormal germinal center response. However, balancing immune suppression and activation in autoimmune patients is challenging due to the increased risk of infection with immunosuppressive treatments [377, 378]. In fact, infection is one of the leading causes of the mortality of SLE patients [379, 380]. Notably, a study of 665 SLE patients found that those receiving LD IL-2 had a substantially lower rate of infection compared to those on conventional therapy [381], indicating a potential benefit for autoimmune patients at high risk of infection.

Th17 cells, which produce large amounts of IL-17, are considered a pathogenic factor in Sjögren's syndrome. Short-term LD IL-2 administration reversed the imbalance between Th17 and Treg cells in patients [382], primarily by directly inhibiting Th17 cells rather than by potentiating Tregs [383].

Furthermore, an open-label phase 1/2a clinical study demonstrated the safety and efficacy of LD IL-2 therapy across multiple autoimmune diseases, including rheumatoid arthritis (RA), Behçet's disease, ankylosing spondylitis, granulomatosis with polyangiitis and autoimmune hepatitis that were rarely investigated before, regarding the clinical benefits of LD IL-2 treatment [374]. Another study of 888 RA patients revealed that LD IL-2 therapy tripled Treg cell counts and significantly alleviated disease activity [384].

Administration of LD IL-2 for five days significantly increased Treg cells in patients with dermatomyositis/polymyositis, leading to clinical improvement and better remission rates [385]. In idiopathic inflammatory myopathies, 77.8% of patients under LD IL-2 therapy reached the definition of improvement by the International Myositis Assessment and Clinical Studies definition of improvement [386].

In the context of autoimmune hepatitis (AIH), a preclinical study in mice and a case report in humans have shown that LD IL-2 not only increases systemic Treg cells but also enhances their accumulation in the liver, which was associated with improved level of liver-

34

specific alanine transaminase [387]. Correspondingly, a case report with two refractory AIH patients receiving LD IL-2 therapy showed a safe and effective response with reduced liver damage [388].

Ongoing clinical trials are further exploring the potential of LD IL-2 therapy in inflammatory diseases such as ischemic heart disease, ulcerative colitis (UC), and Crohn's disease [389]. A phase 1b/2a study in ischemic heart disease yielded encouraging results with no significant adverse events [390]. Although limited, early results in UC patients show that daily LD IL-2 injections significantly increased Treg cells in peripheral blood within 14 days. In a humanized mouse colitis model, LD IL-2 expanded human Tregs and reduced experimental colitis [391].

Due to its potent ability to expand Tregs *in vivo*, LD IL-2 therapy is also being tested in patients with other diseases like subarachnoid hemorrhage injury [392], severe alopecia areata [393], and myelodysplastic syndromes [394]. Currently, there are more than 20 registered clinical trials of LD IL-2 therapy in patients with autoimmunity or beyond, with early results demonstrating the profound safety and efficacy of LD IL-2 therapy. Overall, low-dose IL-2 therapy leveraging its potent ability to expand Tregs *in vivo* emerges as a promising approach to restoring immune balance in a broad spectrum of autoimmune and inflammatory diseases, and GvHD [360-362, 364, 367, 369, 370, 395]. Despite the differences in particular regiments, patients typically receive 1,000,000 IU/day subcutaneously for 5-14 days, then once every 2 weeks for 6-9 months.

I.3. IL-2-based immunotherapeutics

IL-2 therapy has elicited significant clinical responses in a subset of cancer patients, illustrating its potential as an effective treatment modality. However, its broader application is considerably restricted due to severe dose-limiting toxicities. These adverse effects necessitate extensive monitoring and comprehensive supportive care to mitigate risks to patients. Additionally, HD IL-2 therapy may also activate Treg cells, which can suppress the immune response to self-antigens, including certain tumor antigens, thereby undermining its efficacy. While LD IL-2 has shown benefits in managing autoimmune diseases, it may also inadvertently stimulate NK cells [376]. This is a significant issue, particularly over prolonged treatments, complicating its use in autoimmune contexts. Moreover, a major limitation of IL-2 therapy is its short half-life, necessitating frequent dosing to maintain effective therapeutic levels, which complicates treatment schedules and challenges patient compliance. The heterogeneity among patient responses further complicates the determination of an optimal dose, presenting a significant barrier to standardizing IL-2 treatment protocols.

These limitations have spurred the development of improved IL-2 immunotherapeutics designed to achieve better selectivity for specific immune cells and reduced toxicity [94]. A pivotal advancement in this research was the elucidation of the crystal structure of IL-2 bound to its trimeric receptor [102]. This discovery has facilitated the creation of new IL-2 analogs that are tailored to target specific immune cells. These engineered products are designed either to selectively activate Treg cells, helping to modulate the immune response in autoimmune and inflammatory disorders, or to enhance the responses of effector T cells, memory T cells, and NK cells, thereby boosting their antitumor activity (Figure 13).

a Cancer therapy

IL-2
IL-2Rβ
IL-2Rγc

Teff

Expansion and activation of Teff cells

Immunostimulation to promote an antitumor response

IL-2 superkine
Nemvaleukin
PEGylated IL-2 (NKTR-214)
Non-PEGylated IL-2 agonists
IL-2 fusion proteins
IL-2/anti-IL-2 mAb complexes
IL-2 immunocytokines

b Autoimmune disease therapy

IL-2Rα
IL-2
IL-2Rβ
IL-2Rγc

Treg

Expansion and activation of Tregs

Immunosuppression to promote immunologic tolerance

IL-2 muteins
PEGylated IL-2 (NKTR-358)
IL-2/anti-IL-2 mAb complexes

Figure 13. Mechanisms of action of IL-2-based immunotherapeutics for the treatment of cancer and autoimmune diseases. (a) Cancer can be treated using IL-2-based immunotherapeutics that target the intermediate-affinity IL-2Rβγc receptor that is constitutively expressed on Teffs, memory T cells, and NK cells, while (b) autoimmune diseases can be treated using agents that target the high-affinity IL-2Rαβγc receptor that is constitutively expressed on Tregs. Adapted from Annu Rev Med [79].

Some IL-2 immunotherapeutics have shown efficacy in preclinical models, leading to a surge in clinical trials for improved IL-2-based agents in recent years (Figure 14). These studies will determine whether novel IL-2 immunotherapeutics can harness the IL-2/IL-2R pathway as effective therapies for autoimmunity and cancer, either alone or in combination with other treatments.
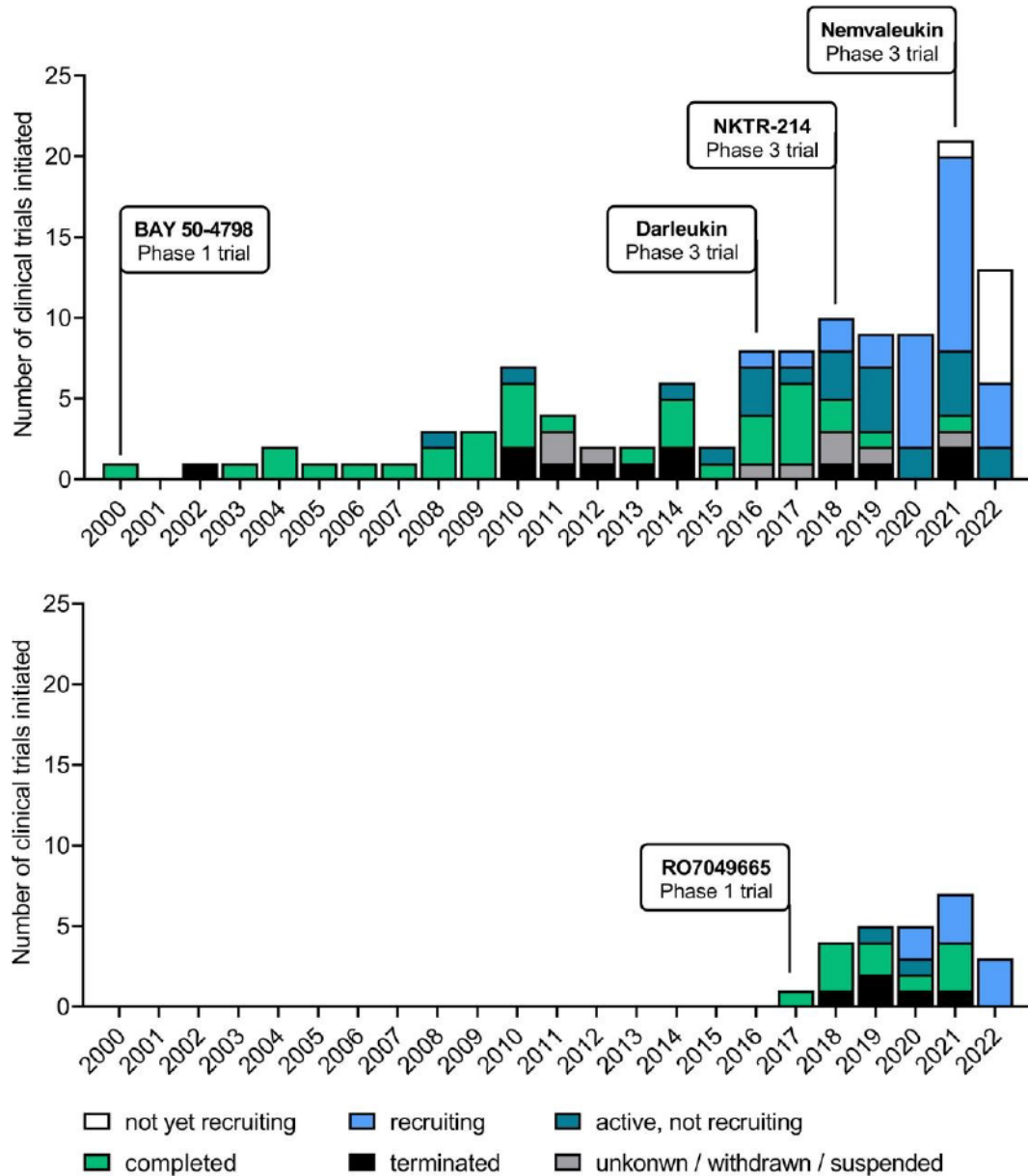
Figure 14. Registered clinical trials testing improved IL-2-based immunotherapeutics. The top panel displays trials in cancer and the bottom panel trials in autoimmune diseases. Adapted from EBioMedicine [396].

I.3.1 IL-2 muteins with altered binding to the IL-2R

This strategy involves creating IL-2 muteins (IL-2 molecules with introduced mutations that alter the amino acid sequence but still bind to IL-2R), designed to exhibit altered affinities for IL-2Rα, IL-2Rβ, and/or IL-2Rγ$_c$. These IL-2 analogs produce varying signaling responses - agonistic, mixed, or antagonistic - through the IL-2Rαβγ$_c$ and IL-2Rβγ$_c$ pathways. Such differential signaling crucially influences the balance between Tregs and Teffs, a key aspect of immune modulation.

I.3.1.1 IL-2 muteins with reduced IL-2Rα binding or enhanced affinity for IL-2Rβ

Researchers have developed several IL-2 muteins with decreased binding to IL-2Rα and, in some cases, increased affinity for IL-2Rβ. These modifications aim to preferentially stimulate CD8$^+$ T cells (effector and memory ones) and NK cells without stimulating CD25$^+$ Treg cells and endothelial cells. Such engineered variants have shown improved antitumor efficacy and reduced toxicity in preclinical animal models [369-372], leading to their testing in clinical trials (NCT05267626, NT02983045, NCT04855929).

Levin et al. introduced an IL-2 variant termed "superkine" (also known as Super-2), which exhibits enhanced affinity for IL-2Rβ. Crystallographic studies of this molecule, both alone and when complexed with its receptor, demonstrated that specific mutations (L80F, R81D, L85V, I86V, and I92F) in the core of the cytokine stabilized IL-2, reducing the flexibility of a C-helix in the IL-2Rβ binding site. This stabilization fosters an optimal receptor-binding conformation similar to that when IL-2 is bound to CD25, thereby mimicking its functional effects and leading to ~ 200 times increased affinity for IL-2Rβ. These changes lead to potent STAT5 phosphorylation and vigorous T cell proliferation independent of CD25 presence. The Super-2 substantially increases the proliferation of cytotoxic T cells *in vivo*, thereby improving antitumor responses while minimizing Treg cell expansion and pulmonary edema [397].

Nemvaleukin alfa (Nemvaleukin, ALKS 4230), a fusion protein combining circularly permuted IL-2 with IL-2Rα, is designed to target the intermediate-affinity IL-2Rβγ$_c$ found on CD8$^+$ T and NK cells. This selectivity reduces Treg cell expansion [398], enhancing the anti-tumor immune response. In a murine model of small-cell lung cancer, the mouse variant of Nemvaleukin significantly inhibited tumor growth and extended survival, effects that were amplified when combined with chemotherapy. Tumor analysis showed an increase in tumor-infiltrating NK and CD8$^+$ T cells, indicative of a potent anti-tumor immune response, especially when combined with chemotherapy [399]. Following these promising results, Nemvaleukin has entered Phase I-III clinical trials, both as a monotherapy and in combination with checkpoint inhibitors like Pembrolizumab or chemotherapy [400-402]. These studies underscore Nemvaleukin's efficacy and tolerability, demonstrating sustained responses in patients with diverse and advanced tumor types, thereby justifying further clinical investigation [402].

I.3.1.2 IL-2 muteins with improved binding to IL-2Rαβγ$_c$

Another human IL-2 mutein denoted BAY 50-4798, was designed using site-directed mutagenesis to contain a single mutation, N88R, in the IL-2/IL-2Rβ interface. This mutation ablated cytokine binding to IL-2Rβ and weakened interactions to the IL-2Rβγ$_c$ heterodimer by five orders of magnitude, while maintaining the same affinity for IL-2Rα, resulting in >3,000-fold greater selectivity in stimulating proliferation of T cells over NK cells compared to wildtype IL-2 [403]. In preclinical studies, BAY 50-4798 induced the proliferation of activated human T cells with a potency comparable to IL-2 but caused less proliferation in NK cells and reduced activation of secondary cytokine cascades [404]. Despite these promising results, at concentrations where BAY 50-4798 demonstrated peak biological activity, it lost T cell selectivity and induced pro-inflammatory cytokines [405]. In a follow-up study, AIC284 (renamed from BAY 50-4798) preferentially expanded Treg cells over CD4$^+$ effector T cells *in vivo* while ameliorating clinical symptoms in EAE, a rodent model of MS [406]. BAY 50-4798

underwent a Phase I clinical trial in patients with advanced melanoma and renal cell carcinoma—both malignancies that respond to HD IL-2 therapy. While some clinical responses were noted, BAY 50-4798 did not show a significant improvement over conventional IL-2 therapy [407]. Currently, BAY 50-4798 is being tested in Phase II trials, both as a potential adjunct to standard chemotherapy for various cancers and as a possible treatment for HIV infection.

Concurrently, other research groups have focused on developing IL-2 muteins with increased IL-2Rα binding. Fallon and colleagues reported an IL-2 mutein that exhibits enhanced endosomal recycling due to altered pH sensitivity between IL-2 and IL-2Rα [55]. Similarly, Rao and others have created IL-2 muteins with increased affinity to IL-2Rα [408, 409]. Unlike wild-type IL-2, these muteins persist longer on the cell surface, thus sustaining durable signaling similar to IL-15 [410]. The clinical efficacy of these IL-2 muteins, and the specific conditions under which they might be effective, remain under investigation.

I.3.1.3 IL-2 muteins with antagonist activity

In addition to efforts aimed at enhancing or refining IL-2 signaling, significant work has also been devoted to the development of IL-2 muteins that act as antagonists [411, 412]. For example, Liu et al. [411] engineered an IL-2 antagonist that exhibits high affinity binding to IL-2Rα while lacking binding to IL-2Rβγ$_c$. These molecules are designed to selectively block high-affinity IL-2 signaling pathways and could, for instance, be used to suppress Treg cell activity. This approach represents a strategic redirection of IL-2 interactions to modulate the immune system in a targeted manner. While mutant IL-2 molecules have promise, it is also worth mentioning that Tsytsikov and others [413] reported natural variants of IL-2, generated by alternative splicing, that may competitively inhibit full-length IL-2. The existence of these natural variants further complicates the biological landscape of IL-2 signaling and suggests additional layers of regulation that could be exploited therapeutically.

I.3.2 Modified IL-2 and IL-2 muteins with improved half-life and biological activity

I.3.2.1 IL-2 mutein fusion proteins

Like their WT counterpart, IL-2 muteins suffer from limited bioavailability *in vivo*. As a remedy, they are frequently fused with a mAb or its Fc part or albumin [220, 414, 415]. One of them is RO7049665 (Melredableukin alfa), a fusion protein that consists of a human IgG1κ fused to a hIL-2 mutein (point mutation N88D) with reduced binding to the intermediate affinity IL-2Rβγ$_c$ receptor. Although Melredableukin alfa preferentially expanded Treg cells but not effector T cells in cynomolgus monkeys and humanized mice [416], Phase I and II clinical studies testing its clinical benefit in ulcerative colitis and autoimmune hepatitis (NCT04790916, NCT03943550) were terminated due to the lack of superior efficacy over standard treatment.

Another significant fusion mutein is MDNA11, with a higher binding affinity for IL-2Rβ and blocked IL-2Rα interaction. MDNA11 is a fusion protein composed of mutated Super-2 (with two additional changes: F42A and E62A) and human albumin, used to increase the molecular size and improve the *in vivo* half-life. This long-acting superkine predominantly

stimulates NK and naive CD8$^+$ T cells over Treg cells. MDNA11 exhibits a favorable pharmacodynamic profile, translating to strong therapeutic efficacy in preclinical tumor models and robust, durable immune responses in non-human primates [417].

I.3.2.2 Pegylated IL-2

In addition to enhancing the specificity of IL-2, other strategies seek to improve the half-life and biological activity of IL-2. Pegylation of recombinant proteins can improve half-life [418-420], and pegylated IL-2 (PEG-IL-2) molecules have been generated with an increased half-life, enhanced biological activity, and antitumor activity in comparison to non-pegylated IL-2 [421-426]. Pegylated IL-2 has shown promising efficacy in clinical trials for metastatic melanoma and renal cell carcinoma [427], indicating its potential as a potent immunomodulator.

An added benefit of pegylation, besides increasing the half-life through increased molecular weight, is the potential alteration of the IL-2 molecule to redirect its cellular target specificity. Prodrug versions of rhIL-2, decorated with releasable PEG chains, allowed: (i) a sustained release of the cytokine; (ii) a prolonged stimulation of the IL-2R signaling pathway; and (iii) a biased binding of IL-2 either to IL-2Rα/CD25 or IL-2Rβ/CD122, depending on the sites of PEGylation [428]. For instance, NKTR-214 (Bempegaldesleukin, BEMPEG) is an engineered Aldesleukin prodrug with six pegylated surface lysines which extends its half-life and reduces its ability to bind to IL-2Rα. Thus, this molecule is therefore biased to the IL-2Rβ (Figure 15) [428, 429]. When administered *in vivo*, the PEG chains slowly release, creating a cascade of increasingly active IL-2 protein conjugates bearing fewer PEG chains [428]. Due to its limited activation of the high-affinity trimeric IL-2Rαβγ$_c$ expressed on Tregs, NKTR-214 was predicted to induce only mild Treg cell expansion compared to the expansion and activation of T and NK cells, which only express the intermediate affinity dimeric IL-2R. In early preclinical studies, NKTR-214 monotherapy induced tumor regression accompanied by preferential peripheral and intratumoral expansion of Teff over Tregs in various immunogenic murine tumor models [423]. Mechanistically, intratumoral Treg depletion was mediated by CD8$^+$ Teff-associated cytokines IFN-γ and TNF-α. Similar trends of peripheral and intratumoral Treg and Teff dynamics together with tumor shrinkage and durable regression were observed in a small cohort of patients treated with NKTR-214, and without causing serious toxicity [430]. In adjuvant therapy, NKTR-214 combined with the PD-1 inhibitor Nivolumab progressed to Phase III trials, showing prolonged survival in patients with completely resected stage III/IV melanoma at high risk of recurrence [431]. However, a study combining NKTR-214 with another PD-1 inhibitor, Pembrolizumab, did not meet its primary endpoints of improved objective response rate and progression-free survival in metastatic melanoma. With 20 registered clinical trials NKTR-214 is the most studied IL-2-based compound, however, due to a lack of efficacy reported in two phase 3 trials clinical development of NKTR-214 was terminated in 2022 [432, 433]. Since October 2022, two other non-alpha IL-2 variants, NL-201 and Thor-707 (SAR444245) have been discontinued or deprioritized from clinical development.

Figure 15. Model demonstrating region of PEGylation sites at IL-2 interface with IL2Rα. NKTR-214 is IL-2 at its core (green), sites of PEGylation are depicted by red circles. The γ_c receptor is depicted in pink, IL2Rβ in aqua blue and IL2Rα in dark blue. Adapted from [423].

Conversely, NKTR-358, a PEGylated IL-2 variant with a lower affinity for IL-2Rβ compared to IL-2Rα, preferentially stimulates Tregs over conventional T cells (Tconv). Initial studies in murine and simian models of SLE and cutaneous hypersensitivity showed that NKTR-358 could restore Treg cell function [434]. In humans, a Phase I study indicated that NKTR-358 was well-tolerated, had a suitable pharmacokinetic profile allowing biweekly dosing, and significantly increased CD25^{bright} Tregs without affecting Tconv cells [435]. These promising results support further clinical evaluation of NKTR-358 in SLE and other inflammatory diseases. However, of the nine registered trials testing NKTR-358, only one Phase I study (NCT03556007) reports clinical results. These results did not reveal any significant treatment-related changes in the validated SLE Disease Activity Index or the counts of affected joints in SLE patients. Nonetheless, a dose-dependent improvement in skin manifestations, measured using the Cutaneous Lupus Erythematosus Disease Area and Severity Index, was observed.

I.3.2.3   Targeted IL-2 and IL-2 muteins

To mitigate the toxicity associated with the systemic administration of HD IL-2, various IL-2-based immunocytokines (IC)s have been developed. Some ICs consist of IL-2 fused to antibodies targeting tumor-associated antigens (TAA) and such ICs have shown promising results in preclinical models [436-441]. Once bound to the TAA, these IL-2-based ICs promote the *in situ* recruitment and activation of NK and cytotoxic CD8$^+$ T cells. This recruitment facilitates a shift in the tumor microenvironment towards a classical Th1 anti-tumor immune response, which is further supported by the interaction between NK cells and DCs. Additionally, some tumor-targeted IL-2-based ICs have been demonstrated to induce tumor cell

killing through antibody-dependent cellular cytotoxicity (ADCC) via engagement of Fcγ receptors [442, 443].

Darleukin (L19IL2) is a fully human immunostimulatory product consisting of the human L19 antibody fused to the rhIL-2 (Figure 16). The fusion of IL-2 to the L19 antibody, specific to the human fibronectin extra-domain B results in a tumor-targeted molecule, which selectively localizes at the site of disease, while sparing healthy organs [444]. Darleukin, given i.v. or intratumorally, shows strong anti-cancer activity, especially when combined with other therapeutic modalities. Mechanistically, Darleukin activates tumor-specific T cells and NK cells at the site of disease, i.e. directly within the tumor mass. Darleukin has been tested in numerous clinical studies (I-III) and numerous tumors (metastatic melanoma, various carcinomas of the skin, etc.), both as monotherapy and in combination with other drugs [445]. Promising phase I results have been obtained especially when Darleukin was combined with stereotactic ablative radiotherapy (SABR). In collaboration with the IMMUNOSABR European Consortium, Darleukin is currently being studied in a phase II clinical trial in patients with advanced non-small cell lung cancer in combination with SABR and anti-PD-1 therapy [446].
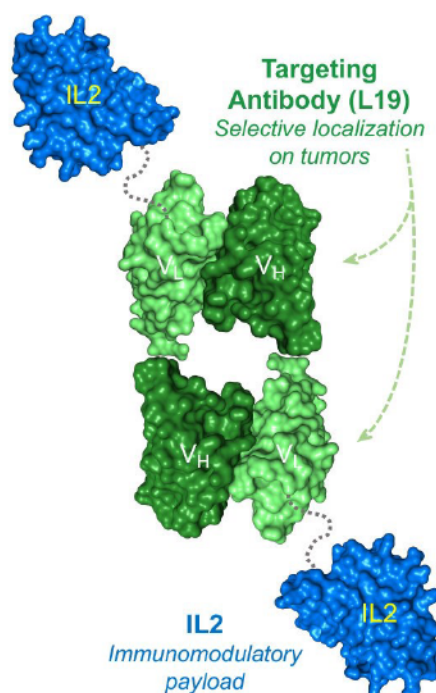
Figure 16. Darleukin (L19IL2) consists of the humanized L19 mAb fused to the hIL-2. Adapted from Philogen.com

ALT-801 is another IC composed of an IL-2 linked to a single-chain TCR domain recognizing amino acids 264–272 of human p53 antigen, thus shuttling IL-2 to the tumor [447, 448]. Hu14.18-IL2 consists of two hIL-2 molecules fused to an anti-ganglioside GD2 mAb [449-451] and DI-Leu16–IL2 is a fusion protein of IL-2 and a CD20-targeting mAb [452]. All these molecules advanced to clinical trials; however, they have either been completed, terminated, or withdrawn, indicating that further clinical development has been suspended.

Furthermore, the modulation of the tumor microenvironment (TME) can also be achieved using IL-2-based ICs. A novel class of monomeric tumor-targeted IC in which a single-engineered IL-2 variant (IL-2v) with abolished CD25 binding is fused to the C-terminus of an antibody against the CEA has been described [442]. CEA-IL-2v demonstrated superior safety, pharmacokinetics, and tumor targeting while lacking preferential induction of Treg cells due to abolished CD25 binding. At the same time, this construct showed monovalency and high-affinity tumor targeting as compared to classical IL-2-based ICs. Moreover, CEA-IL-2v retains the capacity to activate and expand NK and CD8$^+$ effector T cells through IL-2R$\beta\gamma_c$ in the periphery and the TME. CEA-IL2v treatment resulted in superior efficacy when administered in combination with PD-L1 checkpoint blockade or with ADCC-competent antibodies, such as trastuzumab and cetuximab [442].

However, targeting proteins expressed on the surface of tumor cells possesses several limitations. These include the transient expression of TAAs, and rapid internalization and degradation of ICs in the lysosomal compartment, all of which contribute to the failure to achieve the expected therapeutic effect. Furthermore, the higher affinity of IL-2 for its receptor compared to the antibody for its antigen may limit effective tumor targeting. Recent studies also suggest that the efficacy and biodistribution of IL-2 variants may not adequately be attributed solely to TAA targeting [453, 454]. Additionally, the systemic delivery of ICs may activate T cells in both lymphoid and non-lymphoid tissues, contributing to severe toxicity and limited anti-tumor efficacy.

IL-2R$\beta\gamma_c$-biased IL-2 agonists have also been directed to specific T cell subsets with 'bispecific' antibodies, referred to as *cis*-targeting, for example, to CD8$^+$ T cells or T cells expressing PD-1 [455, 456]. These approaches are expected to increase the IL-2 effect within the tumor microenvironment and/or bias IL-2 away from interaction with NK cells and Tregs. CD8 *cis*-targeted IL-2 promoted robust effector T cell responses and potent antitumor immunity [455] and drove potent antiviral response against hepatitis B virus [457]. A recent publication indicates that *cis*-targeting of non-alpha IL-2 mutein to T-cells may bypass the requirement for CD25 binding needed for the generation of better effectors [456]. In this way, a specific IL-2 delivery to CD8$^+$ PD1$^+$ T cells, which are found particularly in tumors, is ensured using a chimeric molecule of anti-PD-1 mAb fused to IL-2 variants binding specifically to intermediate affinity IL-2R$\beta\gamma_c$. Promising preclinical data [456, 458, 459] encouraged clinical trials with immunocytokine PD1-IL2v, either alone or combined with Atezolizumab, in advanced tumors (NCT04303858).

I.3.3 Complexes of IL-2 and anti-IL-2 mAbs

Another strategy to reduce the limitations of IL-2 therapy involves complexing IL-2 with specific anti-IL-2 mAbs, creating IL-2/anti-IL-2 mAb complexes (IL-2co). These complexes exhibit significantly enhanced biological activity *in vivo* [74]. Moreover, they possess selective stimulatory activity for distinct IL-2-responsive immune cell subsets governed by the clone of mAb used.

I.3.3.1 CD122-biased IL-2co

Complexes formed by the S4B6 mAb (mIL2-specific; IL-2/S4B6 henceforth) and MAB602 (hIL-2-specific; IL-2/MAB602 henceforth) are CD122-biased. This IL-2co requires only the IL-2R$\beta\gamma_c$ to exert its biological activity and preferentially stimulates CD122^{high} cell populations, such as memory CD8$^+$ T and NK cells [94]. In mice, administration of IL-2/S4B6 has been shown to increase memory-phenotype (MP) CD8$^+$ T cell counts up to 100-fold and significantly boost NK cell numbers by day 7 post-administration, primarily in the spleen and lymph nodes, with only minimal increases in CD4$^+$ T cells or B cells [74, 460, 461]. Interestingly, IL-2/S4B6 complexes also stimulate Tregs, albeit to a lesser extent (<2-fold increase), in a CD25-independent manner [74].

Krieg *et al.* reported that severe pulmonary edema, a notable side effect of IL-2 therapy, does not result from cytokine release by activated NK cells but rather from the direct interaction of IL-2 with trimeric IL-2R on CD31$^+$ lung endothelial cells [94]. This adverse effect can be mitigated either by using CD122-biased IL-2co or by employing blocking antibodies against CD25 [94, 214].

Preclinical studies in melanoma-bearing mice revealed the superiority of IL-2/S4B6 over free IL-2 because: (i) the IL-2 interaction with IL-2Rα^+ endothelial cells was disrupted and vascular leak syndrome was prevented; and (ii) naive IL-2R$\beta\gamma_c^+$ CD8$^+$ T and NK cells were preferentially amplified over IL-2R$\alpha\beta\gamma_c^+$ Tregs. These complexes not only exhibit higher antitumor activity but also show potential synergy with immune checkpoint inhibitors [94, 462, 463]. For instance, in an autochthonous lung adenocarcinoma model, combining IL-2/MAB602 with anti-PD-1 mAb increased CD8$^+$ T cell infiltration in the lung and controlled tumor growth. Even in models resistant to checkpoint inhibitors, such as B16-OVA, combining IL-2/MAB602 with either PD-1 or CTLA-4 pathway blockade could reverse resistance. These effects can be attributed to reinvigorating exhausted intratumoral CD8$^+$ T cells similar to those induced by PD-1 + IL-2 combination therapy in chronic infection. Moreover, IL-2/MAB602 combined with anti-CTLA-4 mAb uniquely rescued NK cell antitumor function by modulating intratumoral Treg cells. This demonstrates that combining IL-2/MAB602 with PD-1 or CTLA-4 pathway blockade operates through different cellular mechanisms, suggesting a path toward the rational design of combinatorial antitumor therapies [462]. In other studies, IL-2/S4B6 treatment prevented lethal toxoplasmosis through IL-12- and IL-18-dependent IFN-γ production by non-CD4 immune cells [464] and significantly reduced viral loads during persistent virus infections [465].

To proceed toward clinical development, Arenas-Ramirez and colleagues [466] developed a mAb to hIL-2, named NARA1, which binds to the CD25-binding epitope in IL-2. This prevents the association of IL-2 with CD25 and forms CD122-biased hIL-2/NARA1 complexes [466]. Compared to unbound hIL-2 and similarly to IL-2/S4B6 complexes, such hIL-2/NARA1 complexes prolong the half-life of hIL-2 and preferentially activate CD122^{high} CD8$^+$ T and NK cells, while reducing the association with CD25-expressing Treg and endothelial cells. This results in enhanced expansion of tumor-specific as well as other CD8$^+$ T cells with robust IFN-γ production and low levels of exhaustion markers (PD-1, LAG-3, TIM-3), leading to superior CD8$^+$ T cell-mediated tumor control in several melanoma mouse models [466].

ANV419, a second-generation IL-2co fusion protein of IL-2 fused to the anti-IL-2 mAb NARA1 [467], has entered Phase I/II clinical testing as a monotherapy or in combination with anti-PD-1 or anti-CTLA-4 mAbs (clinical trials NCT04855929, NCT05578872). First-generation IL-2 complexes, AU-007 and SLC-3010, where IL-2 is non-covalently complexed to specific anti-IL-2 mAbs are also in clinical development (clinical trials NCT05267626, NCT05525247).

I.3.3.2 CD25-biased IL-2co

In contrast to CD122-biased complexes, CD25-biased IL-2co, utilizing mAbs such as mouse JES6-1A12 (IL-2/JES6 henceforth) and human 5344, interact highly selectively with cells expressing high levels of CD25 along with IL-2Rβγ$_c$ [94]. This specificity effectively excludes CD25$^-$ cell populations that do not utilize IL-2/JES6 even if they express both CD122 and CD132, making these complexes highly selective for Treg cells and activated T cells [74].

This selective stimulation has significant implications: expanded Treg cells exhibit at least similar suppressive activity compared to normal Treg cells [468]. The phenotype of expanded Treg cells is characterized by a considerable, albeit transient, increase in molecules critical for their suppressive potential, including CD25, ICOS, CTLA-4, and GITR. Additionally, these IL-2co induce a mild transient rise in other markers like CD44, TGF-β, ICAM-1, and PD-1, typically found on Treg cells. There is also a considerable build-up of IL-10 mRNA production with a respective increase in the suppressive activity *in vitro* and with the same transient character as is seen for the surface molecules [352].

Interestingly, a similar response is observed in recently activated CD8$^+$ T cells, which upon TCR stimulation express CD25, making them receptive to IL-2/JES6. The expansion of these cells can increase their count by more than three orders of magnitude within one week, creating a robust population of memory phenotype CD8$^+$ T cells (CD44^{high}CD122^{high}) capable of executing effector functions upon receiving a TCR signal [469]. Thus, CD25-biased IL-2co are capable of inducing selective expansion of CD25$^+$CD4$^+$ Tregs and recently activated T cells much more efficiently than IL-2 administration alone [74, 94].

Létourneau and colleagues demonstrated that the *in vivo* activity of CD25-biased IL-2co is heavily dependent on the presence of neonatal Fc receptor (FcRn), while the function of CD122-biased IL-2co benefits from a prolonged half-life and reduced interaction with CD25 [463]. It has been observed that depleting CD8$^+$ T and NK cells extends the half-life of CD122-biased IL-2co to approximate that of CD25-biased ones. This suggests that the rapid consumption of IL-2 by dividing MP CD8$^+$ T and NK cells limits the half-life of CD122-biased IL-2co to about 24 h. In contrast, CD25-biased IL-2co selectively binds to a smaller population of CD25-expressing cells, primarily CD25$^+$CD4$^+$ T cells, which results in a lifespan of approximately 72 h. The differential consumption of these IL-2co provides insight into their varying half-lives and FcRn dependency. This is supported by findings that the half-life of CD25-biased IL-2co is significantly shorter in FcRn$^{-/-}$ mice, while the half-life of CD122-biased IL-2co remains largely unchanged. Importantly, FcRn is known to play a crucial role in the serum IgG half-life [470].

These observations underscore the potential of CD25-biased IL-2co as a strategic tool for improving IL-2-based immunotherapies. By mimicking the biological effects of IL-2 monotherapy but at a targeted and lower concentration, these complexes could minimize the

undesirable side effects associated with IL-2. The efficacy of IL-2/JES6 administration has been confirmed in various preclinical models, including experimental autoimmune encephalomyelitis [352], diabetes [357], allergy [471], and solid organ transplantation [357]. Additional studies have shown that IL-2/JES6 treatment can suppress collagen-induced arthritis [472], promote long-term acceptance of islet allografts [352], attenuate atherosclerosis [473], and reduce experimental myasthenia in mice [468], further advocating for its role in treating autoimmune disorders.

Moreover, in a study by Diaz-de-Durana and colleagues [474], IL-2/JES6 treatment was associated with increased pancreatic islet β-cell proliferation, indicating a possible role for IL-2 immunotherapy in β-cell regeneration. However, the specific mechanisms underlying this effect remain unclear, highlighting the need for further investigation into how IL-2/JES6 may contribute to β-cell regeneration.

In preclinical studies, F5111.2, a first-generation clinical-grade pro-Treg anti-IL-2 mAb complexed with rhIL-2, has shown effectiveness in inducing T1D remission in diabetic mice and in reducing the severity of xenogeneic GvHD and EAE [475].

II.   Aims

The aims of this thesis are focused on making progress in the field of immunotherapy by developing and evaluating the biological activities of innovative IL-2-based immunotherapeutics with enhanced therapeutic profiles for the treatment of cancer and autoimmune diseases. Specifically, this research focuses on overcoming the limitations associated with native IL-2 therapy, such as its short half-life and dose-dependent adverse effects, by designing and testing novel IL-2 formulations. Through a combination of molecular engineering and protein chemistry, the thesis is aimed to:

1. **Design and develop novel IL-2 formulations**:
   - **IL-2-poly(HPMA) conjugate**: an IL-2 modified with poly(N-(2-hydroxypropyl)methacrylamide), designed to improve the pharmacokinetic properties and biological activity of IL-2 *in vivo*.
   - **Immunocytokines**:
     1. **scIL-2/S4B6 IC**: a protein chimera where IL-2 is covalently linked to the light chain of the S4B6 mAb via a flexible $(Gly_4Ser)_3$ spacer, designed to increase the biological activity of IL-2 while minimalizing limitations associated with IL-2co (stoichiometry, possible dissociation of IL-2co), and to selectively stimulate CD122^{high} cells.
     2. **JY3 IC**: an engineered IL-2-JES6 protein chimera preserves the unique mechanism of action of CD25-biased IL-2co without the well-known limitations (stoichiometry, possible dissociation of IL-2co), designed to selectively stimulate Treg cell expansion and their suppressive activity.

2. **Evaluate biological activity and therapeutic efficacy**:
   - Conduct comprehensive *in vitro* and *in vivo* assessments to determine the biological activity of the developed IL-2 variants.
   - Test the therapeutic efficacy of these IL-2 formulations in experimental models of vaccination and autoimmune disease, examining their potential to enhance immune responses and control disease progression.

3. **Provide mechanistic insights**:
   - Explore the distinct interactions of IL-2R subunits with IL-2 bound to either S4B6 or JES6-1A12 anti-IL-2 mAbs.
   - Elucidate how these interactions affect the balance between the stimulation of CD122^{high} effector T and NK cells and CD25^{high} Treg cells, contributing to the observed biological activities and therapeutic outcomes.

4. **Address safety concerns of CD25-biased IL-2co**:
   - Investigate the unexpectedly powerful sensitization of mice to LPS-mediated shock and mortality through CD25-biased IL-2co.
   - Elucidate the mechanism of this extraordinarily strong sensitization and identify the key cell subsets as well as the molecular mediators involved.
   -

III. Materials and methods

All further described methods were conducted using murine models. We utilized the following mouse strains: inbred strains C57BL/6 (B6 henceforth), BALB/c; TCR transgenic OT-I and OT-II on B6 background; congenic strain B6.SJL (Ly5.1); athymic CD1 nude (Nu/Nu); mice deficient in particular gene IFN-$\gamma^{-/-}$ (B6 background), and Rag1$^{-/-}$ (BALB/c background). Both male and female mice aged between 8 and 16 weeks were used in the experiments. Age- and sex-matched pairs of animals were used in the experimental groups. All animals were bred in the animal facilities of the Institute of Molecular Biology or the Institute of Physiology under Czech Republic laws. They were housed in individually ventilated cages under specific pathogen-free conditions. Animal protocols were approved by the Czech Academy of Sciences, Czech Republic.

The most common approach of the following studies was the execution of *in vivo* or *ex vivo* experiments, followed by flow cytometry. Other *in vivo* approaches included survival monitoring, body temperature measurements, or assessment of vascular leak syndrome in the lungs. *In vitro* and *ex vivo* assays used during my PhD studies included ELISA, MACS-based cell isolations, proliferation assays *via* [^{3}H]-thymidine incorporation *in vitro* and *via* CTV or CFSE labeling of purified cell subsets *ex vivo*, *in vivo* BrdU incorporation, *ex vivo* detection of intracellular cytokines in immune cells with *in vivo* injection of Brefeldin A. Methods are described in detail within the relevant publications. Methods not included in published papers involve Treg suppression assays *in vitro*, isolation of bone marrow cells, isolation of peritoneal macrophages, and phosphorylated STAT5 staining. Additionally, I optimized within my work the protocols for i) isolation of leukocytes from the liver, lungs, and peritoneal fluid, ii) isolation of cells from bone marrow, and iii) isolation of monocytes and dendritic cells from the spleen.

The methods described herein enabled us to obtain some of the data presented in the attached publications, but these methods are not described in sufficient detail within those papers. While some experiments did not yield significant results, others contributed to my participation in a manuscript entitled "Temporal optimization of CD25-biased IL-2 agonists and immune checkpoint blockade leads to synergistic anti-cancer activity despite robust regulatory T cell expansion" currently prepared for submission. This manuscript describes a key role of timing for the antitumor efficacy of immune checkpoint blockade combined with IL-2 agonist with selective stimulatory activity for CD25$^+$ T cells and the ability of this IL-2 agonist to overcome Treg cell-mediated suppression of CD8$^+$ T cells.

Isolation of bone marrow cells

Mice were sacrificed by cervical dislocation, and the abdomen and hind legs were washed with 70% ethanol. An incision was made along the abdominal midline, and the skin was peeled outward to expose the hind legs. All muscle tissue was removed from the femur using scissors and cleaned with sterile gauze sprayed with 70% ethanol. Both femur ends were cut off. A sterile 18G needle was used to pierce a hole in the bottom of a sterile 0.5 mL Eppendorf tube. The 0.5 mL tube was placed into a 1.5 mL tube (with its cap removed) containing 0.5 mL of RPMI media supplemented with 20 mM HEPES. The bones were placed into the 0.5 mL tube. The Eppendorf tubes were centrifuged (500 x g, 15 min). Cells in the 1.5

mL tube were passed through a 70 μm cell strainer and washed with a complete RPMI medium. The cells were counted and plated in a complete RPMI media.

Isolation of Liver Leukocytes

Mice were sacrificed by cervical dislocation, and the skin was washed using 70% ethanol. An incision was made along the abdominal midline, and the skin was peeled outward to expose the peritoneum, which was then incised. The liver, excluding the gall bladder, was aseptically dissected and placed into a 60 mm Petri dish containing 6 mL of HANKS buffer. The liver tissue was homogenized using the plunger of a 5 ml syringe and cell strainer (70 μm) mesh. The resulting single-cell suspension was filtered through a sterile cell strainer into a 50 mL conical tube. This suspension was then transferred to a 15 mL conical tube, adding 2 mL of HANKS buffer to rinse the 50 mL tube, making the total volume 8 mL. Subsequently, 4.5 mL of isotonic Percoll and 125 μL of heparin were added to each 15 mL tube, achieving a final Percoll concentration of 33 %. The tubes were centrifuged for 20 min at 400 x g at room temperature. The supernatant, containing parenchymal cells, was carefully aspirated, leaving a pellet composed of red blood cells (RBCs) and leukocytes. These cells were washed with 12 mL HANKS buffer and centrifuged at 226 x g for 5 min at 4°C. RBCs were lysed using 1X ACK lysing buffer (5 mL/liver) and incubated at room temperature for 10 min. Lysis was stopped by adding HANKS buffer containing 5 % FTS, followed by centrifugation at 226 x g for 5 min at 4°C. After aspirating the supernatant, the pellet was resuspended in 1-10 ml of RPMI medium. Finally, the cells were counted and analyzed using flow cytometry.

Isolation of lymphocytes from lungs

Mice were sacrificed by cervical dislocation, and the skin was washed using 70% ethanol. An incision was made along the abdominal midline, and the skin was peeled outward to expose the peritoneum, which was then incised. Lungs were aseptically dissected and placed into a 60 mm Petri dish containing 6 mL of HANKS buffer. The lungs were cut into small pieces (~ 3 mm) and placed in MACS C tubes containing up to 5 mL of collagenase solution with 1 mg/ml Collagenase IV. GentleMACS program LUNGS 1.1 was applied followed by incubation at 37°C for 30 min. Collagenase IV was stopped by adding 1 mL of 50 mM EDTA (pH 7) to each tube, and the mixture was left for 5 min. Subsequently, the GentleMACS program LUNGS 2.1 was applied. The homogenized tissue was then strained through a 70 μm cell strainer. Cells were spun for 10 min at 145 x g at 20°C and the supernatant was discarded. ACK Lysing buffer, approximately 2-3 mL per lung, was added to each sample and incubated for 10 min to lyse RBC. Lysis was stopped by adding a 10 times bigger volume of FACS buffer. Cells were spun for 10 min at 145 x g at 4°C and the supernatant was discarded. Finally, 0.5-1 mL of the appropriate buffer was added to each tube to resuspend the cells for further analysis.

Isolation of peritoneal macrophages

The mice were euthanized, sprayed with 70% ethanol, and mounted on its back on the styrofoam block. An incision was made along the abdominal midline, and the skin was peeled outward to expose the peritoneum. 5 mL ice-cold PBS (with 3 % FBS) was injected into the peritoneal cavity using a 27G needle. The needle was pushed slowly into the peritoneum, being careful not to puncture any organs. After injection, the peritoneum was gently massaged to

dislodge any attached cells into the PBS solution. A 25G needle, bevel up, attached to a 5 ml syringe, was inserted into the peritoneum, and the fluid was collected while moving the tip of the needle gently to avoid clogging by fat tissue or other organs. As much fluid as possible was collected and deposited into tubes kept on ice after removing the needle from the syringe. An incision was made in the inner skin of the peritoneum, and while holding up the skin with forceps, a plastic Pasteur pipette was used to collect the remaining fluid from the cavity. The sample was discarded if visible blood contamination was detected. The collected cell suspension was spun at 226 x g for 8 min and the supernatant was discarded. The cells were resuspended in the desired media or PBS.

Treg suppression assay

Round-bottom 96-well plates were coated with either αCD3 mAb (10 μg/ml) alone or in combination with αCD28 mAb (10 μg/ml). The plates were incubated at 37°C for 3 h and then thoroughly washed. B6 mice were euthanized, and their skin was washed with 70% ethanol. An incision was made along the abdominal midline, and the skin was peeled outward to expose the peritoneum. Single-cell suspensions were prepared from harvested lymph nodes (inguinal, axillary, mandibular, brachial, mesenteric, and lumbar) and spleens. Tregs (CD4$^+$CD25$^+$) and Tconv (CD4$^+$ or CD8$^+$ T cells with naïve phenotype) were isolated using respective MACS kits on a MACS separator. The cells were counted, and their numbers were adjusted in a T-cell culture medium (complete RPMI 1640 supplemented with antibiotics, 2-Mercaptoethanol, and HEPES). Tregs and either naïve CD4$^+$ or CD8$^+$ T cells were then co-cultured at various ratios in medium only, with IL-2 or IL-2/JES6. The plates were incubated at 37°C in 5% CO$_2$ for 72 h. Plates were pulsed with 0.1 μCi [^{3}H]-thymidine/well for the last 16 h of incubation. The cultures were then harvested using a commercial cell harvester and counts per minute were determined using a plastic scintillator and beta counter. Alternatively, naïve CD4$^+$ or CD8$^+$ T cells were stained with CTV before the assay setup and analyzed by flow cytometry after 72 h of co-culture.

Phosphorylated STAT5 staining within the cells by the use of methanol permeabilization

Initially, the staining of cells for surface antigens was performed as described in publications. Then, treated and untreated cells were fixed by adding 16% formaldehyde directly into the culture medium to obtain a final concentration of 1.5% formaldehyde. Cells were incubated in fixative for 10 min at room temperature and pelleted. The cells were then permeabilized by resuspending with vigorous vortexing in 500 μl ice-cold MeOH per 10^6 cells and incubated at 4°C for 20 min. Cells were washed twice in staining media (PBS containing 1% BSA) and then resuspended in staining media at 0.5-1 × 10^6 cells per 100 μl. The anti-phosphorylated STAT5 (pY694)-PE antibody was diluted according to the manufacturer's recommendation. The volume in each tube was normalized using staining media so that the final staining volume was 100 μL. The antibody master mix was added to each tube, and the contents were mixed by pipetting up and down. The tubes were incubated for 30 min at room temperature. The cells were thoroughly washed as described above and analyzed by flow cytometry.

IV. Results

The thesis is based on the following publications:

IV.1   Tomala J., Kovarova J., Kabesova M., **Votavova P.**, Chmelova H., Dvorakova B., Rihova B., Kovar M. **Chimera of IL-2 linked to light chain of anti-IL-2 mAb mimics IL-2/anti-IL-2 mAb complexes both structurally and functionally.** ACS Chem Biol. 2013; 17;8(5):871-6. ($IF_{2013} = 5.356$)

IV.2   **Votavova P.**, Tomala J., Subr V., Strohalm J., Ulbrich K., Rihova B., Kovar M.: **Novel IL-2-Poly(HPMA)Nanoconjugate Based Immunotherapy**. J Biomed Nanotechnol. 2015; 11(9):1662-73. ($IF_{2015} = 3.929$)

IV.3   Spangler J.B., Tomala J., Luca V.C., Jude K.M., Dong S., Ring A.M., **Votavova P.**, Pepper M., Kovar M., Garcia K.C.: **Antibodies to Interleukin-2 elicit selective T cell subsets potentiation through distinct conformational mechanisms**. Immunity 2015; 42(5):815-25. ($IF_{2015} = 24.082$)

IV.4   Spangler J.B., Trotta E., Tomala J., Peck A., Young T.A., Savvides C.S., Silveria S, **Votavova P.**, Salafsky J., Pande V.J., Kovar M, Bluestone J.A., Garcia K.C.: **Engineering a single-agent cytokine-antibody fusion that selectively expands regulatory T cells for autoimmune disease therapy**. J Immunol. 2018; 201(7): 2094-2106. ($IF_{2018} = 4.718$)

IV.5   Tomala J., **Weberova P.**, Tomalova B., Jiraskova Zakostelska Z., Sivak L., Kovarova J., Kovar M.: **IL-2/JES6-1 mAb complexes dramatically increase sensitivity to LPS through IFN-γ production by CD25$^+$Foxp3$^-$ T cells.** eLife 2021; 10:e62432. (IF_{2021} = 8,713)

Other impacted publications (not included):

Votavova P., Tomala J., Kovar M.: **Increasing the biological activity of IL-2 and IL-15 through complexing with anti-IL-2 mAbs and IL-15Rα-Fc chimera.** Immunol Lett. 2014; 159(1-2):1-10. ($IF_{2014} = 2.512$)

I confirm that Petra Weberová, the author of this thesis, has contributed significantly to the publications listed above. P. Weberová conducted most of the experimental work and significantly contributed to the manuscript preparation in the case of her first-author publication.

RNDr. Marek Kovář, Ph.D.

IV.1   Chimera of IL-2 linked to light chain of anti-IL-2 mAb mimics IL-2/anti-IL-2 mAb complexes both structurally and functionally

Previous studies have demonstrated that IL-2/anti-IL-2 mAb IL-2co exhibits significantly higher biological activity than free IL-2 *in vivo*. Building upon this, we engineered a chimeric fusion protein that consists of IL-2 linked to the light chain of the anti-IL-2 mAb S4B6 through a flexible oligopeptide spacer $(Gly_4Ser)_3$, thus creating an IC. Such IC effectively replicates the structure and function of the IL-2/S4B6 IL-2co while overcoming its inherent limitations, such as the potential excess of IL-2 or anti-IL-2 mAb within the prepared IL-2co and the possibility of dissociation to free IL-2 and antiIL-2 mAb, particularly at low concentrations. We provided evidence that our IC maintains intramolecular interaction between IL-2 and the S4B6 mAb binding site, similar to the native IL-2co. We also proved that our IC stimulates the proliferation of activated OT-I $CD8^+$ T cells comparably to IL-2/S4B6 IL-2co *in vitro*. Furthermore, *in vivo* studies showed that the IC induces a more pronounced expansion of CFSE-labeled OT-I $CD8^+$ T cells activated by a low dose of SIINFEKL peptide than the IL-2/S4B6 IL-2co, highlighting its superior stimulatory activity.

P. Weberová's contribution to this publication:

I was involved in ELISA assays, *in vitro* cultures, and *in vivo* experiments with CFSE-labeled OT-I $CD8^+$ cells, as well as in data acquisition and analysis. I also participated in the preparation of the manuscript. Overall contribution ~ 15%.

Chimera of IL-2 Linked to Light Chain of anti-IL-2 mAb Mimics IL-2/anti-IL-2 mAb Complexes Both Structurally and Functionally

Jakub Tomala, Jirina Kovarova, Martina Kabesova, Petra Votavova, Helena Chmelova, Barbora Dvorakova, Blanka Rihova, and Marek Kovar*

Laboratory of Tumor Immunology, Institute of Microbiology of Academy of Sciences of the Czech Republic, v.v.i., Prague, Czech Republic

S *Supporting Information*

ABSTRACT: IL-2/anti-IL-2 mAb immunocomplexes were described to have dramatically higher activity than free IL-2 *in vivo*. We designed protein chimera consisting of IL-2 linked to light chain of anti-IL-2 mAb S4B6 through flexible oligopeptide spacer $(Gly_4Ser)_3$. This protein chimera mimics the structure of IL-2/S4B6 mAb immunocomplexes but eliminates general disadvantages of immunocomplexes like possible excess of either IL-2 or anti-IL-2 mAb and their dissociation to antibody and IL-2 at low concentrations. This novel kind of protein chimera is characterized by an intramolecular interaction between IL-2 and binding site of S4B6 mAb similarly as in IL-2/S4B6 mAb immunocomplexes. Our protein chimera has biological activity comparable to IL-2/S4B6 mAb immunocomplexes *in vitro*, as shown by stimulation of proliferation of purified and activated OT-I $CD8^+$ T cells. The protein chimera exerts higher stimulatory activity to drive expansion of purified CFSE-labeled OT-I $CD8^+$ T cells activated by an injection of a low dose of SIINFEKL peptide than IL-2/S4B6 mAb immunocomplexes *in vivo*.
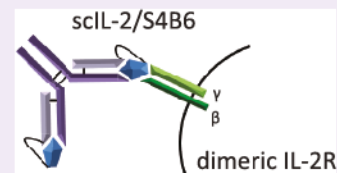
The *in vivo* biological activity of IL-2 can be dramatically increased by complexing IL-2 with certain anti-IL-2 mAb.[1] Moreover, these IL-2 immunocomplexes have selective stimulatory activity depending on the clone of anti-IL-2 mAb used (Supplementary Figure 1). IL-2/S4B6 mAb immunocomplexes (henceforth, IL-2ic) are highly stimulatory for memory $CD8^+$ T and NK cells ($CD122^{high}$ populations).[1,2] They have also moderate stimulatory activity for T_{reg} cells.[3] Conversely, IL-2/JES6.1 mAb immunocomplexes have no effect on $CD122^{high}$ cell populations, but they considerably expand T_{reg} cells ($CD25^{high}$ population).[1,4] Interestingly, both IL-2 immunocomplexes are very potent in expanding recently activated naïve $CD8^+$ T cells *in vivo*,[5] and IL-2ic possess significant antitumor activity.[2,3]

IL-2ic are prepared simply by mixing rmIL-2 and S4B6 mAb at molar ratio 2:1 (Figure 1A). In theory, this should lead to formation of IL-2/antibody complexes without either protein left (omitting the K_d). However, it is likely that one protein will be in small excess since it is very hard to exactly quantify and handle S4B6 mAb and IL-2, especially when small batches of IL-2ic are prepared (typically, 10−100 μg of IL-2 is complexed for laboratory experiments). In order to make a more defined structure, we designed chimeric protein of IL-2 and S4B6 mAb (henceforth, scIL-2/S4B6) where the C-terminus of IL-2 is linked via a flexible oligopeptide spacer to N-terminus of light chain of S4B6 mAb (Figure 1B). IL-2 could not dissociate far away from scIL-2/S4B6 like from IL-2ic where the interaction between IL-2 and binding site of S4B6 mAb is interrupted (Figure 1A,B). Instead, IL-2 stays in the vicinity of the binding site of S4B6 mAb (the length of the spacer defines maximal distance), and thereby, it is continuously available for reassociation (Figure 1B). Although this difference between

scIL-2/S4B6 and IL-2ic does not have probably any measurable effect on biological activity at sufficiently high and stable concentrations, it might play a significant role at low and gradually decreasing concentrations, and thus, it could be the factor making scIL-2/S4B6 superior to IL-2ic in certain situations, for example, *in vivo*. The structure of scIL-2/S4B6 is a novel one since fusion protein of cytokine linked to N-terminus of light chain of respective anticytokine mAb has not been, to our best knowledge, described so far. Chimeras where IL-2 was linked to the C-terminus of the heavy chain of mAb (Figure 1C) recognizing tumor antigens were reported.[6−8] Nevertheless, these protein chimeras were designed to deliver IL-2 into tumor microenvironment and thereby induce antitumor immunity. IL-2 is linked to mAb molecule, but at very different sites, and there is not any binding interaction between IL-2 and antibody. These chimeras thus do not mimic cytokine/anticytokine mAb immunocomplexes at all. IL-2 was also linked to the Fc part of the antibody (Figure 1D), the structure known as immunocytokine, with the aim to prolong the half-life of the cytokine in circulation.[9,10]

The aim of this study was to design and produce scIL-2/S4B6 as a recombinant protein. We wanted also to characterize the protein we produced and to verify whether it contains antibody and IL-2 within one protein molecule and possess predicted molecular weight both in reducing and nonreducing conditions. Further characterization of our protein chimera was focused on proving that IL-2 in this chimera interacts with the binding site of antibody in cis and thus showing that this
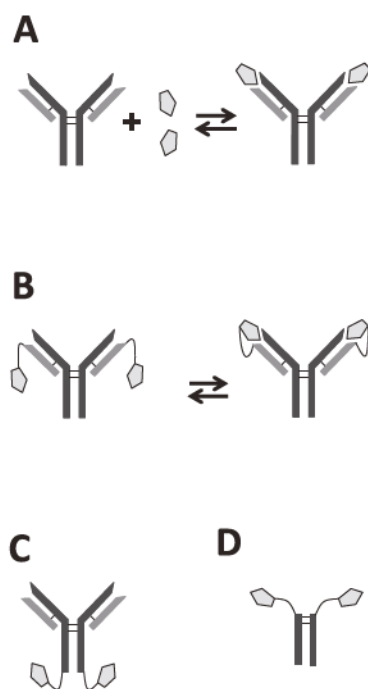
Figure 1. Schematic chart showing approaches of how to increase the biological activity of IL-2 *in vivo*. (A) IL-2 and anti-IL-2 mAb form immunocomplexes, but these can also dissociate back to free IL-2 and anti-IL-2 mAb. (B) Protein chimera mimicking IL-2 immunocomplexes. IL-2 can dissociate from its interaction with antibody; however, these two structures are linked through a short flexible peptide linker, and thus, it remains close to the binding site of the antibody, increasing the probability of reassociation. (C) IL-2 fused to the C-terminal part of heavy chains of selected mAb. (D) IL-2 linked to the Fc-part of the antibody, a structure also called immunocytokine.

chimera structurally mimics IL-2/S4B6 mAb immunocomplexes. Finally, we decided to determine the biological activity of our protein chimera and compare it with biological activity of IL-2/S4B6 mAb immunocomplexes both *in vitro* and *in vivo* and thus confirm that it mimics IL-2/S4B6 mAb immunocomplexes also functionally.

Flexible oligopeptide linker of 15 amino acids $(Gly_4Ser)_3$ has been used to link C-terminal amino acid of IL-2 to N-terminal amino acid of κ light chain of S4B6 mAb. Sequences encoding this fusion polypeptide and heavy chain of S4B6 mAb were cloned separately in two distinct expression vectors (Supplementary Figure 2) and could be seen in Supplementary Figure 3. Cotransfection of CHO-S cells with both prepared expression vectors should lead to production of scIL-2/S4B6. Indeed, we detected a protein in the supernatant of cotransfected CHO-S cells by our customized sandwich ELISA calibrated with IL-2ic (Figure 2A), which reacted both with antirat IgG2a mAb and anti-rκ light chain mAb. Thus, we decided to designate this produced protein as scIL-2/S4B6, to further characterize it and to confirm its structure and features. The production of scIL-2/S4B6 by transiently cotransfected CHO-S cells was considerably increased by valproic acid,[11] approximately from 25 to 80 ng/mL of IL-2 equivalent (Figure 2B). We also established stable transfected CHO-S clone entitled 104/53 after two runs of single cell cloning and selection process, which continuously produce scIL-2/S4B6 (Supplementary Figure 4). However, the production of chimeric protein scIL-2/S4B6 by 104/53 clone was quite low (about 5−10 ng/mL), and we thus decided to use mainly
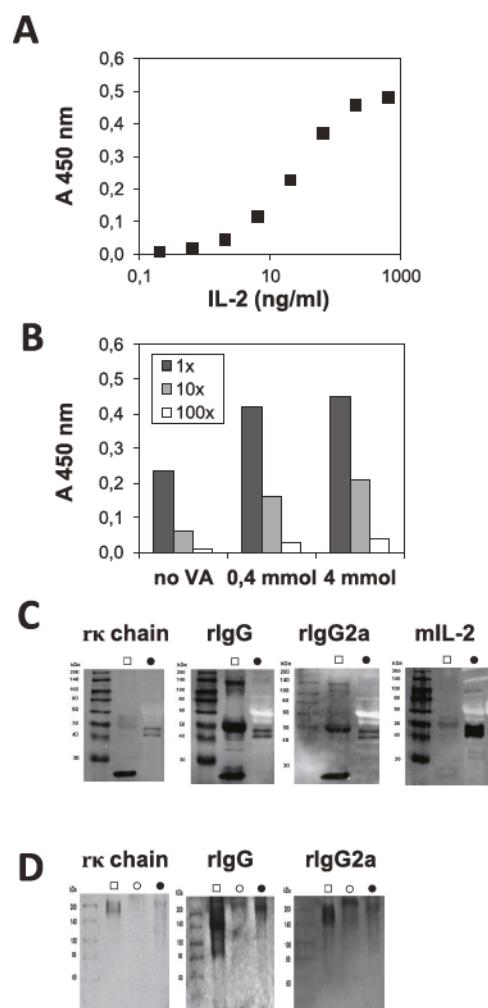

Figure 2. *In vitro* characterization of supernatant of CHO-S cells cotransfected with both expression vectors identifies a protein with biochemical features predicted for scIL-2/S4B6. (A) IL-2 was mixed with S4B6 mAb at a molar ratio 2:1, and resultant IL-2ic were used to calibrate sandwich ELISA for detection of scIL-2/S4B6. (B) Supernatant of CHO-S cells after cotransfection and 5 day cultivation either without (no VA) or with 0.4 or 4 mmol valproic acid (VA) were analyzed by ELISA calibrated as in panel A either undiluted or 10 times and 100 times diluted (black, gray, and empty bars, respectively). (C) Western blot of S4B6 mAb (●) and 50 times concentrated and extensively dialyzed supernatant of CHO-S cells cotransfected with both expression vectors (□). The specificity of each antibody used for detection is shown above each individual SDS-PAGE gel. Gels were run under reductive conditions. (D) Western blot of S4B6 mAb (●), 25 times concentrated and extensively dialyzed supernatant of CHO-S cells cotransfected with both expression vectors (○), and 50 times concentrated and extensively dialyzed supernatant of clone 104/53 (□). The specificity of each antibody used for detection is shown above each individual SDS-PAGE gel. Gels were run under nonreductive conditions.

transient transfection as the source of scIL-2/S4B6. Next, we analyzed our produced scIL-2/S4B6 by Western blot. Supernatants were concentrated 20−40 times on 100 kDa membranes, extensively dialyzed against PBS and ran together with S4B6 mAb on SDS-PAGE under reductive (Figure 2C) and nonreductive conditions (Figure 2D). Nonreduced S4B6 mAb and scIL-2/S4B6 gave bands of predicted M_w 150 and 190 kDa, respectively, when detected either with anti-rIgG2a mAb or anti-rIgG polyclonal antibody. The same antibodies under

reductive condition detected S4B6 mAb as 50 and 25 kDa bands corresponding to heavy and light chains, respectively, and scIL-2/S4B6 as 50 and 45 kDa bands corresponding to heavy and IL-2-linker-light chains, respectively. Anti-rκ chain mAb under reductive condition detected S4B6 mAb as single band of 25 kDa and scIL-2/S4B6 as 45 kDa band. Unexpectedly, anti-rκ chain mAb also detected a 50 kDa band. Notably, anti-mIL-2 mAb under reductive conditions gave no signal in the case of S4B6 mAb, but a nice 45 kDa band was detected in the case of scIL-2/S4B6. All these data collectively show that the scIL-2/S4B6 we produce by cotransfection of CHO-S cells with both prepared expression plasmids has M_w of about 200 kDa and contains mIL-2, rκ light chain, and rIgG2a structures. Further, detection with anti-mIL-2 mAb and anti-rκ light chain mAb under reductive conditions provides the identical band with M_w of neither of these two proteins but with M_w corresponding to the sum of M_w of these two proteins. Since the produced scIL-2/S4B6 has all important features as theoretically predicted, we thus conclude that this protein is indeed scIL-2/S4B6 as we designed it.

Further, we decided to prove that IL-2 is bound to the binding site of S4B6 mAb in scIL-2/S4B6. Thus, we modified our sandwich ELISA by using anti-mIL-2 mAb instead of anti-rκ light chain mAb as the detection antibody. We used biotinylated S4B6, JES6.1, JES6.5 anti-mIL-2 mAbs, and control anti-IFNγ mAb as detection antibodies. Antirat IgG2a mAb was still used as catching antibody. When IL-2ic were analyzed in such ELISA, the only detection mAb that provided positive signal was JES6.1 (Figure 3A). It seems that IL-2 is significantly washing out from IL-2ic during numerous washing steps in the ELISA since only relatively high concentrations of IL-2ic (at least 100 ng/mL) provided reasonably strong signal. IL-2ic are not washed out from anti-IgG2a-coated wells since the same catching antibody is used for detection of produced scIL-2/S4B6 where we are able to detect much lower concentrations of IL-2ic (1 ng/mL being usually the detection limit). Next, scIL-2/S4B6 was bound to the wells coated with anti-rIgG2a mAb and detected by selected mAb (Figure 3B). JES6.1 mAb provided the highest signal, which is in concordance with the fact that this mAb recognizes the epitope located oppositely to the S4B6 mAb epitope. However, S4B6 mAb provided slightly higher signal than control anti-mIFN-γ mAb. This shows that probably a very little fraction of scIL-2/S4B6 is in conformation where IL-2 is available to bind S4B6 in trans. A slightly higher signal obtained with JES6.5H4 mAb reflects that JES6.5H4 mAb epitope is close, but not identical to, S4B6 mAb epitope, and thereby, these two mAbs significantly compete with each other in binding to IL-2. We also show that neither S4B6 mAb nor JES6.5 mAb compete with binding of JES6.1 mAb to IL-2 in IL-2ic (Figure 3C) and in scIL-2/S4B6 (Figure 3D).

Finally, we determined the biological activity of scIL-2/S4B6 *in vitro* and *in vivo*. We found that scIL-2/S4B6 added in titrated doses to naive CD8^{+} T cells activated via TCR signal potently stimulated their proliferation *in vitro*. The maximal proliferation activity reached by scIL-2/S4B6 was the same as that reached by IL-2ic (Figure 4A,B). Interestingly, calculated concentrations of scIL-2/S4B6 in supernatants on the basis of this assay corresponded very well to those determined by sandwich ELISA calibrated with IL-2ic as shown in Figure 2A. Thus, it seems that scIL-2/S4B6 and IL-2ic possess very similar biological activity *in vitro* (Figure 4C). To assess the biological activity of scIL-2/S4B6 *in vivo*, we employed adoptive transfer of CFSE-labeled OT-I CD8^{+} T cells into congeneic CD45.1
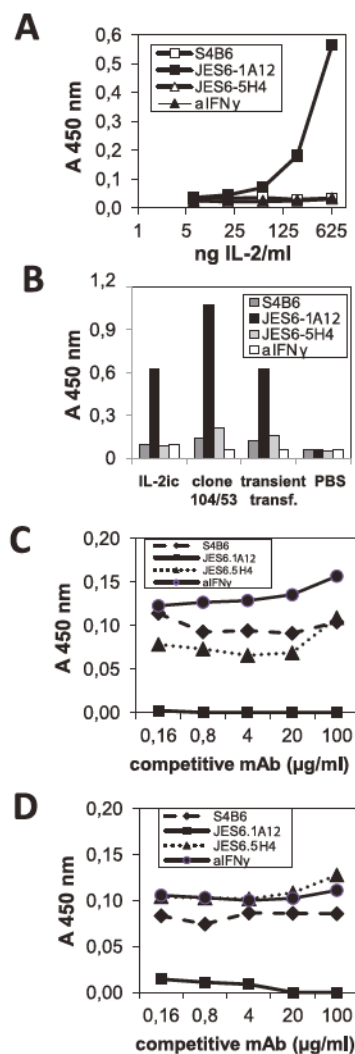
Figure 3. IL-2 moiety binds to the binding site of antibody moiety in scIL-2/S4B6 chimera, which structurally resembles IL-2/anti-IL-2 S4B6 mAb immunocomplexes. (A) IL-2ic were analyzed in a wide range of concentrations by ELISA with anti-rIgG2a mAb as coating antibody and S4B6, JES6.1, JES6.5H4, and anti-IFN-γ as detection mAbs. (B) IL-2ic, 50 times concentrated supernatant of clone 104/53 and 25 times concentrated supernatant from transient transfection were analyzed by ELISA with anti-rIgG2a mAb as coating antibody and with S4B6, JES6.1, JES6.5H4, and anti-IFN-γ as detection mAbs (dark gray, black, pale gray, and empty bars, respectively). The background of the assay is shown for each detection mAb by the use of PBS. (C) IL-2ic were analyzed by ELISA with anti-rIgG2a mAb as the coating antibody and with JES6.1 as the detection mAb. Detection with JES6.1 mAb was proceeded by incubation with S4B6, JES6.1, JES6.5H4, and anti-IFN-γ mAbs as competitive antibodies. (D) The same assay as that in panel C, but 25 times concentrated supernatant from transient transfection was used.

mice. Transferred T cells were activated by injection of a low dose of SIINFEKL peptide, and either IL-2ic or scIL-2/S4B6 were used to stimulate their proliferation and expansion (Figure 4D). The same supernatant as above was used as a source of scIL-2/S4B6, and the dose was determined by both ELISA and *in vitro* proliferation assay. Surprisingly, the results show that, unlike *in vitro*, biological activity of scIL-2/S4B6 is higher than IL-2ic *in vivo* (Figure 4D).
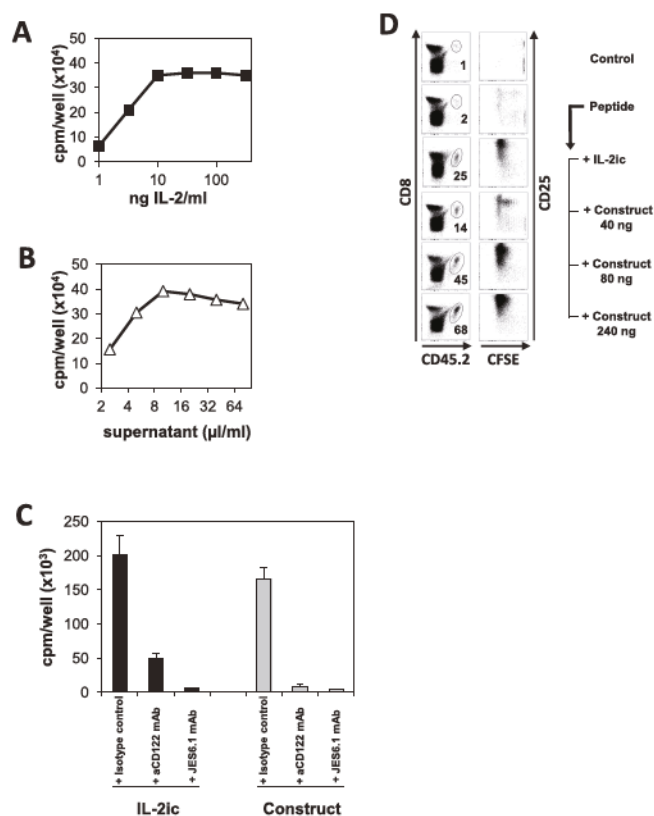
Figure 4. Biological activity of scIL-2/S4B6 mimicking IL-2/S4B6 immunocomplexes *in vitro* and *in vivo*. (A) CD8$^+$ T cells purified from the spleen of OT-I transgeneic mice were cultured with 50 nM SIINFEKL peptide and different concentrations of IL-2ic. CTLA-4-Ig protein chimera (2.5 μg/mL) was added to cultivated T cells to lower proliferation background. Proliferation was determined by [^{3}H]-thymidine incorporation assay. (B) The same assay as that in panel A, but 25 times concentrated supernatant from transient transfection was used. (C) CD8$^+$ T cells purified from the spleen of OT-I trangeneic mice were cultured with 50 nM SIINFEKL peptide and either with IL-2ic or with supernatant from transient transfection. Control, anti-CD122, and anti-IL-2 JES6.1 mAbs were added to cells on the beginning of cultivation. CTLA-4-Ig protein chimera (2.5 μg/mL) was added to cultivated T cells to lower proliferation background. Proliferation was determined by [^{3}H]-thymidine incorporation assay. (D) CD8$^+$ T cells purified from spleen of OT-I transgeneic mice were labeled with CFSE and adoptively transferred into Ly5.1 mice. Next day, all mice except controls were i.p. injected with 2 nmol SIINFEKL peptide. IL-2ic and scIL-2/S4B6 were injected i.p. the same day and then 24 and 48 h later. Spleen cells were analyzed by flow cytometry one day after the last dose. Numbers show expansion of transferred CD8$^+$ T cells relative to control.

■ METHODS

Animals and Cell Lines. Transgenic OT-I, congeneic B6.SJL (Ly5.1), and C57BL/6 mice were bred and kept at the GMO facility of the Institute of Molecular Genetics of ASCR, v.v.i. Mice were used at 9 to 15 weeks of age. All experiments were approved by the Animal Welfare Committee at the Institute of Microbiology of ASCR, v.v.i. CHO-S cell line was purchased from Invitrogen.

Monoclonal Antibodies and Other Reagents. The following antimouse mAbs were used for experiments: aCD8-PerCP-Cy5.5, aCD45.2-APC, and aCD25-PE (eBioscience) for flow cytometry analysis; funtional grade aIFN-γ, aCD122, anti-IL-2 mAb JES6.1-A12, anti-IL-2 mAb JES6.1.5H4 (eBioscience), anti-IL-2 mAb JES6.5H4-biotin, and aIFN-γ-biotin (eBioscience) for ELISA, proliferation assays, and Western blot. Unconjugated anti-IL-2 mAb S4B6 was purchased from Bioport. The following antirat mAbs were used for Western blot: anti-κ-biotin, anti-IgG2a (BD Biosciences), and polyclonal anti-IgG-biotin (eBioscience). CTLA-4Ig fusion protein chimera was purchased from BD Biosciences. Antibiotin-HRP and anti-IgG-HRP conjugates were purchased from Cell Signaling Tech. Extravidin−peroxidase conjugate was purchased from Sigma.

Biotinylation. Anti-IL-2 mAb JES6.1-A12 and S4B6 were biotinylated by EZ-Link Sulfo-NHS-LC-Biotin (Pierce) according to the standard protocol.

Preparation of Expression Vectors. Total RNA was isolated from *Mus musculus* C57BL/6 spleen cells stimulated for 24 h with aCD3 (5 μg/mL) and aCD28 (20 μg/mL) mAb and then from *Rattus rattus* S4B6 hybridoma cells using TRIZOL reagent (Gibco) according to the manufacturer protocol. DNaseI-treated total RNA (2 μg) were reverse-transcribed using oligo(dT)$_{12-18}$ and Superscript II Reverse Transcriptase (Invitrogen) to cDNA and then used in PCR. Mouse IL-2 cDNA was amplified by primers *F-IL2/R-IL2-SPACER*, and light rκ chain cDNA was amplified by primers *VKB1*-SPACER/*VKF MYS* using Platinum Taq DNA Polymerase (Invitrogen), resulting in specific PCR products (Table 1). Both products were digested by *Bam*HI (Fermentas) and ligated in one fused fragment linked by a 30bp spacer. The fragment was digested by *Kpn*I/*Xho*I and cloned into *Kpn*I/*Xho*I restriction site of pcDNA3.1(+)/HYGRO vector, which was then transformed into TOP 10F′cells. Rat heavy chain cDNA was amplified similarly to the light chain, yet by primers *VHB1NEW RF/VHFRAT2A*. The PCR product was digested with *Hind*III/*Kpn*I and then ligated into *Hind*III/*Kpn*I digested pSecTagA/ZEO, which was then transformed into TOP 10F′cells.

Transient Expression and Production of scIL-2/S4B6. Transient expression was carried out in CHO-S cells and mediated by FuGene transfecting reagent (Promega) according to the standard protocol in OptiMEM protein-free medium (Invitrogen). Cells were cotransfected by two expression vectors containing IL-2-κ light chain sequence and heavy chain, respectively. Transfectomas were grown in OptiMEM protein-free medium with desired concentration of valproic acid (R&D Systems), and supernatants were collected, dialyzed against PBS, concentrated, and stored in −70 °C.

Establishing of Stable Transfectant. Stable transfectant clone 104/53 was made using the same reagents, media, and expression vectors as in the transient transfection. CHO-S cells were first transfected by an expression vector containing IL-2-κ light chain sequence with Hygromycin B selection cassette, followed by cotransfection with an expression vector containing a heavy chain sequence with Zeocin selection cassette. Stable clone was obtained out of two subsequent single cell cloning and selection cycles with rising concentrations of Hygromycin B (10−75 μg/mL) and Zeocin (5−25

Table 1

primer	nucleotide sequence (5′−3′)	purpose	restriction site
F-IL2	GCAA*GGTACC*ATGTACAGCATGCAGCTCGC	IL-2	*Kpn*I
R-IL2-*SPACER*	CA*GGATCC*TCCTCCTCCAGAACCTCCGCCACCTTGAGGGCTTGTTGAG		*Bam*HI
VKB1-*SPACER*	GT*GGATCC*GGTGGCGGAGGTTCTGACATYCAGRTGACCCAGTCTC	light κ chain	*Bam*HI
VKF MYS	GCCA*CTCGAG*ctaACACTCATTCCTGTTG		*Xho*I
VHB1NEW RF	GTGT*AAGCTT*CRAGGTGCARCTGCAGGAGTCTG	heavy chain	*Hind*III
VHFRAT2A	GCA*GGTACC*TCATTTACCAGGAGAGTGGGAG		*Kpn*I

$\mu g/mL$). Clones were screened for production of scIL-2/S4B6 by ELISA, cryopreserved, and stored in −152 °C.

IL-2/S4B6 Immunocomplexes. These immunocomplexes[1,5] were prepared by adding rmIL-2 (Prospec) into a solution of anti-IL-2 mAb S4B6 (both reagents in PBS) at a molar ratio 2:1. After a 15 min incubation at RT, the immunocomplexes were diluted with PBS to the desired concentration.

Surface Staining and Flow Cytometry Analysis. A single cell suspension was prepared from harvested spleens of OT-I mice by GentleMACS Dissociator (Miltenyi Biotech). After RBC lysis, cells were resuspended in FACS buffer (PBS, 2% FCS, and 2 mmol EDTA), blocked by 10% mouse serum for 30 min on ice, and stained with fluorochrome-labeled mAbs for 30 min on ice in dark. Cells were washed twice after each step in FACS buffer and fixed in 4% paraformaldehyde prior to analysis. Flow cytometric analysis was performed on LSRII (BD Biosciences) and data were analyzed using FlowJo software (Tree Star).

ELISA. NUNC MaxiSorp 96-well flat-bottom plates were plated with 5 $\mu g/mL$ anti-IgG2a mAb and incubated overnight in 4 °C. Wells were rinsed and then blocked with 1% gelatin in PBS (2 h, RT), and samples were plated in a desired dilution or concentration, alone or in the presence of competitive mAbs, along with blank (PBS) and titrated IL-2/S4B6 as standard (2 h, RT, agitated). After rinsing, detection antibodies were added in dilution buffer (PBS, 0.5% gelatin, 3% PEG 6000, and 0.1% Tween 20) in a concentration of 0.05 $\mu g/mL$ (1.5 h, RT), followed by rinsing and incubation with extravidin–peroxidase conjugate (1 h, RT). After the last rinse, a plate was developed using 3,3′,5,5′-tetramethylbenzidine (Sigma) for 10 min maximum, stopped by 2 M H_2SO_4, and analyzed on Tecan Rainbow ELISA reader and BIOLISA software (Tecan).

Proliferation Assay *in Vitro*. A single cell suspension was prepared from the spleen of OT-I mice by GentleMACS Dissociator (Miltenyi Biotech). After RBC lysis, cells were washed, centrifuged for 5 min at 300g, resuspended in fresh culture medium, and seeded into Nunc 96-well flat-bottom plates in 0.2 mL volume and 5×10^4 cells/mL density. SIINFEKL peptide (50 nM) (MBL international), CTLA-4-Ig protein chimera (2.5 $\mu g/mL$), and either IL-2ic or supernatant from transient transfection was added, together with control, anti-CD122, and anti-IL-2 JES6.1 mAbs on the beginning of cultivation. The plates were then cultured in 5% CO_2 for 72 h at 37 °C, and 18.5 kBq of [^{3}H]-thymidine was added for the final 8 h of cultivation before harvesting.

Western Blot. Cells ($1–5 \times 10^7$) were washed twice with an ice-cold Tris-buffered saline (TBS) with 1 μM Na_3VO_4 and centrifuged (4000g, 4 °C). Cells were then resuspended in extract buffer composed of 1% Nonidet P-40 (Pierce), 1 mM Na_3VO_4, 1 mM EDTA, 2 mM EGTA, 10 mM NaF, 1 mM DTT, 5% Protease mix (Sigma), 1 mM PMSF, and TBS at pH 7.4 and passed ten times through a needle (25–30G). Cell lysates were centrifuged at 4000g (4 °C) and protein concentration in aspirated supernatants was determined. 20 μg of protein was loaded per lane and run on SDS-PAGE either under standard or denaturing conditions using 10% polyacrylamide gel. Semidry blotting procedure with nitrocellulose membrane was performed, and scIL-2/S4B6 was detected by one of the primary antibodies (anti-rκ-biotin, anti-rIgG-biotin, anti-rIgG2a, or anti-mIL-2 JES6.5H4-biotin) together with a secondary antibody (antibiotin-HRP or anti-mIgG-HRP).

Adoptive Transfer. Purified OT-I CD8$^+$ T cells (Ly5.2) were labeled with CFSE and injected i.v. into B6.SJL recipients (Ly5.1) at 1 $\times 10^6$ cells per mouse. The next day, the mice were injected i.p. with PBS, 4 nmol SIINFEKL peptide (MBL International), 4 nmol SIINFEKL peptide plus IL-2ic, or 4 nmol SIINFEKL peptide plus scIL-2/S4B6 (40, 80, or 240 ng of IL-2 equiv). IL-2ic and scIL-2/S4B6 were injected 24 and 48 h later (total of 3 doses). Mice were sacrificed 24 h after the last dose, and spleens were harvested.

CFSE Labeling. Labeling of the cells with CFSE was carried out as described elsewhere.[1]

■ ASSOCIATED CONTENT

ⓢ Supporting Information
Scheme of two kinds of IL-2 immunocomplexes; scheme showing the cloning of genes; protein sequences cloned into expression vectors; identification of stabile transfected CHO-S clone 104/53. This material is available free of charge via the Internet at http://pubs.acs.org.

■ AUTHOR INFORMATION

Corresponding Author
*Tel: +420 241 062 362. Fax: +420 241 721 143. E-mail: makovar@biomed.cas.cz.

Notes
The authors declare the following competing financial interest(s): Marek Kovar is listed as co-inventor on patent entitled Methods for Improving Immune Function and Methods for Prevention or Treatment of Disease in a Mammalian subject, which was filed on February 16, 2007, and now bears International Application Number PCT/US2007/0623631.

■ ACKNOWLEDGMENTS

■ REFERENCES

(1) Boyman, O., Kovar, M., Rubinstein, M. P., Surh, C. D., and Sprent, J. (2006) Selective stimulation of T cell subsets with antibody–cytokine immune complexes. *Science 311*, 1924−1927.

(2) Kamimura, D., Sawa, Y., Sato, M., Agung, E., Hirano, T., and Murakami, M. (2006) IL-2 *in vivo* activities and antitumor efficacy enhanced by an anti-IL-2 mAb. *J. Immunol. 177*, 306−314.

(3) Tomala, J., Chmelova, H., Strohalm, J., Ulbrich, K., Sirova, M., Rihova, B., and Kovar, M. (2011) Antitumor activity of IL-2/anti-IL-2 mAb immunocomplexes exerts synergism with that of N-(2-hydroxypropyl)methacrylamide copolymer-bound doxorubicin conjugate due to its low immunosuppressive activity. *Int. J. Cancer 129*, 2002−2012.

(4) Webster, K. E., Walters, S., Kohler, R. E., Mrkvan, T., Boyman, O., Surh, C. D., Grey, S. T., and Sprent, J. (2009) *In vivo* expansion of T reg cells with IL-2-mAb complexes: induction of resistance to EAE and long-term acceptance of islet allografts without immunosuppression. *J. Exp. Med. 206*, 751−760.

(5) Tomala, J., Chmelova, H., Mrkvan, T., Rihova, B., and Kovar, M. (2009) *In vivo* expansion of activated naive CD8+ T cells and NK cells driven by complexes of IL-2 and anti-IL-2 monoclonal antibody as novel approach of cancer immunotherapy. *J. Immunol. 183*, 4904−4912.

(6) Hornick, J. L., Khawli, L. A., Hu, P., Lynch, M., Anderson, P. M., and Epstein, A. L. (1997) Chimeric CLL-1 antibody fusion proteins containing granulocyte-macrophage colony-stimulating factor or interleukin-2 with specificity for B-cell malignancies exhibit enhanced effector functions while retaining tumor targeting properties. *Blood 89*, 4437−4447.

(7) Hornick, J. L., Khawli, L. A., Hu, P., Sharifi, J., Khanna, C., and Epstein, A. L. (1999) Pretreatment with a monoclonal antibody/interleukin-2 fusion protein directed against DNA enhances the delivery of therapeutic molecules to solid tumors. *Clin. Cancer Res. 5*, 51−60.

(8) Xiang, R., Lode, H. N., Dolman, C. S., Dreier, T., Varki, N. M., Qian, X., Lo, K. M., Lan, Y., Super, M., Gillies, S. D., and Reisfeld, R. A. (1997) Elimination of established murine colon carcinoma metastases by antibody-interleukin 2 fusion protein therapy. *Cancer Res. 57*, 4948−4955.

(9) Craiu, A., Barouch, D. H., Zheng, X. X., Kuroda, M. J., Schmitz, J. E., Lifton, M. A., Steenbeke, T. D., Nickerson, C. E., Beaudry, K., Frost, J. D., Reimann, K. A., Strom, T. B., and Letvin, N. L. (2001) An IL-2/Ig fusion protein influences CD4+ T lymphocytes in naive and simian immunodeficiency virus-infected Rhesus monkeys. *AIDS Res. Hum. Retroviruses 17*, 873−886.

(10) Budagian, V., Nanni, P., Lollini, P. L., Musiani, P., Di Carlo, E., Bulanova, E., Paus, R., and Bulfone-Paus, S. (2002) Enhanced inhibition of tumour growth and metastasis, and induction of antitumour immunity by IL-2-IgG2b fusion protein. *Scand. J. Immunol. 55*, 484−492.

(11) Fan, S., Maguire, C. A., Ramirez, S. H., Bradel-Tretheway, B., Sapinoro, R., Sui, Z., Chakraborty-Sett, S., and Dewhurst, S. (2005) Valproic acid enhances gene expression from viral gene transfer vectors. *J. Virol. Methods 125*, 23−33.

IV.2   Novel IL-2-Poly(HPMA) Nanoconjugate Based Immunotherapy

This study introduces a novel approach by covalently attaching synthetic semitelechelic polymers based on N-(2-hydroxypropyl)methacrylamide (HPMA) to IL-2 through aminolysis of the ε-amino groups within the lysine residues. The resultant IL-2-poly(HPMA) conjugate, averaging 2-3 polymer chains per IL-2 molecule, exhibited reduced *in vitro* biological activity compared to native IL-2 due to poly(HPMA) chains partially preventing the interaction with IL-2R. However, this approach substantially increased the half-life of IL-2-poly(HPMA) conjugate in circulation (~4 h for the conjugate compared to < 10 min for free IL-2), which, together with its partially CD122-biased activity, led to enhanced biological activity *in vivo*. This conjugate significantly expanded memory CD8$^+$ T, NK, NKT, γδ T, and Treg cells. Furthermore, the conjugate markedly potentiated the CD8$^+$ T cell response following peptide-based vaccinations. These findings underscored the potential of polymer-modified IL-2 in improving the therapeutic profile of cytokine-based treatments, providing a groundbreaking proof-of-concept for polymer/protein modifications in enhancing their biological activity for immunotherapy applications.

P. Weberová's contribution to this publication:

All biological studies reported in this manuscript resulted from my work, including experiments' design, execution, data analysis, and interpretation of results. I significantly contributed to the preparation of the manuscript. Overall contribution ~ 60%.

Novel IL-2-Poly(HPMA)Nanoconjugate Based Immunotherapy

Petra Votavova[1], Jakub Tomala[1], Vladimir Subr[2], Jiri Strohalm[2], Karel Ulbrich[2], Blanka Rihova[1], and Marek Kovar[1, *]

[1] Department of Immunology and Gnotobiology, Institute of Microbiology ASCR, v.v.i., Videnska 1083, Prague 14220, Czech Republic
[2] Department of Biomedical Polymers, Institute of Macromolecular Chemistry ASCR, v.v.i., Heyrovskeho namesti 2, Prague 16202, Czech Republic

Interleukin-2 (IL-2) possesses a strong stimulatory activity for activated T and NK cells and it is an attractive molecule for immunotherapy. Nevertheless, extremely short half-life and severe toxicities associated with high-dose IL-2 treatment are serious and limiting drawbacks. In order to increase IL-2 half-life in vivo, we covalently conjugated synthetic semitelechelic polymeric carrier based on N-(2-hydroxypropyl)methacrylamide (HPMA) to IL-2. Thus, we synthesized IL-2-poly(HPMA) conjugate containing 2–3 polymer chains per IL-2 molecule in average. Such conjugate has lower biologic activity in comparison to IL-2 in vitro. However, it exerts much higher activity than IL-2 in vivo as shown by expansion of memory CD8$^+$ T, NK, NKT, $\gamma\delta$T and Treg cells. Moreover, IL-2-poly(HPMA) extremely effectively potentiates CD8$^+$ T cell peptide-based vaccination. IL-2-poly(HPMA) shows also much longer half-time in circulation than IL-2 ($\sim$4 h versus $\sim$5 min). Collectively, modification of IL-2 with poly(HPMA) chains dramatically improves its potency and pharmacologic features in vivo, which have implications for immunotherapy. To our knowledge, this is the first proof-of-concept report of the use of polymer/protein modification of IL-2 to obtain more pronounced biological activity.

KEYWORDS: Interleukin-2, N-(2-hydroxypropyl)Methacrylamide, Poly(HPMA) Conjugate, CD8$^+$ T Cells, Vaccination, Immunostimulation.

INTRODUCTION

Interleukin-2 (IL-2) is a small glycoprotein produced by activated T cells. IL-2 plays a crucial role in T cell-mediated immune responses as it promotes proliferation and survival of activated T cells and NK cells and it induces expression of effector functions in these cells. This cytokine further stimulates proliferation of memory CD8$^+$ T cells and, to a lesser extent, also activated B cells.[1] IL-2 is thus a very attractive molecule for immunotherapy and vaccination. However, due to its small molecular size, IL-2 is rapidly cleared through the kidneys, where it is metabolized completely.[2–4] This results into limited bioavailability and therefore low bioactivity of IL-2 when administered as a recombinant protein.[5] Attempts to administer IL-2 in high doses lead to many types of serious toxicities like vascular leak syndrome, severe pulmonary oedema[6] and many others.[7, 8]

Increasing the molecular size of IL-2 may lead to reduced renal clearance, thereby achieving prolonged circulation.[9, 10] IL-2 has been modified with synthetic polymeric carrier polyethylene glycol (PEG) for the first time more than 25 years ago. The IL-2-PEG conjugate was shown to have up to 20-fold increased plasma half-life in comparison to IL-2 and IL-2-PEG was thus considered as promising drug.[9] Although earlier studies in animals[9, 11, 12, 15, 16] and humans[13, 14] suggested positive effects in the treatment of various cancers, more recent data, however, failed to clearly demonstrate an advantage for IL-2-PEG in comparison to IL-2.[17–20] Other alternative strategies such as fusion or conjugation of IL-2 to serum proteins like albumin (Albuleukin)[21] or IgG[22] were also employed and showed to be effective in terms of increasing the bioavailability and also antitumor activity of IL-2.

PEG is the gold standard in the emerging field of polymer-based drug delivery, although the situation regarding PEGylated proteins is rather complicated. Since a vast

amount of clinical experience has been gained with PEGylated products up to this time, not only benefits but possible side effects and complications have also been found.[23] Among them, adverse effects in the body that can be provoked by the PEG itself or by side products formed during synthesis that lead to hypersensitivity are the most frequent ones.[25–28] Furthermore, PEG may possess antigenic and immunogenic properties as a hapten.[24] With all these potential drawbacks of PEGylated proteins in mind, we focused on another well characterized, but chemically significantly different synthetic polymeric carrier based on *N*-(2-hydroxypropyl)methacrylamide (HPMA). Poly(HPMA) is water-soluble and entirely biocompatible, i.e., non-immunogenic polymer which is easily eliminated from the body when chains up to 40 kDa are used.[30–32] Importantly, when comparing immunogenicity of protein-polymer conjugates, our laboratory showed that conjugates containing PEG possess higher ability to provoke hosts immunity than that ones with poly(HPMA).[33–35] Superoxide dismutase (SOD), bovine seminal ribonuclese (BSR) and α-chymotrypsin were conjugated to semitelechelic poly(HPMA). The conjugation decreased the immunogenicity of conjugates, increased the temperature stability of poly(HPMA)-SOD conjugates and proteolytic stability of poly(HPMA)-BSR conjugates.[36, 37]

In this study, we designed and synthesized an *in vivo* superagonistic form of IL-2 through its modification with well-defined polymeric carrier based on HPMA. By covalent conjugation of semitelechelic poly(HPMA) chains (MW$\sim$20 kDa) to IL-2 through aminolysis of ε-amine group in lysine residues, we synthesized IL-2-poly(HPMA) conjugate containing in average 2–3 polymer chains per IL-2 molecule and with relatively narrow size distribution ($\sim$Đ $= 1.9$). We determined the biological activity of IL-2-poly(HPMA) conjugate on activated CD8$^+$ T and NK cells *in vitro* and on CD8$^+$ T, NK, NKT, $\gamma\delta$T and Treg cells *in vivo* and we demonstrate here the benefits of this conjugate over unmodified IL-2. This study was not focused to develop new form of IL-2 for tumor immunotherapy, but rather much broadly to generally increase the biological activity and improve pharmacological features of IL-2 *in vivo* and thus potentially enable the use of this cytokine and, theoretically, also other cytokines in various biomedical applications like vaccination, immunodeficiency, and reconstitution of immune system after BMT, etc.

MATERIALS AND METHODS
Chemicals

Methacryloyl chloride, 1-aminopropan-2-ol, 4,4′-azobis (4-cyanopentanoic acid) 4,5-dihydro-thiazole-2-thiol, N,N′-dicyclohexylcarbodiimide (DCC) were purched from Sigma-Aldrich, Czech Republic. Mouse recombinant interleukin-2 (IL-2) was purchased from ProSpec-Tany TechnoGene Ltd. (Israel). All other chemicals and solvents

were of analytical grade. The solvents were dried and purified by conventional procedures and distilled before use.

Synthesis of Monomer and Semitelechelic Poly(HPMA)

N-(2-Hydroxypropyl)methacrylamide (HPMA) was synthesized by a modified reaction of methacryloyl chloride with 1-aminopropan-2-ol in dichloromethane in the presence of sodium carbonate.[38] Azo initiator 3,3′-azobis (4-cyano-4-methyl-1-oxobutane-1.4-diyl)bis(thiazolidine-2-thione) (ABIC-TT) was prepared by reaction of 4,4′-azobis (4-cyanopentanoic acid) with thiazolidine-2 thione in the presence of DCC in THF.[39] Semitelechelic poly(HPMA) containing thiazolidine-2-thione reactive group (polyHPMA-TT) at the polymer end chain was prepared by radical solution polymerization of HPMA (0.5 g, 3.5 mmol) initiated with azo initiator ABIC-TT (0.228 g) in DMSO (3.5 mL) in a sealed ampule under nitrogen atmosphere at 60 °C for 6 h. Yield of polymerization was 0.299 g (59.8%) of polyHPMA-TT with molecular weight 24 kDa and polydispersity Đ $= 1.9$.

Synthesis and Characterization of IL-2-poly(HPMA) Conjugate

IL-2 (4 mg) was dissolved in PBS buffer pH 7.4 (0.8 mL), cooled to 0 °C and then polyHPMA-TT (12 mg) was added. Reaction mixture was stirred for 6 h and the pH $=$ 8.2 was maintained by addition of sodium borate using pH-stat. Polymer conjugate IL-2-poly(HPMA) was separated from unbound polymer by size exclusion chromatography (SEC) on AKTAexplorer equipped with Superpose 6 column and UV detector set to 280 nm using 0.3 M sodium acetate buffer pH 6.5 as mobile phase. Fraction containing IL-2-poly(HPMA) conjugate was concentrated on Vivaspin with cut off 10 000 kDa, desalted using PD-10 column and lyophilized. The yield was 10 mg of IL-2-poly(HPMA) conjugate with molecular weight Mw 62 300 and polydispersity Đ $= 1.9$.

Number-average molecular weight (Mn), weight-average molecular weight (Mw), and polydispersity (Đ) of poly(HPMA)-TT and IL-2-poly(HPMA) conjugate were measured using SEC on a HPLC Shimadzu system equipped with UV, an Optilab rEX differential refractometer and multiangle light scattering DAWN 8 (Wyatt Technology, USA) detectors using Superose 6 column. The 0.3 M sodium acetate buffer pH 6.5 was used as mobile phase.

The content of IL-2 in the IL-2-poly(HPMA) conjugate (59 wt%) was determined by amino acid analysis of hydrolyzed conjugate (6 M HCl, 115 °C, 18 h in a sealed ampule) on a reverse-phase column Chromolith HighResulution RP-18e, 100 × 4.6 mm (Merck, Germany) using precolumn derivatization with phthalaldehyde (OPA) and 3-sulfanylpropanoic acid (excitation at 229 nm, emission at

61

450 nm). Gradient elution with 10–100% of solvent B for 35 min at a flow rate of 1.0 mL/min was used (solvent A, 0.05 M sodium acetate buffer, pH 6.5; solvent B, 300 mL of 0.17 M sodium acetate and 700 mL of methanol).

Mice

Female and male C57BL/6 mice were obtained from a breeding colony at the Institute of Physiology (Academy of Sciences of the Czech Republic, v.v.i., Prague, Czech Republic). Transgenic OT-I mice and B6.SJL (Ly5.1) mice were bred and kept at the genetically modified organism facility of the Institute of Molecular Genetics (Academy of Sciences of the Czech Republic). The mice were used at 9–15 wk of age. All experiments were approved by the Animal Welfare Committee at the Institute of Microbiology (Academy of Sciences of the Czech Republic, v.v.i., Prague, Czech Republic).

Cell Lines and mAbs

Murine YAC-1 cell line was purchased from American Type Culture Collection. The following anti-mouse mAbs were used: CD3-eF450, CD4-APC (/allophy-cocyanin), CD8-A700, CD8-PerCP-Cy5.5, CD44-APC, CD45.2-APC, Ly5.2-A700, DX5-PE, IFN-γ-PE mAb, IgG2b-PE, NK1.1-PerCP-Cy55, CD25-PE, Foxp3-PE, IL-2 clone JES6-1A12 and IL-2 clone JES6.5H4, CD122-PE (eBioscience), CTLA-4-IgG mAb (BD Pharmingen). CD25-APC and S4B6 mAb were provided by Drbal (Institute of Molecular Genetics, Academy of Sciences of the Czech Republic, v.v.i., Prague, Czech Republic). Functional grade purified blocking anti-mouse mAbs anti-CD25 (PC61.5) and anti-CD122 (Tm-b1) were purchased from eBioscience.

Proliferation Assay *In Vitro*

Purified CD8$^+$ T cells were seeded into Nunc 96-well flat-bottom plates in 0.2 ml volume and density of 2.5×10^5 cells/ml, cultured with 5 μg/ml soluble anti-CD3 and 1 μg/ml CTLA-4-IgG plus titrated amounts of free IL-2 or IL-2-poly(HPMA) conjugate. The plates were then cultured in 5% CO_2 for 72 h at 37 °C. A 18.5 kBq of [^{3}H]thymidine was added for the final 8 h of cultivation before harvesting. Purified NK cells were cultured at 1.25×10^6 cells/ml with IL-2 or IL-2-poly(HPMA) conjugate. The plates were cultured in 5% CO_2 for 72 h at 37 °C. A 18.5 kBq of [^{3}H]thymidine was added for the final 18 h of cultivation before harvesting.

Adoptive Transfer of OT-I Cells

Purified OT-I CD8$^+$ T cells (Ly5.2) were labeled with CFSE and injected i.v. into B6.SJL recipients (Ly5.1) at 1,2 x 10^6 cells per mouse. Next day, the mice were injected i.p. with PBS, SIINFEKL peptide (2 nmol, MBL International), SIINFEKL peptide plus polyinosinic-polycytidylic acid (poly(I:C), 75 μg), IL-2-poly(HPMA) conjugate plus

SIINFEKL peptide, or free IL-2 plus SIINFEKL peptide. Detailed schedule of the treatment is indicated at each experiment.

Staining for Surface and Intracellular Markers

Cells were resuspended in FACS buffer (PBS with 2% FCS, 2 mmol EDTA and 0,05% sodium azide), blocked by 10% mouse serum for 30 min on ice and stained with fluorochrome labeled mAbs for 30 min on ice in the dark. Cells were washed twice after each step in FACS buffer and fixed in 4% paraformaldehyde before analysis. When intracellular markers were stained, cells were additionally incubated in Fixation Buffer (eBioscience) 30 min on ice in the dark. Then washed twice in 1× Permeabilisation Buffer (eBioscience) and stained with fluorochrome labeled mAbs for 30 min on ice in the dark. Cells were washed three times in 1× Permeabilisation Buffer and resuspended in FACS buffer before analysis. Labelling the cells with CFSE was conducted as described elsewhere.[40] Flow cytometric analysis was performed on LSRII (BD Biosciences), and data were analyzed using FlowJo software (Tree Star).

Measuring of Intracellular IFN-γ Expression

Spleen cell suspensions from B6.SJL (Ly 5.1) mice were seeded into Nunc 12-well flat-bottom plates in 2 ml volume and restimulated with 50 nM SIINFEKL peptide. The plates were then cultured in 5% CO_2 for 6 h at 37 °C. Brefeldin A (Sigma-Aldrich) was added for last 4 h of cultivation at final concentration of 2,5 μg/ml. IFN-γ-PE or IgG2b-PE mAb (isotype control) were used in intracellular staining followed by flow cytometric analysis.

Detection of Antigen-Specific T-Cells with MHC-Dextramers

C57BL/6 mice were immunized i.p. with SIINFEKL peptide (40 μg) plus poly(I:C) (75 μg) with or without the IL-2-poly(HPMA) conjugate (4 μg of IL-2) administered i.p. on the same day and for next 3 consecutive days. Second and third round of immunization was performed in the same schedule and given with 10-day intervals between the courses. Splenocytes were isolated 10 days after the third immunisation and stained with the H-2Kb/SIINFEKL-PE dextramers (Immudex) at 2×10^6 cells per tube according to the manufacturer's protocol. All samples were then incubated for 30 min at 4 °C in the dark with CD3-FITC, CD4-PerCP, and CD8-Horizon V500 mAb in conditions recommended by the manufacturer (Immudex).

Kinetics of IL-2-Poly(HPMA) in Circulation

C57BL/6 mice were injected i.p. with free IL-2 (2 μg) or IL-2-poly(HPMA) conjugate (2 μg of IL-2). Blood from the mice was collected 3 min, 15, and 75 min (for IL-2) and 3 min, 15 min, 1 h, 2, 4, 6, 8, 24

and 48 hours (for IL-2-poly(HPMA)) after the injection and kept on ice. Tubes with blood were left for 30 min at 5 °C, and then repeatedly centrifuged (14 000 rpm, 10 min, 4 °C) to obtain blood sera. Serum IL-2 concentrations were determined by standard sandwich ELISA with anti-mouse JES6.1A12 and anti-mouse JES6.5H4-biotin mAbs. Detection was performed using extravidin-HRP (Sigma) and 3,3′,5,5′-tetramethylbenzidine as a substrate (TMB, Sigma). Absorbance was read for each well with a microplate reader BIOLISA set to 450 nm.

Determination of the Maximum Tolerated DOSE (MTD) of IL-2-Poly(HPMA) Conjugate

B6.SJL mice were injected i.p. with PBS or IL-2-poly(HPMA) (1.25, 2.50 or 3.75 mg/kg of IL-2) on day 1. Weight of each mouse (3 mice/group) was recorded prior to injection (day 0) and each day for next 7 days. Survival was evaluated on day 9. Next, B6.SJL mice were injected i.p. with PBS or IL-2-poly(HPMA) daily for 5 consecutive days (one dose 0.2, 0.3 or 0.4 mg/kg of IL-2) starting on day 1. Weight of each mouse (5 mice/group) was recorded prior to injection (day 0) and each day for next 9 days. Survival was evaluated on day 13.

RESULTS

The semitelechelic polymer containing TT reactive groups at the end of polymer chain (polyHPMA-TT) was prepared by radical solution polymerization. The molecular weight of polyHPMA-TT was controlled by concentration of monomer, azo initiator ABIC-TT and polymerization temperature. The amino groups from lysine residues of IL-2 were reacted with semitelechelic polyHPMA-TT forming the IL-2-polyHPMA conjugate in which the polymer chains are attached to IL-2 via a single polymer end-chain amide bond (Scheme 1). The conjugation reaction was carried in buffer solution at pH = 8.2. At these conditions the difference between the rate of aminolysis and hydrolysis of polyHPMA-TT is significantly more pronounced and aminolysis is prevailing.

The IL-2-polyHPMA conjugate was synthesized with the aim to improve the biological activity and pharmacological features of IL-2 *in vivo*. However, we decided first to determine the biological activity of IL-2-poly(HPMA) *in vitro* and to compare it with unmodified IL-2. We used the same batch of IL-2 both for conjugation to poly(HPMA) and as the source of unmodified IL-2 just to make sure that we are starting with the protein of the identical biological activity.

Stimulatory Activity of IL-2-Poly(HPMA) for Activated CD8+ *T* and NK Cells In Vitro

Since IL-2 potently stimulates proliferation of activated T cells and NK cells, we used purified CD8+ T and NK cells from B6 mice as an experimental system. We activated
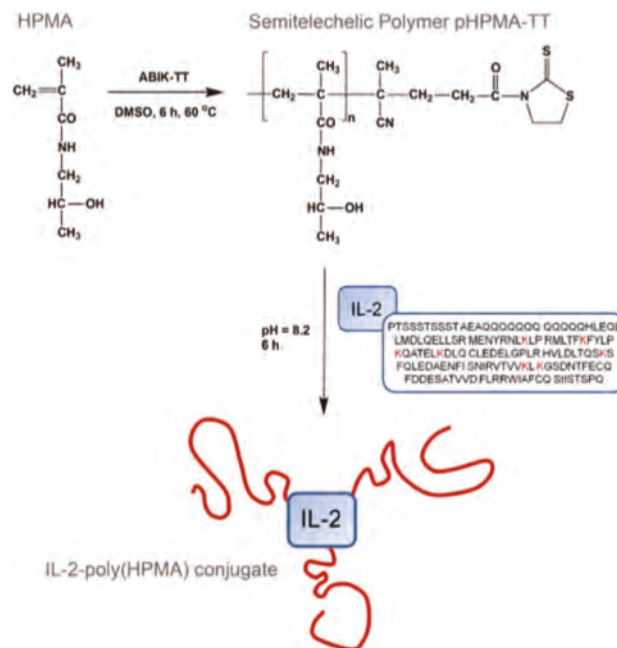
Scheme 1. Scheme showing a key steps in synthesis of IL-2-poly(HPMA) conjugate. The box at bottom right corner of IL-2 shows the primary amino acid sequence of this cytokine with lysines shown in red. ξ-amino groups of lysine residues are potentially modified with reactive semitelechelic poly(HPMA) precursor (pHPMA-TT).

CD8+ T cells by anti-CD3 mAb and we also added CTLA-4-Ig to cultures to minimize the proliferation background, i.e., the level of proliferation without IL-2, since CD8+ T cells upregulate expression of costimulatory molecule CD86 upon TCR signalling. NK cells do not need any stimulation to be responsive to IL-2. We found that IL-2-poly(HPMA) conjugate was able to stimulate proliferation of both activated CD8+ T and NK cells, albeit at higher concentrations (∼30–50 times) than IL-2 *in vitro* (Figs. 1(A) and (D)).

Such decrease of *in vitro* biological activity probably reflects the fact that modification of IL-2 molecule with several poly(HPMA) chains could impede the interaction with IL-2 receptor to some extent. To further investigate this hypothesis, we determined the effect of blocking anti-CD25 and anti-CD122 mAbs in cultures of activated CD8+ T (CD25high) and NK (CD122high) cells stimulated with IL-2 and IL-2-poly(HPMA) conjugate. Both blocking mAbs inhibited stimulatory activity of IL-2-poly(HPMA) conjugate more severely than that of IL-2, except of anti-CD122 mAb in NK cells where complete inhibition was achieved both in IL-2 and IL-2-poly(HPMA) conjugate stimulated cells (Figs. 1(B), (C), (E) and (F)). Thus, modification of IL-2 with poly(HPMA) chains decreased the ability of IL-2 to interact with its receptor subunits, particularly with CD25, and leads to significantly lowered biological activity *in vitro*.
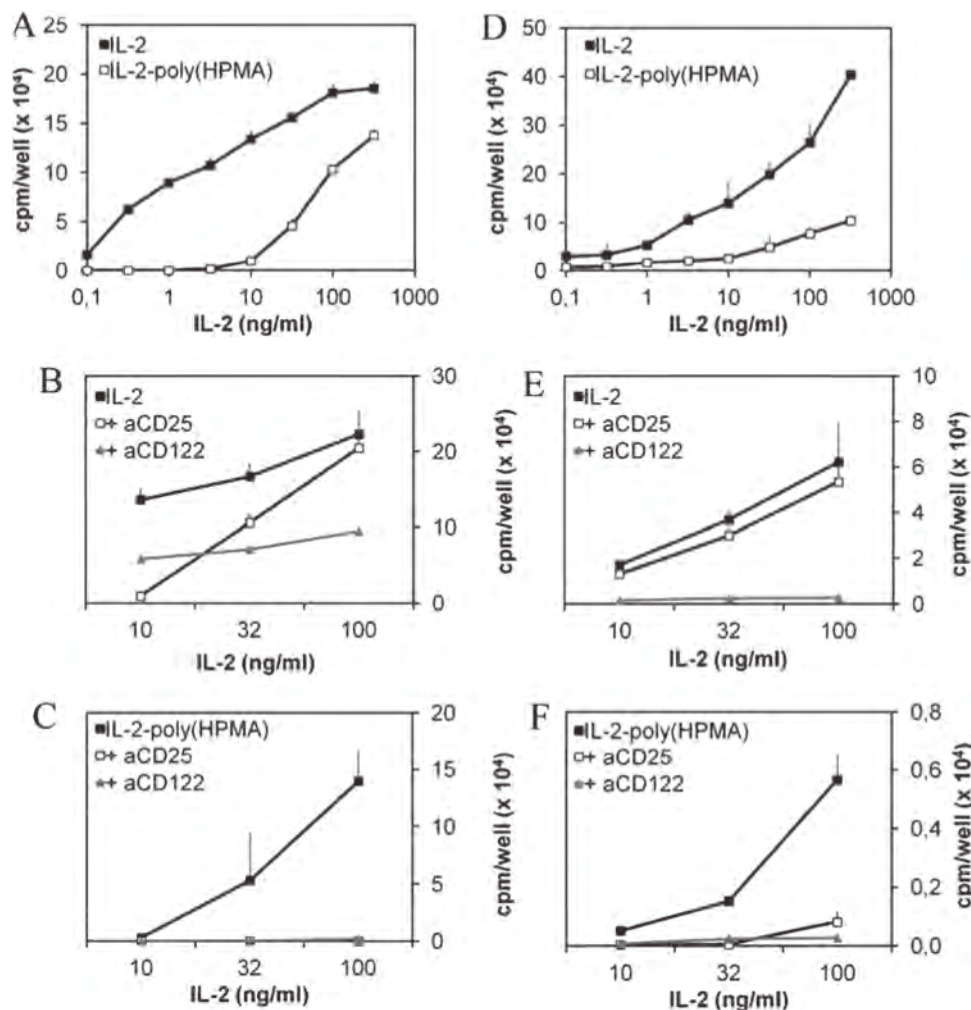
Figure 1. IL-2 covalently modified by poly(HPMA) is capable of stimulating proliferation of activated CD8$^+$ T cells and NK cells *in vitro*. (A), Purified CD8$^+$ T cells were cultured at 5×10^4 cells per well with anti-CD3 mAb (5 μg/ml), CTLA-4-Ig (1 μg/ml) and IL-2 or IL-2-poly(HPMA) conjugate. (B) and (C), Purified CD8$^+$ T cells were cultured at 6.6×10^4 cells per well under the same cell conditions as in A plus 10 μg/ml anti-CD25 mAb or anti-CD122 mAb. (D), Purified NK cells were cultured at 2.5×10^5 cells per well with IL-2 or IL-2-poly(HPMA) conjugate. (E) and (F), Purified NK cells were cultured at 2.5×10^4 cells per well with IL-2 or IL-2-poly(HPMA) plus 10 μg/ml anti-CD25 mAb or anti-CD122 mAb. Data show mean levels $\pm$ SD of [^{3}H]thymidine incorporation for triplicate cultures on day 3. Data are representative of at least two independent experiments with similar results.

IL-2-Poly(HPMA) Acts as an IL-2 Superagonist *In Vivo*

Next, we asked whether IL-2-poly(HPMA) conjugate also possess a biological activity *in vivo*. We decided to investigate the effect of IL-2-poly(HPMA) in comparison to IL-2 on several subsets of immunocompetent cells which are naturally responsive to IL-2 per se. Thus, we injected naive B6 mice with IL-2 and equivalent dose of IL-2-poly(HPMA) daily for four consecutive days and analyzed spleen cells by flow cytometry one day after the last injection. IL-2-poly(HPMA) conjugate was found to be far more potent than IL-2 (Fig. 2(A)) in terms of expansion of memory CD8$^+$ T cells (CD3$^+$CD8$^+$CD44^{high}CD122^{high}), NK cells (CD3$^-$NK1.1$^+$DX5$^+$), NKT cells (CD3$^+$NK1.1$^+$),

$\gamma\delta$ T cells (CD3$^+\gamma\delta$TCR$^+$) and T regulatory cells (CD4$^+$Foxp3$^+$; henceforth Treg).

Memory CD8$^+$ T cells and NK cells had very high relative counts in spleen of mice treated with IL-2-poly(HPMA) conjugate, being about 25% and 15% of all splenocytes, respectively (Fig. 2(B)). Dramatic expansion of IL-2 responsive cell subsets was also reflected by considerably increased spleen cellularity in mice treated with IL-2-poly(HPMA) conjugate while spleen cellularity in mice treated with IL-2 remained comparable to PBS treated controls (Fig. 2(C)). Memory CD8$^+$ T, NK and NKT cells increased their absolute numbers in mice treated with IL-2-poly(HPMA) about 90–120 times relatively to controls and 50–90 times relatively to IL-2 treated mice (Fig. 2(D)). Absolute numbers of $\gamma\delta$ T and Treg cells in mice treated with IL-2-poly(HPMA) were increased about
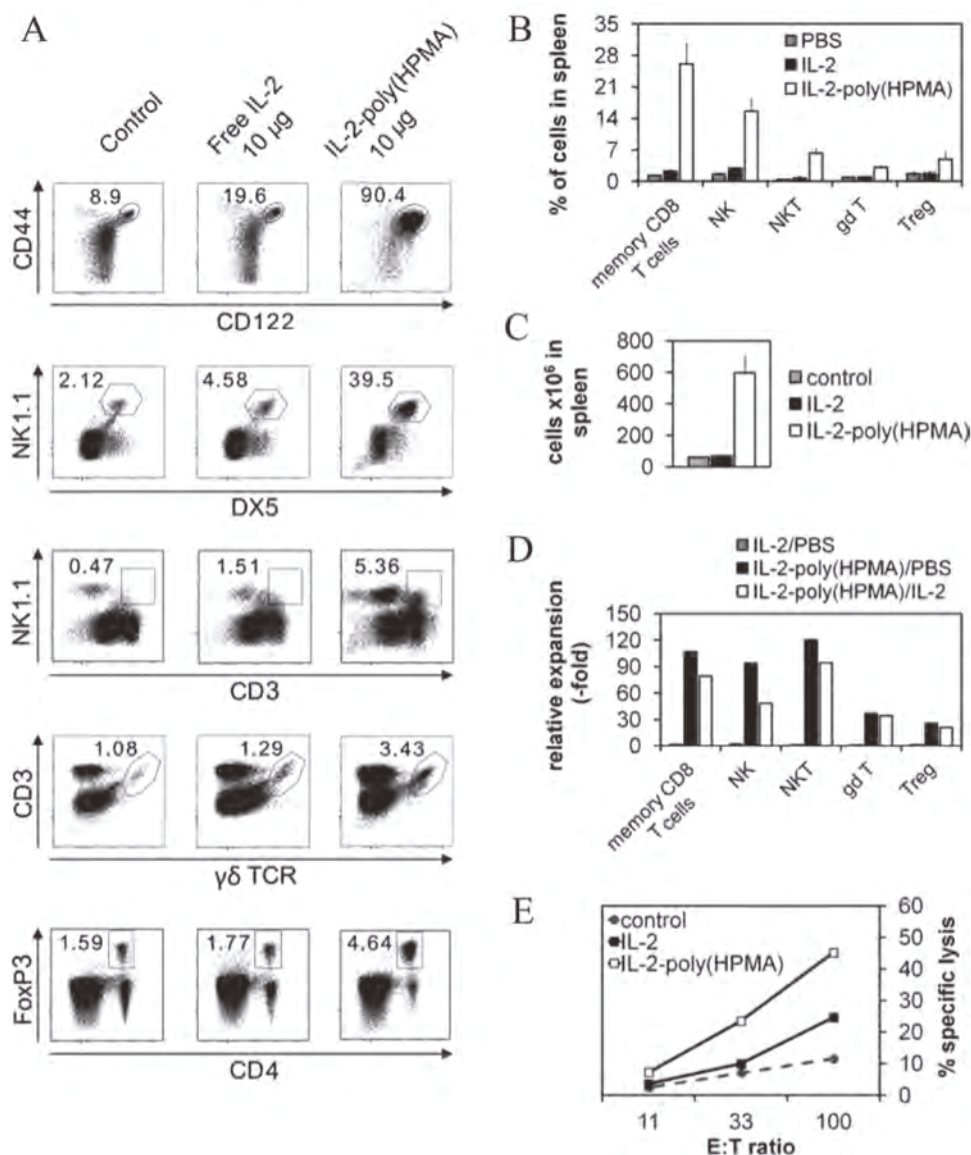
Figure 2. IL-2-poly(HPMA) conjugate potently drives expansion of memory CD8^{+} T, NK, NKT, $\gamma\delta$ T, and Treg cells. B6.SJL mice were injected i.p. with PBS (control), IL-2 (10 μg) or IL-2-poly(HPMA) (10 μg of IL-2) daily for 4 days. Mice were euthanized 1 day after last injection and their spleen cells were analyzed. (A), Relative expansion of CD44^{+}CD122^{+} cell population within CD3^{+}CD8^{+} cells (memory CD8^{+} T cells; upper row), NK1.1^{+}DX5^{+} cell population within CD3^{−} cells (NK cells; second row from top), CD3^{+}NK1.1^{+} cell population within all splenocytes (NKT cells; middle row), CD3^{+}$\gamma\delta$TCR^{+} cell population within all splenocytes ($\gamma\delta$ T cells; second row from bottom) and CD4^{+}Foxp3^{+} cell population within all splenocytes (Treg cells; bottom row). One representative mouse of 2 mice per each condition is shown. (B), Relative size of cell populations described above in spleen. Average of 2 mice per condition$\pm$SD is shown. (C), Spleen cellularity of mice treated as in (A). Average of 4 mice per condition$\pm$SD is shown. (D), Total numbers of memory CD8^{+} T, NK, NKT, $\gamma\delta$ T and Treg cells in spleen were calculated. Relative expansion of these cell populations is given as a ratio calculated from their total numbers in each condition (PBS, IL-2 and IL-2-poly(HPMA) treatment). (E), B6.SJL mice were injected i.p. with PBS (control), IL-2 (2 μg) or IL-2-poly(HPMA) (2 μg of IL-2) on day 1. Mononuclear cells (effectors; E) were isolated from spleens on day 6 and incubated with [^{3}H]thymidine-labeled target (*T*) YAC-1 cells at various E:T ratios for 4 h. Lysis of target YAC-1 cells by cytolytic effector cells was determined as loss of radioactivity in the harvested cells relative to appropriate controls. Data are representative of two independent experiments with similar results.

20–35 times relatively to controls as well as IL-2 treated mice (Fig. 2(D)). We also wanted to address the question whether IL-2-poly(HPMA) is capable of increasing the NK cytolytic activity in spleen cells of treated mice. We injected B6 mice with single dose of IL-2-poly(HPMA) or IL-2 and analyzed cytolytic activity of mononuclear cells isolated from spleens of these mice by JAM assay on day 6. Indeed, cytolytic activity of mononuclear cells from spleen was markedly increased by treatment with IL-2-poly(HPMA) but only slight increase was observed

after the treatment with IL-2 (Fig. 2(E)). Thus, based on much higher stimulatory activity to expand naturally IL-2 responsive immunocompetent cell populations, we can conclude that IL-2-poly(HPMA) acts as IL-2 superagonist *in vivo*.

IL-2-Poly(HPMA) Enormously Potentiates CD8+ *T* Cell Response

We demonstrated above that IL-2-poly(HPMA) conjugate possesses much higher stimulatory activity than IL-2 to expand naturally IL-2 responsive immune cell subsets *in vivo*. We further asked whether IL-2-poly(HPMA) has also such a potent stimulatory activity for activated T cells. Thus, we employed adoptive transfer of purified and CFSE-labeled OT-I CD8$^+$ T cells from Ly5.2$^+$ OT-I mice into congeneic Ly5.1$^+$ mice. OT-I CD8$^+$ T cells were then selectively activated by injection of SIINFEKL peptide one day post transfer followed by daily treatment with IL-2-poly(HPMA) conjugate or IL-2 for four days. The IL-2-poly(HPMA) conjugate exhibited extremely high efficacy to stimulate the proliferation (Fig. 3(A)) and expansion (Fig. 3(B)) of activated OT-I CD8$^+$ T cells, while IL-2 showed practically no activity even at 10 μg IL-2/dose. Moreover, OT-I CD8$^+$ T cells expanded by injection of SIINFEKL peptide plus IL-2-poly(HPMA) conjugate showed high expression of CD25 as long as 5 days after

Figure 3. IL-2-poly(HPMA) conjugate has dramatically increased potential to expand activated CD8$^+$ T cells in comparison to IL-2 *in vivo*. Purified OT-I CD8$^+$ T cells (Ly5.2) were labeled with CFSE and injected i.v. into congeneic B6.SJL recipients (Ly5.1) at 1.2 × 10^6 cells per mouse on day 1. On day 2, the mice were injected i.p. with PBS (control), SIINFEKL peptide (2 nmol) plus poly (I:C) (75 μg), SIINFEKL peptide plus IL-2 (10 μg) or SIINFEKL peptide plus IL-2-poly(HPMA) (1 μg or 10 μg of IL-2). IL-2 and IL-2-poly(HPMA) were injected i.p. also on days 3, 4, and 5. (A), CFSE dilution, CD25 expression and expansion of Ly5.2$^+$CD8$^+$ T cells relative to control (bottom left corner of each dot plot) in spleen were analyzed 1 day after last injection. One representative mouse of 2 mice per each condition is shown. (B), Relative counts of Ly5.2$^+$CD8$^+$ cells in spleens of experimental mice. Average of 2 mice per condition ± SD is shown. Data are representative of at least two independent experiments with similar results.

activation, whereas OT-I CD8$^+$ T cells expanded by injection of SIINFEKL peptide plus poly (I:C) were CD25^{low} (Fig. 3(A)).

Expansion of activated T cells is a key process for primary T cell response; however, the complete T cell response should to be finalized by the establishment of long-lived functional memory T cells which provide rapid and efficient immune response in the case of second antigen encounter. Thus, we asked whether activated CD8$^+$ T cells massively expanded by IL-2-poly(HPMA) conjugate are able to establish memory CD8$^+$ T cells which would persist in the organism for long time. We used the same experimental system as above, i.e., adoptive transfer of purified OT-I CD8$^+$ T cells from Ly5.2$^+$ OT-I mice into congeneic Ly5.1$^+$ mice and activation of transferred cells by injection of SIINFEKL peptide. IL-2-poly(HPMA) conjugate or IL-2 was injected only once together with SIINFEKL peptide, but at significantly higher dose (50 μg IL-2) than in previous experiments. The reason was that such schedule is much more convenient for the potential use of IL-2-poly(HPMA) as adjuvant for boosting T cell-based vaccination and we thus wanted to explore whether this schedule of administration is effective. OT-I CD8$^+$ T cells expanded only slightly in mice treated with SIINFEKL peptide plus IL-2 in comparison to mice treated with peptide alone (~3 times) on day 4 post treatment (Fig. 4(A)).

Nevertheless, OT-I CD8$^+$ T cells were able to form long-lived cell population in mice treated with SIINFEKL peptide plus IL-2 albeit the population was very tiny on day 50. On the other hand, OT-I CD8$^+$ T cells dramatically expanded in mice treated with SIINFEKL peptide plus IL-2-poly(HPMA) in comparison to mice treated with peptide alone (more than 100 times) on day 4 post treatment. Almost 10% of all splenocytes were OT-I CD8$^+$ T cells on day 4 and these cells formed very distinguishable population of long-lived cells with phenotype of memory CD8$^+$ T cells on day 50, i.e., most of them were CD44^{high}CD122^{high} (Figs. 4(A) and (B)).

To elucidate whether memory OT-I CD8$^+$ T cells formed in mice injected with SIINFEKL peptide plus IL-2-poly(HPMA) conjugate are also functional in terms of rapid expression of effector functions upon TCR signal, we isolated spleen cells from these mice on day 50, cultivated them with SIINFEKL peptide *in vitro* and analyzed their intracellular expression of IFN-γ by flow cytometry. Indeed, nearly all memory OT-I CD8$^+$ T cells isolated from mice treated with SIINFEKL peptide plus IL-2-poly(HPMA) conjugate expressed high levels of IFN-γ upon stimulation with SIINFEKL peptide *ex vivo* (Fig. 4(C)). Thus, we have shown that IL-2-poly(HPMA) conjugate is extremely potent in driving the expansion of antigen-activated CD8$^+$ T cells even if administered only in one dose together with the antigen and that such expanded CD8$^+$ T cells form robust population of functional memory CD8+ T cells.
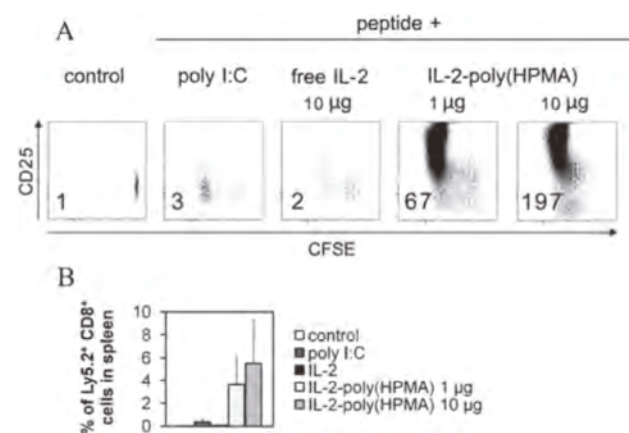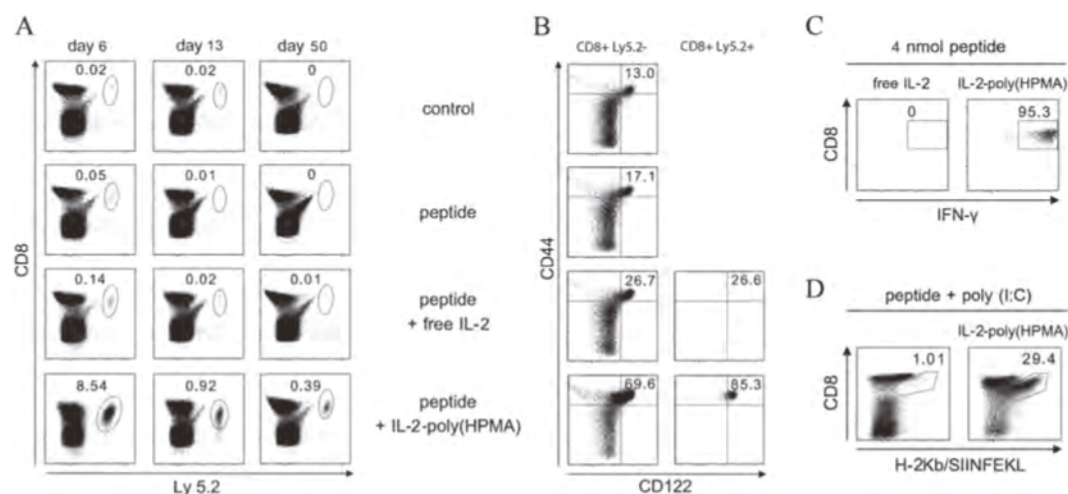
1668

Figure 4. Activated CD8+ T cells expanded by the IL-2-poly(HPMA) conjugate establish a robust population of functional memory cells. Purified OT-I CD8+ T cells (Ly5.2) were injected i.v. into B6.SJL recipients (Ly5.1) on day 1. Mice were injected i.p. with PBS (control), 4 nmol SIINFEKL peptide (peptide), SIINFEKL peptide plus IL-2 (50 μg), or SIINFEKL peptide plus IL-2-poly(HPMA) conjugate (50 μg of IL-2) on day 2. (A), Counts of Ly5.2+ CD8+ T cells relative to all splenocytes were assessed on days 6, 13 and 50 (upper part of each dot plot, in %). (B), Host and transferred CD8+ T cells (left and right column, respectively) were stained for CD44 and CD122 on day 50. (C), On day 50, spleen cells were stimulated by SIINFEKL peptide for 6 h *ex vivo*. Brefeldin A was added for last 4 h, and expression of IFN-γ was determined in Ly5.2+CD8+ cells. (D), C57BL/6 mice were immunized i.p. with SIINFEKL peptide (40 μg) plus poly(I:C) (75 μg) with or without the IL-2-poly(HPMA) conjugate (4 μg of IL-2) administered i.p. on the same day and for next 3 consecutive days. Second and third round of immunization was performed in the same schedule and given with 10-day intervals between the courses. Splenocytes were isolated 10 days after the third immunization and stained with the H-2Kb/SIINFEKL-PE dextramers. Live CD3+ cells are plotted. One representative mouse of 2 mice per each condition is shown. Data are representative of at least two independent experiments with similar results.

Since previous experiments on stimulatory activity of IL-2-poly(HPMA) conjugate were done using OT-I transgenic system, i.e., by using monoclonal CD8+ T cells, we decided to prove the potential of IL-2-poly(HPMA) to dramatically enhance CD8+ T cell responses also in polyclonal model, i.e., in B6 mice. We injected B6 mice with SIINFEKL peptide plus poly I:C and either treated mice with IL-2-poly(HPMA) for four days or not. This immunization was repeated twice with 10 day gap. Spleen cells isolated from the mice 10 days after the last immunization were analyzed by flow cytometry and SIINFEKL-specific CD8+ T cells were identified by H-2Kb/SIINFEKL-PE dextramers. Almost one third of CD8+ T cells were SIINFEKL-specific in mice where immunization with SIINFEKL peptide plus poly I:C was boosted by IL-2-poly(HPMA) while very low counts of SIINFEKL-specific CD8+ T cells were found in mice immunized with SIINFEKL peptide plus poly I:C only (Fig. 4(D)). Thus, we clearly showed that very high potential of IL-2-poly(HPMA) conjugate to boost CD8+ T cell immune response is not limited to monoclonal OT-I experimental model but it works also in wild type B6 mice.

IL-2-Poly(HPMA) Conjugate has much Longer Half-Life in Circulation than IL-2

IL-2 is reported to be rapidly eliminated from the circulation upon i.v. injection with elimination half-life of 3 to 13 min.[2,5] Since IL-2-poly(HPMA) conjugate has significantly higher molecular weight than IL-2, we wanted to determine the half-life of IL-2-poly(HPMA) in circulation upon i.v. administration. Thus, we established ELISA for detection of IL-2 and IL-2-poly(HPMA) in mouse serum with detection limit 0,004 ng IL-2/ml and 0,006 ng IL-2/ml, respectively (see Material and Methods).

As expected, IL-2 was rapidly eliminated from the circulation after i.v. administration (Fig. 5). We found just very low concentration of IL-2 (60 ng/ml) in mouse serum as early as 3 min after i.v. injection of 2 μg IL-2 and IL-2 was undetectable in serum 75 min after the administration. IL-2-poly(HPMA) conjugate was detected in serum even 48 h after i.v. injection of 2 μg IL-2 equivalent and with concentration actually higher than that determined 15 min after injection of IL-2. Moreover, there is a remarkably high concentration of IL-2-poly(HPMA) in serum (almost 400 ng IL-2/ml) which is stable for at least 1 h post administration. We determined the half-life of IL-2-poly(HPMA) in circulation to be approximately 4 h. In other words, modification of IL-2 with poly(HPMA) chains prolonged the half-life of IL-2 in circulation nearly 50 times.

Maximal Tolerated DOSE of IL-2-Poly(HPMA) Conjugate

Next, we decided to estimate the maximal tolerated dose (MTD) of IL-2-poly(HPMA) to further characterize the pharmacological features of this conjugate. We defined the MTD as highest possible dose which causes no mortality
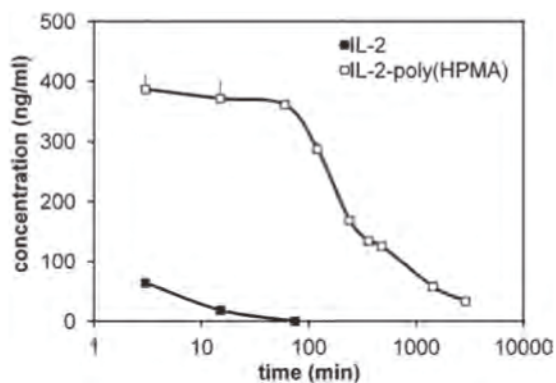
Figure 5. Short half-life of IL-2 in circulation upon i.v. administration is enormously extended when IL-2 is modified with poly(HPMA). C57BL/6 mice were i.v. injected with IL-2 (2 μg) or IL-2-poly(HPMA) conjugate (2 μg of IL-2). IL-2 concentrations were determined in sera isolated 3, 15, and 75 min after IL-2 administration and 3 min, 15 min, 1, 2, 4, 6, 8, 24 and 48 h after IL-2-poly(HPMA) administration. Concentration of IL-2 in serum was determined by sandwich ELISA with anti-mouse IL-2 mAb JES6.1A12 as capture antibody and anti-mouse IL-2 mAb JES6.5H4 labeled with biotin as detecting mAb. Data presented are average of 2 mice per each condition±SD. Data are representative of three independent experiments with similar results.
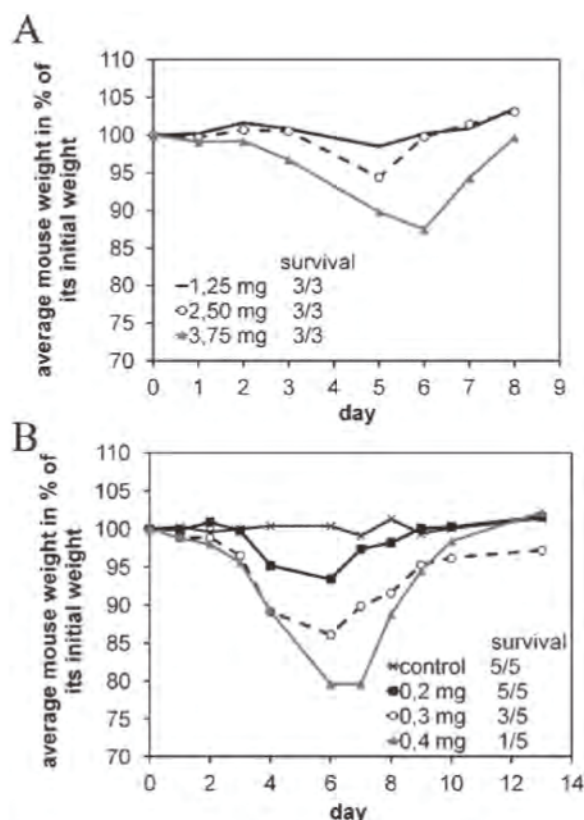

Figure 6. Maximum tolerated dose of IL-2-poly(HPMA) after i.p. administration of single dose or five daily doses. A, B6.SJL mice were injected i.p. with IL-2-poly(HPMA) conjugate (1.25, 2.50 or 3.75 mg/kg of IL-2) on day 1. Body weight of each mouse (3 mice per group) was recorded prior to injection (day 0) and then daily up to day 8. B, B6.SJL mice were injected i.p. with PBS (control) or IL-2-poly(HPMA) (one dose 0.2, 0.3 or 0.4 mg/kg of IL-2) on days 1, 2, 3, 4, and 5. Weight of each mouse (5 mice per group) was recorded prior to injection (day 0) and then daily up to day 13. Survival of mice in each group is indicated in graph legend.

and weight loss not higher than 15%. Titrated doses of IL-2-poly(HPMA) administered as single i.p. injection showed that MTD of the conjugate is approximately 3.75 mg IL-2/kg (Fig. 6(A)). Such dose corresponds to about 75 μg IL-2 per mouse showing that we used IL-2-poly(HPMA) still bellow MTD in experiments analyzing the potential of the conjugate to boost CD8^{+} T cell immune response.

Finally, we determined the MTD of IL-2-poly(HPMA) when given i.p. daily for 5 consecutive days. Of note, IL-2-poly(HPMA) showed to be much more toxic when using this administration schedule in comparison to single bolus injection. MTD was found to be 0.2 mg IL-2/kg per dose, i.e., cumulative total dose 1 mg IL-2/kg (Fig. 6(B)). Even slightly higher dosage 0.3 mg IL-2/kg per dose, i.e., cumulative total dose 1.5 mg IL-2/kg was lethal for 2 out of 5 experimental mice. This finding further supports the use of IL-2-poly(HPMA) in single high dose as an adjuvant for potentiation of T cell-based vaccines.

DISCUSSION

Cytokines are key immunomodulatory agents that shape immune responses. Our growing understanding of the biological basis of immunity and of ways in which this can potentially be affected ultimately led to the use of recombinant cytokines as a new approach to immunotherapy. IL-2 has potent stimulatory effect on T and NK cells and also some other cells of the immune system and IL-2 immunotherapy has been shown to be beneficial in a variety of clinical trials.[41–44] However, the major problem of

this immunotherapeutic approach is the toxicity of high dosage IL-2 therapy and the resultant decrease in curative effect with low doses of IL-2.[7, 45, 46]

Conjugation of IL-2 to carrier molecules such as PEG or albumin and thereby increasing the hydrodynamic radius of IL-2, which leads to a decrease in renal elimination, and thus increasing the half-life of IL-2 upon parenteral administration, has revealed as a promising approach.[9–14, 21] We have explored an alternative strategy of using poly(HPMA) as polymeric carrier for IL-2 to create a new drug with improved pharmacological properties. HPMA homopolymers and copolymers have been proposed for a wide variety of biomedical applications. Initially they were explored as biomaterials and then as drug delivery systems; both hydrogels and polymer-drug conjugates have been explored. The latter became a particular focus of attention.[47–49] HPMA homopolymers and copolymers are being currently explored in a diverse range of applications including their proposed use as coatings for

68

viruses[50], promotion of sub-cellular organelle (mitochon-drial) targeting,[51–51] and as second-generation anticancer conjugates containing combination therapy.[53, 54] Our deci-sion to choose poly(HPMA) was based mainly on our data indicating that proteins modified with HPMA polymer are less immunogenic than proteins modified with PEG polymer[33–35] and that the activity of enzymes is not damp-ened after their conjugation to HPMA copolymers.[36]

The *in vitro* results showed that IL-2-poly(HPMA) con-jugate promotes the proliferation of activated CD8^{+} T cells and NK cells and it competes with blocking anti-CD25 and anti-CD122 mAbs for binding to IL-2 receptor. *In vitro*, the biological activity of IL-2-poly(HPMA) conjugate was about 30–50 times lower than that of IL-2 which is, how-ever, consistent with results obtained with PEG or albumin protein conjugates.[21, 55] This probably reflects the fact that modification of IL-2 molecule with several poly(HPMA) chains could impede the interaction with IL-2 receptor to some extent. However, the decreased *in vitro* potency of IL-2-poly(HPMA) was far outweighed by the significant increase in the half-life of circulating conjugate *in vivo*, which yielded a greater biological activity *in vivo*.

The striking differences in the pharmacokinetic charac-teristics of IL-2-poly(HPMA) and IL-2 is approximately 50-fold difference in the elimination half-life following i.v. injection. As expected[2, 5], IL-2 was rapidly cleared from the blood upon i.v. administration. In contrast, IL-2-poly(HPMA) had a much more prolonged circulation in blood, with a remarkably high concentration which was stable for at least 1 h post administration. This new approach for developing long-acting IL-2 thus showed to be more successful than that creating IL-2-PEG or human IL-2-albumin fusion protein (Albuleukin).[9, 11, 21]

So far, other studies have solely described the phar-macokinetics of PEG- or albumin-modified IL-2 and efficacy of the treatment in various tumor models *in vivo*.[9, 11, 12, 16, 17, 19, 21, 56, 57] We are, to our knowledge, the first group showing the data concerning the changes in bio-logical attributes of IL-2 after modification with polymer carrier. First of all, we found that the IL-2-poly(HPMA) conjugate possesses extremely high stimulatory activity *in vivo* as shown by strong expansion of memory CD8^{+} T cells, NK, NKT, $\gamma\delta$ T cells and T regulatory cells, i.e., cell subsets naturally responsive to IL-2. Actually, mem-ory CD8^{+} T cells and NK cells (CD122^{high} cells) showed up to be even more sensitive to IL-2-poly(HPMA) con-jugate than other cells which was reflected by their very high relative counts in spleen of mice treated with IL-2-poly(HPMA) conjugate. Such a high expansion of NK cells could be useful in cancer immunotherapy, especially in case of tumors that are known to express low levels of MHC class I. However, these expanded NK cells must retain their cytolytic activity. Indeed, we found that NK cell activity of spleen cells isolated from mice injected with IL-2-poly(HPMA) conjugate, detected as killing of

YAC-1 cells by JAM assay, was significantly higher than those isolated from control mice or from mice injected with the same dose of IL-2.

The above mentioned ability of IL-2-poly(HPMA) con-jugate to induce superior expansion of IL-2-responsive cells could be beneficial in various immunotherapeutic interventions. First of all, IL-2 administered as consolidat-ing immunotherapeutic agent early after allogenic HSCT at a time of minimal residual disease might reduce the relapse rate and increase the immunocompetence status of these patients. Exogenous IL-2 might thus lead to an enhance-ment of the autologous GVL effect.[58] There are currently several clinical trials just completed or still ongoing in the allogeneic HSCT setting and it is believed that these will define the use of IL-2 (e.g., http://ClinicalTrials.gov iden-tifiers NCT00003962, and NCT00941928). In addition to that, studies to identify antigen-nonspecific strategies for enhancing immune reconstitution in individuals with HIV infection include those focusing on the use of IL-2.[59]

We further showed that IL-2-poly(HPMA) conjugate can be used *in vivo* to strongly expand activated naive CD8^{+} T cells and that such expanded cells are able to form a robust population of long-lived memory cells which are functional in terms of effective IFN-γ production upon re-activation. Notably, this report is the first describing the powerful stimulatory activity of a modified form of IL-2, the IL-2-poly(HPMA) conjugate in this case, for acti-vated naive CD8^{+} T cells. These results suggest that IL-2-poly(HPMA) conjugate could be used to potently boost CD8^{+} T cell responses and thus it could significantly improve vaccination protocols aimed to trigger responses mediated by cytotoxic T lymphocytes (CTL). Indeed, we further demonstrated that three immunizations with antigen given together with IL-2-poly(HPMA) conjugate resulted in markedly increased number of antigen-specific CD8^{+} T cells. Therefore, especially low immunogenic vaccines, which are known to cause weak immunostimulation and thus provide only low or short-lasting protection should benefit from being coadministered with IL-2-poly(HPMA) conjugate. Based on the above mentioned findings, we assume that the use of IL-2-poly(HPMA) as an adjuvant should receive a considerable attention. We also hypothe-size that IL-2-poly(HPMA) conjugate would improve vac-cination also in the case in which CD4^{+} T cells or B cells play the main role. However, this question remains to be verified in appropriate experiments.

CONCLUSION

Our results show improved pharmacological features of IL-2 covalently conjugated to poly(HPMA) carrier and they also provide a detailed view of the superior biologic activity of the IL-2-poly(HPMA) conjugate. To our knowl-edge, this is the first proof-of-concept report of the use of polymer/protein modification of IL-2 to obtain more pronounced biological activity. We believe that our results

provide a rationale for the use of IL-2-poly(HPMA) in various immunological interventions.

General Disclosure Statement

The authors have nothing to disclose.

REFERENCES

1. K. Smith, Interleukin-2: inception, impact, and implications. *Science* 240, 1169 (**1988**).
2. J. H. Donohue and S. A. Rosenberg, The fate of interleukin-2 after *in vivo* administration. *J. Immunol.* 130, 2203 (**1983**).
3. H. Ohnishi, J. T. Chao, K. K. Lin, H. Lee, and T. M. Chu, Role of the kidney in metabolic change of interleukin-2. *Tumour Biol.* 10, 202 (**1989**).
4. J. A. Gibbons, Z. P. Luo, E. R. Hannon, R. A. Braeckman, and J. D. Young, Quantitation of the renal clearance of interleukin-2 using nephrectomized and ureterligated rats. *J. Pharmacol. Exp. Ther.* 272, 119 (**1995**).
5. P. M. Anderson and M. A. Sorenson, Effects of route and formulation on clinical pharmacokinetics of interleukin-2. *Clin. Pharmacokinet.* 27, 19 (**1994**).
6. D. F. McDermott and M. B. Atkins, Application of IL-2 and other cytokines in renal cancer. *Expert Opin Biol Ther.* 4, 455 (**2004**).
7. U. S. Kammula, D. E. White, and S. A. Rosenberg, Trends in the safety of high dose bolus interleukin-2 administration in patients with metastatic cancer. *Cancer* 83, 797 (**1998**).
8. R. N. Schwartz, L. Stover, and J. Dutcher, Managing toxicities of high-dose interleukin-2. *Oncology (Williston Park)* 16, 11 (**2002**).
9. N. V. Katre, M. J. Knauf, and W. J. Laird, Chemical modification of recombinant interleukin 2 by polyethylene glykol increases its potency in the murine Meth A sarcoma model. *Proc. Natl. Acad. Sci. U.S.A* 84, 1487 (**1987**).
10. J. Lei, B. Guan, B. Li, Z. Duan, Y. Chen, H. Li, and J. Jin, Expression, purification and characterization of recombinant human interleukin-2-serum albumin (rhIL-2-HSA) fusion protein in Pichia pastoris. *Protein Expression Purif.* 84, 154 (**2012**).
11. J. C. Yang, S. L. Schwarz, D. M. Perry-Lalley, and S. A. Rosenberg, Murine studies using polyethylene glycol-modified recombinant human interleukin 2 (PEG-IL-2): antitumor effects of PEG-IL2 alone and in combination with adoptive cellular transfer. *Lymphokine Cytokine Res.* 10, 475 (**1991**).
12. V. Mattijssen, L. T. Balemans, P. A. Steerenberg, and P. H. de Mulder, Polyethylene-glycol-modified interleukin-2 is superior to interleukin-2 in locoregional immunotherapy of established guinea-pig tumors. *Int. J. Cancer* 51, 812 (**1992**).
13. F. J. Meyers, C. Paradise, S. Scudder, G. Goodman, and M. Konrad, A phase I study including pharmacokinetics of polyethylene glycol conjugated interleukin-2. *Clin. Pharmacol. Ther.* 49, 307 (**1991**).
14. T. Menzel, A. Schomburg, A. Körfer, M. Hadam, M. Meffert, I. Dallmann, S. Casper, H. Kirchner, H. Poliwoda, and J. Atzpodien, Clinical and preclinical evaluation of recombinant PEG-IL-2 in human. *Cancer Biother.* 8, 199 (**1993**).
15. X. S. Feng, *In vivo* antitumor activities of polyethylene glycol modified recombinant interleukin 2 (PEG-rIL-2) against murine hepatoma. *Zhonghua Zhong Liu Za Zhi* 15, 256 (**1993**).
16. L. Wang, Y. Wu, and Y. Zhang, *In vivo* antitumor effects of polyethylene glycol-modified recombinant human interleukin-2 on mouse uterine cervical carcinoma. *Zhonghua Zhong Liu Za Zhi* 18, 253 (**1996**).

17. R. J. Zimmerman, S. L. Aukerman, N. V. Katre, J. L. Winkelhake, and J. D. Young, Schedule dependency of the antitumor activity and toxicity of polyethylene glycol-modified interleukin 2 in murine tumor models. *Cancer Res.* 49, 6521 (**1989**).
18. R. M. Bukowski, J. Young, G. Goodman, F. Meyers, B. F. Issell, J. S. Sergi, D. McLain, G. Fyfe, and J. Finke, Polyethylene glycol conjugated interleukin-2: clinical and immunologic effects in patients with advanced renal cell carcinoma. *Invest. New Drugs* 11, 211 (**1993**).
19. M. R. Bernsen, H. F. Dullens, W. den Otter, and P. M. Heintz, Reevaluation of the superiority of polyethylene glycol-modified interleukin-2 over regular recombinant interleukin-2. *J. Interferon Cytokine Res.* 15, 641 (**1995**).
20. J. C. Yang, S. L. Topalian, D. J. Schwartzentruber, D. R. Parkinson, F. M. Marincola, J. S. Weber, C. A. Seipp, D. E. White, and S. A. Rosenberg, The use of polyethylene glycol-modified interleukin-2 (PEG-IL-2) in the treatment of patients with metastatic renal cell carcinoma and melanoma. A phase I study and a randomized prospective study comparing IL-2 alone versus IL-2 combined with PEG-IL-2. *Cancer* 76, 687 (**1995**).
21. R. J. Melder, B. L. Osborn, T. Riccobene, P. Kanakaraj, P. Wei, G. Chen, D. Stolow, W. G. Halpern, T. S. Migone, Q. Wang, K. J. Grzegorzewski, and G. Gallant, Pharmacokinetics and *in vitro* and *in vivo* anti-tumor response of an interleukin-2-human serum albumin fusion protein in mice. *Cancer Immunol. Immunother.* 54, 535 (**2004**).
22. A. Craiu, D. H. Barouch, X. X. Zheng, M. J. Kuroda, J. E. Schmitz, M. A. Lifton, T. D. Steenbeke, C. E. Nickerson, K. Beaudry, J. D. Frost, K. A. Reimann, T. B. Strom, and N. L. Letvin, An IL-2/Ig fusion protein influences CD4+ T lymphocytes in naive and simian immunodeficiency virus-infected Rhesus monkeys. *AIDS Res. Hum. Retroviruses* 17, 873 (**2001**).
23. K. Knop, R. Hoogenboom, D. Fischer, and U. S. Schubert, Poly(ethylene glycol) in drug delivery: pros and cons as well as potential alternatives. *Angew Chem. Int. Ed. Engl.* 49, 6288 (**2010**).
24. A. W. Richter and E. Akerblom, Antibodies against polyethylene glycol produced in animals by immunization with monomethoxy polyethylene glycol modified proteins. *Int. Arch. Allergy Appl. Immunol.* 70, 124 (**1983**).
25. A. Chanan-Khan, J. Szebeni, S. Savay, L. Liebes, N. M. Rafique, C. R. Alving, and F. M. Muggia, Complement activation following first exposure to pegylated liposomal doxorubicin (Doxil): Possible role in hypersensitivity reactions. *Ann. Oncol.* 14, 1430 (**2003**).
26. J. Szebeni, Complement activation-related pseudoallergy: A new class of drug-induced acute immune toxicity. *Toxicology* 216, 106 (**2005**).
27. P. Dewachter and C. Mouton-Faivre, Anaphylaxis to macrogol 4000 after a parenteral corticoid injection. *Allergy* 60, 705 (**2005**).
28. N. J. Ganson, S. J. Kelly, E. Scarlett, J. S. Sundy, and M. S. Hershfield, Control of hyperuricemia in subjects with refractory gout, and induction of antibody against poly(ethylene glycol) (PEG), in a phase I trial of subcutaneous PEGylated urate oxidase. *Arthritis Res. Ther.* 8, R12 (**2006**).
29. J. K. Armstrong, G. Hempel, S. Koling, L. S. Chan, T. Fisher, H. J. Meiselman, and G. Garratty, Antibody against poly(ethylene glycol) adversely affects PEG-asparaginase therapy in acute lymphoblastic leukemia patients. *Cancer* 110, 103 (**2007**).
30. L. Sprincl, J. Exner, O. Sterba, and J. Kopecek, New types of synthetic infusion solutions. III. Elimination and retention of poly-[N-(2-hydroxypropyl)methacrylamide] in a test organism. *J. Biomed. Mater. Res.* 10, 953 (**1976**).
31. B. Rihova, J. Kopecek, K. Ulbrich, M. Pospisil, and P. Mancal, Effect of the chemical structure of N-(2-hydroxypropyl)methacrylamide copolymers on their ability to induce antibody formation in inbred strains of mice. *Biomaterials* 5, 143 (**1984**).
32. B. Rihova, J. Kopecek, K. Ulbrich, and V. Chytry, Immunogenicity of N-(2-hydroxypropyl)-methacrylamide copolymers. *Die Makromolekulare Chemie* 9, 13 (**1985**).

33. P. A. Flanagan, R. Duncan, V. Subr, and J. Kopecek, Immunogenicity of protein—*N*-(2-hydroxypropyl)methacrylamide copolymer conjugate in A/J and B10 mice. *J. Bioact. Compat. Polym.* 5, 151 (**1990**).

34. B. Rihova, Immunomodulating activities of soluble synthetic polymer-bound drugs. *Adv. Drug Deliv. Rev.* 54, 653 (**2002**).

35. B. Rihova and M. Kovar, Immunogenicity and immunomodulatory properties of HPMA-based polymers. *Adv. Drug Deliv. Rev.* 62, 184 (**2010**).

36. D. Oupicky, K. Ulbrich, and B. Rihova, Conjugates of semitelechelic poly[*N*-(2-hydroxypropyl)methacrylamide] with enzymes for protein delivery. *J. Bioact. Compat. Polym.* 14, 213 (**1999**).

37. V. Subr, T. Etrych, K. Ulbrich, T. Hirano, T. Kondo, T. Todoroki, M. Jelinkova, and B. Rihova, J. Synthesis and properties of poly [*N*-(2-hydroxypropyl)methacrylamide] conjugates of superoxide dismutase. *Bioact. Compat. Polym.* 17, 105 (**2002**).

38. K. Ulbrich, V. Subr, J. Strohalm, D. Plocova, M. Jelinkova, and B. Rihova, Polymeric drugs based on conjugates of synthetic and natural macromolecules. I. Synthesis and physico-chemical characterisation. *J. Controlled Release* 64, 63 (**2000**).

39. V. Subr, C. Konak, R. Laga, and K. Ulbrich, Coating of DNA/poly(L-lysine) complexes by covalent attachment of poly[*N*-(2-hydroxypropyl)methacrylamide]. *Biomacromolecules* 7, 122 (**2006**).

40. O. Boyman, M. Kovar, M. P. Rubinstein, C. D. Surh, and J. Sprent, Selective stimulation of T cell subsets with antibody-cytokine immune complexes. *Science* 311, 1924 (**2006**).

41. S. A. Rosenberg, J. C. Yang, S. L. Topalian, D. J. Schwartzentruber, J. S. Weber, D. R. Parkinson, C. A. Seipp, J. H. Einhorn, and D. E. White, Treatment of 283 Consecutive Patients With Metastatic Melanoma or Renal Cell Cancer Using High-Dose Bolus Interleukin 2. *JAMA* 271, 907 (**1994**).

42. B. J. Johnson, L. G. Bekker, R. Rickman, S. Brown, M. Lesser, S. Ress, P. Willcox, L. Steyn, and G. Kaplan, RhuIL-2 adjunctive therapy in multidrug resistant tuberculosis: a comparison of two treatment regimens and placebo. *Tuber. Lung Dis.* 78, 195 (**1997**).

43. M. B. Atkins, M. T. Lotze, J. P. Dutcher, R. I. Fisher, G. Weiss, K. Margolin, J. Abrams, M. Sznol, D. Parkinson, M. Hawkins, C. Paradise, L. Kunkel, and S. A. Rosenberg, Dose Recombinant Interleukin 2 Therapy for Patients With Metastatic Melanoma: Analysis of 270 Patients Treated Between 1985 and 1993. *J. Clin. Oncol.* 17, 2105 (**1999**).

44. S. C. Piscitelli, N. Bhat, and A. Pau, A risk-benefit assessment of interleukin-2 as an adjunct to antiviral therapy in HIV infection. *Drug Saf.* 22, 19 (**2000**).

45. G. Fyfe, R. I. Fisher, S. A. Rosenberg, M. Sznol, D. R. Parkinson, and A. C. Louie, Results of treatment of 255 patients with metastatic renal cell carcinoma who received high-dose recombinant interleukin-2 therapy. *J. Clin. Oncol.* 13, 688 (**1995**).

46. J. P. Dutcher, M. Atkins, R. Fisher, G. Weiss, K. Margolin, F. Aronson, J. Sosman, M. Lotze, M. Gordon, T. Logan, and J. Mier, Interleukin-2-based therapy for metastatic renal cell cancer: The Cytokine working group experience. *Cancer J. Sci. Am.* 3, S73 (**1997**).

47. L. W. Seymour, D. R. Ferry, D. Anderson, S. Hesslewood, P. J. Julyan, R. Poyner, J. Doran, A. M. Young, S. Burtles, and D. J. Kerr, Hepatic drug targeting: phase I evaluation of polymer bound doxorubicin. *J. Clin. Oncol.* 20, 1668 (**2002**).

48. L. W. Seymour, D. R. Ferry, D. J. Kerr, D. Rea, M. Whitlock, R. Poyner, C. Boivin, S. Hesslewood, C. Twelves, R. Blackie, A. Schatzlein, D. Jodrell, D. Bissett, H. Calvert, M. Lind, A. Robbins, S. Burtles, R. Duncan, and J. Cassidy, Phase II studies of polymer-doxorubicin (PK1, FCE28068) in the treatment of breast, lung and colorectal cancer. *Int. J. Oncol.* 34, 1629 (**2009**).

49. D. P. Nowotnik and E. Cvitkovic, ProLindac™ (AP5346): a review of the development of an HPMA DACH platinum Polymer Therapeutic. *Adv. Drug Deliv. Rev.* 61, 1214 (**2009**).

50. K. D. Fisher and L. W. Seymour, HPMA copolymers for masking and retargeting of therapeutic viruses. *Adv. Drug Deliv. Rev.* 62, 240 (**2010**).

51. J. Callahan and J. Kopecek, Semitelechelic HPMA copolymers functionalized with triphenylphosphonium as drug carriers for membrane transduction and mitochondrial localization. *Biomacromolecules* 7, 2347 (**2006**).

52. V. Cuchelkar, P. Kopeckova, and J. Kopecek, Novel HPMA copolymer-bound constructs for combined tumor and mitochondrial targeting. *Mol. Pharmacol.* 5, 776 (**2008**).

53. E. Jäger, A. Jäger, P. Chytil, T. Etrych, B. Rihova, F. C. Giacomelli, P. Stepanek, and K. Ulbrich, J. Combination chemotherapy using core–shell nanoparticles through the self-assembly of HPMA-based copolymers and degradable polyester. *Controlled Release* 152, 153 (**2013**).

54. N. Larson, J. Yang, A. Ray, D. L. Cheney, H. Ghandehari, and J. Kopecek, Biodegradable multiblock poly(*N*-2-hydroxypropyl)methacrylamide gemcitabine and paclitaxel conjugates for ovarian cancer cell combination treatment. *Int. J. Pharm.* 454, 435 (**2013**).

55. S. Bowen, N. Tare, T. Inoue, M. Yamasaki, M. Okabe, I. Horii, and J. F. Eliason, Relationship between molecular mass and duration of activity of polyethylene glycol conjugated granulocyte colony-stimulating factor mutein. *Exp. Hematol.* 27, 425 (**1999**).

56. L. T. Balemans, P. A. Steerenberg, F. J. Koppenhagen, B. H. Kremer, P. H. de Mulder, A. M. Claessen, R. J. Scheper, and W. den Otter, PEG-IL-2 therapy of advanced cancer in the guinea pig. Impact of the primary tumor and beneficial effect of cyclophosphamide. *Int. J. Cancer.* 58, 871 (**1994**).

57. L. T. Balemans, P. A. Steerenberg, B. H. Kremer, F. J. Koppenhagen, P. H. de Mulder, and W. den Otter, Specific tumor memory induced by polyethylene-glycol-modified interleukin-2 requires both helper and cytotoxic T cells. *Cancer Immunol. Immunother.* 40, 125 (**1995**).

58. R. Seggewiss and H. Einsele, Immune reconstitution after allogeneic transplantation and expanding options for immunomodulation: An update. *Blood* 115, 3861 (**2010**).

59. M. Joly and D. Odloak, Modeling interleukin-2-based immunotherapy in AIDS pathogenesis. *J. Theor. Biol.* 335, 57 (**2013**).

IV.3 Antibodies to Interleukin-2 elicit selective T cell subsets potentiation through distinct conformational mechanisms

IL-2 mediates its effects by signaling through IL-2Rβ:IL-2Rγc heterodimers on cells that express varying levels of IL-2Rα. The differential expression of IL-2Rα delineates cells into high-expressing Treg cells and low-expressing effector cells. Utilizing anti-IL-2 mAbs, such as JES6-1A12 (JES6) and S4B6, modulates this pathway to preferentially expand either Treg or effector cells, respectively, presenting a targeted approach for therapeutic interventions. Our research has revealed that JES6 sterically blocks the interactions of IL-2 with IL-2Rβ and IL-2Rγ, while simultaneously decreasing the affinity of IL-2 for IL-2Rα through an allosteric mechanism, thereby selectively enhancing the potential of IL-2Rα^{high} Treg cells to utilize such IL-2co as high amounts of surface IL-2Rα were required to displace JES6 mAb by mass action. IL-2/JES6 augments IL-2Rα expression, establishing a beneficial feedback loop for Treg cell activation. In contrast, S4B6 selectively blocks the IL-2:IL-2Rα interaction and stabilizes the IL-2:IL-2Rβ interaction by inducing an affinity-enhancing conformational change in IL-2. Allosteric enhancement of IL-2:IL-2Rβ interaction by S4B6 leads to increased stimulatory activity that particularly favors IL-2Rβ^{high} effector cells. These findings provide a detailed molecular framework for the development of selectively enhancing therapeutic antibodies, offering significant potential for precision immunotherapy.

P. Weberová's contribution to this publication:

I participated in the experiments *in vivo*. I have assessed the expansion of various immune cell subsets in response to IL-2, IL-2/S4B6, and IL-2/JES6 and levels of IL-2Rα expression in these cells. Overall contribution ~ 10%.

Antibodies to Interleukin-2 elicit selective T cell subset potentiation through distinct conformational mechanisms

Jamie B. Spangler[1,2,3], **Jakub Tomala**[4], **Vincent C. Luca**[1,2,3], **Kevin M. Jude**[1,2,3], **Shen Dong**[1,2,3], **Aaron M. Ring**[1,2,3], **Petra Votavova**[4], **Marion Pepper**[5], **Marek Kovar**[4], and **K. Christopher Garcia**[1,2,3,*]

[1]Howard Hughes Medical Institute, Stanford University School of Medicine, Stanford, California, USA

[2]Department of Molecular and Cellular Physiology, Stanford University School of Medicine, Stanford, California, USA

[3]Department of Structural Biology, Stanford University School of Medicine, Stanford, California, USA

[4]Laboratory of Tumor Immunology, Institute of Microbiology of the Academy of Sciences of the Czech Republic, Prague, Czech Republic

[5]Department of Immunology, University of Washington, Seattle, Washington, USA

SUMMARY

Interleukin-2 (IL-2) is a pleiotropic cytokine that regulates immune cell homeostasis, and has been used to treat a range of disorders such as cancer and autoimmune disease. IL-2 signals via interleukin-2 receptor-β (IL-2Rβ):IL-2Rγ heterodimers on cells expressing high (regulatory T cells, Treg) or low (effector cells) amounts of IL-2Rα (CD25). When complexed with IL-2, certain anti-cytokine antibodies preferentially stimulate expansion of Treg (JES6-1) or effector (S4B6) cells, offering a strategy for targeted disease therapy. We found that JES6-1 sterically blocked the IL-2:IL-2Rβ and IL-2:IL-2Rγ interactions, but also allosterically lowered the

---

IL-2:IL-2Rα affinity through a 'triggered exchange' mechanism favoring IL-2Rα^hi Treg cells, creating a positive feedback loop for IL-2Rα^hi cell activation. Conversely, S4B6 sterically blocked the IL-2:IL-2Rα interaction, while also conformationally stabilizing the IL-2:IL-2Rβ interaction, thus stimulating all IL-2 responsive immune cells, particularly IL-2Rβ^hi effector cells. Our insights provide a molecular blueprint for engineering selectively potentiating therapeutic antibodies.
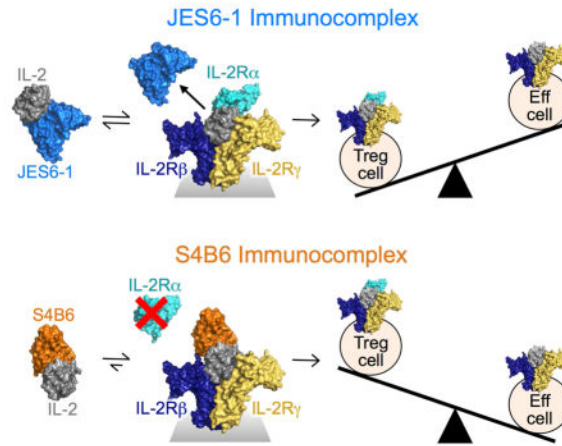
INTRODUCTION

Interleukin (IL)-2 is a four-helix bundle cytokine that plays a critical role in immune cell differentiation, growth, and activity. IL-2 signals through formation of either a high-affinity quaternary complex with the interleukin-2 receptor-α (IL-2Rα, CD25), IL-2Rβ, and IL-2Rγ chains ($K_d \approx 10$ pM), or an intermediate-affinity ternary complex ($K_d \approx 1$ nM) with only the IL-2Rβ and IL-2Rγ chains (Boyman and Sprent, 2012; Liao et al., 2013). Consequently, expression of the non-signaling IL-2Rα subunit regulates cytokine sensitivity. IL-2Rα is robustly expressed on regulatory T (Treg) cells but is virtually absent from naïve effector cells such as memory-phenotype (MP) CD8^{+} T cells and natural killer (NK) cells, resulting in differential responsiveness of these immune cell subsets to IL-2 (Fontenot et al., 2005; Josefowicz et al., 2012; Malek and Bayer, 2004). Upon IL-2 complex formation, intracellular Janus kinase (JAK) proteins constitutively associated with IL-2Rβ and IL-2Rγ phosphorylate tyrosine residues in the receptor intracellular domains, which recruit and activate signal transducer and activator of transcription (STAT)-5 to coordinate immune-related gene expression programs (Malek, 2008). The IL-2 complex also signals secondarily through the mitogen-activated protein kinase (MAPK) and phosphatidylinositol 3-kinase (PI3K) pathways (Malek, 2008; Taniguchi and Minami, 1993).

IL-2 exerts paradoxical effects on immune cell homeostasis, promoting activation and proliferation of both immunostimulatory effector cells and immunosuppressive Treg cells and its vital role in immune regulation has made IL-2 an attractive therapeutic target in a range of immune-linked diseases, both to promote the immune response, as in cancer and infectious disease, and to repress the immune response, as in autoimmune disorders and graft versus host disease (Boyman and Sprent, 2012; Brusko et al., 2008; Liao et al., 2013; Waldmann, 2006). However, the clinical performance of IL-2 has been limited by the

multifarious nature of its activities, which can thwart efficacy and lead to toxicity or harmful off-target effects (Boyman et al., 2006b; Rosenberg, 2012; Shevach, 2012). It would thus be of tremendous therapeutic value to decouple the immunostimulatory and immunosuppressive activities of IL-2 to cater to particular disease applications.

One strategy for selectively modulating the effects of IL-2 is development of cytokine-directed antibodies that bias activity toward specific T cell subsets. Co-administration of antibodies with IL-2 offers important therapeutic advantages such as prolonged *in vivo* half-life due to Fc receptor interactions (Boyman et al., 2006b; Finkelman et al., 1993; Letourneau et al., 2010). Boyman and colleagues established that immunocomplexes formed by pre-association of two anti-mouse IL-2 (mIL-2) antibodies with the cytokine elicit contrasting effects: mIL-2:JES6-1 immunocomplexes actively induce proliferation of IL-2Rα^{hi} cells, preferentially expanding Treg cells over effector cells, whereas mIL-2:S4B6 immunocomplexes stimulate proliferation of all immune cells, but particularly favor effector cells (Boyman et al., 2006a) (Figure 1A). Subsequent work has validated a vast array of therapeutic applications for these two antibodies: JES6-1 immunocomplexes promote graft tolerance (Park et al., 2010; Webster et al., 2009) and show efficacy in preclinical models of diabetes (Grinberg-Bleyer et al., 2010; Tang et al., 2008) and S4B6 immunocomplexes exhibit potent anti-tumor activity (Jin et al., 2008; Verdeil et al., 2008) without inducing toxicity (Krieg et al., 2010). Boyman and Sprent proposed that biased immunocomplex activity results from antibody obstruction of specific epitopes on the cytokine, namely that JES6-1 blocks only the IL-2Rβ binding site on mIL-2 to disrupt interaction with IL-2Rα^{lo} effector cells whereas S4B6 blocks the mIL-2Rα binding site on mIL-2 to prevent high-affinity interactions with IL-2Rα^{hi} Treg cells (Boyman and Sprent, 2012). However, in the absence of structural or molecular characterization, the mechanistic basis for selective cytokine potentiation remains speculative.

In this report, we have combined crystallographic, biophysical, and functional data to elucidate the molecular rationale for antibody-induced bias of cytokine activity. We show that JES6-1 and S4B6 exerted complex steric and allosteric effects on IL-2 to differentially activate immune cell subsets based on their IL-2 receptor surface expression profiles and that this biased activation was further propagated through transcriptional feedback. Our findings provide a direct link between the molecular interactions of cytokine-antibody complexes and their unique functional outcomes. These mechanistic insights into immune cell subset-specific potentiation establish a paradigm for antibody-mediated modulation of IL-2 behavior that will inform the design of enhanced cytokine-targeted therapeutics.

RESULTS

IL-2-targeted antibodies inhibit cytokine signaling to induce biased T cell subset proliferation

To elucidate the molecular properties of JES6-1 and S4B6 that contribute to their functional behavior, we probed antibody effects on mIL-2-induced signaling in IL-2Rα^- and IL-2Rα^+ human YT-1 NK cells as a surrogate for their effects on IL-2Rα^{lo} versus IL-2Rα^{hi} immune cell subsets. Cross-reactivity between mouse and human receptors (Figure S1A) enabled interrogation of murine cytokine signaling on human cells, although its potency was reduced

compared to the human cytokine due to its weaker affinity for the human IL-2 receptor subunits. On IL-2Rα⁻ cells, JES6-1 abolished IL-2-mediated STAT5 activation. S4B6 slightly inhibited activation, which was unexpected but is rationalized by structural and mechanistic experiments presented later in this report. On IL-2Rα⁺ cells, both JES6-1 and S4B6 greatly reduced IL-2 potency (Figure 1B). Importantly, IL-2 activity was greater on IL-2Rα⁺ cells in the presence of JES6-1 and greater on IL-2Rα⁻ cells in the presence of S4B6, consistent with preferential activation of IL-2Rα^{hi} Treg cells and IL-2Rα^{lo} effector cells, respectively. STAT5 signaling modulation was independent of antibody bivalency, as the single-chain variable fragment (scFv) of JES6-1 and the Fab fragment of S4B6 induced the same qualitative effects as their corresponding antibodies, albeit with attenuated potency (Figure S1B), presumably a consequence of the >25-fold higher apparent affinity of the bivalent versus monovalent antibodies (Figure S1C).

In vitro IL-2Rα expression-based signaling blockade translated into *in vivo* skewing of the effector cell:Treg cell ratio. IL-2Rα^{hi} Treg cells were enriched three-fold following mIL-2:JES6-1 immunocomplex injection into mice and, conversely, IL-2Rα^{lo} MP CD8⁺ T cells and NK cells were enriched five-fold following mIL-2:S4B6 immunocomplex injection compared to unbound cytokine administration (Figure 1C).

JES6-1 induces potentiation of Treg cell growth and inhibits autoimmune disease progression in mice

As the effector cell bias induced by S4B6 has promising implications for cancer treatment (Jin et al., 2008; Krieg et al., 2010; Verdeil et al., 2008), we sought to explore the therapeutic potential of the Treg cell bias induced by JES6-1 in the context of autoimmunity using a mouse model of inflammatory bowel disease (IBD). To this end, we assessed the ability of mIL-2:JES6-1 complexes to prevent disease in the dextran sodium sulfate (DSS) colitis model. Prior to DSS exposure, mice were treated with a vehicle control, a Treg cell-depleting anti-mIL-2Rα antibody, or mIL-2:JES6-1 complexes, which enriched relative Treg cell (IL-2R α⁺Foxp3⁺ cell) numbers ten-fold (Figure 1D). We also observed three-fold enrichment of IL-2Rα⁺Foxp3⁻ cells, consistent with previous reports that JES6-1-containing immunocomplexes induce expansion of IL-2Rα-expressing activated T cells (Castro et al., 2012; Tomala et al., 2009). One week after colitis induction, we observed that mIL-2:JES6-1 immunocomplex pretreatment yielded significant improvements in colon length and histopathology and drastically reduced disease activity, with treated mice exhibiting similar characteristics to those in which disease was not induced (Figure 1E,F). Notably, mice treated with PBS exhibited nearly identical disease severity to Treg cell-depleted mice (anti-mIL-2Rα antibody cohort), indicating that in the absence of expansion, background amounts of Treg cells in these mice provide no protective advantage. In combination with our signaling and proliferation studies, this mouse model demonstrates the therapeutic utility of selective immune cell subset stimulation.

mIL-2:JES6-1 and mIL-2:S4B6 complex structures reveal contrasting IL-2 receptor steric competition properties

To study the biochemical and structural mechanisms underlying JES6-1 and S4B6 effects, we isolated the variable region sequences of JES6-1 and S4B6 and expressed them in scFv

and Fab formats. We separately determined the crystal structures of the mIL-2:scFv-JES6-1 and mIL-2:Fab-S4B6 complexes to resolutions of 2.8 and 2.2 Å, respectively (Figure S2A,B and Table S1), and compared them to the human IL-2 quaternary complex structure (Wang et al., 2005) (Figure 2A,B). We observed that JES6-1 binds ventrally, or 'underneath' mIL-2 as it would be disposed in the signaling complex, between the IL-2Rβ and IL-2Rγ interfaces on the cytokine, directly occluding both subunits. Conversely, S4B6 binds dorsally, or on 'top' of mIL-2, directly occluding the IL-2Rα subunit (Figure 2C). JES6-1 makes extensive contacts in the region between the A helix and the N-terminal end of the AB loop of mIL-2 through complementarity-determining regions (CDRs) 2 and 3 of the JES6-1 heavy chain (HC) and CDRs 1 and 3 of the JES6-1 light chain (LC) (Figure S2C). In particular, mIL-2 residues Q36 and E37, which correspond to hIL-2 residues (Q22 and M23) essential to the IL-2:IL-2Rβ and IL-2:IL-2Rγ interactions, respectively, engage in hydrogen bonds with JES6-1 LC CDRs 1 and 3, illustrating the basis for steric competition between JES6-1 and both the IL-2Rβ and IL-2Rγ subunits. In contrast, S4B6 primarily interacts with IL-2Rα-binding residues in the B and C helices of mIL-2, through contacts with S4B6 HC CDR3 and LC CDRs 1 and 2 (Figure S2D). Our crystallographic findings are consistent with recent epitope mapping studies performed for JES6-1 (Rojas et al., 2014) and S4B6 (Rojas et al., 2013).

Anti-cytokine mAbs elicit allosteric effects on cytokine-receptor interactions

Our structural analysis also revealed allosteric effects of antibody binding on IL-2 complex formation that are key to function. No structure of the mouse IL-2:IL-2Rα complex has yet been determined to compare with the mIL-2:JES6-1 complex; however, the human IL-2:IL-2Rα complex structure serves as an accurate model for comparison since human and mouse IL-2 show a high degree of sequence and structural conservation in residues that engage their receptors. Although there is no steric clash between JES6-1 and IL-2Rα (Figure 2B), key residues that contact IL-2Rα 'switch' conformations upon binding to JES6-1. Superposition of the hIL-2:hIL-2Rα and mIL-2:JES6-1 interfaces reveals a large-scale remodeling of the AB loop in the respective complexes, with drastic changes in both side chain and main chain positioning of residues important for both JES6-1 *and* receptor binding (Figure 3). More specifically, two mIL-2 residues (K49 and R52) at the N-terminal end of the AB loop that contact JES6-1 (Figure S2C) also mediate contacts between hIL-2 (residues K35 and R38) and hIL-2Rα. JES6-1 binding distorts the entire AB loop of mIL-2, repositioning K49 and K52 as well as K57 (hIL-2 residue K43) and Y59 (hIL-2 residue Y45) from their presumed receptor-bound states as seen in the human complex. Potentially, IL-2Rα engagement is initiated by interaction with residues K49 and R52 at the N-terminal end of the AB loop that could, then, progressively 'peel off' the cytokine from JES6-1 in a zipper-like mechanism ultimately leading to dissociation of JES6-1 (Figure 3). Once JES6-1 dissociates, the IL-2Rα-bound cytokine is liberated to recruit IL-2Rβ and IL-2Rγ to form the functional signaling complex. These allosteric changes cannot be explained by differences in structure between the cytokine species, as the AB loop region of mIL-2 from the S4B6-bound structure overlays closely (RMSD=0.771 Å for S4B6 versus 3.15 Å for JES6-1) with receptor-bound hIL-2 (Figure S3). Moreover, the conformational flexibility in the AB loop region contrasts with the close correlation between JES6-1-bound mIL-2 and receptor-bound hIL-2 in other regions of the structures (RMSD=3.15 Å for AB loops versus 0.729 Å for

remainder of structures). Thus JES6-1 capitalizes on the previously noted malleability of the IL-2Rα binding site on IL-2 (Thanos et al., 2006; Thanos et al., 2003), and conformational changes are confined locally to this region of the cytokine. We suggest that JES6-1 binding to one site allosterically impairs IL-2Rα binding to a non-overlapping site, and this impaired binding (*i.e.* lowered affinity for IL-2Rα) renders JES6-1-bound IL-2 selective for IL-2Rα^{hi} cells, which express sufficient IL-2Rα to displace the antibody by mass action and initiate the exchange mechanism.

Overlaying the IL-2 receptor subunits with S4B6-bound mIL-2 clearly illustrates direct occlusion of IL-2Rα binding by the antibody (Figure 2B), to the extent that S4B6 appears to be a structural mimic of IL-2Rα. Comparison of the hIL-2:hIL-2Rα and mIL-2:S4B6 interfaces portrays the striking similarity between these two interactions (Figure 4A). Both the side chain and main chain positioning of the AB loop and B helix are highly conserved, particularly for interacting residues that are shared between the structures. Here again, close examination of the structural effects of S4B6 binding illuminates an unanticipated conformational consequence of the antibody on IL-2 engagement of IL-2Rβ. We previously noted that human IL-2 undergoes a slight repositioning of the C helix following IL-2Rα engagement (Wang et al., 2005) and showed that this structural change in the cytokine is recapitulated by a variant of IL-2 (denoted super-2) that exhibits 200-fold higher affinity for the IL-2Rβ subunit than the wild-type cytokine (Levin et al., 2012). S4B6 engages IL-2 in a similar manner to IL-2Rα, and we find that the antibody does indeed induce a shift in the C helix compared to the unbound cytokine, coinciding with the structures of both IL-2Rα-bound hIL-2 and super-2 (Figure 4B and Figure S4A). Thus S4B6 mediates steric blockade but also, to a lesser extent, allosteric effects, eliciting structural changes distal from its binding site that could impact IL-2Rβ binding. Overlay of the IL-2Rβ subunit from the hIL-2 quaternary complex with the S4B6-bound mIL-2 also reveals that the antibody may slightly obstruct accessibility of IL-2Rβ through a tangential steric clash between S4B6 LC CDR1 and domain 1 of IL-2Rβ (Figure S4B) which could partially mitigate the affinity-enhancing effect of S4B6 binding on the IL-2:IL-2Rβ interaction. S4B6-mediated blockade of IL-2Rα binding together with stabilization of the IL-2Rβ-binding conformation of IL-2 would be expected to promote proliferation of all T and NK cells bearing IL-2Rβ and IL-2Rγ, particularly favoring IL-2Rβ^{hi} effector cells, consistent with the functional activity of this antibody.

Anti-IL-2 antibodies exert distinct effects on IL-2 cytokine:receptor interactions

To rationalize our structural analysis in the context of biophysical measurements, we displayed mIL-2 on the surface of yeast and characterized antibody-receptor competition. Both JES6-1 and S4B6 potently blocked the mIL-2:mIL-2Rα interaction and JES6-1 also blocked the mIL-2:mIL-2Rβ interaction. S4B6 partially impaired the mIL-2:mIL-2Rβ interaction (Figure 5A,B), accounting for its mild inhibition of STAT5 signaling (Figure 1B, top), which presumably results resulted from the steric clash between the antibody and IL-2Rβ (Figure S4B). Consistent with our structural findings, these competition studies demonstrate that both antibodies impact cytokine engagement of the IL-2Rα and IL-2Rβ subunits.

We probed the kinetics of mIL-2 interactions with its receptor chains in the absence or presence of the JES6-1 and S4B6 antibodies using surface plasmon resonance (SPR). We immobilized mIL-2Rα and then flowed over pre-incubated mIL-2:antibody complexes containing a fixed mIL-2 concentration and variable concentrations of competitor antibody. The two antibodies exhibited qualitatively different effects on binding: Whereas S4B6 completely abrogated binding of mIL-2, residual cytokine binding occurred in the presence of JES6-1, even when it was in 40-fold excess over mIL-2 (Figure 5C), implying that mIL-2 can simultaneously, but transiently, engage both JES6-1 and mIL-2Rα in an exchanging intermediate state wherein JES6-1 'releases' as mIL-2Rα engages a low-affinity binding site. Upon JES6-1 dissociation, the mIL-2Rα binding site on mIL-2 remodels into the high-affinity state. Accordingly, kinetic profiles of JES6-1-modulated mIL-2:mIL-2Rα interactions indicated that the antibody concurrently decreased the association rate (K_{on}) and increases the dissociation rate (K_{off}) of the mIL-2:mIL-2Rα complex (Figure S5A). In contrast, S4B6 competes with IL-2Rα for binding to mIL-2 in a classical manner, in that IL-2α has to disengage before S4B6 can access mIL-2: dissociation of IL-2Rα from mIL-2 is unaffected by S4B6 (Figure S5C). These distinct modes of IL-2Rα displacement by JES6-1 and S4B6 reflect their unique structural properties and are essential to their biological activities.

We also analyzed the mIL-2:mIL-2Rβ interaction through SPR studies by immobilizing mIL-2Rβ and flowing over immunocomplexes containing variable ratios of competitor antibody to mIL-2. JES6-1 fully blocked mIL-2:mIL-2Rβ interaction whereas S4B6-conjugated mIL-2 bound to mIL-2Rβ (Figure 5D). Kinetic profiles showed that JES6-1 eliminated binding without impacting k_{off}, consistent with direct competitive inhibition (Figure S5B), and S4B6 led to an increase in the molecular mass of bound analyte reflecting mIL-2Rβ engagement of both the cytokine and antibody (Figure S5D).

We modified the topology of our binding studies, immobilizing either JES6-1 or S4B6, saturating the antibody-coated surface with mIL-2, and subsequently measuring mIL-2Rα or mIL-2Rβ binding to the immobilized mIL-2:antibody complexes. mIL-2Rα did not bind to the immobilized mIL-2:S4B6 immunocomplex (Figure 5E and Figure S5I) but bound to the mIL-2:JES6-1 immunocomplex with 200-fold weaker affinity compared to its interaction with mIL-2 alone (Figure 5E). The kinetic profile revealed a dramatic increase in the mIL-2Rα K_{off} in the presence of JES6-1 (Figure S5E,G), reiterating the exchange between receptor and antibody binding to the cytokine. Steric inhibition precluded binding of mIL-2Rβ to the immobilized mIL-2:JES6-1 immunocomplex (Figure 5F and Figure S5H) but, interestingly, we observed 6-fold enhancement in the binding of mIL-2Rβ to the mIL-2:S4B6 immunocomplex compared to its binding to free mIL-2 (Figure 5F). This affinity improvement was a net consequence of simultaneous decreases in K_{on} and K_{off} for the mIL-2:mIL-2Rβ interaction in the presence of S4B6 (Figure S5F,J). The kinetics of this immunocomplex:mIL-2Rβ interaction were rationalized by structural observations, as the predicted clash between S4B6 and mIL-2Rβ (Figure S4B) would presumably impede accessibility of the receptor binding site on mIL-2, hampering K_{on}. However, this effect was counteracted by the conformational change in the mIL-2 C helix induced by S4B6 binding (Figure 4B), which improved complex stability and would be predicted to lower K_{off}. Indeed, it was found that super-2 primarily achieves its IL-2Rβ affinity enhancement relative

to wild-type IL-2 by decreasing K_{off} (Levin et al., 2012). Taken together, our competitive binding studies validate the steric and allosteric effects of anti-IL-2 antibodies seen in the crystal structures, which manifest as biased functional activities *in vivo*.

IL-2:JES6-1 immunocomplex signaling feeds back onto IL-2Rα expression to perpetuate Treg cell proliferation

To further explore the mechanistic basis of the JES6-1-mediated Treg cell proliferation bias, we directly compared proliferation and IL-2Rα expression in five immune cell subsets following immunocomplex treatment. As anticipated, per cell IL-2Rα expression and the proportion of IL-2Rα$^+$ cells were substantially higher on Treg cells compared to effector cells and other subsets (Figure 6A,B). Both IL-2Rα surface density and the percentage of IL-2Rα$^+$ cells in the Treg cell subset (Figure 6C) and all other subsets (Figure 6A,B) increased in response to IL-2:JES6-1 immunocomplex treatment compared to mIL-2:S4B6 immunocomplex treatment or unbound mIL-2 treatment. However, the JES6-1-induced rise in receptor expression only corresponded with increased cell proliferation in the Treg cell subset, implying that a threshold amount of surface IL-2Rα is required to induce proliferation in the presence of JES6-1 (Figure 6D,E). This finding resonates with our proposed triggered release mechanism, wherein sufficient amounts of surface IL-2Rα are required to displace JES6-1 by mass action. Elevation of IL-2Rα expression following mIL-2:JES6-1 treatment in turn heightens sensitivity to the immunocomplex, creating a positive feedback loop that further biases immune cell homeostasis to favor IL-2Rα^{hi} Treg cells (Figure S6A).

In the case of mIL-2:S4B6 treatment, we found that induced proliferation did not correlate with surface IL-2Rα quantities, as the immunocomplex promotes proliferation of all IL-2 responsive immune subsets, particularly IL-2Rα^{lo} but IL-2Rβ^{hi} effector cell subsets (Figure 6A–E). This corroborates our proposed S4B6 mechanism of action, wherein steric blockade renders IL-2 insensitive to IL-2Rα expression and allosteric enhancement of IL-2Rβ binding directs IL-2's effects toward IL-2Rβ^{hi} effector cells (Figure S6B). Collectively, these subset expansion and IL-2Rα profiling studies reveal an additional layer through which IL-2-directed antibodies regulate immune homeostasis by altering transcriptional behavior.

DISCUSSION

Since the discovery that certain anti-IL-2 antibodies evoke selective immune cell proliferation, there has been a great deal of interest in exploiting these molecules to treat immune diseases. However, in order to harness their therapeutic potential, it is critical to understand the mechanistic basis for their activities. Half-life extension alone cannot explain their effects since different high-affinity IL-2 antibodies exhibit distinct potentiation profiles. Therefore, we explored the atomic basis for their IL-2 interactions as a possible explanation. It was previously thought that antibody selectivity was achieved by strict steric blockade of specific epitopes on the cytokine (Boyman and Sprent, 2012), but we found the mechanism to be more complex. Based on our collective structural and functional studies, we propose that the mechanisms for selective immune cell subset potentiation by JES6-1

and S4B6 are multi-layered, but ultimately rooted in the unique structural properties of each antibody.

JES6-1 acted through a three-tiered mechanism that induced IL-2 to potently and exclusively activate IL-2Ra^{hi} cells, skewing the immune cell balance to favor Treg cells. The first layer of IL-2 modulation involved extension of the cytokine's *in vivo* half-life. Complexing cytokines with antibodies has long been pursued as a strategy for enhancing activity through prolonged persistence in the bloodstream (Finkelman et al., 1993) and Fc receptor-mediated half-life extension has been previously shown to be necessary though not sufficient for maximal activity of anti-IL-2 antibody immunocomplexes (Letourneau et al., 2010). The second layer of the JES6-1 mechanism of action comprised the combined steric and allosteric effects of antibody binding on the IL-2 structure. JES6-1 sterically blocked binding of IL-2Rβ and IL-2Rγ and also allosterically impeded binding of IL-2Rα to the cytokine. Allosteric disruption of the mIL-2:mIL-2Rα interaction conferred exquisite sensitivity for Treg cells, as high amounts of IL-2Rα expression were required to overcome this disruption to allow for IL-2 complex formation and signal activation. IL-2Ra^{lo} effector cells were unresponsive to mIL-2:JES6-1 immunocomplex treatment since IL-2Rβ and IL-2Rγ interactions with the cytokine were occluded and there were not sufficient quantities of IL-2Rα to displace the antibody. The third layer of JES6-1 action consisted of IL-2Rα expression upregulation to create a positive feedback loop that perpetuated proliferation of IL-2Ra^{hi} cells. Increased IL-2Rα expression following mIL-2:JES6-1 treatment presumably resulted from a coalescence of two effects: (1) Increased IL-2Rα transcription, which has been shown to occur in response to IL-2 signaling (Depper et al., 1985), and (2) selective proliferation of cells with particularly high surface densities of IL-2Rα. Elevated IL-2Rα expression resulted in enhanced sensitivity to the mIL-2:JES6-1 immunocomplex, further heightening selectivity for IL-2Ra^{hi} Treg cell expansion.

An important component to the action of JES6-1 is its monovalent affinity for IL-2. The mIL-2:JES6-1 affinity is closely matched to that of the mIL-2:mIL-2Rα complex, allowing the antibody to directly compete with the receptor for access to mIL-2. One can imagine that a higher affinity antibody might bind too tightly to the cytokine and fail to let go and enable IL-2 complex formation. Conversely, a lower affinity antibody might dissociate more readily from the cytokine to allow interaction with IL-2Rβ and IL-2Rγ on all cell types, diminishing the advantage JES6-1 affords Treg cells. The mIL-2:mIL-2Rβ affinity is two orders of magnitude weaker than that of the mIL-2:JES6-1 interaction, positioning the antibody in an affinity 'sweet spot' that primes it for IL-2Ra^{hi} Treg cell bias.

S4B6 also acted through a multiple-tiered mechanism to preferentially direct IL-2 toward potentiation of effector cells. As with JES6-1, the first layer of S4B6-mediated IL-2 modification occurred through extension of *in vivo* half-life (Letourneau et al., 2010). However, as the functional consequences of S4B6 are unique to this antibody, increased half-life alone cannot account for the biased potentiation it orchestrates. The second layer of S4B6 action included the collection of steric and allosteric structural effects it exerts on mIL-2. S4B6 sterically occluded IL-2Rα binding and mildly obstructed IL-2Rβ binding but it also allosterically strengthened the mIL-2:mIL-2Rβ interaction by inducing an affinity-enhancing conformational change in mIL-2. The net result was that sensitivity to IL-2Rα

expression was lost as S4B6-bound mIL-2 signals equivalently through the IL-2 ternary complex on all IL-2 responsive immune cells, and susceptibility to IL-2 signaling was governed by IL-2Rβ expression. Allosteric enhancement of IL-2:IL-2Rβ interaction by S4B6 led to increased stimulatory activity that particularly favored IL-2Rβ^{hi} effector cells. As it has been established that IL-2 signaling induces IL-2Rβ upregulation (Siegel et al., 1987), it is enticing to speculate that, analogous to the JES6-1 immunocomplex, S4B6 exerts a third layer of regulation on mIL-2 activity, initiating a positive feedback cycle for IL-2Rβ expression to further bias stimulation in favor of IL-2Rβ^{hi} effector cells.

The complementary JES6-1 and S4B6 pair of IL-2-targeted antibodies serves as an archetypal system for exploring the molecular mechanisms underlying selective immune cell subset potentiation. Future work could expand upon our findings to design antibody variants with altered affinities and receptor subunit competition propensities that accentuate immune cell biasing effects. One could also envision applying our mechanistic insights to other systems by evolving cytokine- or growth factor-directed antibodies with desired receptor competitive properties. While JES6-1 and S4B6 have limited cross-reactivity with hIL-2 and IL-2Rα expression in activated effector T cells is more pervasive in human versus mouse tissues (Malek, 2008), the structural and biophysical studies we present illuminate a clear engineering-based path to modify these antibodies so that they may exert analogous effects on hIL-2 and serve as biased T cell subset-selective potentiating agents for a wide range of immunotherapeutic objectives.

EXPERIMENTAL PROCEDURES

Protein expression and purification

mIL-2 was expressed in the periplasm of *Escherichia coli* cells. hIL-2 and the mouse and human IL-2 receptor subunits were secreted from a baculovirus expression system. Sequences for the JES6-1 and S4B6 antibodies were isolated from their respective hybridoma cell lines and used to recombinantly express scFv and Fab fragments in a baculovirus expression system. Details are provided in the Supplemental Experimental Procedures.

Cell Lines

Procedures for culturing YT-1 cells and sorting for IL-2Rα expression are described in the Supplemental Experimental Procedures.

YT-1 cell STAT5 phosphorylation studies

YT-1 or IL-2Rα$^+$ YT-1 cells were stimulated with mIL-2, mIL-2:antibody immunocomplexes, or mIL-2:antibody fragment complexes (2:1 molar ratio of antibody or antibody fragment to mIL-2). STAT5 activation was analyzed via flow cytometry as described previously (Ring et al., 2012). Details are provided in the Supplemental Experimental Procedures.

82

Immune cell subset proliferation and receptor expression studies

For relative effector cell:Treg cell proliferation studies (Figure 1C), C57BL/6 mice were injected *i.p.* with mIL-2 immunocomplexes (2:1 cytokine:antibody molar ratio) or free mIL-2 on days 1, 2, 3, and 4. For immune cell subset expansion and IL-2Rα profiling studies (Figures 6A–E), C57BL/6 mice were injected *i.p.* with mIL-2 immunocomplexes or free mIL-2 on days 1, 2, and 3. In both studies, mice were sacrificed on day 5 and spleens were harvested, homogenized, and analyzed for surface and intracellular markers via flow cytometry. Cells were profiled and average relative expansion of various immune cell subsets compared to untreated control mice was determined for each cohort. Details are described in the Supplemental Experimental Procedures.

Mouse dextran sodium sulfate (DSS)-induced colitis model

BALB/c mice were injected *i.p.* either daily for seven days with PBS, once on day 6 with anti-mIL-2Ra antibody (EXBIO, clone PC61.5), or daily for seven days with mIL-2:JES6-1 immunocomplexes (2:1 cytokine:antibody molar ratio). On day 8, two mice per condition were sacrificed to assess spleen Treg cell counts by flow cytometry. The remaining pretreated mice from each cohort were administered 3% DSS (MP Biomedicals Inc.) in their drinking water beginning on day 8 to induce colitis. On day 15, disease severity was assessed by a clinical disease activity index (CDAI) and on day 16, mice were sacrificed for colon measurement and histological analysis. See Supplemental Experimental Procedures for details.

Yeast surface and SPR affinity titrations

hIL-2 and mIL-2 were displayed on the surface of yeast as described previously (Boder and Wittrup, 1997; Rao et al., 2004). For SPR studies, biotinylated human and mouse IL-2 receptors or biotinylated anti-IL-2 antibodies were immobilized to streptavidin-coated chips and binding of hIL-2 and mIL-2 was analyzed on a Biacore T100 instrument (GE Healthcare). Protocol details are provided in the Supplemental Experimental Procedures.

Crystallization and data collection

Purified mIL-2 and JES6-1 scFv or mIL-2 and S4B6 Fab were complexed overnight at 4° C in the presence of carboxypeptidases-A and B (Sigma), co-eluted over a Superdex-200 size-exclusion chromatography column, and concentrated to >10 mg/mL. mIL-2:JES6-1 scFv crystals were grown in sitting drops at 22° C from 0.1 M Bis-tris propane pH 6.4, 0.2 M sodium citrate, and 19% PEG 3350 and flash frozen in liquid nitrogen, cryoprotected with the addition of 25% 2-Methyl-2,4-pentanediol (Sigma). A 2.8 Å dataset was collected at beamline 8-2 at the Advanced Light Source. mIL-2:S4B6 Fab crystals were grown in sitting drops at 22° C from 0.1 M Bis-tris propane pH 6.5, 0.2 M sodium fluoride, and 20% PEG 3350 and flash frozen in liquid nitrogen, cryoprotected with the addition of 25% glycerol (Sigma). A 2.2 Å dataset was collected at beamline 11-1 at the Stanford Synchrotron Radiation Laboratory. Diffraction data were processed using HKL2000. Crystallographic data collection and refinement statistics are reported in Table S1.

Structure determination and refinement

The mIL-2:JES6-1 scFv and mIL-2:S4B6 Fab complex structures were solved by molecular replacement using PHASER (McCoy, 2007). For mIL-2, a one-to-one threaded model of mIL-2 to a human IL-2 structure (PDB ID 2B5I) generated in Phyre (Kelley and Sternberg, 2009) was used, and for the JES6-1 and S4B6 VH and VL domains, multiple-threaded models obtained from the I-TASSER server (Roy et al., 2010; Zhang, 2008) were used. Models of the S4B6 CH1 and CL domains were obtained from the previously solved structure of a rat Fab (PDB ID 1LK3). Iterative model rebuilding and refinement were performed using the Phenix software (Adams et al., 2002) and COOT (Crystallographic Object-Oriented Toolkit) (Emsley and Cowtan, 2004). For initial refinement, rigid body, coordinate, and real-space refinement were used with individual atomic displacement parameter refinement. Translation, libration, and screw-rotation refinement was added in later iterations. Ramachandran and rotamer analysis were performed using MolProbity (Davis et al., 2007). Electron density connected to N31 of the JES6-1 VH was modeled as an N-linked $GlcNAc_2$ with α-1,6 and α-1,3 difucosylation of the proximal GlcNAc. Interacting residues were identified using the protein interfaces, surfaces, and assemblies (PISA) service at the European Bioinformatics Institute (Krissinel and Henrick, 2007). Structural figures were created using PyMOL (DeLano, The PyMOL Molecular Graphics System, 2002).

Yeast surface and SPR antibody-receptor competitive IL-2 binding assays

For yeast surface competition studies, mIL-2-displaying yeast were incubated concurrently with saturating concentrations of mIL-2Ra or mIL-2Rβ and serial dilutions of unlabeled competitor antibody and subsequently analyzed for receptor binding via flow cytometry.

SPR-based competition studies were performed on a Biacore T100 instrument in two different topologies. In one orientation, biotinylated mIL-2Ra or mIL-2Rβ was immobilized to a streptavidin-coated chip and binding of pre-incubated complexes containing saturating amounts of mIL-2 and serial dilutions of competitor antibody was evaluated. In the other orientation, biotinylated antibodies JES6-1 or S4B6 were immobilized to a streptavidin-coated chip, a saturating amount of mIL-2 was then captured on the immobilized antibodies, and binding of soluble mIL-2Rα or mIL-2Rβ was evaluated. See Supplemental Experimental Procedures for details.

Supplementary Material

Refer to Web version on PubMed Central for supplementary material.

Acknowledgments

References

Adams PD, Grosse-Kunstleve RW, Hung LW, Ioerger TR, McCoy AJ, Moriarty NW, Read RJ, Sacchettini JC, Sauter NK, Terwilliger TC. PHENIX: building new software for automated crystallographic structure determination. Acta Crystallogr D Biol Crystallogr. 2002; 58:1948–1954. [PubMed: 12393927]

Boder ET, Wittrup KD. Yeast surface display for screening combinatorial polypeptide libraries. Nature biotechnology. 1997; 15:553–557.

Boyman O, Kovar M, Rubinstein MP, Surh CD, Sprent J. Selective stimulation of T cell subsets with antibody-cytokine immune complexes. Science. 2006a; 311:1924–1927. [PubMed: 16484453]

Boyman O, Sprent J. The role of interleukin-2 during homeostasis and activation of the immune system. Nat Rev Immunol. 2012; 12:180–190. [PubMed: 22343569]

Boyman O, Surh CD, Sprent J. Potential use of IL-2/anti-IL-2 antibody immune complexes for the treatment of cancer and autoimmune disease. Expert Opin Biol Ther. 2006b; 6:1323–1331. [PubMed: 17223740]

Brusko TM, Putnam AL, Bluestone JA. Human regulatory T cells: role in autoimmune disease and therapeutic opportunities. Immunological reviews. 2008; 223:371–390. [PubMed: 18613848]

Castro I, Dee MJ, Malek TR. Transient enhanced IL-2R signaling early during priming rapidly amplifies development of functional CD8+ T effector-memory cells. Journal of immunology. 2012; 189:4321–4330.

Davis IW, Leaver-Fay A, Chen VB, Block JN, Kapral GJ, Wang X, Murray LW, Arendall WB 3rd, Snoeyink J, Richardson JS, Richardson DC. MolProbity: all-atom contacts and structure validation for proteins and nucleic acids. Nucleic acids research. 2007; 35:W375–383. [PubMed: 17452350]

DeLano, WL. The PyMOL Molecular Graphics System. DeLano Scientific; San Carlos, CA, USA: 2002.

Depper JM, Leonard WJ, Drogula C, Kronke M, Waldmann TA, Greene WC. Interleukin 2 (IL-2) augments transcription of the IL-2 receptor gene. Proceedings of the National Academy of Sciences of the United States of America. 1985; 82:4230–4234. [PubMed: 2987968]

Emsley P, Cowtan K. Coot: model-building tools for molecular graphics. Acta Crystallogr D Biol Crystallogr. 2004; 60:2126–2132. [PubMed: 15572765]

Finkelman FD, Madden KB, Morris SC, Holmes JM, Boiani N, Katona IM, Maliszewski CR. Anti-cytokine antibodies as carrier proteins. Prolongation of in vivo effects of exogenous cytokines by injection of cytokine-anti-cytokine antibody complexes. Journal of immunology. 1993; 151:1235–1244.

Fontenot JD, Rasmussen JP, Gavin MA, Rudensky AY. A function for interleukin 2 in Foxp3-expressing regulatory T cells. Nature immunology. 2005; 6:1142–1151. [PubMed: 16227984]

Grinberg-Bleyer Y, Baeyens A, You S, Elhage R, Fourcade G, Gregoire S, Cagnard N, Carpentier W, Tang Q, Bluestone J, et al. IL-2 reverses established type 1 diabetes in NOD mice by a local effect on pancreatic regulatory T cells. The Journal of experimental medicine. 2010; 207:1871–1878. [PubMed: 20679400]

Jin GH, Hirano T, Murakami M. Combination treatment with IL-2 and anti-IL-2 mAbs reduces tumor metastasis via NK cell activation. International immunology. 2008; 20:783–789. [PubMed: 18448458]

Josefowicz SZ, Lu LF, Rudensky AY. Regulatory T cells: mechanisms of differentiation and function. Annual review of immunology. 2012; 30:531–564.

Kelley LA, Sternberg MJ. Protein structure prediction on the Web: a case study using the Phyre server. Nature protocols. 2009; 4:363–371.

Krieg C, Letourneau S, Pantaleo G, Boyman O. Improved IL-2 immunotherapy by selective stimulation of IL-2 receptors on lymphocytes and endothelial cells. Proceedings of the National

Academy of Sciences of the United States of America. 2010; 107:11906–11911. [PubMed: 20547866]

Krissinel E, Henrick K. Inference of macromolecular assemblies from crystalline state. Journal of molecular biology. 2007; 372:774–797. [PubMed: 17681537]

Letourneau S, van Leeuwen EM, Krieg C, Martin C, Pantaleo G, Sprent J, Surh CD, Boyman O. IL-2/ anti-IL-2 antibody complexes show strong biological activity by avoiding interaction with IL-2 receptor alpha subunit CD25. Proceedings of the National Academy of Sciences of the United States of America. 2010; 107:2171–2176. [PubMed: 20133862]

Levin AM, Bates DL, Ring AM, Krieg C, Lin JT, Su L, Moraga I, Raeber ME, Bowman GR, Novick P, et al. Exploiting a natural conformational switch to engineer an interleukin-2 'superkine'. Nature. 2012; 484:529–533. [PubMed: 22446627]

Liao W, Lin JX, Leonard WJ. Interleukin-2 at the crossroads of effector responses, tolerance, and immunotherapy. Immunity. 2013; 38:13–25. [PubMed: 23352221]

Malek TR. The biology of interleukin-2. Annual review of immunology. 2008; 26:453–479.

Malek TR, Bayer AL. Tolerance, not immunity, crucially depends on IL-2. Nat Rev Immunol. 2004; 4:665–674. [PubMed: 15343366]

McCoy AJ. Solving structures of protein complexes by molecular replacement with Phaser. Acta Crystallogr D Biol Crystallogr. 2007; 63:32–41. [PubMed: 17164524]

Park YH, Koo SK, Kim Y, Kim HM, Joe IY, Park CS, Kim SC, Han DJ, Lim DG. Effect of in vitroexpanded CD4(+)CD25(+)Foxp3(+) regulatory T cell therapy combined with lymphodepletion in murine skin allotransplantation. Clinical immunology. 2010; 135:43–54. [PubMed: 20006940]

Rao BM, Driver I, Lauffenburger DA, Wittrup KD. Interleukin 2 (IL-2) variants engineered for increased IL-2 receptor alpha-subunit affinity exhibit increased potency arising from a cell surface ligand reservoir effect. Mol Pharmacol. 2004; 66:864–869. [PubMed: 15385640]

Ring AM, Lin JX, Feng D, Mitra S, Rickert M, Bowman GR, Pande VS, Li P, Moraga I, Spolski R, et al. Mechanistic and structural insight into the functional dichotomy between IL-2 and IL-15. Nature immunology. 2012; 13:1187–1195. [PubMed: 23104097]

Rojas G, Cabrera Infante Y, Pupo A, Carmenate T. Fine epitope specificity of antibodies against interleukin-2 explains their paradoxical immunomodulatory effects. mAbs. 2014; 6:273–285. [PubMed: 24253188]

Rojas G, Pupo A, Leon K, Avellanet J, Carmenate T, Sidhu S. Deciphering the molecular bases of the biological effects of antibodies against Interleukin-2: a versatile platform for fine epitope mapping. Immunobiology. 2013; 218:105–113. [PubMed: 22459271]

Rosenberg SA. Raising the bar: the curative potential of human cancer immunotherapy. Science translational medicine. 2012; 4:127ps128.

Roy A, Kucukural A, Zhang Y. I-TASSER: a unified platform for automated protein structure and function prediction. Nature protocols. 2010; 5:725–738.

Shevach EM. Application of IL-2 therapy to target T regulatory cell function. Trends in immunology. 2012; 33:626–632. [PubMed: 22951308]

Siegel JP, Sharon M, Smith PL, Leonard WJ. The IL-2 receptor beta chain (p70): role in mediating signals for LAK, NK, and proliferative activities. Science. 1987; 238:75–78. [PubMed: 3116668]

Tang Q, Adams JY, Penaranda C, Melli K, Piaggio E, Sgouroudis E, Piccirillo CA, Salomon BL, Bluestone JA. Central role of defective interleukin-2 production in the triggering of islet autoimmune destruction. Immunity. 2008; 28:687–697. [PubMed: 18468463]

Taniguchi T, Minami Y. The IL-2/IL-2 receptor system: a current overview. Cell. 1993; 73:5–8. [PubMed: 8462103]

Thanos CD, DeLano WL, Wells JA. Hot-spot mimicry of a cytokine receptor by a small molecule. Proceedings of the National Academy of Sciences of the United States of America. 2006; 103:15422–15427. [PubMed: 17032757]

Thanos CD, Randal M, Wells JA. Potent small-molecule binding to a dynamic hot spot on IL-2. Journal of the American Chemical Society. 2003; 125:15280–15281. [PubMed: 14664558]

Tomala J, Chmelova H, Mrkvan T, Rihova B, Kovar M. In vivo expansion of activated naive CD8+ T cells and NK cells driven by complexes of IL-2 and anti-IL-2 monoclonal antibody as novel approach of cancer immunotherapy. Journal of immunology. 2009; 183:4904–4912.

Verdeil G, Marquardt K, Surh CD, Sherman LA. Adjuvants targeting innate and adaptive immunity synergize to enhance tumor immunotherapy. Proceedings of the National Academy of Sciences of the United States of America. 2008; 105:16683–16688. [PubMed: 18936481]

Waldmann TA. The biology of interleukin-2 and interleukin-15: implications for cancer therapy and vaccine design. Nat Rev Immunol. 2006; 6:595–601. [PubMed: 16868550]

Wang X, Rickert M, Garcia KC. Structure of the quaternary complex of interleukin-2 with its alpha, beta, and gammac receptors. Science. 2005; 310:1159–1163. [PubMed: 16293754]

Webster KE, Walters S, Kohler RE, Mrkvan T, Boyman O, Surh CD, Grey ST, Sprent J. In vivo expansion of T reg cells with IL-2-mAb complexes: induction of resistance to EAE and long-term acceptance of islet allografts without immunosuppression. The Journal of experimental medicine. 2009; 206:751–760. [PubMed: 19332874]

Zhang Y. I-TASSER server for protein 3D structure prediction. BMC bioinformatics. 2008; 9:40. [PubMed: 18215316]

HIGHLIGHTS

- JES6-1 blocks IL-2/IL-2Rβ interaction and allosterically disrupts IL-2/IL-2Rα binding

- JES6-1 selectivity for IL-2Rα^{hi} cells perpetuated by transcriptional feedback loop

- S4B6 sterically blocks IL-2/IL-2Rα interaction but enhances IL-2/IL-2Rβ interaction

- JES6-1-mediated IL-2Rα^{hi} cell growth bias inhibits colitis pathogenesis in mice
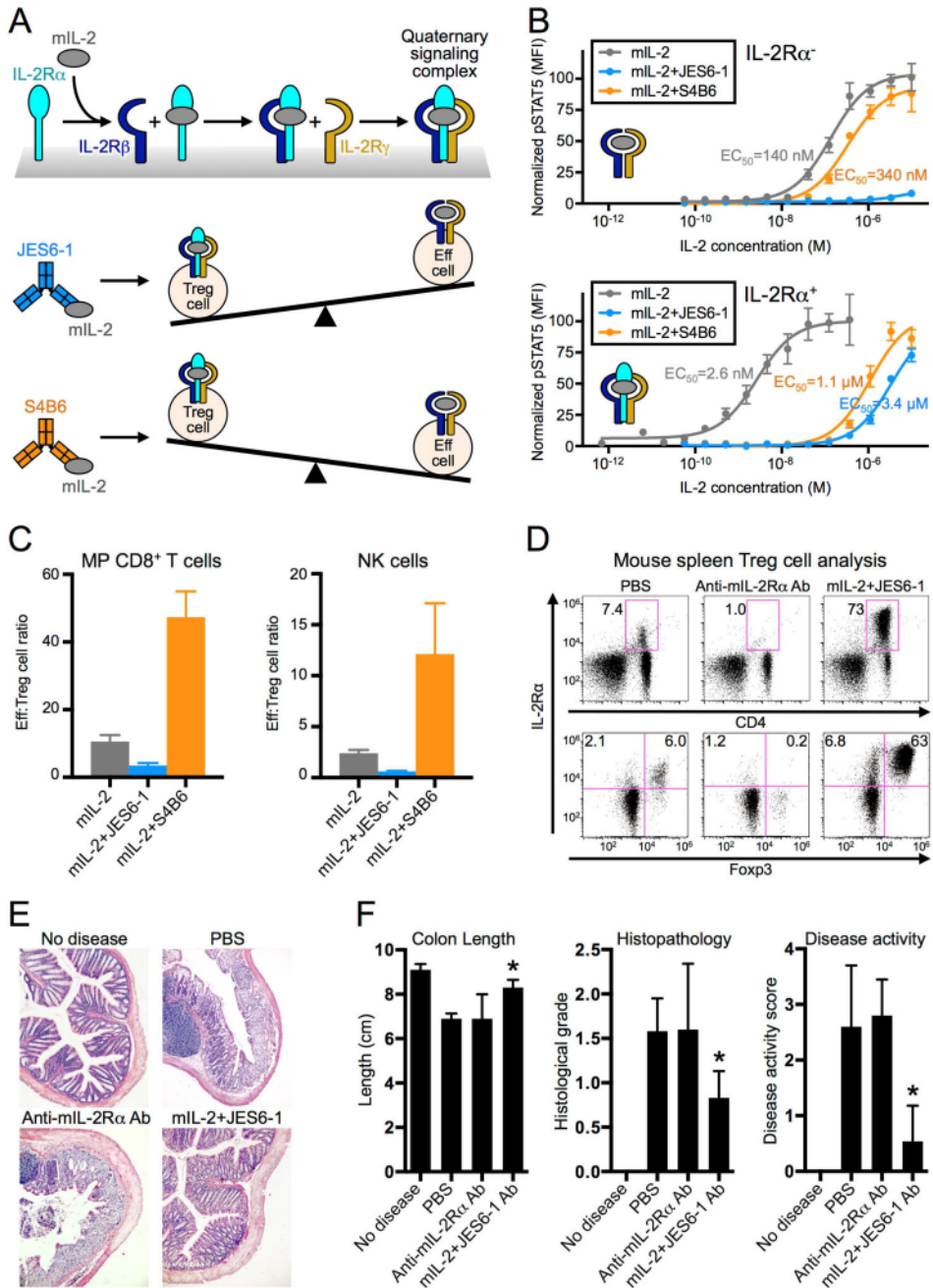
Figure 1. Anti-IL-2 antibodies bias cytokine signaling and functional outcomes
(A) Schematic of IL-2 cytokine-receptor quaternary complex formation (top) and regulatory
(Treg) versus effector (Eff) immune cell proliferation biases induced by mIL-2:JES6-1
(middle) and mIL-2:S4B6 (bottom) immunocomplexes. (B) STAT5 phosphorylation
response to mIL-2 or mIL-2:antibody immunocomplex treatment in IL-2Ra$^-$ (top) or
IL-2Ra$^+$ (bottom) YT-1 human NK cells. Half-maximal effective concentrations (EC$_{50}$s) for
STAT5 activation are indicated. Data are representative of three independent experiments.
(C) C57BL/6 mouse spleen effector cell:Treg cell ratios following mIL-2 or
immunocomplex treatment. Data are representative of two independent experiments. (D)

Treg cell expansion in BALB/c mouse spleens in response to anti-mIL-2Rα antibody (Ab) or mIL-2:JES6-1 treatment. Top plots display the percentage of CD4$^+$ cells that are IL-2Rα$^+$. Bottom plots show only CD4$^+$ cells and the percentages of Treg (IL-2Rα$^+$FoxP3$^+$) cells and IL-2Rα$^+$FoxP3$^-$ cells are shown for each treatment condition. (E) Colon histopathology of colitis-induced BALB/c mice pretreated with anti-mIL-2Rα Ab or mIL-2:JES6-1. (F) Evaluation of disease progression indicators for treated mice. *$P<0.05$ by Student's *t*-test (colon length) or Mann-Whitney *U* test (histological grade and disease activity score). All error bars indicate SD. Also see Figure S1.
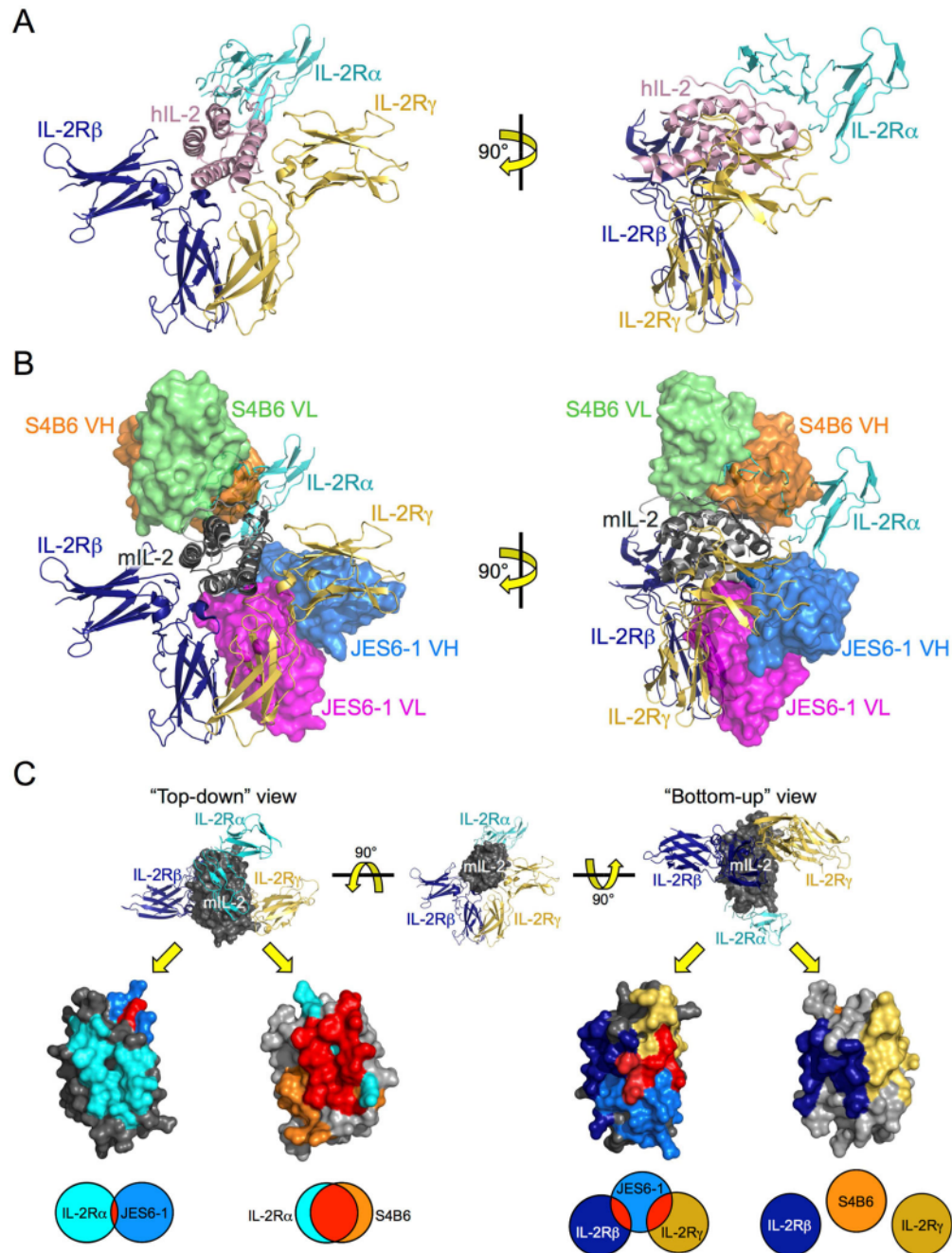
Figure 2. mIL-2:JES6-1 and mIL-2:S4B6 complex structures reveal basis for competitive binding between anti-IL-2 antibodies and IL-2 receptor

(A) Orthosteric views of the hIL-2 cytokine-receptor quaternary complex (PDB ID 2B5I) comprised of hIL-2 (pink), IL-2Rα (cyan), IL-2Rβ (navy), and IL-2Rγ (gold). (B) Overlay of the mIL-2:JES6-1 and mIL-2:S4B6 complex structures on the hIL-2 quaternary complex. Both JES6-1-bound mIL-2 (dark gray) and S4B6-bound mIL-2 (light gray) are presented, with the JES6-1 variable heavy (VH, blue) and light (VL, magenta) and the S4B6 VH (orange) and VL (green) chains shown as surface representations. Crystallographic statistics for mIL-2:antibody complexes are provided in Table S1. (C) "Top-down" (left) and

"bottom-up" (right) views of JES6-1-bound mIL-2 (dark gray) and S4B6-bound mIL-2 (light gray) with the predicted binding epitopes of IL-2Ra (cyan), IL-2Rβ (navy), IL-2R (gold), JES6-1 (blue), and S4B6 (orange) on the mIL-2 cytokine shaded. Residues shared between the mIL-2:antibody and the mIL-2:IL-2Ra, mIL-2:IL-2Rβ, or mIL-2:IL-2R interfaces are colored red. Venn diagrams at bottom indicate the relative extent of overlap between the antibody and receptor epitopes. Also see Figure S2.
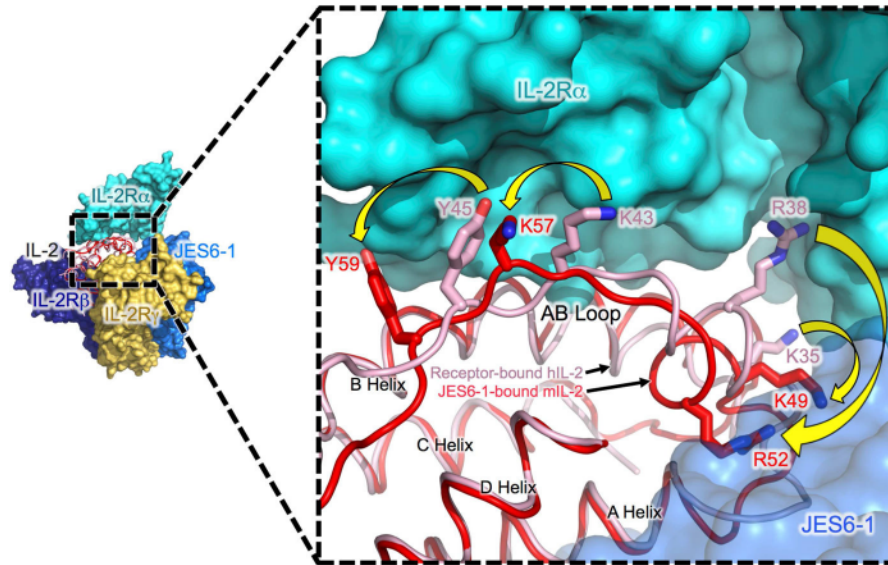
Figure 3. JES6-1 allosterically obstructs IL-2Rα binding to IL-2 via epitope distortion
Overlay of the hIL-2 quaternary complex (PDB ID 2B5I) with the mIL-2:JES6-1 complex. Surface depictions of the IL-2Rα (cyan), IL-2Rβ (navy), and IL-2Rγ (gold) subunits and the JES6-1 antibody (blue) and cartoon representations of receptor-bound hIL-2 (pink) and JES6-1-bound mIL-2 (red) are shown. An enlargement of the IL-2Rα binding site is provided at right with key IL-2Ra-interacting residues in the hIL-2 AB loop and the corresponding JES6-1-bound mIL-2 residues labeled. Arrows highlight differences between the structures. Also see Figure S3.
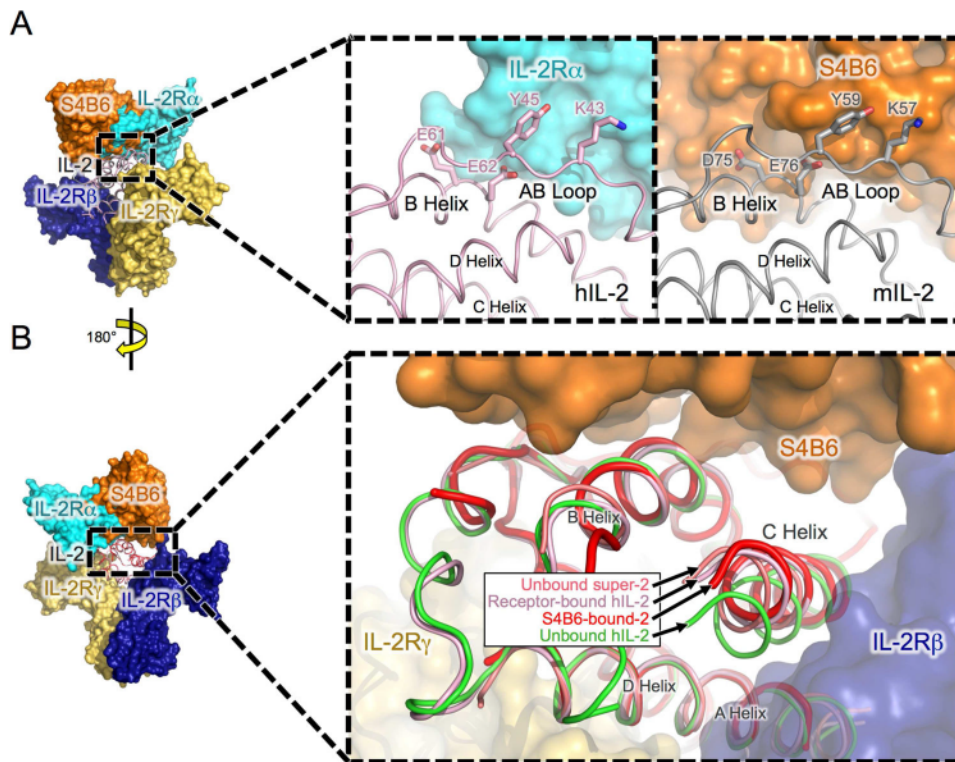
Figure 4. S4B6 mimics the IL-2Ra subunit, allosterically enhancing binding of IL-2Rβ
(A) Overlay of hIL-2 (pink) bound to IL-2Rα (cyan), IL-2Rβ (navy), and IL-2Rγ and mIL-2 (light gray) bound to S4B6 (orange) with detailed views of the hIL-2:hIL-2Ra (left) and mIL-2:S4B6 (right) interfaces in the AB loops and B helices of the cytokines juxtaposed at right. Analogous human and mouse IL-2 residues implicated in both interactions are labeled. (B) Superposition of cytokine orientations proximal to the IL-2Rβ binding site for unbound super-2 (PDB ID 3QB1, salmon), receptor-bound hIL-2 from the quaternary complex (PDB ID 2B5I, pink), S4B6-bound mIL-2 (red), and unbound hIL-2 (PDB ID 3INK, green). Also see Figure S4.
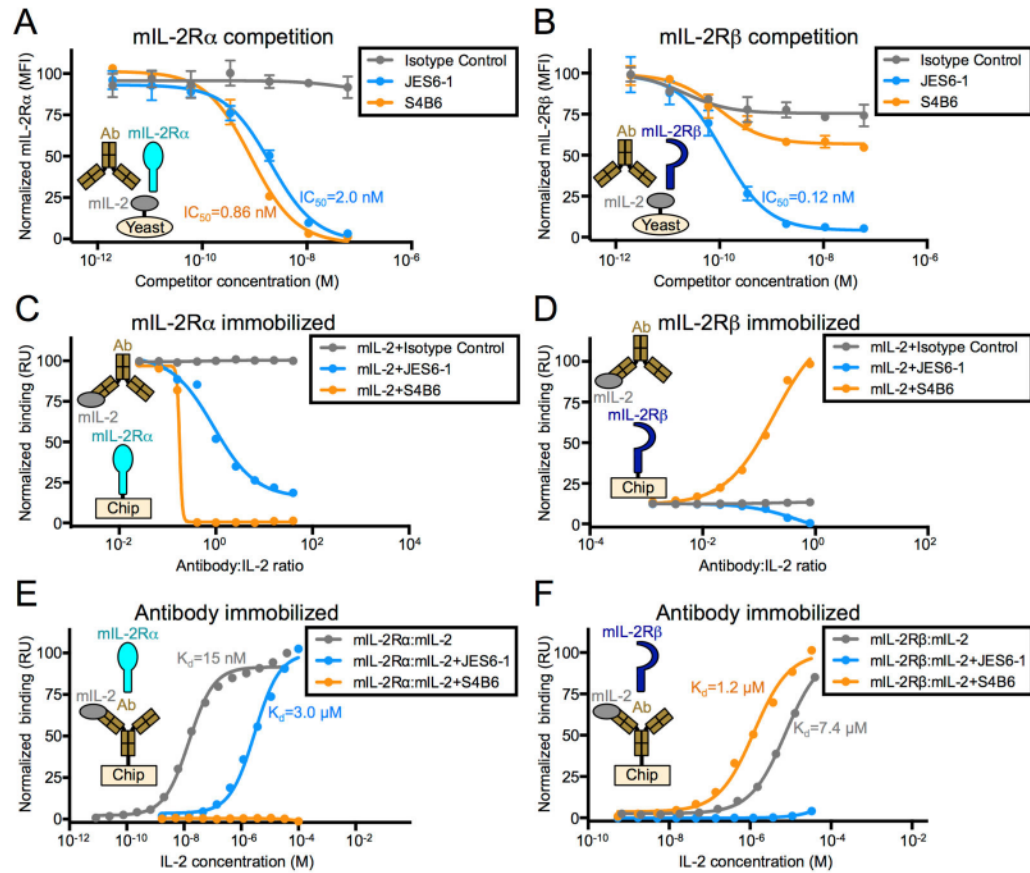
Figure 5. Anti-IL-2 antibodies and IL-2 receptor compete for cytokine binding
Yeast surface mIL-2 competition studies between anti-mIL-2 antibodies (Abs) and saturating concentrations of mIL-2Rα (A) or mIL-2Rβ (B) are shown (Error bars, SD). Data are representative of three independent experiments. Half maximal inhibitory concentrations (IC$_{50}$s) of the antibodies are indicated. Equilibrium surface plasmon resonance titrations of mIL-2:antibody immunocomplex interactions with immobilized mIL-2Rα (C) or mIL-2Rβ (D) and mIL-2Rα (E) or mIL-2Rβ (F) interactions with unbound mIL-2 compared to interactions with immobilized mIL-2:antibody immunocomplexes are presented. Also see Figure S5.
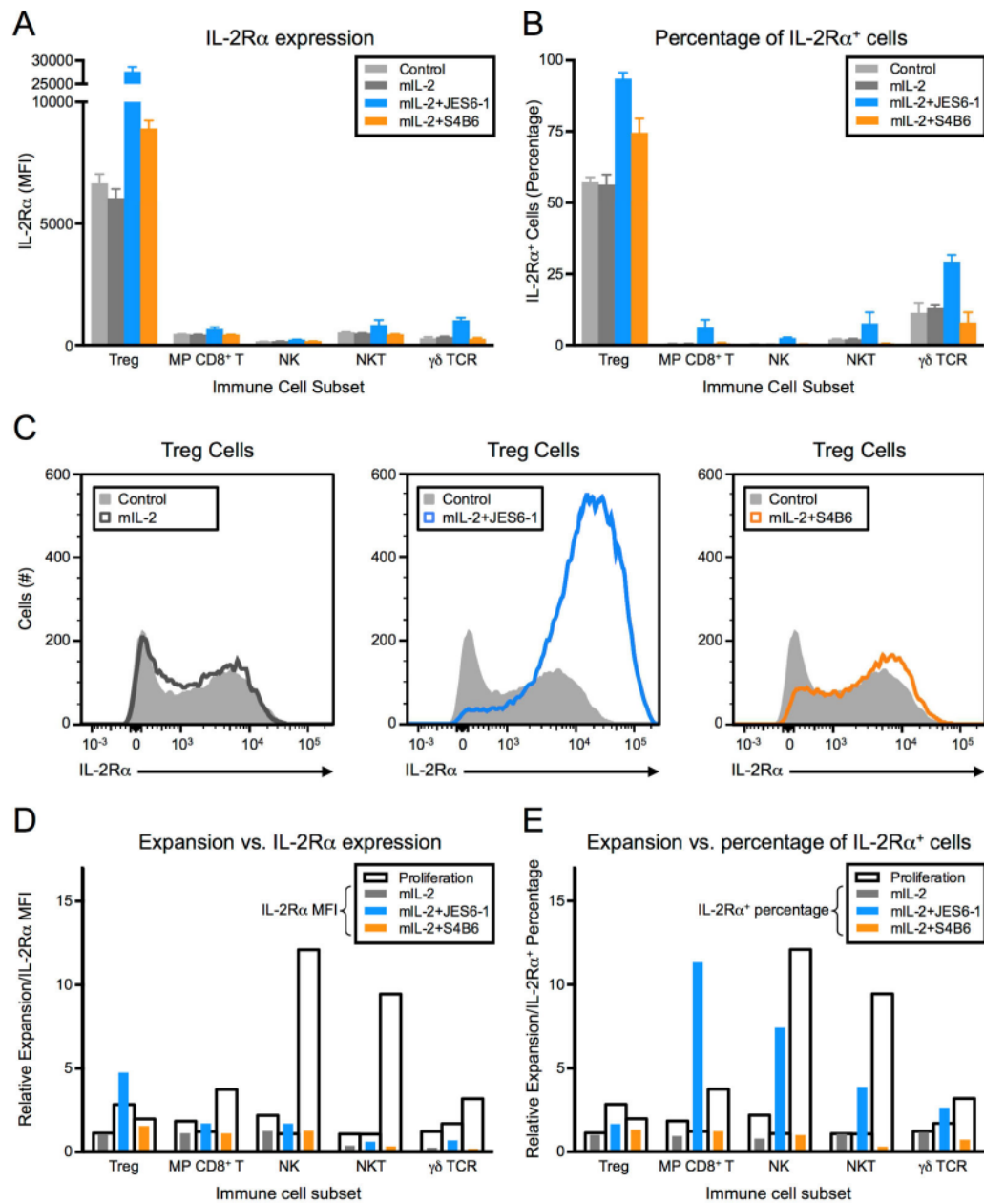
Figure 6. mIL-2:JES6-1 immunocomplex induces increased IL-2Rα expression to create a positive feedback loop favoring IL-2Rα^hi cell signaling

(A) IL-2Rα expression quantification (mean fluorescence intensity, MFI) for five immune cell subsets (Treg, MP CD8$^+$ T, NK, NKT, and γ^d TCR) in BALB/c mouse spleens following treatment with mIL-2 or mIL-2:antibody immunocomplex. (B) Percentage of IL-2Rα$^+$ cells within each immune cell subset in treated mouse spleens. (C) IL-2Rα expression histograms for Treg cells isolated from treated mouse spleens. Representative plots from one mouse per cohort are presented. (D) Relative cell expansion (transparent thick bars) and IL-2Rα expression quantification (solid thin bars) in treated mouse spleens. Responses for each treatment cohort are normalized to those of untreated control mice for each cell subset. (E) Relative cell expansion (transparent thick bars) and IL-2Rα$^+$ cell

percentage (solid thin bars) in treated mouse spleens, normalized as in (D). Error bars indicate SD. Data are representative of two independent experiments.

SUPPLEMENTAL INFORMATION

Figures S1-S6

Table S1

Supplemental Experimental Procedures

Supplemental References
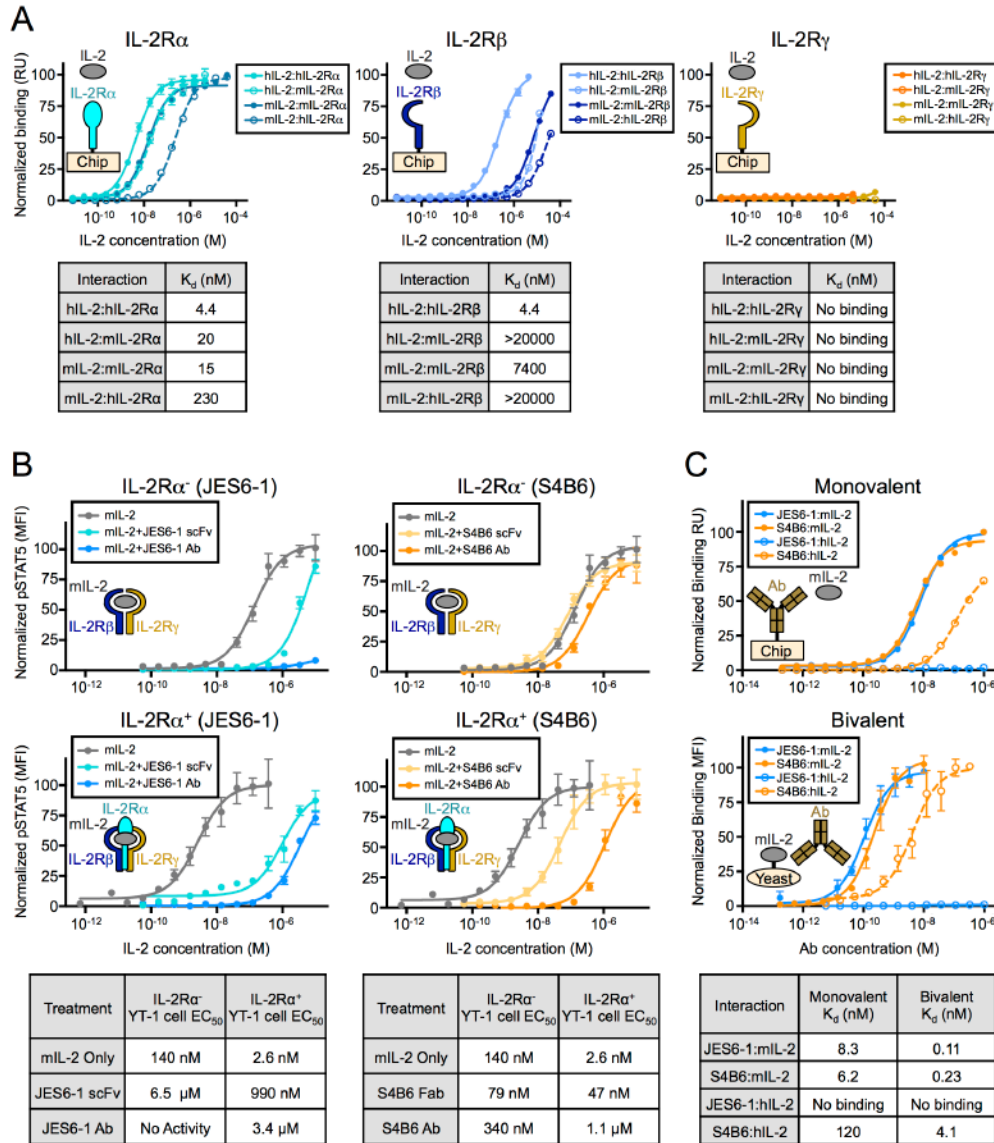
Figure S1, Related to Figure 1: Human and mouse IL-2 receptor subunits cross-react, anti-IL-2 antibodies and antibody fragments induce similar signaling effects, and bivalent affinities of anti-IL-2 antibodies are >25-fold tighter than their respective monovalent affinities. (A) Surface plasmon resonance (SPR) equilibrium titrations of mouse or human IL-2Rα, IL-2Rβ, or IL-2Rγ subunits binding to either the mouse or human IL-2 cytokine. Fitted equilibrium dissociation constant (K_d) values are presented below, assuming first-order binding interactions. Note the formidable cross-species reactivity for both the IL-2/IL-2Rα and hIL-2/IL-2Rβ interactions. IL-2Rγ does not bind IL-2 independently, but rather requires cooperativity with the IL-2Rβ subunit. (B) STAT5 phosphorylation response to either unbound mIL-2, mIL-2 pre-bound to the JES6-1 scFv, and mIL-2 pre-bound to the full JES6-1 antibody (Ab, left) or to unbound mIL-2, mIL-2 pre-bound to the S4B6 Fab, and mIL-2 pre-bound to the full S4B6 antibody (right) in IL-2Rα⁻ (top) or IL-2Rα⁺ (bottom) YT-1 human NK cells. Data are representative of three independent experiments. Fitted half maximal effective

concentrations (EC$_{50}$s) for each treatment condition are tabulated below. Note that antibody fragments exert the same effects on IL-2 signaling as do the full antibodies, but with attenuated potency due to their reduced affinities for the cytokine. (C) SPR equilibrium titrations of mIL-2 and hIL-2 binding to immobilized JES6-1 or S4B6 antibodies (top) and equilibrium titrations of bivalent JES6-1 and S4B6 antibodies binding to yeast surface-displayed mIL-2 and hIL-2 (bottom). Computed equilibrium dissociation constant (K$_d$) values are provided in the table below, assuming first-order binding interactions. Note that the mIL-2 affinities of the monovalent antibodies are >25-fold weaker than those of their bivalent counterparts. Also, hIL-2 has limited cross-reactivity with S4B6 and no cross-reactivity with JES6-1. All error bars represent SD.
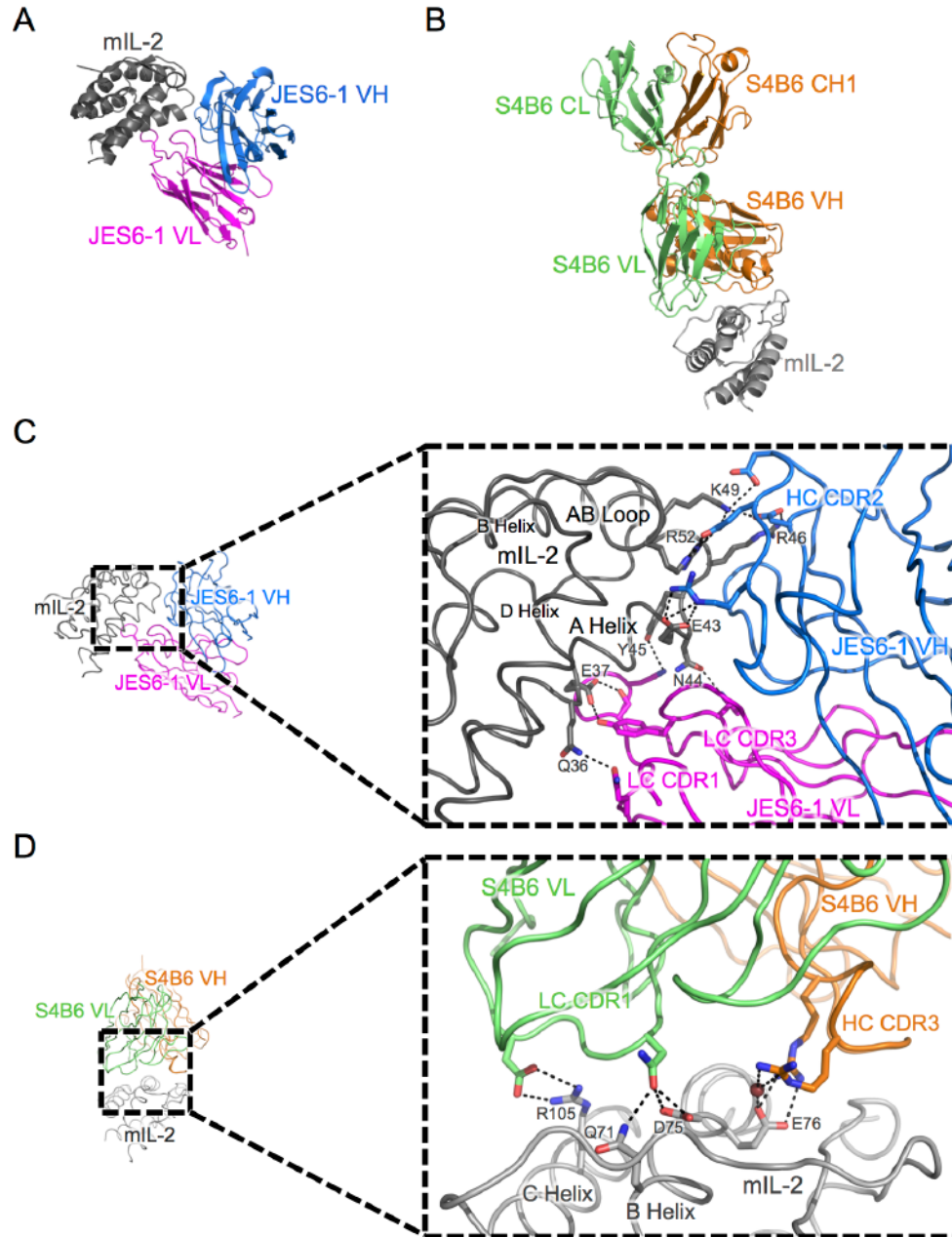
Figure S2, Related to Figure 2: JES6-1 and S4B6 engage mIL-2 with distinct binding topologies and form extensive interaction interfaces with the cytokine. (A) Crystal structure of mIL-2 (dark gray) bound to the scFv fragment of JES6-1 with the variable heavy (VH, blue) and light (VL, magenta) chains indicated. (B) Crystal structure of mIL-2 (light gray) bound to the S4B6 Fab with the VH (orange), VL (green), constant heavy 1 (CH1, orange), and constant light (CL, green) chains denoted. (C)-(D) Detailed views of the mIL-2/JES6-1 (C) and mIL-2/S4B6 (D) interfaces (colored as in panels (A) and (B), respectively), with key interacting residues on the cytokine and antibody shown as sticks. The mIL-2/JES6-1 interface primarily comprises the mIL-2 A helix and AB loop and heavy chain (HC) complementarity determining region (CDR)-2, light chain (LC) CDR1, and LC CDR3 of JES6-1, whereas the mIL-2/S4B6 interface is localized to

the mIL-2 B and C helices and HC CDR3 and LC CDR1 of S4B6. Black dashes represent hydrogen bonds and salt bridges. A coordinated water molecule is shown in brown. Crystallographic statistics for mIL-2/antibody complexes are provided in **Table S1**.
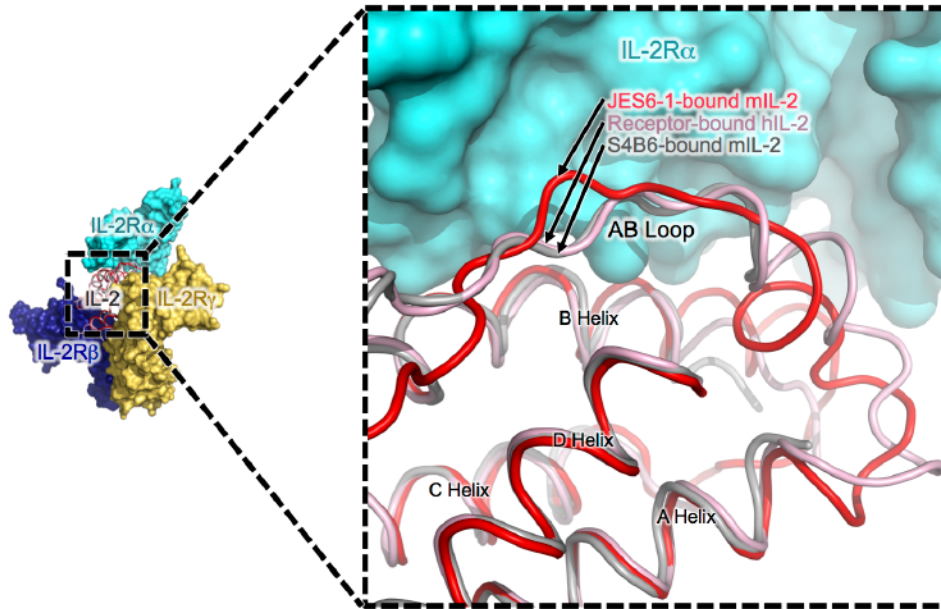
Figure S3, Related to Figure 3: JES6-1 allosterically distorts the IL-2 structure proximal to the IL-2Rα binding site. JES6-1-bound mIL-2 (red), receptor-bound hIL-2 from the quaternary complex (PDB ID 2B5I, pink), and S4B6-bound mIL-2 (light gray) are aligned. Surface representations of IL-2Rα (cyan), IL-2Rβ (navy), and IL-2Rγ (gold) are provided for context. A detailed view of the main chains for the three aligned cytokines near the IL-2Rα binding site is presented at right. Note that the structures overlay well in all regions of the cytokine with the exception of the IL-2Rα-interacting AB loop, where the JES6-1-bound cytokine diverges drastically from the receptor-bound hIL-2, which overlays closely with the S4B6-bound mIL-2. JES6-1-induced distortion of the AB loop disrupts binding of IL-2Rα in the presence of the antibody.
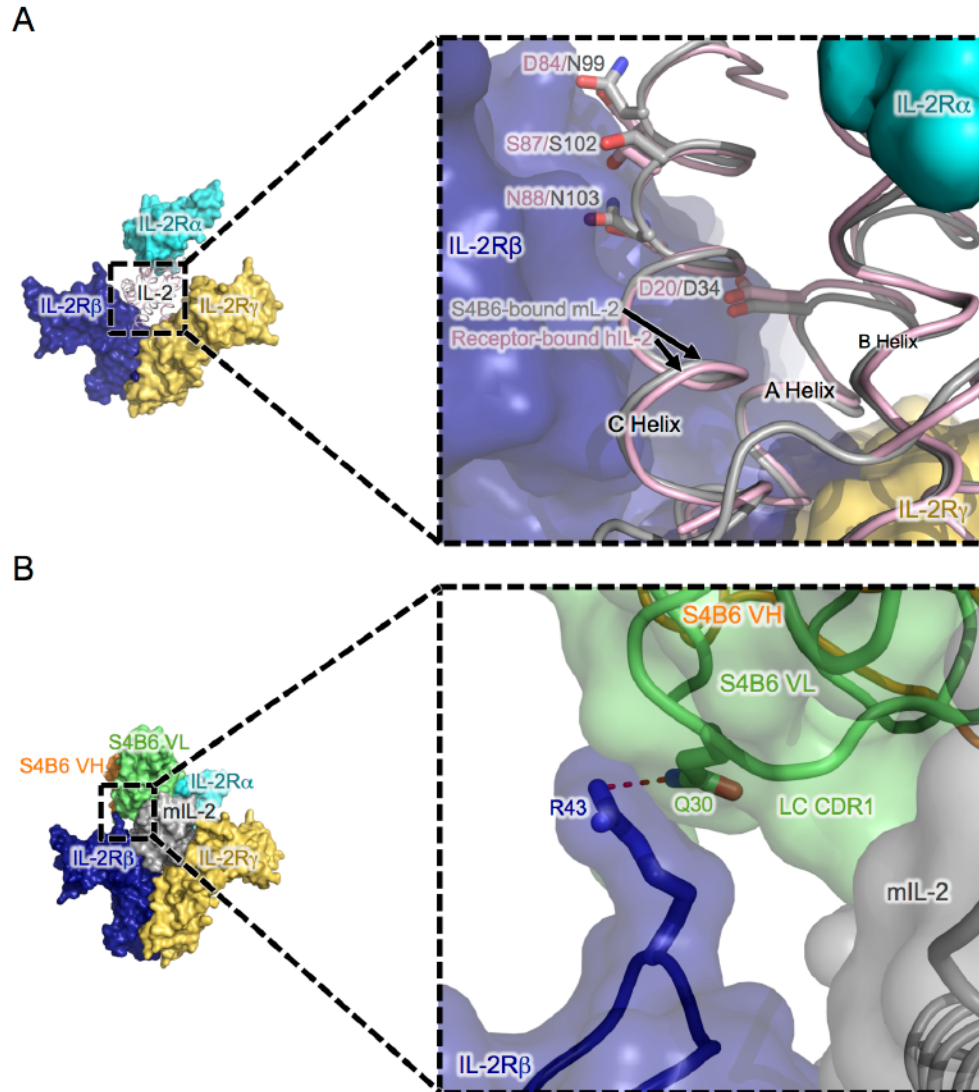
Figure S4, Related to Figure 4: The IL-2/IL-2Rβ interface is highly conserved between receptor-bound and S4B6-bound IL-2 but a steric clash impairs the IL-2/IL-2Rβ interaction in the presence of antibody. (A) S4B6-bound mIL-2 (light gray) and receptor-bound hIL-2 from the quaternary complex structure (PDB 2B5I, pink) are overlaid with surface renderings of the IL-2Rα (cyan), IL-2Rβ (navy), and IL-2Rγ (gold) subunits shown for context. Critical hIL-2 residues involved in the hIL-2/IL-2Rβ interaction are labeled, as are their mIL-2 counterparts in the S4B6-bound structure. Note the similarity between the antibody-bound and receptor-bound cytokine structures in the vicinity of the IL-2Rβ binding site (the A and C helices of the cytokine). (B) Overlay of the mIL-2/S4B6 and hIL-2 quaternary complex structures, colored as in (A), with surface representations of the S4B6 variable heavy (VH, orange) and light (VL, green) chains also shown. The predicted clash between the S4B6 LC CDR1 and domain 1 of IL-2Rβ is indicated with a red dashed line. This unfavorable interaction is predicted to hinder IL-2/IL-2Rβ association when the S4B6 antibody is bound to the cytokine.
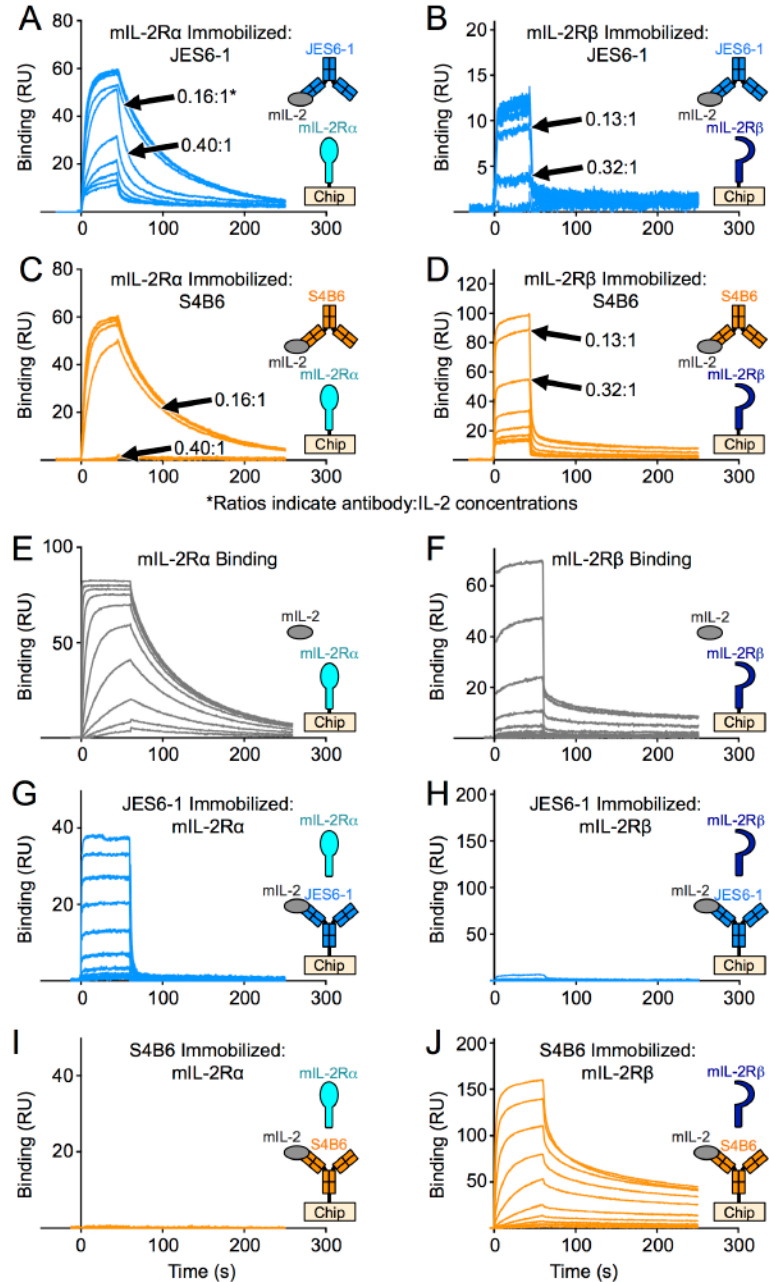
Figure S5, Related to Figure 5: Kinetic characterization illustrates anti-IL-2 antibody effects on IL-2 cytokine-receptor interactions. SPR kinetic profiles for soluble mIL-2/JES6-1 immunocomplex interactions with immobilized mIL-2Rα (A) and mIL-2Rβ (B) and soluble IL-2/S4B6 immunocomplex interactions with immobilized mIL-2Rα (C) and mIL-2Rβ (D) are presented. Individual curves in panels (A)-(D) represent unique antibody (Ab):receptor ratios. Note the fundamental differences in the JES6-1- and S4B6-bound cytokine interactions with the receptor subunits: mIL-2 exhibits an increased mIL-2Rα dissociation rate with increasing JES6-1:mIL-2 ratios whereas mIL-2 loses binding to mIL-2Rα when S4B6:mIL-2 ratios exceed 0.4:1, and mIL-2 binding to mIL-2Rβ is drastically reduced between JES6-1:mIL-2 ratios of 0.13:1 and 0.32:1 whereas mIL-2 simultaneously binds mIL-2Rβ and S4B6. SPR kinetic profiles for

mIL-2 interactions with immobilized mIL-2Rα (E) or mIL-2Rβ (F), soluble mIL-2Rα (G) or mIL-2Rβ (H) interactions with immobilized mIL-2/JES6-1 immunocomplex, and soluble mIL-2Rα (I) or mIL-2Rβ (J) interactions with immobilized mIL-2/S4B6 immunocomplex are also shown. Individual curves in panels (E)-(J) represent unique concentrations of the soluble species. JES6-1 accelerates the dissociation rate of the mIL-2/mIL-2Rα complex whereas S4B6 blocks mIL-2/mIL-2Rα complex formation altogether and JES6-1 abrogates mIL-2/mIL-2Rβ binding whereas S4B6 slows both the association and dissociation rates of the mIL-2/mIL-2Rβ complex.
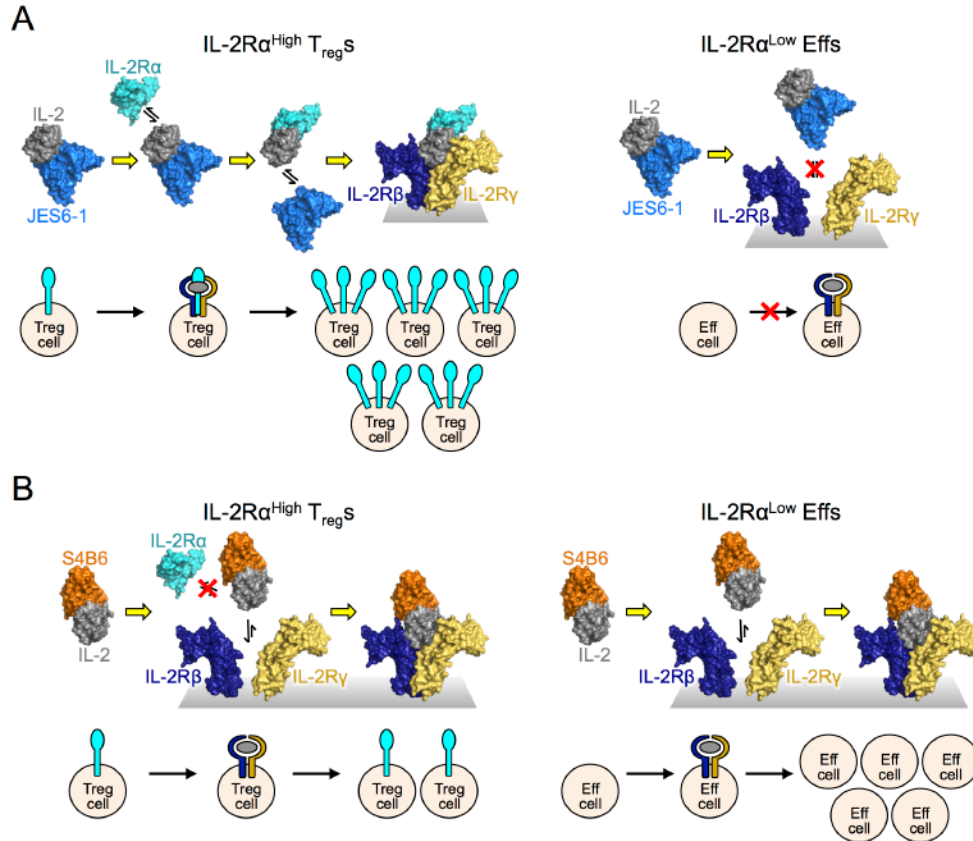
Figure S6. Proposed structure-based mechanistic model rationalizes biased immune cell proliferation responses to anti-IL-2 antibodies. (A) On IL-2Rα^{hi} Treg cells (left), the IL-2Rα subunit displaces the JES6-1 antibody from mIL-2 to allow for formation of the high-affinity IL-2 quaternary complex. Signal activation and preferential stimulation of IL-2Rα^{hi} cells leads to IL-2Rα upregulation, creating a positive feedback loop for IL-2Rα expression that heightens cytokine sensitivity. On IL-2Rα^{lo} effector cells (right), JES6-1-bound mIL-2 is sterically obstructed from binding to the IL-2Rβ and IL-2Rγ subunits and thus cannot form a functional signaling complex. (B) On IL-2Rα^{hi} Treg cells (left), S4B6-bound mIL-2 is sterically obstructed from binding to the IL-2Rα subunit but is primed for binding to the IL-2Rβ subunit and forms the IL-2 ternary complex. On IL-2Rα^{lo} effector cells (right), S4B6-bound mIL-2 also forms the IL-2 ternary complex. Thus, S4B6-bound mIL-2 stimulates growth of both IL-2Rα[hi] and IL-2Rα^{lo} cells, and immunocomplex sensitivity is determined by IL-2Rβ expression, favoring potentiation of IL-2Rβ^{hi} effector cells.

	mIL-2/JES6-1 scFv	mIL-2/S4B6 Fab
Data Collection		
Space Group	P 31 2 1	P 21 21 21
Cell Dimensions (a, b, c [Å])	99.0, 99.0, 198.7	43.08, 77.56, 169.04
(α, β, γ [°])	90.0, 90.0, 120.0	90.0, 90.0, 90.0
Resolution (Å)	49.67-2.82 (2.92-2.82)[a]	57.15-2.19 (2.27-2.19)
R_{merge}	0.101 (0.580)	0.107 (1.468)
I/σ	12.3 (1.7)	12.11 (1.26)
Completeness (%)	99.0 (81.8)	99.0 (96.0)
Redundancy	2.4 (1.9)	6.5 (6.3)
Refinement Statistics		
Resolution range (Å)	48.04-2.83 (2.93-2.83)	57.15-2.19 (2.27-2.19)
R_{work} reflections ($F > 0$)	27531 (2519)	29457 (2835)
R_{free} reflections	1359 (128)	1475 (143)
R_{work}	0.1694 (0.2301)	0.2032 (0.3278)
R_{free}	0.2041 (0.3202)	0.2316 (0.3496)
Atoms		
Protein	5668	4227
Ligand-ion	76	6
Water	81	223
B-factors		
Protein	63.58	54.67
Ligand-ion	106.76	58.50
Water	49.02	49.01
RMSD		
Bond-lengths (Å)	0.005	0.008
Bond-angles (°)	0.86	1.19
Ramachandran favored (outliers) %	98.0 (0.14)	99.0 (0.0)

Table S1, Related to Figure 2: Crystallographic statistics for mIL-2/antibody complexes Data collection and refinement statistics are provided for solution of the crystal structures of the mIL-2/JES6-1 single-chain variable fragment (scFv) and mIL-2/S4B6 Fab complexes. [a]Values in parentheses are for highest-resolution shell.

SUPPLEMENTAL EXPERIMENTAL PROCEDURES

Protein expression and purification. The sequence encoding hexahistidine-tagged mIL-2 (amino acids 1-149) was cloned into the pMal vector with an N-terminal maltose-binding protein (MBP) followed by a 3C protease site. mIL-2 was expressed in the periplasm of BL21(DE3) *Escherichia coli* cells by 20 h induction at 22° C with 1 mM isopropyl β-d-thiogalactopyranoside (IPTG). Protein in the periplasmic compartment was isolated by osmotic shock and purified by nickel-nitrilotriacetic acid (Ni-NTA) (Qiagen) affinity chromatography. Purity was improved through size-exclusion chromatography on a Superdex-75 column (GE Healthcare) in HEPES-buffered saline (HBS) (150 mM NaCl in 10 mM HEPES pH 7.3). For crystallization, a truncated version of mIL-2 (amino acids 27-149) was used, eliminating the N-terminal poly-glutamine sequence.

hIL-2 (amino acids 1-133), hIL-2Rα ectodomain (amino acids 1-217), hIL-2Rβ ectodomain (amino acids 1-214), hIL-2Rγ ectodomain (amino acids 1–232), mIL-2Rα ectodomain (amino acids 1-213), mIL-2Rβ ectodomain (amino acids 1-215), and mIL-2Rγ ectodomain (amino acids 34-233) were secreted and purified using a baculovirus expression system, as previously described (Wang et al., 2005). All proteins were purified to >98% homogeneity with a Superdex 200 sizing column (GE Healthcare) equilibrated in HBS.

For biotinylated protein expression, human or mouse IL-2 receptor subunits with C-terminal biotin acceptor peptides (BAP)-LNDIFEAQKIEWHE were expressed and purified via Ni-NTA affinity chromatography and then biotinylated with the soluble BirA

ligase enzyme in 0.5 mM Bicine pH 8.3, 100 mM ATP, 100 mM magnesium acetate, and 500 mM biotin (Sigma). Excess biotin was removed by size exclusion chromatography on a Superdex 200 column equilibrated in HBS.

The JES6-1 hybridoma cell line (Abrams et al., 1992) was kindly provided by Onur Boyman and the S4B6 hybridoma cell line (Zurawski et al., 1986) (commercially available as ATCC clone HB-10968) was obtained. The variable heavy (VH) and light (VL) chains of both JES6-1 and S4B6 were cloned out of their respective hybridoma cell lines by isolating and reverse transcribing DNA and subsequently extracting the variable chains via PCR using conserved rat IgG2A framework and constant domain primers for the HC and conserved rat kappa framework and constant domain primers for the LC, as described previously (Dubel et al., 1994). Antibody variable domain framework and CDR regions were delineated using the International Immunogenetics Information System (IMGT) V-QUEST tool (Brochet et al., 2008; Giudicelli et al., 2011). For JES6-1 scFv expression, the identified antibody VH and VL domains separated by a (Gly$_4$Ser)$_3$ linker were cloned into the pAcGP67A vector for transfection. For S4B6 Fab expression, the identified VH followed by the rat IgG2A constant heavy 1 (CH1) domain and the identified VL domain followed by the rat kappa constant light (CL) domain were separately cloned into the pAcGP67A plasmid containing 3C protease-cleavable basic and acidic leucine zippers, respectively, for high-fidelity pairing of the Fab chains, as detailed previously (Bankovich et al., 2007; Chang et al., 1994). The S4B6 Fab HC and LC constructs were transfected independently and their corresponding viruses were co-titrated to determine optimal infection ratios for equivalent expression of the two chains.

Insect cell secretion and purification of the JES6-1 scFv and the S4B6 Fab proceeded as described for IL-2 cytokine and receptor subunits. The S4B6 Fab was treated with 3C to remove the leucine zippers prior to FPLC purification.

Full-length JES6-1 antibody was purchased commercially (eBioscience) and full-length S4B6 antibody, secreted and purified from the publicly available hybridoma cell line, was generously provided by Onur Boyman. For surface plasmon resonance (SPR) studies, antibodies were biotinylated using the EZ-Link Sulfo-NHS-LC-Biotinylation kit (Pierce) according to the manufacturer's protocol.

Cell Lines. Unmodified YT-1 (Yodoi et al., 1985) and IL-2Rα^+ YT-1 human natural killer cells (Kuziel et al., 1993) were cultured in RPMI complete medium (RPMI 1640 medium supplemented with 10% fetal bovine serum, 2 mM L-glutamine, minimum non-essential amino acids, sodium pyruvate, 25 mM HEPES, and penicillin-streptomycin [Gibco]) and maintained at 37º C in a humidified atmosphere with 5% CO_2.

The subpopulation of YT-1 cells expressing IL-2Rα was purified via magnetic selection as detailed previously (Ring et al., 2012). Ten million unsorted IL-2Rα^+ YT-1 cells were washed with FACS buffer (phosphate-buffered saline [PBS] pH 7.2 containing 0.1% bovine serum albumin) and incubated in FACS buffer with PE-conjugated anti-human IL-2Rα antibody (Biolegend, clone BC96) for 2 hr at 4° C. PE-labeled IL-2Rα^+ cells were then conjugated to paramagnetic microbeads coated with an anti-PE IgG for 20 min at 4º C, washed once with cold FACS buffer, and sorted on an LS MACS separation

column (Miltenyi Biotec) according to the manufacturer's protocol. Purified eluted cells were re-suspended and grown in RPMI complete medium. Enrichment of IL-2Rα cells was evaluated using an Accuri C6 flow cytometer (BD Biosciences) and persistence of IL-2Rα expression was monitored by PE-conjugated anti-human IL-2Rα antibody labeling and flow cytometric analysis of sorted IL-2Rα$^+$ YT-1 cells.

YT-1 cell STAT5 phosphorylation studies. Approximately 2×10^5 YT-1 or IL-2Rα$^+$ YT-1 cells were plated in each well of a 96-well plate and re-suspended in RPMI complete medium containing serial dilutions of mIL-2, mIL-2/antibody immunocomplexes, or mIL-2/antibody fragment complexes. Complexes were formed by incubating a 2:1 molar ratio of antibody or antibody fragment to mIL-2 for 30 min at room temperature. Cells were stimulated for 15 min at 37º C and immediately fixed by addition of formaldehyde to 1.5% and incubation for 10 min at room temperature. Permeabilization of cells was achieved by resuspension in ice-cold 100% methanol for 30 min at 4º C. The fixed and permeabilized cells were washed twice with FACS buffer and incubated with Alexa Fluor® 488-conjugated anti-STAT5 pY694 (BD Biosciences) diluted in FACS buffer for 2 hr at room temperature. Cells were then washed twice in FACS buffer and MFI was determined on an Accuri C6 flow cytometer. Dose-response curves were fitted to a logistic model and half-maximal effective concentrations (EC$_{50}$s) were calculated using GraphPad Prism data analysis software after subtraction of the MFI of unstimulated cells and normalization to the maximum signal intensity. Experiments were conducted in triplicate and performed three times with similar results.

Immune cell subset proliferation and receptor expression studies. For relative Eff:T_{reg} proliferation studies (**Figure 1C**), C57BL/6 mice (6 per cohort) were injected *i.p.* with mIL-2 immunocomplexes (prepared by pre-incubating 2 µg mIL-2 (Peprotech) with S4B6 or JES6-1 in a 2:1 cytokine:antibody molar ratio in PBS) or 10 µg of free mIL-2 on days 1, 2, 3, and 4. Mice were sacrificed on day 5 by cervical dislocation and spleens were harvested. Single-cell suspensions were prepared by homogenization (GentleMACS Dissociator, Miltenyi Biotec). Cells were resuspended in PBE buffer (PBS with 2.5% fetal calf serum [FCS], 2.5 mmol EDTA), blocked with 10% C57BL/6 mouse serum for 30 min on ice, and subsequently stained for 30 min on ice with fluorophore-conjugated anti-mouse monoclonal antibodies (mAbs) for phenotyping of: T_{reg}s (CD3$^+$CD4$^+$IL-2Rα^+Foxp3$^+$) - eFluor 450®-conjugated anti-CD3 (eBioscience, clone 17A2), PerCP-conjugated anti-CD4 (BD Biosciences, clone RM4-5), and APC-conjugated anti-IL-2Rα (eBioscience, clone PC61.5) mAbs; memory phenotype (MP) CD8$^+$ T cells (CD3$^+$CD8$^+$CD44$^+$IL-2Rβ^+) - eFluor 450®-conjugated anti-CD3, PerCP-Cy5.5-conjugated anti-CD8 (eBioscience, clone 53-7.62), APC-conjugated anti-CD44 (eBioscience, clone IM7), and PE-conjugated anti-IL-2Rβ (eBioscience, clone 5H4) mAbs; and NK cells (CD3$^-$CD49b$^+$NK1.1$^+$) - eFluor 450®-conjugated anti-CD3, FITC-conjugated anti-CD49b (eBioscience, clone DX5), and APC-conjugated anti-NK1.1 (eBioscience, clone PK136) mAbs. Cells were then washed twice with PBE buffer and fixed in Fixation/Permeabilization Buffer (BD Biosciences) for 1 hr on ice. After two washes in Permeabilization Buffer (BD Biosciences), cells were stained with PE-conjugated anti-mouse/rat Foxp3 mAb (eBioscience, clone FJK-16s) for 30 min on ice. Two final washes were conducted in Permeabilization Buffer and cells were resuspended

in PBE buffer for flow cytometric analysis on an LSRII (BD Biosciences). Data were analyzed using FlowJo software (Tree Star). The experiment was performed twice with similar results. Average ratios of the relative expansion of the indicated subsets are plotted.

For immune cell subset expansion and IL-2Rα profiling studies (**Figures 6A-E**), C57BL/6 mice (3 or 4 per cohort) were injected *i.p.* with mIL-2 immunocomplexes (prepared by pre-incubating 2 μg mIL-2 with S4B6 or JES6-1 in a 2:1 cytokine:antibody molar ratio in PBS) or 10 μg of free mIL-2 on days 1, 2, and 3. Mice were sacrificed on day 5 by cervical dislocation and spleens were harvested, homogenized, and analyzed by flow cytometry as described for relative Eff:T_{reg} proliferation studies. Five immune cell subsets were distinguished and profiled for IL-2Rα expression using the following fluorophore-conjugated anti-mouse mAbs: T_{reg}s ($CD3^+CD4^+Foxp3^+$) - V500 Horizon®-conjugated anti-CD3 (BD Biosciences, clone 500A2), PerCP-conjugated anti-CD4, PE-conjugated anti-mouse/rat Foxp3 (eBioscience, clone FJK-16s), and APC-conjugated anti-IL-2Rα mAbs; MP $CD8^+$ T cells ($CD3^+CD8^+CD44^+IL-2R\beta^+$) - V500 Horizon®-conjugated anti-CD3, PerCP-Cy5.5-conjugated anti-CD8, APC-conjugated anti-CD44, PE-conjugated anti-IL-2Rβ, and eFluor 450®-conjugated anti-IL-2Rα (eBioscience, clone PC61.5) mAbs; NK ($CD3^-CD49b^+CD161^+$) and NKT cells ($CD3^+CD49b^+CD161^+$) - V500 Horizon®-conjugated anti-CD3, PE-conjugated anti-CD49b (eBioscience, clone DX5), APC-conjugated anti-CD161 (eBioscience, clone PK136), and eFluor 450®-conjugated anti-IL-2Rα mAbs; and γδ TCR cells ($CD3^+CD49b^+\gamma\delta TCR^+$) - V500 Horizon®-conjugated anti-CD3, PE-conjugated anti-CD49b, PE-conjugated anti-γδ TCR

(eBioscience, clone GL3), and APC-conjugated anti-IL-2Rα mAbs. The experiment was performed twice with similar results. Average relative expansion compared to untreated control mice was determined for each cohort. Histograms show IL-2Rα expression profiles for one representative mouse out of 3 or 4 per cohort.

Mouse dextran sodium sulfate (DSS)-induced colitis model. BALB/c mice (six per condition) were injected *i.p.* either daily for seven days with PBS, once on day 6 with 150 mg anti-mIL-2Rα antibody (EXBIO, clone PC61.5), or daily for seven days with mIL-2/JES6-1 immunocomplexes (prepared by pre-incubating 1.5 μg mIL-2 with JES6-1 in a 2:1 molar ratio in PBS). On day 8, two mice per condition were sacrificed by cervical dislocation to assess spleen T_{reg} cell counts by flow cytometry. Spleen harvesting, homogenization, and T_{reg} marker analysis (CD3, CD4, IL-2Rα, and Foxp3) were performed as described for *in vivo* immune cell proliferation and receptor expression studies. Representative dot plots from one mouse per condition are shown.

The remaining four pretreated mice from each cohort were administered 3% DSS (MP Biomedicals Inc.) in their drinking water beginning on day 8 to induce colitis. On day 15, disease severity was assessed by a clinical disease activity index. CDAI was calculated on day 15 as described previously (Cooper et al., 1993), using the following parameters: body weight decrease (0= no change to 4 = >20% change); stool consistency (0 = solid to 4 = liquid stools that stick to the anus); and bleeding (0 = none to 4 = gross bleeding). Scores for each parameter were summed and divided by three to determine CDAI. On day 16, mice were sacrificed and their entire colons were removed (from

cecum to anus). Colon length was measured and shortening was used as an indirect marker of inflammation. Histological scoring of paraffin-embedded and hematoxylin and eosin-stained transversal colon sections was implemented in a blinded manner using a weighted score, ranging from 0 (no signs of inflammation) to 3 (severe inflammation). The final histological score was calculated as the mean score from 4 independently analyzed sections from each sample. One representative section from each condition is shown. The "no disease" cohort refers to an untreated group of mice in which colitis was not induced. Statistical significance was determined by either Student's *t*-test (colon length) or by Mann-Whitney *U* test (histological grade and disease activity score).

Yeast surface and SPR affinity titrations. For yeast studies, full-length human and mouse IL-2 were cloned into the pCT302 vector and presented on the surface of yeast as described previously (Boder and Wittrup, 1997; Rao et al., 2004). Yeast displaying hIL-2 and mIL-2 were incubated in FACS buffer containing serial dilutions of the full-length S4B6 or JES6-1 antibodies for 2 hr at room temperature. Cells were then washed and incubated for 20 min at 4º C with PE-conjugated anti-Rat IgG2A antibody (eBioscience, clone R2A-21B2) diluted in FACS buffer. After a final wash, cells were analyzed for antibody binding using an Accuri C6 flow cytometer. Background-subtracted and normalized binding curves were fitted to a first-order binding model and equilibrium dissociation constants (K_ds) were determined using GraphPad Prism. Studies were performed in triplicate and reproduced three times with similar results.

For SPR studies, biotinylated human and mouse IL-2Rα, IL-2Rβ, and IL-2Rγ receptors or biotinylated anti-IL-2 antibodies were immobilized to streptavidin-coated chips for analysis on a Biacore T100 instrument (GE Healthcare). An irrelevant biotinylated protein was immobilized in the reference channel to subtract non-specific binding. Less than 100 response units (RU) of each ligand was immobilized to minimize mass transfer effects. Serial dilutions of human or mouse IL-2 were flowed over the immobilized ligands for 60 s and dissociation was measured for 240 s. Surface regeneration for all interactions was conducted using 15 s exposure to 1 M $MgCl_2$ in 10 mM sodium acetate pH 5.5, with the exception of the mIL-2/antibody interactions, for which surface generation was implemented using 15 s exposure to 1 M $MgCl_2$ in 10 mM sodium acetate pH 4.5. Experiments were carried out in HBS-P+ buffer (GE Healthcare) supplemented with 0.2% bovine serum albumin (BSA) at 25 ºC and all binding studies were performed at a flow rate of 30 μL/min to prevent analyte rebinding. Data was visualized and processed using the Biacore T100 evaluation software version 2.0 (GE Healthcare). Equilibrium titration curve fitting and determination of K_d values was implemented using GraphPad Prism assuming all binding interactions to be first order.

Yeast surface and SPR antibody-receptor competitive IL-2 binding assays. For yeast competition studies, approximately 2×10^5 mIL-2-displaying yeast per well were plated in a 96-well plate and washed with FACS buffer. Yeast cells were incubated with saturating concentrations of biotinylated mIL-2Rα (100 nM) or mIL-2Rβ (2 μM) and serial dilutions of unlabeled competitor antibody (either an isotype control [rat IgG 2A kappa antibody, eBioscience clone eBR2A], S4B6, or JES6-1) in FACS buffer for 2 hr at room

temperature. Cells were then washed and stained with fluorophore-conjugated streptavidin diluted in FACS buffer for 20 min at 4° C. Cells were washed again and assessed for mIL-2 receptor subunit binding on an Accuri C6 flow cytometer. Background-subtracted fluorescent signal as a fraction of receptor subunit binding in the absence of competitor was plotted. Curves were fitted to a logistic model and half maximal inhibitory concentrations (IC_{50}s) were computed using GraphPad Prism. Assays were performed in triplicate and repeated three times with consistent results.

SPR-based competition studies were performed in two different topologies. In the first series of studies, biotinylated mIL-2Rα or mIL-2Rβ was immobilized to a streptavidin-coated chip. Saturating amounts of mIL-2 (100 nM for mIL-2Rα studies and 2 μM for mIL-2Rβ studies) were pre-incubated with serial dilutions of competitor antibody (either isotype control antibody, JES6-1, or S4B6) for 30 min at room temperature. The various ratios of cytokine/antibody immunocomplexes were then flowed over the receptor-coated chip and both equilibrium binding and interaction dynamics were visualized using the Biacore T100 evaluation software. Equilibrium binding curves were fitted using GraphPad Prism, assuming a first-order model for all interactions with the exception of the mIL-2+S4B6 interaction on immobilized IL-2Rα, which was instead fitted to a cooperative binding model. In the second series of studies, the orientation was reversed such that biotinylated antibodies JES6-1 or S4B6 were immobilized. A saturating amount of mIL-2 (100 nM) was then captured on the immobilized antibodies and serial dilutions of soluble mIL-2Rα or mIL-2Rβ were immediately flowed over to quantify binding to the chip-bound mIL-2/antibody immunocomplexes. Equilibrium and kinetic binding

curves were generated in the Biacore T100 evaluation software, with the binding sensogram of mIL-2 in the absence of soluble receptor subtracted from each profile. Equilibrium titration curve fits and K_d values were calculated using GraphPad Prism, assuming first-order binding interactions. Binding profiles for soluble receptor interactions with antibody-complexed mIL-2 were compared to those of the unbound mIL-2 binding to immobilized mIL-2Rα or mIL-2Rβ, detailed under SPR affinity titrations. For both series of SPR competitive binding studies, immobilization, buffer, flow, regeneration, and analysis conditions were as described for SPR affinity titrations.

SUPPLEMENTAL REFERENCES

Abrams, J.S., Roncarolo, M.G., Yssel, H., Andersson, U., Gleich, G.J., and Silver, J.E. (1992). Strategies of anti-cytokine monoclonal antibody development: immunoassay of IL-10 and IL-5 in clinical samples. Immunological reviews *127*, 5-24.

Bankovich, A.J., Raunser, S., Juo, Z.S., Walz, T., Davis, M.M., and Garcia, K.C. (2007). Structural Insight into Pre-B Cell Receptor Function. Science *316*, 291-294.

Boder, E.T., and Wittrup, K.D. (1997). Yeast surface display for screening combinatorial polypeptide libraries. Nature biotechnology *15*, 553-557.

Brochet, X., Lefranc, M.P., and Giudicelli, V. (2008). IMGT/V-QUEST: the highly customized and integrated system for IG and TR standardized V-J and V-D-J sequence analysis. Nucleic acids research *36*, W503-508.

Chang, H.C., Bao, Z., Yao, Y., Tse, A.G., Goyarts, E.C., Madsen, M., Kawasaki, E., Brauer, P.P., Sacchettini, J.C., Nathenson, S.G., and et al. (1994). A general method for

facilitating heterodimeric pairing between two proteins: application to expression of alpha and beta T-cell receptor extracellular segments. Proceedings of the National Academy of Sciences of the United States of America *91*, 11408-11412.

Cooper, H.S., Murthy, S.N., Shah, R.S., and Sedergran, D.J. (1993). Clinicopathologic study of dextran sulfate sodium experimental murine colitis. Laboratory investigation; a journal of technical methods and pathology *69*, 238-249.

Dubel, S., Breitling, F., Fuchs, P., Zewe, M., Gotter, S., Welschof, M., Moldenhauer, G., and Little, M. (1994). Isolation of IgG antibody Fv-DNA from various mouse and rat hybridoma cell lines using the polymerase chain reaction with a simple set of primers. Journal of immunological methods *175*, 89-95.

Giudicelli, V., Brochet, X., and Lefranc, M.P. (2011). IMGT/V-QUEST: IMGT standardized analysis of the immunoglobulin (IG) and T cell receptor (TR) nucleotide sequences. Cold Spring Harbor protocols *2011*, 695-715.

Kuziel, W.A., Ju, G., Grdina, T.A., and Greene, W.C. (1993). Unexpected effects of the IL-2 receptor alpha subunit on high affinity IL-2 receptor assembly and function detected with a mutant IL-2 analog. Journal of immunology *150*, 3357-3365.

Rao, B.M., Driver, I., Lauffenburger, D.A., and Wittrup, K.D. (2004). Interleukin 2 (IL-2) variants engineered for increased IL-2 receptor alpha-subunit affinity exhibit increased potency arising from a cell surface ligand reservoir effect. Mol Pharmacol *66*, 864-869.

Ring, A.M., Lin, J.X., Feng, D., Mitra, S., Rickert, M., Bowman, G.R., Pande, V.S., Li, P., Moraga, I., Spolski, R._, et al._ (2012). Mechanistic and structural insight into the functional dichotomy between IL-2 and IL-15. Nature immunology _13_, 1187-1195.

Wang, X., Rickert, M., and Garcia, K.C. (2005). Structure of the quaternary complex of interleukin-2 with its alpha, beta, and gammac receptors. Science _310_, 1159-1163.

Yodoi, J., Teshigawara, K., Nikaido, T., Fukui, K., Noma, T., Honjo, T., Takigawa, M., Sasaki, M., Minato, N., Tsudo, M., and et al. (1985). TCGF (IL 2)-receptor inducing factor(s). I. Regulation of IL 2 receptor on a natural killer-like cell line (YT cells). Journal of immunology _134_, 1623-1630.

Zurawski, S.M., Mosmann, T.R., Benedik, M., and Zurawski, G. (1986). Alterations in the amino-terminal third of mouse interleukin 2: effects on biological activity and immunoreactivity. Journal of immunology _137_, 3354-3360.

IV.4 Engineering a single-agent cytokine-antibody fusion that selectively expands regulatory T cells for autoimmune disease therapy

The selective stimulatory activity of IL-2/JES6 for Treg cells makes it an enticing candidate for the treatment of autoimmune diseases in humans, but clinical administration of IL-2co, i.e. mixture of IL-2 and anti-IL-2 mAb at a molar ratio 2:1, is complicated by logistical challenges in drug formulation including optimization of the dosing ratio and instability of the cytokine/antibody complex. Addressing these challenges, our study introduces a structure-guided engineered fusion of IL-2 with the JES6-1A12 mAb. However, to enable CD25-mediated triggered exchange of IL-2, it was necessary to lower the affinity of JES6-1A12 mAb to IL-2 by about 6-fold through two point mutations (Y41A+Y101A) introduced into the binding site of the VL domain of the antibody. The resulting JY3 IC maintains the crucial cytokine exchange property of the parental IL-2/JES6 IL-2co, selectively promoting Treg cell expansion, and exhibiting superior disease control to the non-covalent IL-2/JES6 complex in a murine model of colitis. This breakthrough provides a foundational engineering blueprint to overcome significant obstacles associated with implementation of IL-2co for clinical application in human diseases.

P. Weberová's contribution to this publication:

I performed several experiments *in vivo*. I assessed the expansion of various immune cell subsets in response to IL-2/JES6 complexes, IL-2/JES6 IC, or its affinity-mutated forms, and participated in adoptive T cell transfer experiments. Overall contribution ~ 10 %.

Engineering a single-agent cytokine-antibody fusion that selectively expands regulatory T cells for autoimmune disease therapy.

Jamie B. Spangler[1,2,3,†], **Eleonora Trotta**[4], **Jakub Tomala**[5], **Ariana Peck**[6], **Tracy A. Young**[7], **Christina S. Savvides**[8], **Stephanie Silveria**[4], **Petra Votavova**[5], **Joshua Salafsky**[7], **Vijay S. Pande**[9], **Marek Kovar**[5], **Jeffrey A. Bluestone**[4,10], and **K. Christopher Garcia**[1,2,3,*]

[1]Howard Hughes Medical Institute, Stanford University School of Medicine, Stanford, California, USA.

[2]Department of Molecular and Cellular Physiology, Stanford University School of Medicine, Stanford, California, USA.

[3]Department of Structural Biology, Stanford University School of Medicine, Stanford, California, USA.

[4]Diabetes Center, University of California San Francisco, San Francisco, California, USA.

[5]Laboratory of Tumor Immunology, Institute of Microbiology of the Academy of Sciences of the Czech Republic, Prague, Czech Republic.

[6]Department of Biochemistry, Stanford University, Stanford, California, USA.

[7]Biodesy, Inc. South San Francisco, California, USA.

[8]Department of Biology, Stanford University, Stanford, California, USA.

[9]Department of Bioengineering, Stanford University, Stanford, California, USA.

[10]Sean N. Parker Autoimmune Research Laboratory, University of California San Francisco, San Francisco, California, USA.

Abstract

*kcgarcia@stanford.edu.

123

Interleukin-2 (IL-2) has been used to treat diseases ranging from cancer to autoimmune disorders, but its concurrent immunostimulatory and immunosuppressive effects hinder efficacy. IL-2 orchestrates immune cell function through activation of a high-affinity heterotrimeric receptor (comprised of IL-2 receptor-α [IL-2Rα], IL-2Rβ, and common γ [γ_c]). IL-2Rα, which is highly expressed on regulatory T (T$_{Reg}$) cells regulates IL-2 sensitivity. Previous studies have shown that complexation of IL-2 with the JES6–1 antibody preferentially biases cytokine activity toward T$_{Reg}$ cells through a unique mechanism whereby IL-2 is exchanged from the antibody to IL-2Rα. However, clinical adoption of a mixed antibody-cytokine complex regimen is limited by stoichiometry and stability concerns. Here, through structure-guided design, we engineered a single agent fusion of the IL-2 cytokine and JES6–1 antibody that, despite being covalently linked, preserves IL-2 exchange, selectively stimulating T$_{Reg}$ expansion, and exhibiting superior disease control to the mixed IL-2/JES6–1 complex in a mouse colitis model. These studies provide an engineering blueprint for resolving a major barrier to the implementation of functionally similar IL-2/antibody complexes for treatment of human disease.

INTRODUCTION

Interleukin-2 (IL-2) is a pleiotropic cytokine that orchestrates the proliferation, survival, and function of both immune effector cells and regulatory T (T$_{Reg}$) cells to maintain immune homeostasis. IL-2 signals through activation of either a high-affinity (~100 pM) heterotrimeric receptor (composed of IL-2 receptor-α [IL-2Rα], IL-2Rβ, and the shared common gamma [γ_c]) or an intermediate-affinity (~1 nM) heterodimeric receptor (composed of only the IL-2Rβ and γ_c chains) (1–3). Consequently, IL-2 sensitivity is dictated by the non-signaling IL-2Rα chain, which is abundantly expressed on the surface of T$_{Reg}$ cells, but virtually absent from naïve immune effector cells (*i.e.* natural killer [NK] cells and memory phenotype [MP] CD8$^+$ T cells) (1, 2, 4). Formation of the IL-2 cytokine-receptor complex leads to activation of intracellular Janus kinase (JAK) proteins, which are constitutively associated with IL-2Rβ and γ_c. JAK proteins phosphorylate key tyrosine residues in the receptor intracellular domains, leading to recruitment and activation of signal transducer and activator of transcription (STAT)-5 to effect immune-related gene expression and regulate functional outcomes (1, 5, 6).

Due to its essential role in the differentiation and growth of T$_{Reg}$ cells, the IL-2 cytokine has been extensively characterized in pre-clinical models to treat a range of autoimmune diseases, including diabetes and multiple sclerosis. These models have underlined the need to administer low doses of the cytokine to take advantage of the enhanced IL-2 sensitivity of T$_{Reg}$ over effector cells (7, 8). More recently, proof-of-concept clinical trials backed by mechanistic studies have demonstrated that low-dose IL-2 therapy specifically activates and expands T$_{Reg}$ cells to ameliorate autoimmune pathologies (9–11). However, careful dose titration is required for these studies and the off-target activation of effector cells (particularly activated cells with upregulated IL-2Rα expression) remains of concern.

Boyman and colleagues demonstrated that treating mice with complexes of IL-2 with the anti-IL-2 antibody JES6–1 biases cytokine activity toward T$_{Reg}$ cells to orchestrate an immunosuppressive response (12), offering an exciting opportunity for targeted autoimmune

disease therapy (13). Subsequent work has demonstrated that IL-2/JES6–1 complexes prevent development of autoimmune diseases (14–17) and promote graft tolerance (18, 19) in mice. We recently determined the molecular structure of the IL-2/JES6–1 complex to elucidate the mechanistic basis for its selective stimulation of T_{Reg} over effector cells. JES6–1 sterically obstructs IL-2 interaction with the IL-2Rβ and $γ_c$ subunits to block signaling on IL-2Rα^{Low} effector cells, but also undergoes a unique allosteric exchange mechanism with the IL-2Rα subunit, wherein surface-expressed IL-2Rα displaces the JES6–1 antibody and liberates the cytokine to signal through the high-affinity heterotrimeric receptor on IL-2Rα^{High} T_{Reg} cells (Fig. 1a). This phenomenon occurs because key residues in the IL-2 AB interhelical loop engage the JES6–1 antibody and the IL-2Rα subunit in distinct orientations; thus, IL-2-antibody and IL-2-receptor binding are mutually exclusive, leading to bidirectional exchange. Activation of the IL-2 signaling pathway on IL-2Rα^{High} cells further upregulates IL-2Rα expression to create a positive feedback loop that exquisitely favors T_{Reg} expansion (17).

The immunosuppressive effects of IL-2/JES6–1 complexes make them enticing candidates for autoimmune disease treatment in humans, but clinical administration of mixed IL-2/antibody complexes is complicated by logistical challenges in drug formulation including optimization of the dosing ratio and instability of the cytokine/antibody complex. Previously, IL-2 has been covalently linked to an anti-IL-2 antibody to enhance its *in vivo* half-life and stability (20). However, this approach is incompatible with the allosteric exchange mechanism enacted by the IL-2/JES6–1 complex as tethering IL-2 to the JES6–1 antibody greatly enhances the apparent antibody-cytokine affinity, obstructing the triggered release that is essential for T_{Reg} bias. To overcome this obstacle to therapeutic development, we utilized a structure-based engineering strategy to design a single-agent IL-2/JES6–1 fusion that preserves antibody-receptor exchange. Through modulation of the cytokine-antibody affinity, we successfully recapitulated the selective T_{Reg} potentiation elicited by mixed IL-2/JES6–1 complex treatment and we demonstrated that our engineered cytokine-antibody fusion controlled autoimmune disease better than the mixed complex in an induced mouse model of colitis. Collectively, our biophysical and functional studies present a mechanism-driven biomolecular engineering approach that enables the therapeutic translation of a cytokine-antibody complex, and that can readily be adapted to other systems for a range of immune disease applications.

MATERIALS AND METHODS

Protein expression and purification.

The sequence encoding hexahistidine-tagged mouse IL-2 (mIL-2, amino acids 1–149) was cloned into the pMal vector with an N-terminal maltose-binding protein (MBP) followed by a 3C protease site. mIL-2 was expressed in the periplasm of BL21(DE3) *Escherichia coli* cells by 20 h induction at 22°C with 1 mM isopropyl β-d-thiogalactopyranoside (IPTG). Protein in the periplasmic compartment was isolated by osmotic shock and purified by nickel-nitrilotriacetic acid (Ni-NTA) (Qiagen) affinity chromatography. Purity was improved via size-exclusion chromatography on a Superdex-75 column (GE Healthcare) in HEPES-buffered saline (HBS, 150 mM NaCl in 10 mM HEPES pH 7.3).

mIL-2Rα (amino acids 1–213) ectodomain, mIL-2Rβ ectodomain (amino acids 1–215), and mγ$_c$ ectodomain (amino acids 34–233) were secreted and purified using a baculovirus expression system, as previously described (3). All proteins were purified to >98% homogeneity with a Superdex 200 sizing column (GE Healthcare) equilibrated in HBS. Purity was verified by SDS-PAGE analysis.

Recombinant JES6–1 antibody and immunocytokine and mutants thereof were co-expressed using the previously described BacMam technique (21) adapted for 293F human embryonic kidney cells (Thermo Life Technologies). For JES6–1 antibody and variants thereof, the JES6–1 variable heavy (V$_H$) chain followed by the rat immunoglobulin (IgG) 2a constant domains was cloned into the pVLAD6 vector with a C-terminal hexahistidine tag. The JES6–1 variable light (V$_L$) chain followed by the rat kappa light chain constant domain was separately cloned into the pVLAD6 vector with with a C-terminal hexahistidine tag. For immunocytokine constructs, mIL-2 was cloned N-terminal to the V$_L$ domain of the light chain construct, spaced by a (Gly$_4$Ser)$_2$ linker. Heavy and light chain constructs were separately transfected into *Spodoptera frugiperda* insect (SF9) cells as previously described (21) and the resulting viral supernatants were used to infect 293F cells (Thermo Life Technologies) in the presence of 10 mM sodium butyrate (Sigma). Heavy and light chain viruses were co-titrated to determine optimal infection ratios for equivalent expression of the two chains. Infected 293F cells were harvested after 72 hours and secreted protein was captured from the supernatant via Ni-NTA (Qiagen) affinity chromatography. Proteins were further purified to >98% homogeneity with a Superdex 200 sizing column (GE Healthcare) equilibrated in HBS, and purity was confirmed by SDS-PAGE analysis. Rat IgG2a isotype control antibody (Clone eBR2a) was purchased commercially (eBioscience).

For expression of biotinylated mouse IL-2 and mouse IL-2 receptor subunits, proteins containing a C-terminal biotin acceptor peptide (BAP)-LNDIFEAQKIEWHE were expressed and purified via Ni-NTA affinity chromatography and then biotinylated with the soluble BirA ligase enzyme in 0.5 mM Bicine pH 8.3, 100 mM ATP, 100 mM magnesium acetate, and 500 mM biotin (Sigma). Excess biotin was removed by size exclusion chromatography on a Superdex 200 column equilibrated in HBS. Antibodies and immunocytokines were biotinylated using the EZ-Link Sulfo-NHS-LC-Biotinylation kit (Pierce) according to the manufacturer's protocol.

Cell Lines.

Unmodified YT-1 (22) and IL-2Rα$^+$ YT-1 human natural killer cells (23) were cultured in RPMI complete medium (RPMI 1640 medium supplemented with 10% fetal bovine serum, 2 mM L-glutamine, minimum non-essential amino acids, sodium pyruvate, 25 mM HEPES, and penicillin-streptomycin [Gibco]) and maintained at 37ºC in a humidified atmosphere with 5% CO$_2$.

The subpopulation of YT-1 cells expressing IL-2Rα was purified via magnetic selection as described previously (24). Ten million unsorted IL-2Rα$^+$ YT-1 cells were washed with FACS buffer (phosphate-buffered saline [PBS] pH 7.2 containing 0.1% bovine serum albumin) and incubated in FACS buffer with PE-conjugated anti-human IL-2Rα antibody (Biolegend, clone BC96) for 2 hr at 4°C. PE-labeled IL-2Rα$^+$ cells were then incubated with

J Immunol. Author manuscript; available in PMC 2019 October 01.

126

paramagnetic microbeads coated with an anti-PE IgG for 20 min at 4° C, washed once with cold FACS buffer, and sorted on an LS MACS separation column (Miltenyi Biotec) according to the manufacturer's protocol. Purified eluted cells were re-suspended and grown in RPMI complete medium. Enrichment of IL-2Rα^+ cells was evaluated using an Accuri C6 flow cytometer (BD Biosciences) and persistence of IL-2Rα expression was monitored by PE-conjugated anti-human IL-2Rα antibody labeling and flow cytometric analysis of sorted IL-2Rα^+ YT-1 cells.

Second harmonic generation antibody-receptor exchange studies.

For cytokine labeling, hexahistidine-tagged mIL-2 was exchanged into labeling buffer (50 mM HEPES pH 8.2, 150 mM NaCl) with a 0.5 mL, 7000 molecular weight cut-off Zeba™ Spin Desalting Column (Thermo). A five-fold molar excess of lysine-reactive (succinimidyl ester chemistry) second harmonic-active dye SHG1-SE (25) (Biodesy, Inc.) was added to the protein. The reaction proceeded on ice for 5 min and was then stopped by removal of unreacted SHG1-SE by buffer exchange into HBS with a 0.5 mL, 7000 molecular weight cut-off Zeba™ Spin Desalting Column (Thermo). The reacted protein was centrifuged at 16,000×g at 4 °C for 20 minutes to pellet any precipitate and the supernatant was analyzed by UV-Vis spectroscopy. The degree of labeling was determined to be 1 (dye:protein stoichiometry).

For target immobilization, Ni-NTA lipid-containing small unilamellar vesicles (SUVs) were generated in tris-buffered saline (TBS, pH 7.6) from the Ni-NTA Bilayer Surface reagent (Biodesy, Inc) according to the manufacturer's protocol. Supported lipid bilayers were formed by fusion of the Ni-NTA SUVs on the glass surface of a 384-well Biodesy Delta plate. The formed bilayer was washed into HBS. SHG1-SE labeled hexahistidine-tagged mIL-2 was added to each well at 500 nM final concentration (20 uL well volume). The protein was allowed to attach to the surface through the Ni-NTA:Hexahistidine-tag interaction overnight at 4°C. The plate was then equilibrated to room temperature for 30 min and unbound protein was washed out. Following 20 min incubation at room temperature, the plate was transferred to the Biodesy Delta for data collection.

To assess JES6–1 exchange, 500 nM IL-2Rα was injected at time t=0 and second harmonic generation (SHG) signal was monitored for 10 minutes. Two-fold serial dilutions of JES6–1 antibody ranging from 2 μM to 31 nM in assay buffer containing 500 nM IL-2Rα (to keep the receptor concentration constant) were injected and percent SHG signal change (ΔSHG) was tracked for 10 min. To assess IL-2Rα exchange, 500 nM JES6–1 was injected at time t=0 and SHG signal was monitored for 10 minutes. Two-fold serial dilutions of IL-2Rα ranging from 32 μM to 0.5 μM in assay buffer containing 500 nM JES6–1 (to keep the antibody concentration constant) were injected and ΔSHG was tracked for 10 min. The percent change in SHG intensity was calculated as $(SHG_F-SHG_B)/SHG_B \times 100$, where SHG_B is the SHG signal at t=0 and SHG_F is the SHG signal at each time point post-injection.

Molecular dynamics simulations.

Atomistic molecular dynamics simulations of mIL-2 were performed using the Gromacs 5.0.4 package (26) with the Amber99SB-ILDN force field (27) and the TIP3P water model (28). Initial conformations were obtained from the crystal structures of the mIL-2:JES6–1 scFv (PDB ID 4YQX), mIL-2:S4B6 Fab (PDB ID 4YUE), and hIL-2:hIL-2Rα (PDB ID: 1Z92) complexes, with the binding partner omitted. The Modeller 9.14 package (29) was used to mutate the hIL-2 conformation to the mouse sequence and to build crystallographically-unresolved loops, with five predicted configurations for each crystal structure. Starting conformations of mIL-2 were positioned in a dodecahedron box with a minimum of 10 Å between the protein's surface and the edge of the box. The protein was solvated with approximately 8400 water molecules; five sodium ions were added to neutralize the charge. Energy minimization was performed using a steepest descent algorithm, and solvent was equilibrated for 500 ps at 300 K and 1 bar with the positions of the protein atoms held fixed. Production simulations were performed using a 2 fs timestep, with trajectory lengths of 150 ns and an aggregate simulation time of 19.4 µs. Constant temperature and pressure were maintained by applying a velocity-rescaling thermostat (30) and a Parrinello-Rahman barostat (31). Bonds were constrained using the LINCS algorithm (32), and electrostatic interactions were treated with the particle mesh Ewald method (33). Adaptive sampling was performed by reseeding simulations from poorly sampled regions of the mIL-2 conformational landscape; conformations in these regions were identified by time-structure independent component analysis (34), an unbiased method to determine the slowest degrees of conformational freedom.

A Markov State model (MSM) with a lag-time of 5 ns was constructed from the simulation data using the MSMBuilder 2.8.2 package (35). Similar to prior analysis of IL-2 simulations (24), conformations were clustered into 50 states using a hybrid k-centers k-medoids algorithm, with distances between all pairs of conformations determined from the root mean square deviation (RMSD) of the backbone atom positions. A representative trajectory of the predicted equilibrium dynamics was constructed using kinetic Monte Carlo sampling of the MSM transition probability matrix. Inter-residue distances, dihedral angles, and RMSD were computed using MDTraj 1.7.2 (36).

Surface plasmon resonance studies.

For IL-2 affinity titration studies, biotinylated mouse IL-2Rα and IL-2Rβ receptors, biotinylated JES6–1 antibody mutants, or biotinylated JES6–1 IC mutants were immobilized to streptavidin-coated chips for analysis on a Biacore T100 instrument (GE Healthcare). An irrelevant biotinylated protein was immobilized in the reference channel to subtract non-specific binding. Less than 100 response units (RU) of each ligand was immobilized to minimize mass transfer effects. Three-fold serial dilutions of mIL-2 were flowed over the immobilized ligands for 60 s and dissociation was measured for 240 s. Surface regeneration for all interactions was conducted using 15 s exposure to 1 M $MgCl_2$ in 10 mM sodium acetate pH 5.5.

For immunocytokine receptor exchange studies, biotinylated mIL-2Rα or mIL-2Rβ receptors were immobilized to streptavidin-coated chips for analysis on a Biacore T100

instrument (GE Healthcare). An irrelevant biotinylated protein was immobilized in the reference channel to subtract non-specific binding. Less than 100 response units (RU) of each ligand was immobilized to minimize mass transfer effects. Three-fold serial dilutions of mIL-2 or JES6–1 IC mutants were flowed over the immobilized ligands for 60 s and dissociation was measured for 240 s. Surface regeneration for all interactions was conducted using 15 s exposure to 1 M MgCl$_2$ in 10 mM sodium acetate pH 5.5.

SPR experiments were carried out in HBS-P+ buffer (GE Healthcare) supplemented with 0.2% bovine serum albumin (BSA) at 25°C and all binding studies were performed at a flow rate of 50 μL/min to prevent analyte rebinding. Data was visualized and processed using the Biacore T100 evaluation software version 2.0 (GE Healthcare). Equilibrium titration curve fitting and equilibrium binding dissociation (K_D) value determination was implemented using GraphPad Prism assuming all binding interactions to be first order.

YT-1 cell STAT5 phosphorylation studies.

Approximately 2×10^5 YT-1 or IL-2Rα$^+$ YT-1 cells were plated in each well of a 96-well plate and re-suspended in RPMI complete medium containing serial dilutions of mIL-2, mIL-2/antibody complexes, JES6–1 IC, or JES6–1 IC mutants. Complexes were formed by incubating a 1:1 molar ratio of antibody or antibody fragment to mIL-2 for 30 min at room temperature. Cells were stimulated for 15 min at 37°C and immediately fixed by addition of formaldehyde to 1.5% and 10 min incubation at room temperature. Permeabilization of cells was achieved by resuspension in ice-cold 100% methanol for 30 min at 4°C. Fixed and permeabilized cells were washed twice with FACS buffer (phosphate-buffered saline [PBS] pH 7.2 containing 0.1% bovine serum albumin) and incubated with Alexa Fluor® 647-conjugated anti-STAT5 pY694 (BD Biosciences) diluted in FACS buffer for 2 hr at room temperature. Cells were then washed twice in FACS buffer and MFI was determined on a CytoFLEX flow cytometer (Beckman-Coulter). Dose-response curves were fitted to a logistic model and half-maximal effective concentrations (EC$_{50}$s) were calculated using GraphPad Prism data analysis software after subtraction of the mean fluorescence intensity (MFI) of unstimulated cells and normalization to the maximum signal intensity. Experiments were conducted in triplicate and performed three times with similar results.

Immune cell subset proliferation studies.

For relative T$_{Reg}$:CD8$^+$/CD4$^+$ T cell proliferation studies, 12 weeks old C57BL/6 mice (3 per cohort) or NOD mice (4 per cohort) were injected *i.p.* with PBS, mixed IL-2/JES6–1 complex (prepared by pre-incubating 1.5 μg mIL-2 [eBioscience] with 6 μg JES6–1 [2:1 cytokine:antibody molar ratio] in PBS for 30 mins), or 6 μg of the indicated JES6–1 IC mutants on days 1, 2, 3 and 4. Mice were sacrificed on day 5 by cervical dislocation and spleens were harvested. Single-cell suspensions were prepared by mechanical homogenization and absolute count of splenocytes was assessed for each spleen by automated cell counter (Vicell, Beckman Coulter). Cells were resuspended in PBS and subsequently stained for 30 min on ice with fluorophore-conjugated anti-mouse monoclonal antibodies (mAbs) for phenotyping of T$_{Reg}$ (CD4$^+$IL-2Rα$^+$Foxp3$^+$) or CD8$^+$ effector T cells (CD8$^+$) using BV605-conjugated anti-CD4 (Biolegend, clone RM4–5), PeCy7-conjugated anti-IL-2Rα (eBioscience, clone PC61.5), PerCP-Cy5.5-conjugated anti-CD8 (eBioscience,

J Immunol. Author manuscript; available in PMC 2019 October 01.

129

clone 53–6.72), and mAbs. Fixable Blue Dead Cell Stain Kit (Life Techonologies) was used
to assess live cells. Cells were then washed twice with FACS buffer (1% BSA, 1% Sodium
Azide) and fixed in Foxp3 Transcription Factor Fixation/Permeabilization Buffer
(eBioscience) for 30 mins on ice. After two washes in Permeabilization Buffer
(eBioscience), T_{Reg} cells were stained with FITC-conjugated anti-mouse/rat Foxp3 mAb
(eBioscience, clone FJK-16s) for 1 hour on ice. Two final washes were conducted in
Permeabilization Buffer and cells were resuspended in FACS buffer for flow cytometric
analysis on an LSRII (BD Biosciences). Data were analyzed using FlowJo X software (Tree
Star). Ratios of the absolute numbers of T_{Reg} cells to either CD8$^+$ effector T cells or total
CD4$^+$ T cells are presented. Statistical significance was determined by two-tailed unpaired
Student's *t*-test. Experiments were performed three times with similar results.

Adoptive T cell transfer studies.

OT-I Ly 5.1$^+$ mice (3 per cohort) were sacrificed by cervical dislocation and lymph nodes
(head, axillary, inquinal and mesenteric) were harvested. Single-cell suspensions were
prepared by homogenization (GentleMACS Dissociator, Miltenyi Biotec) and CD8$^+$ effector
T cells were negatively sorted on AutoMACS (Miltenyi Biotec). Isolated CD8$^+$ T cells were
labeled with carboxyfluorescein succinimidyl ester (CFSE) and injected *i.v.* into C57BL/6
mice (Ly 5.2) (1×10^6 cells/mouse). Mice were then treated *i.p.* on day 1 with PBS or with 2
nmol SIINFEKL peptide alone or in combination with 75 µg polyI:C7, 7.5 µg mIL-2 plus 30
µg Rat IgG2a isotype control antibody (BioXcell, Clone 2A3), mixed mIL-2/JES6–1
complex (formed by pre-incubating 7.5 µg mIL-2 [Peprotech] with 30 µg JES6–1 [2:1
cytokine:antibody molar ratio] in PBS for 15 min), or 30 µg JY3 immunocytokine. On day 2,
3, and 4, mice were treated with the same doses of mIL-2 plus Rat IgG2a isotype control
antibody, mixed mIL-2/JES6–1 complex, or JY3 immunocytokine. Mice were sacrificed on
day 5 by cervical dislocation and spleens were harvested, homogenized, and analyzed by
flow cytometry as described for Immune cell subset proliferation studies. Four immune
populations were distinguished and profiled for IL-2Rα expression using the following
fluorophore-conjugated anti-mouse mAbs: adoptively transferred CD8$^+$ T cells - V500
Horizon®-conjugated anti-CD3 (BD Biosciences, clone 500A2), PerCP-Cy5.5-conjugated
anti-CD8 (eBioscience, clone 53–6.72), APC-conjugated anti-CD45.1 (eBioscience, clone
A20), and eFluor 450®-conjugated anti-IL-2Rα, T_{Reg}s (CD3$^+$CD4$^+$Foxp3$^+$) - V500
Horizon®-conjugated anti-CD3 (BD Biosciences, clone 500A2), PerCP-conjugated anti-
CD4 (BD Biosciences, clone RM4–5), PE-conjugated anti-mouse/rat Foxp3 (eBioscience,
clone FJK-16s), and APC-conjugated anti-IL-2Rα mAbs (eBioscience, clone PC61.5); MP
CD8$^+$ T cells (CD3$^+$CD8$^+$CD44$^+$IL-2Rβ$^+$) - V500 Horizon®-conjugated anti-CD3, PerCP-
Cy5.5-conjugated anti-CD8 (eBioscience, clone 53–6.72), APC-conjugated anti-CD44
(eBioscience, clone IM7), PE-conjugated anti-IL-2Rβ (eBioscience, clone 5H4), and eFluor
450®-conjugated anti-IL-2Rα (eBioscience, clone PC61.5) mAbs; and NK cells
(CD3$^-$CD49b$^+$CD161) - V500 Horizon®-conjugated anti-CD3, PE-conjugated anti-CD49b
(eBioscience, clone DX5), APC-conjugated anti-CD161 (eBioscience, clone PK136), and
eFluor 450®-conjugated anti-IL-2Rα mAbs. Fixable Viability Dye eFluor™ 780
(eBioscience) was used to assess live cells. Data were analyzed using FlowJo X software
(Tree Star). Relative number of cells and mean fluorescence intensity (MFI) of IL-2Rα are
presented for each cohort in all four immune cell subsets. Statistical significance was

determined by two-tailed unpaired Student's *t*-test. The experiment was performed three times with similar results.

Mouse dextran sodium sulfate (DSS)-induced colitis model.

BALB/c mice (6 per cohort) were injected *i.p.* daily for seven days with PBS, 7.5 μg mIL-2 plus 30 μg isotype control antibody (BioXcell, clone 2A3), mixed mIL-2/JES6–1 complex (formed by pre-incubating 7.5 μg mIL-2 [Peprotech] with 30 μg JES6–1 [2:1 cytokine:antibody molar ratio] in PBS for 15 min), or 30 μg JY3 immunocytokine. Beginning on day 8, mice were administered 3% DSS (molecular weight=40000, MP Biomedicals Inc.) in their drinking water to induce colitis. On day 15, body weight was recorded and disease severity was assessed using clinical disease activity index, as described previously (4, 37). On day 16, mice were sacrificed and entire colons were removed (from cecum to anus). Colon length was measured and shortening was used as an indirect marker of pathological inflammation. Statistical significance was determined by one-way ANOVA + Dunnett's multiple comparison post-test. The experiment was performed two times with similar results.

RESULTS

IL-2 undergoes bidirectional exchange between the JES6–1 antibody and the IL-2Rα receptor subunit.

The aforementioned allosteric exchange mechanism allows for displacement of JES6–1 in the cytokine/antibody complex by the surface-bound IL-2Rα receptor subunit (Fig. 1a). This mechanism was supported by structural and surface plasmon resonance (SPR)-based studies (17). To demonstrate the bidirectionality of the antibody-receptor exchange mechanism, we interrogated the capacity of both antibody and receptor to engage bound mouse IL-2 complexes. To this end, we used a second-harmonic generation (SHG) detection platform, which was previously used to detect conformational changes in proteins in time and space (25, 38, 39). IL-2 was labeled with a second-harmonic-active dye and immobilized to a surface. The tethered cytokine was then saturated with either mouse IL-2Rα (Fig. 1b, *top*) or JES6–1 (Fig. 1b, *bottom*). Subsequently, various concentrations of soluble JES6–1 (Fig. 1b, *top*) or IL-2Rα (Fig. 1b, *bottom*) were added and changes in SHG signal, indicative of modulations in average tilt angles of the dye particles conjugated to IL-2, were quantified. In both topologies, dose-dependent conformational changes were observed in IL-2 upon adding soluble protein to the immobilized complex, demonstrating the bidirectional exchange between antibody and receptor engagement of the cytokine.

To further corroborate the allosteric exchange mechanism, we performed molecular dynamics simulations to study the distinct conformational states of IL-2 when bound to the JES6–1 antibody versus the IL-2Rα receptor, as well as the transition between these states. IL-2, and in particular the IL-2Rα-binding epitope of the cytokine, is known to exhibit extensive conformational flexibility (40–42). We constructed an atomically-detailed Markov State model (MSM) of the conformational landscape of free IL-2. The equilibrium dynamics captured by the MSM predicted that IL-2 stably adopts a JES6–1-bound conformation even in the absence of antibody but occasionally relaxes to a distinct metastable state that

resembles the IL-2Rα-bound conformation (Fig. 1c, Supplemental Video 1). The antibody-bound and receptor-bound states of the cytokine diverge significantly with respect to root mean square deviation (RMSD), inter-residue distances, and residue-specific dihedral angles in all three interhelical loops (Fig. 1c). The transition from the JES6–1-bound to the IL-2Rα-bound states involves significant conformational rearrangements and, in particular, destabilization of a salt bridge and a hydrogen bond in the AB and BC loops, respectively, that appear to rigidify these regions (Fig. 1c, *red* and *orange*). These changes coincide with the loss of a cation-pi interaction between the B helix and the beta strand of the CD region, accompanied by increased flexibility of the latter (Fig. 1c, *green*). Inspection of the primary transition path with higher temporal resolution suggests that loss of loop rigidity occurs in sequential fashion. Deformation of the BC loop, which interacts with IL-2Rα, is predicted to precede destabilization of the AB loop, which engages IL-2Rα at its C-terminal end and JES6–1 at its N-terminal end (Fig. 1d). Such a stepwise transition may facilitate allosteric exchange between the JES6–1 antibody and IL-2Rα subunit (17). Taken together, our biophysical and computational studies offer mechanistic insight into the antibody-receptor exchange that drives the T_{Reg} cell bias induced by stimulation with the mixed IL-2/JES6–1 complex.

Design of a single-agent cytokine-antibody fusion.

To stabilize the IL-2/JES6–1 complex with an eye toward translation, we fused the IL-2 cytokine to the full-length JES6–1 antibody, tethering IL-2 to the N-terminal end of the light chain via a flexible $(Gly_4Ser)_2$ linker (Fig. 2a). Based on the IL-2/JES6–1 complex structure (17), the C-terminus of IL-2 is predicted to be 19.9 Å from the N-terminus of the JES6–1 light chain (Supplemental Fig. 1a). Our cytokine/antibody construction (hereafter denoted the JES6–1 immunocytokine [IC]) was designed to allow for intramolecular cytokine engagement. Interaction between IL-2 and JES6–1 within the immunocytokine was confirmed by SPR-based titrations of the IL-2Rα subunit. Whereas untethered IL-2 binds the IL-2Rα subunit with an equilibrium dissociation constant (K_D) of 9.8 nM, JES6–1 IC has a 30-fold weaker IL-2Rα affinity (K_D=290 nM) (Fig. 2b), reflective of cytokine sequestering by the tethered antibody.

The IL-2-JES6–1 affinity (K_D=5.6 nM) is similar to the IL-2-IL-2Rα affinity (K_D=9.8 nM) and significantly stronger than the IL-2-IL-2Rβ affinity (K_D=7.4 µM) (Supplemental Fig. 1b). Thus, effective exchange of the IL-2 cytokine between the JES6–1 antibody and the IL-2Rα subunit is observed when the affinities are closely matched. We hypothesized that tethering IL-2 to the JES6–1 antibody would enhance the apparent cytokine-antibody affinity due to avidity effects, and this increased cytokine-antibody affinity would in turn weaken IL-2-IL-2Rα interaction in the context of the IC. We speculated that changes in the antibody-cytokine affinity and, by consequence, the IC-IL-2Rα affinity, would impact on the exchange mechanism in a biphasic manner. If the affinity of the IL-2-JES6–1 complex was greatly reduced, the antibody would fall off constitutively, leading to the cytokine to behave the same as the naked IL-2 and activate both IL-2Rα^{High} T_{Reg} and IL-2Rα^{Low} effector cells, thus erasing the robust T_{Reg} cell IL-2 signaling bias conferred by JES6–1 (Supplemental Fig. 1c). Conversely, if the affinity of the IL-2-JES6–1 complex was significantly increased, to the limit of an irreversible interaction, the antibody would never be displaced by IL-2Rα,

ablating the exchange mechanism and precluding cytokine activity on both T_{Reg} and effector cells (Supplemental Fig. 1c). Consequently, there exists an optimal IL-2-antibody affinity to maximize T_{Reg} over effector cell expansion, and substantial enhancement of the IL-2-antibody affinity through immunocytokine construction could push this affinity outside of the optimal range.

Parent IL-2-JES6–1 immunocytokine exhibits reduced activation of IL-2Rα^{High} cells and does not promote T_{Reg} expansion *in vivo*.

To examine the functional consequences of antibody-cytokine tethering on cell subset-selective activity, we tested activation of two genotypically matched cell lines based on the YT-1 human NK lineage that differ only in their expression of the IL-2Rα subunit (23), as a surrogate for stimulation of IL-2Rα^{High} T_{Reg} cells compared to IL-2Rα^{Low} effector cells. IL-2 exhibited over 30-fold more potent activation (as measured by STAT5 phosphorylation) on IL-2Rα^+ cells compared to IL-2Rα^- cells, as was expected due to the higher affinity of the heterotrimeric versus the heterodimeric IL-2 receptor complex. The mixed IL-2/JES6–1 complex induced weaker activation of both cell lines but, importantly, showed more pronounced obstruction of signaling on IL-2Rα^- compared to IL-2Rα^+ cells, rationalizing the complex's IL-2Rα^{High} T_{Reg} bias. JES6–1 IC did not activate IL-2Rα^- cells and induced much weaker activation of IL-2Rα^+ cells compared to the mixed complex, consistent with its impaired interaction with the IL-2Rα subunit (Fig. 2c). We explored how this differential *in vitro* signaling would translate into *in vivo* immune cell subset bias. Administration of IL-2 alone to non-obese diabetic (NOD) mice did not induce an increase in T_{Reg} relative to CD8$^+$ effector T cell abundance, but treatment with IL-2/JES6–1 complex doubled the T_{Reg}:CD8$^+$ T cell ratio. However, this increase was completely absent for JES6–1 IC, indicating that stabilization of the IL-2-antibody affinity had disrupted the exchange mechanism, ablating cytokine activity on both T_{Reg} and effector cells (Fig. 2d, Supplemental Fig. 1c). Accordingly, enrichment of T_{Reg} in the total CD4$^+$ T cell population was observed following treatment with IL-2/JES6–1 complex treatment but not JES6–1 IC (Supplemental Fig. 1d).

Affinity mutant immunocytokines demonstrate improved exchange and elicit biased IL-2Rα^+ cell activation.

To rescue the T_{Reg}-biased activity of the immunocytokine, we used crystallographic insights to rationally design a panel of eight single-point alanine mutants of the JES6–1 antibody. We selected four variable heavy (V_H) and four variable light (V_L) chain residues at the cytokine/antibody interface, intentionally avoiding residues proximal to the IL-2Rα chain to circumvent disruption of the allosteric exchange mechanism (Fig. 3a). We formatted each alanine mutant as a full-length antibody and characterized binding to the IL-2 cytokine via SPR titrations. All mutants with the exception of R62A decreased the antibody-cytokine affinity, with a maximum affinity impairment of 89-fold relative to the parent JES6–1 antibody (Fig. 3b and Table I).

To probe the effects of reduced cytokine/antibody affinity on IL-2Rα exchange, we reformatted each of the alanine mutants as IC fusions and measured the binding of these soluble IC variants to immobilized IL-2Rα using SPR. Each of the eight IC mutants tested

exhibited increased receptor affinity compared to the parent JES6–1 IC, indicative of improved exchange due to enhanced antibody displacement. The most pronounced affinity improvement was observed for the Y41A IC mutant, which had a 2.2-fold tighter affinity for IL-2Rα than JES6–1 IC (Fig. 3c, *top* and Table I). Notably, neither the parent JES6–1 IC nor any of the mutant IC constructs bound the immobilized IL-2Rβ subunit, indicating that JES6–1-mediated blockade of the IL-2Rβ remained intact for our engineered IC mutants (Fig. 3c, *bottom*).

We predicted that improved antibody displacement by the IL-2Rα subunit would potentiate mutant JES6–1 IC activity on IL-2Rα$^+$ cells and, indeed, we observed that many of our immunocytokine mutants enhanced STAT5 signaling on IL-2Rα$^+$ YT-1 cells relative to the parent JES6–1 IC. Three IC mutants (S34A, Y41A, and Y101A) recovered the extent of STAT5 signaling induced by the mixed IL-2/JES6–1 complex (Fig. 3d, *top*). None of the engineered IC mutants activated IL-2Rα$^-$ YT-1 cells, consistent with the behavior of the mixed complex (Fig. 3d, *bottom*). Our JES6–1 IC mutant cellular activation assays also offered insight into the relationships between affinity, exchange, and functional response. We hypothesized that activity would correlate with affinity in a biphasic manner (Supplemental Fig. 1c), and our data support this postulate (Fig. 3e). However, additional structural factors appear to contribute to signaling output, as is evidenced by the much greater potency of activation induced by JES6–1 IC mutants with alanine substitutions in the V_L versus the V_H domain. Since the cytokine was linked to the JES6–1 light chain, heavy chain mutants disrupt the cytokine/antibody interface further from the tether and we would thus expect function to be more dramatically affected for V_H versus V_L mutants. Accordingly, the V_H mutants generally impair affinity to a greater extent than do V_L mutants (Fig. 3b, Table I). The discrepancy between V_H and V_L JES6–1 IC mutant constructs is even more apparent when comparing IL-2Rα$^+$ cell activity to exchange (as determined by IL-2Rα affinity). Although activity correlates with exchange within the JES6–1 IC V_L mutants, the JES6–1 IC V_H mutants all elicit weak stimulation of IL-2Rα$^+$ cells, independent of their IL-2Rα exchange propensities (Fig. 3f).

Multi-site immunocytokine mutants exhibit enhanced IL-2Rα exchange, cellular activation, and *in vivo* T$_{Reg}$-biased expansion.

Based on our three most active single-point mutant JES6–1 IC constructs (the V_L domain mutants S34A, Y41A, and Y101A) (Fig. 3d), we designed three double-alanine mutant IC constructs and one triple-alanine JES6–1 IC mutant construct to enhance IL-2Rα exchanging capacity and IL-2Rα$^+$ cell-selective signaling. All multi-residue mutant IC constructs potentiated IL-2Rα exchange compared to the parent JES6–1 IC, with the most actively-exchanging mutants (Y41A+Y101A and S34A+Y101A) exhibiting a 2.6-fold IL-2Rα affinity enhancement relative to the parent JES6–1 IC (Fig. 4a, *top,* Table II). Several of the multi-residue mutants (including Y41A+Y101A) also bound to immobilized IL-2Rβ due to the weakened cytokine-antibody interaction, but all IC mutants bound weaker to IL-2Rβ than to IL-2Rα and had lower IL-2Rβ affinities than the free IL-2 cytokine (Fig. 4a, *bottom*). Signaling activity of the multi-residue IC mutants on IL-2Rα$^+$ YT-1 cells correlated directly with IL-2Rα exchange; all mutants activated IL-2Rα$^+$ cells more potently than the parent JES6–1 IC and three of the four constructs had greater activity than the

mixed IL-2/JES6–1 complex (Fig. 4b, *top*). The Y41A+Y101A and S34+Y101A mutants were again the most active and none of the mutants triggered appreciable activation of IL-2Rα^- YT-1 cells (Fig. 4b, *bottom*).

Guided by our cellular activation results, we chose to further characterize the Y41A+Y101A mutant, which has a 5.6-fold weaker cytokine-antibody affinity than the unmodified JES6–1 (Fig. 4c), and the S34A+Y101A mutant, which had a 1.9-fold weaker cytokine-antibody affinity than the parent JES6–1 (Supplemental Fig. 2a). We assessed the ability of the Y41A+Y101A IC mutant to expand immune cell subset populations in C57BL/6 mice and found that, in contrast with JES6–1 IC, Y41A+Y101A IC induced preferential T_{Reg} versus CD8$^+$ effector T cell expansion to the same extent as the mixed IL-2/JES6–1 complex (Fig. 4d and Supplemental Fig. 3a), indicating that reducing cytokine-antibody affinity had restored biased activity on IL-2Rα^{High} cells. Consistent results were observed for the T_{Reg} versus CD4$^+$ T cell ratio (Supplemental Fig. 3b), confirming specific expansion of T_{Reg} by the Y41A+Y101A IC variant. IC behavior *in vivo* was found to be highly sensitive to affinity and structural modifications, as the S34A+Y101A IC mutant did not elicit biased T_{Reg} expansion (Supplemental Figs. 2b and 3), despite its similar exchange (Fig. 4a) and signaling (Fig 4b) properties to the Y41A+Y101A IC mutant *in vitro*. Further studies demonstrated that the Y41A+Y101A IC mutant (hereafter denoted JY3 IC) effected preferential T_{Reg} over CD8$^+$ effector T cell growth in a dose-dependent manner in C57BL/6 (Supplemental Fig. 2c) and NOD mice (Supplemental Fig. 2e). Moreover, JY3 treatment upregulated IL-2Rα expression on T_{Reg} cells to a much greater extent than the mixed IL-2/JES6–1 complex (Supplemental Figs. 2d and 2f). IC formulation also had benefits in enhancing maximum tolerated dose of the IL-2 cytokine compared to the mixed complex, as administration of a 7.4 μg dose of IL-2 in mixed complex format was lethal to NOD mice (3/4 mice died), but an equivalent dose of the JY3 IC (30 μg) was well tolerated (0/4 mice died). This suggests that tethering the cytokine to the antibody may mitigate toxicity relative to the mixed complex, presumably through increased complex stability, which reduces off-target effects elicited by free IL-2.

Engineered immunocytokine induces cell subset-specific expansion in an adoptive T cell transfer model.

Given that JY3 IC selectively expanded IL-2Rα^{High} cells in a mixed immune population, we wondered whether our construct would be able to precisely control immune cell subset populations in an adoptive T cell transfer model. We purified and CFSE-labeled CD8$^+$ T cells from OT-I mice, transferred the cells into congenic B6 mice, and treated recipient mice with a low dose of the SIINFEKL peptide plus various IL-2-antibody regimens for analysis of recipient immune cell expansion (Fig. 5a). Peptide stimulation with or without poly-L-lysine and IL-2 co-administration with an isotype control antibody failed to expand adoptively transferred activated CD8$^+$ T cells, whereas the mixed IL-2/JES6–1 complex induced robust proliferation of transferred cells, and JY3 IC further enhanced this expansion at equivalent doses (Fig. 5b). An identical trend was observed for IL-2Rα expression on transferred CD8$^+$ T cells, with higher surface levels of IL-2Rα elicited by JY3 IC versus IL-2/JES6–1 complex treatment (Supplemental Fig. 4a).

Characterization of recipient mouse T cell subsets supported our hypothesis that JY3 IC biases IL-2 activity to IL-2Rα^{High} T_{Reg} cells over IL-2Rα^{Low} naïve effector cells. No T_{Reg} cell expansion was induced by IL-2/isotype control antibody treatment, but we observed an increase in T_{Reg} cell number following IL-2/JES6–1 complex treatment and an even more profound increase following JY3 IC treatment (Fig. 5c). In contrast, IL-2/isotype control antibody treatment expanded both MP CD8$^+$ T cells and NK cells, whereas neither IL-2/JES6–1 complex nor JY3 IC promoted proliferation of these effector subsets (Fig. 5d, e). IL-2/JES6–1 complex also upregulated IL-2Rα expression on T_{Reg} and MP CD8+ T cells, although not on NK cells, and JY3 IC increased surface IL-2Rα levels on T_{Reg} and MP CD8$^+$ T cells to a greater extent than the complex and also robustly upregulated IL-2Rα on NK cells (Supplemental Fig. 4b-d). Overall, our adoptive transfer studies establish that JY3 IC specifically targets IL-2 activity to IL-2Rα^{High} immune cell subsets, and that it promotes more robust expansion and receptor upregulation on these subsets compared to the mixed IL-2/JES6–1 complex.

Engineered immunocytokine prevents the development of autoimmune disease in mice.

To explore the therapeutic potential of our engineered IC mutant, we compared the efficacy of JY3 IC to the mixed IL-2/JES6–1 complex in a dextran sodium sulfate (DSS)-induced colitis model. Mice were pre-treated with PBS, IL-2 with an isotype control antibody, IL-2/ JES6–1 complex, or JY3 IC for seven consecutive days and disease was induced beginning on day 8 (Fig. 6a). One week post-colitis induction, as compared to IL-2/isotype control antibody-treated mice, IL-2/JES6–1 complex-treated mice exhibited significant reductions in disease severity, including attenuated weight loss, increased colon length, and lower disease activity index (Fig. 6b–d), consistent with previous findings (17). JY3 IC further enhanced autoimmune disease prevention, with more pronounced improvements in weight loss, colon length, and disease activity score compared to the IL-2/JES6–1 complex (Fig. 6b–d). These results suggest that the JY3 IC could have therapeutic advantages to the mixed cytokine-antibody complex beyond the logistical considerations of stability and ease of formulation.

DISCUSSION

There is a growing interest in the development of antibody-cytokine fusions (immunocytokines) to empower cytokines as drugs (43). Whereas cytokines have short *in vivo* half-lives (often less than five minutes) and thus require frequent dosing (44–46), antibodies benefit from prolonged serum persistence due to neonatal Fc receptor-mediated recycling (47, 48). In addition, fusion to surface antigen-binding antibodies can allow for targeted cytokine delivery tailored to particular disease indications (43, 49–54). However, clinical development of targeted immunocytokines is hampered by the high potency of cytokines, which nullifies the effect of the targeting antibody and leads to toxicity through indiscriminate activation of all cytokine-response immune cell subsets (55–57). To circumvent the issue of potency, recent efforts have focused on reducing cytokine-receptor affinity through directed mutagenesis of the cytokine (58, 59), but cytokine modification may alter functional activity and also raises concerns about immunogenicity.

Here, we describe a novel use of immunocytokines to 'shield' a cytokine from non-specifically engaging immune cells and instead target it preferentially to T_{Reg} cells based on surface receptor expression levels. Our approach relies entirely on antibody engineering, thus obviating the need for cytokine manipulation and keeping both cytokine-receptor affinity and cytokine activity intact. Furthermore, our strategy completely eliminates off-target effects by fully sequestering the cytokine rather than simply lowering its receptor interaction affinity. Although the allosteric receptor-antibody exchange mechanism we describe is specific to the IL-2/JES6–1 system, the structure-based design principles we used to engineer an effective single-agent cytokine-antibody fusion can be extended to other ligand-antibody interactions for exclusive targeting of soluble factors to specific cell subsets of interest.

Our engineering workflow offered new insight into the relationship between antibody-cytokine affinity and signaling activity in the context of allosteric exchange. Previous studies have elucidated correlations between cytokine-receptor affinity and signaling activity (60–65). A systematic study of the interplay between cytokine-receptor complex stability and membrane-proximal signaling for the IL-13/IL-13Rα1/IL-4Rα complex revealed that cytokine activity correlated directly with cytokine-receptor affinity only outside of a 'buffering region,' an affinity regime within 100-fold (in either direction) of the wild-type interaction affinity wherein cytokine activity was insensitive to affinity changes (65). The complexities of activity-affinity relationships in other systems led us to speculate that the antibody-cytokine affinity in the IL-2/JES6–1 single-agent fusion could also exhibit non-linear behavior. Furthermore, since the exchange mechanism depends on the relative strengths of cytokine interaction between the IL-2Rα receptor subunit and the JES6–1 antibody, we would expect the activity of the immunocytokine on various cell subsets to depend strongly on binding parameters.

We predicted biphasic behavior of the IL-2Rα^{High} cell (*i.e.* T_{Reg} cell) activity bias of our engineered JES6–1 mutants with respect to their IL-2 affinities: at very low affinities the antibody would constitutively dissociate, resulting in unbiased activation of all IL-2-responsive cells, and at very high affinities, the antibody would never dissociate, obstructing activity on all cell subsets (Supplemental Fig. 1c). By modulating the affinity of the IL-2/antibody interaction over nearly two orders of magnitude (Fig. 1b, Table I), we aimed to probe the window of antibody-cytokine affinity 'tunability' for optimization of preferential T_{Reg} cell expansion. As illustrated in Fig. 3e, we indeed observed a biphasic activity curve as IL-2 affinity was varied, although the tuning range was found to be surprisingly narrow. JES6–1 mutants with up to a 2.2-fold decrease in IL-2 affinity compared to the parent antibody exhibited improved T_{Reg} selectivity, but no improvements were observed for mutants with IL-2 affinities that were reduced by 10-fold or more (Fig. 3e, Table II).

Other factors such as structural considerations also apparently contribute to the activity of IC mutants. For instance, the E60A and H100A mutants have similar affinities for IL-2, but diverge significantly in their activation potencies (Fig. 3e). The E60A mutation is in the V_H domain whereas the H100A mutation is in the V_L domain, suggesting that the location of the interface disruption with respect to chain affects IC activity. Consistent with this observation, V_L mutants exhibit uniformly stronger signaling activity on IL-2Rα^+ cells than

do V_H mutants. This phenomenon could also be impacted by the topology of the fusion itself, as the greater proximity to tethered IL-2 for V_L compared to V_H may render the V_L interface more robust against affinity disruption. The dramatic (>10-fold) affinity losses observed with 3/4 V_H mutants compared with only 1/4 V_L mutants support the influence of topological factors on IC mutant activity (Table II). Further complicating the affinity-activity relationship is the lack of correlation between biased signal activation *in vitro* and selective cell subset expansion *in vivo*. Although the S34A+Y101A and Y41A+Y101A (JY3) IC mutants behaved similarly with respect to STAT5 signaling on IL-2Rα^+ and IL-2Rα^- cells, there was a clear discrepancy in their *in vivo* promotion of IL-2Rα^{High} versus IL-2Rα^{Low} cell growth (Fig. 3d and Supplemental Fig. 2b).

From a therapeutic development standpoint, the IC format has clear advantages over mixed complex administration as it eliminates dosing ratio considerations and concerns about the free cytokine inducing off-target effects and toxicities or undergoing rapid clearance from the bloodstream (43, 46). However, we unexpectedly found that our engineered IC elicited greater IL-2Rα^{High} cell expansion in an adoptive T cell transfer model (Fig. 4) and prevented DSS-induced colitis more effectively than the mixed complex (Fig. 5), even though the two formats induced similar T_{Reg} to effector cell expansion ratios (Figs. 4d and Supplemental Figs. 2c, 2e, and 3). One possibility for the superior phenotypic behavior of the engineered IC could be that it is positioned more optimally on the biphasic T_{Reg} to effector cell activity curve based on its altered antibody-cytokine affinity (Supplemental Fig. 1c). Alternatively, the more extensive IL-2Rα upregulation induced by JY3 IC versus the mixed complex (Supplemental Figs. 2d and 2f) may present an advantage for the immunocytokine by fueling the transcriptional feedback loop that perpetuates IL-2 signaling (17). Regardless of rationale, the enhanced behavior of JY3 IC over the mixed complex provides an immediately useful reagent for expanding T_{Reg} cells to combat autoimmune disease, and the structure-guided engineering strategy we used to develop this construct will inform the design of other mechanism-driven therapeutic immunocytokines. With a growing number of anti-cytokine antibodies in development, including those against IL-2, −4, −6, −7, and −15 (66), our novel approach can be readily extended to a broad range of cytokine-receptor systems for disease-relevant applications.

Supplementary Material

Refer to Web version on PubMed Central for supplementary material.

ACKNOWLEDGMENTS

REFERENCES

1. Malek TR 2008 The Biology of Interleukin-2. Annu. Rev. Immunol 26: 453–479. [PubMed: 18062768]

2. Boyman O, and Sprent J. 2012 The role of interleukin-2 during homeostasis and activation of the immune system. Nat. Rev. Immunol 12: 180–190. [PubMed: 22343569]

3. Wang X, Rickert M, and Garcia KC. 2005 Structure of the quaternary complex of interleukin-2 with its alpha, beta, and gammac receptors. Science 310: 1159–1163. [PubMed: 16293754]

4. Spangler JB, Moraga I, Mendoza JL, and Garcia KC. 2015 Insights into Cytokine–Receptor Interactions from Cytokine Engineering. Annu. Rev. Immunol 33: 139–167. [PubMed: 25493332]

5. Stroud RM, and Wells JA. 2004 Mechanistic Diversity of Cytokine Receptor Signaling Across Cell Membranes. Sci STKE 2004: re7–re7. [PubMed: 15126678]

6. Murray PJ 2007 The JAK-STAT signaling pathway: input and output integration. J. Immunol. Baltim. Md 1950 178: 2623–2629.

7. Shevach EM 2012 Application of IL-2 therapy to target T regulatory cell function. Trends Immunol 33: 626–632. [PubMed: 22951308]

8. Cheng G, Yu A, and Malek TR. 2011 T-cell tolerance and the multi-functional role of IL-2R signaling in T-regulatory cells. Immunol. Rev 241: 63–76. [PubMed: 21488890]

9. Klatzmann D, and Abbas AK. 2015 The promise of low-dose interleukin-2 therapy for autoimmune and inflammatory diseases. Nat. Rev. Immunol 15: 283–294. [PubMed: 25882245]

10. Saadoun D, Rosenzwajg M, Joly F, Six A, Carrat F, Thibault V, Sene D, Cacoub P, and Klatzmann D. 2011 Regulatory T-Cell Responses to Low-Dose Interleukin-2 in HCV-Induced Vasculitis. N. Engl. J. Med 365: 2067–2077. [PubMed: 22129253]

11. Koreth J, Matsuoka K, Kim HT, McDonough SM, Bindra B, Alyea EPI, Armand P, Cutler C, Ho VT, Treister NS, Bienfang DC, Prasad S, Tzachanis D, Joyce RM, Avigan DE, Antin JH, Ritz J, and Soiffer RJ. 2011 Interleukin-2 and Regulatory T Cells in Graft-versus-Host Disease. N. Engl. J. Med 365: 2055–2066. [PubMed: 22129252]

12. Boyman O, Kovar M, Rubinstein MP, Surh CD, and Sprent J. 2006 Selective stimulation of T cell subsets with antibody-cytokine immune complexes. Science 311: 1924–1927. [PubMed: 16484453]

13. Boyman O, Surh CD, and Sprent J. 2006 Potential use of IL-2/anti-IL-2 antibody immune complexes for the treatment of cancer and autoimmune disease. Expert Opin. Biol. Ther 6: 1323–1331. [PubMed: 17223740]

14. Tang Q, Adams JY, Penaranda C, Melli K, Piaggio E, Sgouroudis E, Piccirillo CA, Salomon BL, and Bluestone JA. 2008 Central role of defective interleukin-2 production in the triggering of islet autoimmune destruction. Immunity 28: 687–697. [PubMed: 18468463]

15. Liu R, Zhou Q, La Cava A, Campagnolo DI, Van Kaer L, and Shi F-D. 2010 Expansion of regulatory T cells via IL-2/anti-IL-2 mAb complexes suppresses experimental myasthenia. Eur. J. Immunol 40: 1577–1589. [PubMed: 20352624]

16. Grinberg-Bleyer Y, Baeyens A, You S, Elhage R, Fourcade G, Gregoire S, Cagnard N, Carpentier W, Tang Q, Bluestone J, Chatenoud L, Klatzmann D, Salomon BL, and Piaggio E. 2010 IL-2 reverses established type 1 diabetes in NOD mice by a local effect on pancreatic regulatory T cells. J. Exp. Med 207: 1871–1878. [PubMed: 20679400]

17. Spangler JB, Tomala J, Luca VC, Jude KM, Dong S, Ring AM, Votavova P, Pepper M, Kovar M, and Garcia KC. 2015 Antibodies to Interleukin-2 Elicit Selective T Cell Subset Potentiation through Distinct Conformational Mechanisms. Immunity 42: 815–825. [PubMed: 25992858]

18. Webster KE, Walters S, Kohler RE, Mrkvan T, Boyman O, Surh CD, Grey ST, and Sprent J. 2009 In vivo expansion of T reg cells with IL-2–mAb complexes: induction of resistance to EAE and long-term acceptance of islet allografts without immunosuppression. J. Exp. Med 206: 751–760. [PubMed: 19332874]

19. Park Y-H, Koo S-K, Kim Y, Kim H-M, Joe I-Y, Park C-S, Kim S-C, Han D-J, and Lim D-G. 2010 Effect of in vitroexpanded CD4+CD25+Foxp3+ regulatory T cell therapy combined with lymphodepletion in murine skin allotransplantation. Clin. Immunol 135: 43–54. [PubMed: 20006940]

20. Tomala J, Kovarova J, Kabesova M, Votavova P, Chmelova H, Dvorakova B, Rihova B, and Kovar M. 2013 Chimera of IL-2 Linked to Light Chain of anti-IL-2 mAb Mimics IL-2/anti-IL-2 mAb Complexes Both Structurally and Functionally. ACS Chem. Biol 8: 871–876. [PubMed: 23419043]

21. Dukkipati A, Park HH, Waghray D, Fischer S, and Garcia KC. 2008 BacMam system for high-level expression of recombinant soluble and membrane glycoproteins for structural studies. Protein Expr. Purif 62: 160–170. [PubMed: 18782620]

22. Yodoi J, Teshigawara K, Nikaido T, Fukui K, Noma T, Honjo T, Takigawa M, Sasaki M, Minato N, and Tsudo M. 1985 TCGF (IL 2)-receptor inducing factor(s). I. Regulation of IL 2 receptor on a natural killer-like cell line (YT cells). J. Immunol. Baltim. Md 1950 134: 1623–1630.

23. Kuziel WA, Ju G, Grdina TA, and Greene WC. 1993 Unexpected effects of the IL-2 receptor alpha subunit on high affinity IL-2 receptor assembly and function detected with a mutant IL-2 analog. J. Immunol 150: 3357–3365. [PubMed: 8468475]

24. Ring AM, Lin J-X, Feng D, Mitra S, Rickert M, Bowman GR, Pande VS, Li P, Moraga I, Spolski R, Ozkan E, Leonard WJ, and Garcia KC. 2012 Mechanistic and structural insight into the functional dichotomy between IL-2 and IL-15. Nat. Immunol 13: 1187–1195. [PubMed: 23104097]

25. Salafsky JS 2006 Detection of protein conformational change by optical second-harmonic generation. J. Chem. Phys 125: 074701. [PubMed: 16942358]

26. Abraham MJ, Murtola T, Schulz R, Páll S, Smith JC, Hess B, and Lindahl E. 2015 GROMACS: High performance molecular simulations through multi-level parallelism from laptops to supercomputers. SoftwareX 1–2: 19–25.

27. Lindorff-Larsen K, Piana S, Palmo K, Maragakis P, Klepeis JL, Dror RO, and Shaw DE. 2010 Improved side-chain torsion potentials for the Amber ff99SB protein force field. Proteins 78: 1950–1958. [PubMed: 20408171]

28. Jorgensen WL, Chandrasekhar J, Madura JD, Impey RW, and Klein ML. 1983 Comparison of simple potential functions for simulating liquid water. J. Chem. Phys 79: 926–935.

29. Šali A, and Blundell TL. 1993 Comparative Protein Modelling by Satisfaction of Spatial Restraints. J. Mol. Biol 234: 779–815. [PubMed: 8254673]

30. Bussi G, Donadio D, and Parrinello M. 2007 Canonical sampling through velocity rescaling. J. Chem. Phys 126: 014101. [PubMed: 17212484]

31. Parrinello M, and Rahman A. 1981 Polymorphic transitions in single crystals: A new molecular dynamics method. J. Appl. Phys 52: 7182–7190.

32. Hess B, Bekker H, Berendsen HJC, and Fraaije JGEM. 1997 LINCS: A linear constraint solver for molecular simulations. J. Comput. Chem 18: 1463–1472.

33. Essmann U, Perera L, Berkowitz ML, Darden T, Lee H, and Pedersen LG. 1995 A smooth particle mesh Ewald method. J. Chem. Phys 103: 8577–8593.

34. Schwantes CR, and Pande VS. 2013 Improvements in Markov State Model Construction Reveal Many Non-Native Interactions in the Folding of NTL9. J. Chem. Theory Comput 9: 2000–2009. [PubMed: 23750122]

35. Beauchamp KA, Bowman GR, Lane TJ, Maibaum L, Haque IS, and Pande VS. 2011 MSMBuilder2: Modeling Conformational Dynamics on the Picosecond to Millisecond Scale. J. Chem. Theory Comput 7: 3412–3419. [PubMed: 22125474]

36. McGibbon RT, Beauchamp KA, Harrigan MP, Klein C, Swails JM, Hernández CX, Schwantes CR, Wang L-P, Lane TJ, and Pande VS. 2015 MDTraj: A Modern Open Library for the Analysis of Molecular Dynamics Trajectories. Biophys. J 109: 1528–1532. [PubMed: 26488642]

37. Cooper HS, Murthy SN, Shah RS, and Sedergran DJ. 1993 Clinicopathologic study of dextran sulfate sodium experimental murine colitis. Lab. Investig. J. Tech. Methods Pathol 69: 238–249.

38. Salafsky JS 2007 Second-harmonic generation for studying structural motion of biological molecules in real time and space. Phys. Chem. Chem. Phys. PCCP 9: 5704–5711. [PubMed: 17960260]

39. Moree B, Connell K, Mortensen RB, Liu CT, Benkovic SJ, and Salafsky J. 2015 Protein Conformational Changes Are Detected and Resolved Site Specifically by Second-Harmonic Generation. Biophys. J 109: 806–815. [PubMed: 26287632]

J Immunol. Author manuscript; available in PMC 2019 October 01.

140

40. Thanos CD, Randal M, and Wells JA. 2003 Potent Small-Molecule Binding to a Dynamic Hot Spot on IL-2. J. Am. Chem. Soc 125: 15280–15281. [PubMed: 14664558]

41. Thanos CD, DeLano WL, and Wells JA. 2006 Hot-spot mimicry of a cytokine receptor by a small molecule. Proc. Natl. Acad. Sci 103: 15422–15427. [PubMed: 17032757]

42. Levin AM, Bates DL, Ring AM, Krieg C, Lin JT, Su L, Moraga I, Raeber ME, Bowman GR, Novick P, Pande VS, Fathman CG, Boyman O, and Garcia KC. 2012 Exploiting a natural conformational switch to engineer an interleukin-2 "superkine". Nature 484: 529–533. [PubMed: 22446627]

43. Pasche N, and Neri D. 2012 Immunocytokines: a novel class of potent armed antibodies. Drug Discov. Today 17: 583–590. [PubMed: 22289353]

44. Lotze MT, Matory YL, Ettinghausen SE, Rayner AA, Sharrow SO, Seipp CA, Custer MC, and Rosenberg SA. 1985 In vivo administration of purified human interleukin 2. II. Half life, immunologic effects, and expansion of peripheral lymphoid cells in vivo with recombinant IL 2. J. Immunol 135: 2865–2875. [PubMed: 2993418]

45. Kontermann RE 2011 Strategies for extended serum half-life of protein therapeutics. Curr. Opin. Biotechnol 22: 868–876. [PubMed: 21862310]

46. Vazquez-Lombardi R, Roome B, and Christ D. 2013 Molecular Engineering of Therapeutic Cytokines. Antibodies 2: 426–451.

47. Finkelman FD, Madden KB, Morris SC, Holmes JM, Boiani N, Katona IM, and Maliszewski CR. 1993 Anti-cytokine antibodies as carrier proteins. Prolongation of in vivo effects of exogenous cytokines by injection of cytokine-anti-cytokine antibody complexes. J. Immunol 151: 1235–1244. [PubMed: 8393043]

48. Roopenian DC, and Akilesh S. 2007 FcRn: the neonatal Fc receptor comes of age. Nat. Rev. Immunol 7: 715–725. [PubMed: 17703228]

49. Becker JC, Pancook JD, Gillies SD, Furukawa K, and Reisfeld RA. 1996 T cell-mediated eradication of murine metastatic melanoma induced by targeted interleukin 2 therapy. J. Exp. Med 183: 2361–2366. [PubMed: 8642346]

50. Halin C, Rondini S, Nilsson F, Berndt A, Kosmehl H, Zardi L, and Neri D. 2002 Enhancement of the antitumor activity of interleukin-12 by targeted delivery to neovasculature. Nat. Biotechnol 20: 264. [PubMed: 11875427]

51. Gillies SD, Lan Y, Williams S, Carr F, Forman S, Raubitschek A, and Lo K-M. 2005 An anti-CD20–IL-2 immunocytokine is highly efficacious in a SCID mouse model of established human B lymphoma. Blood 105: 3972–3978. [PubMed: 15692062]

52. Schrama D, Reisfeld RA, and Becker JC. 2006 Antibody targeted drugs as cancer therapeutics. Nat. Rev. Drug Discov 5: 147. [PubMed: 16424916]

53. Schliemann C, Palumbo A, Zuberbühler K, Villa A, Kaspar M, Trachsel E, Klapper W, Menssen HD, and Neri D. 2009 Complete eradication of human B-cell lymphoma xenografts using rituximab in combination with the immunocytokine L19-IL2. Blood 113: 2275–2283. [PubMed: 19005180]

54. Schilbach K, Alkhaled M, Welker C, Eckert F, Blank G, Ziegler H, Sterk M, Müller F, Sonntag K, Wieder T, Braumüller H, Schmitt J, Eyrich M, Schleicher S, Seitz C, Erbacher A, Pichler BJ, Müller H, Tighe R, Lim A, Gillies SD, Strittmatter W, Röcken M, and Handgretinger R. 2015 Cancer-targeted IL-12 controls human rhabdomyosarcoma by senescence induction and myogenic differentiation. OncoImmunology 4: e1014760. [PubMed: 26140238]

55. Shusterman S, London WB, Gillies SD, Hank JA, Voss SD, Seeger RC, Reynolds CP, Kimball J, Albertini MR, Wagner B, Gan J, Eickhoff J, DeSantes KB, Cohn SL, Hecht T, Gadbaw B, Reisfeld RA, Maris JM, and Sondel PM. 2010 Antitumor Activity of Hu14.18-IL2 in Patients With Relapsed/Refractory Neuroblastoma: A Children's Oncology Group (COG) Phase II Study. J. Clin. Oncol 28: 4969–4975. [PubMed: 20921469]

56. Yu AL, Gilman AL, Ozkaynak MF, London WB, Kreissman SG, Chen HX, Smith M, Anderson B, Villablanca JG, Matthay KK, Shimada H, Grupp SA, Seeger R, Reynolds CP, Buxton A, Reisfeld RA, Gillies SD, Cohn SL, Maris JM, and Sondel PM. 2010 Anti-GD2 Antibody with GM-CSF, Interleukin-2, and Isotretinoin for Neuroblastoma. N. Engl. J. Med 363: 1324–1334. [PubMed: 20879881]

57. Tzeng A, Kwan BH, Opel CF, Navaratna T, and Wittrup KD. 2015 Antigen specificity can be irrelevant to immunocytokine efficacy and biodistribution. Proc. Natl. Acad. Sci 112: 3320–3325. [PubMed: 25733854]

58. Gillies SD, Lan Y, Hettmann T, Brunkhorst B, Sun Y, Mueller SO, and Lo K-M. 2011 A Low-Toxicity IL-2–Based Immunocytokine Retains Antitumor Activity Despite Its High Degree of IL-2 Receptor Selectivity. Clin. Cancer Res 17: 3673–3685. [PubMed: 21531812]

59. Garcin G, Paul F, Staufenbiel M, Bordat Y, der Heyden JV, Wilmes S, Cartron G, Apparailly F, Koker SD, Piehler J, Tavernier J, and Uzé G. 2014 High efficiency cell-specific targeting of cytokine activity. Nat. Commun 5: 3016. [PubMed: 24398568]

60. Pearce Kenneth H., Cunningham BC, Fuh G, Teeri T, and Wells JA. 1999 Growth Hormone Binding Affinity for Its Receptor Surpasses the Requirements for Cellular Activity. Biochemistry (Mosc.) 38: 81–89.

61. Junttila IS, Creusot RJ, Moraga I, Bates DL, Wong MT, Alonso MN, Suhoski MM, Lupardus P, Meier-Schellersheim M, Engleman EG, Utz PJ, Fathman CG, Paul WE, and Garcia KC. 2012 Redirecting cell-type specific cytokine responses with engineered interleukin-4 superkines. Nat. Chem. Biol 8: 990. [PubMed: 23103943]

62. Piehler J, Thomas C, Garcia KC, and Schreiber G. 2012 Structural and dynamic determinants of type I interferon receptor assembly and their functional interpretation. Immunol. Rev 250: 317–334. [PubMed: 23046138]

63. Walter MR 2014 The molecular basis of IL-10 function: from receptor structure to the onset of signaling. Curr. Top. Microbiol. Immunol 380: 191–212. [PubMed: 25004819]

64. Moraga I, Spangler J, Mendoza JL, and Garcia KC. 2014 Multifarious determinants of cytokine receptor signaling specificity. Adv. Immunol 121: 1–39. [PubMed: 24388212]

65. Moraga I, Richter D, Wilmes S, Winkelmann H, Jude K, Thomas C, Suhoski MM, Engleman EG, Piehler J, and Garcia KC. 2015 Instructive roles for cytokine-receptor binding parameters in determining signaling and functional potency. Sci. Signal 8: ra114. [PubMed: 26554818]

66. Mostböck S 2009 Cytokine/Antibody complexes: an emerging class of immunostimulants. Curr. Pharm. Des 15: 809–825. [PubMed: 19275644]

J Immunol. Author manuscript; available in PMC 2019 October 01.

142
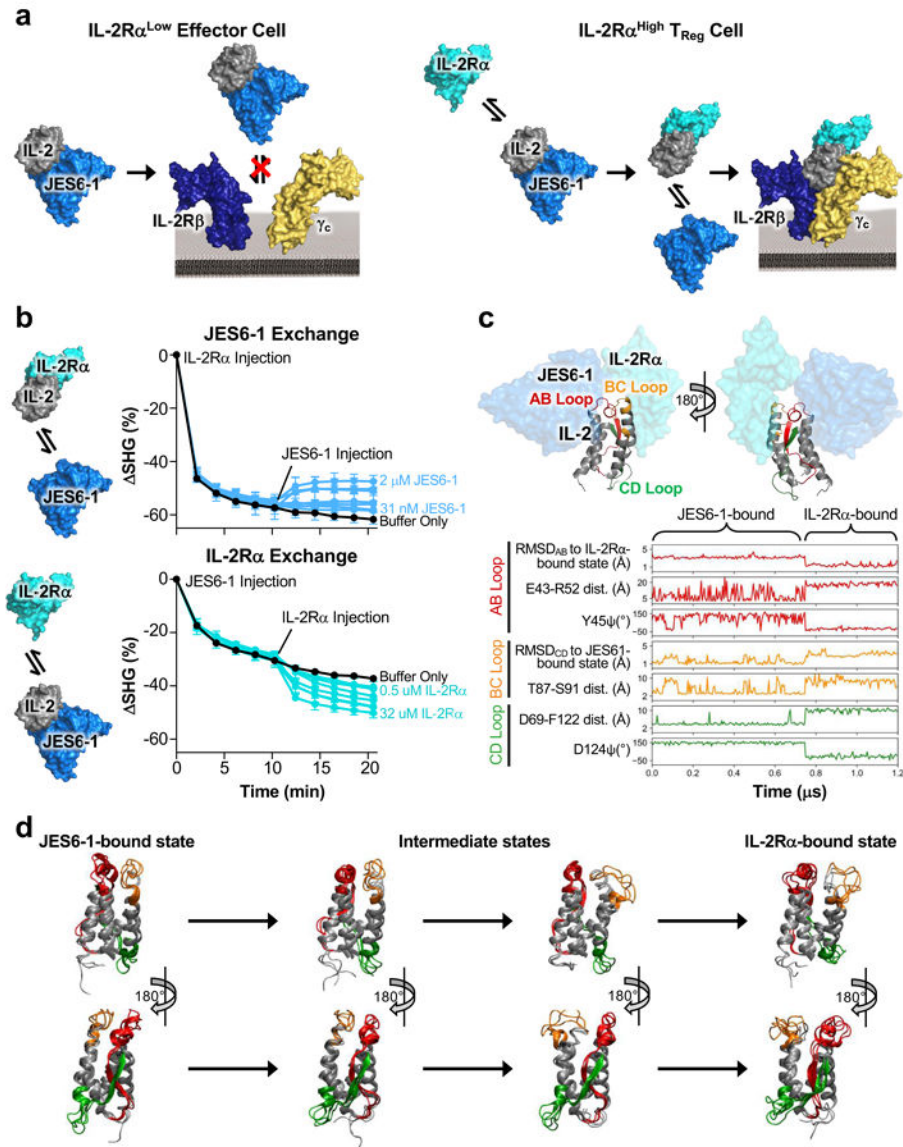
Figure 1. Unique antibody-receptor exchange mechanism underlies T$_{Reg}$ bias of mixed IL-2/JES6–1 complex.
(**a**) Schematic of the mechanistic rationale for IL-2/JES6–1 complex-mediated selective potentiation of T$_{Reg}$ cells. The JES6–1 antibody (shown in single-chain format) sterically obstructs IL-2 engagement of the IL-2Rβ and γ_c subunits, preventing activation of IL-2Rα^{Low} effector cells (*left*). However, allosteric exchange between JES6–1 and the IL-2Rα subunit allows for exclusive signaling on IL-2Rα^{High} T$_{Reg}$s, biasing toward an immunosuppressive response (*right*). (**b**) IL-2 was immobilized and 500 nM IL-2Rα (*top*) or 500 nM JES6–1 antibody (*bottom*) was injected at time 0 min. After 10 minutes, various concentrations of JES6–1 antibody ranging from 31 nM to 2 μM (*top*) or various concentrations of IL-2Rα ranging from 0.5 μM to 32 μM (*bottom*) were added and second-harmonic generation signal change (ΔSHG) was monitored. Exchange schemes are shown at *left*. (**c**) Molecular structure of the IL-2 cytokine bound to JES6–1 (PDB ID 4YQX) (17) overlaid with the IL-2Rα subunit from the IL-2 cytokine-receptor quaternary complex

structure (PDB ID 2B5I) (3), highlighting the AB (*red*), BC (*orange*), and CD (*green*) interhelical loops of the cytokine (*top*). Molecular dynamics simulations of free IL-2 were conducted starting from the cytokine's conformations in the crystallographic structures of IL-2 bound to the JES6–1 and S4B6 antibodies and the IL-2Rα subunit. Root mean square deviation (RMSD), dihedral angles, and inter-residue distances for the interhelical loops and flanking residues are plotted for a representative transition between the JES6–1-bound and IL-2Rα-bound states (*bottom*). **(d)** Overlay of three representative simulated conformations each from the JES6–1-bound state, the intermediate states, and the IL-2Rα-bound state of IL-2 that form the primary transition path, with interhelical regions colored as in (**c**).
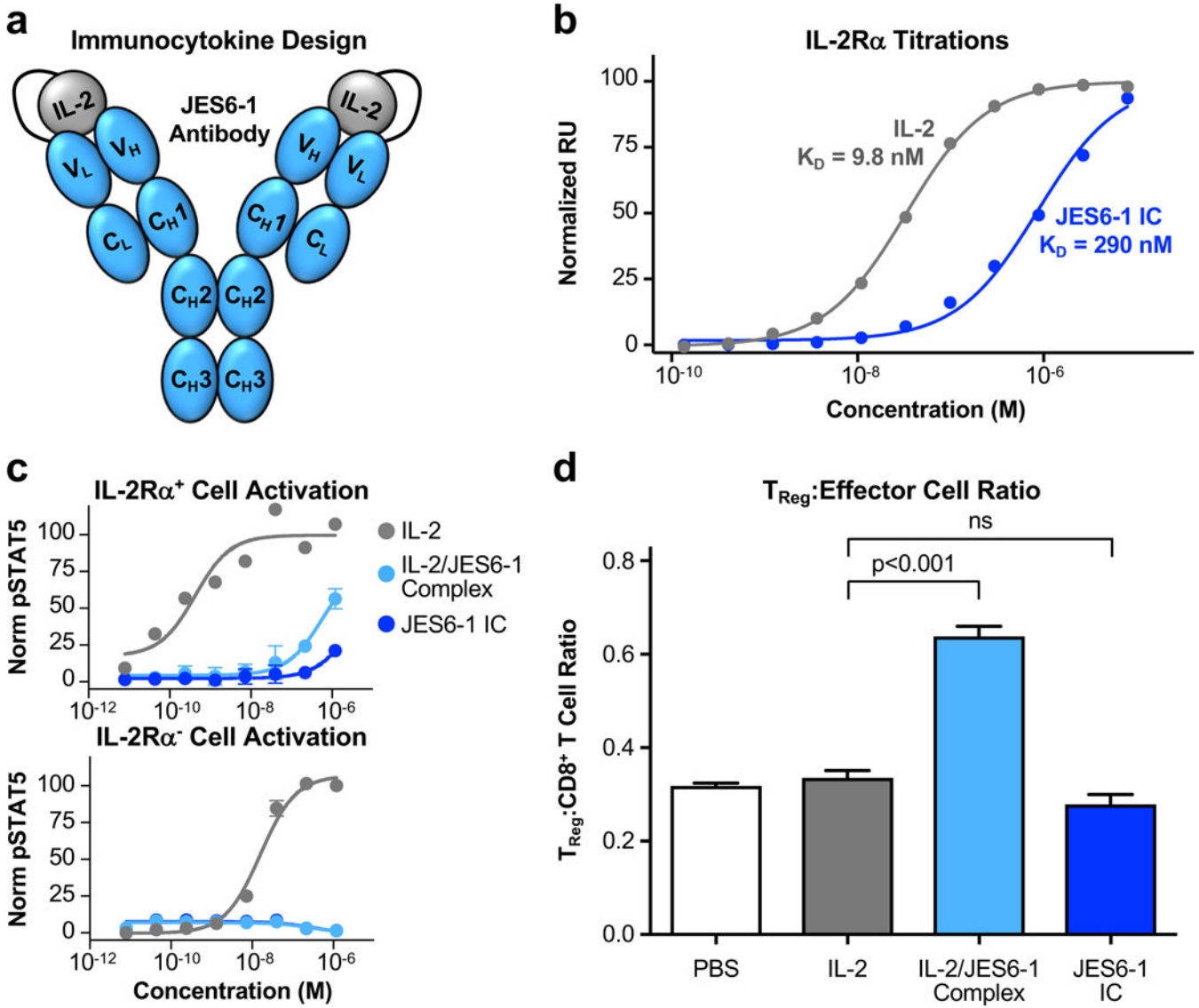
Figure 2. IL–2/JES6–1 immunocytokine fusion fails to recapitulate T_Reg-promoting activity of the mixed antibody-cytokine complex.
(a) Schematic of the IL-2/JES6–1 single-chain immunocytokine (IC) fusion with the C-terminus of the cytokine tethered to the N-terminus of the antibody light chain via a $(Gly_4Ser)_2$ flexible linker. (b) Equilibrium surface plasmon resonance titrations of soluble IL-2 (gray) or JES6–1 IC (blue) binding to immobilized IL-2Rα. Fitted equilibrium dissociation constants (K_D) are indicated. (c) STAT5 phosphorylation response (mean ± S.D.) of IL-2Rα$^+$ (*top*) or IL-2Rα$^-$ (*bottom*) YT-1 human NK cells stimulated with IL-2, IL-2/JES6–1 complex, or JES6–1 IC. (d) Ratio of T_Reg to CD8$^+$ effector T cell abundance in spleens harvested from non-obese diabetic (NOD) mice (*n*=4 per cohort) treated with PBS, IL-2, IL-2/JES6–1 complex, or JES6–1 IC for four consecutive days. Data represents mean ± s.d. Statistical significance was determined by two-tailed unpaired Student's *t*-test. The experiment was performed three times with similar results.

J Immunol. Author manuscript; available in PMC 2019 October 01.

145
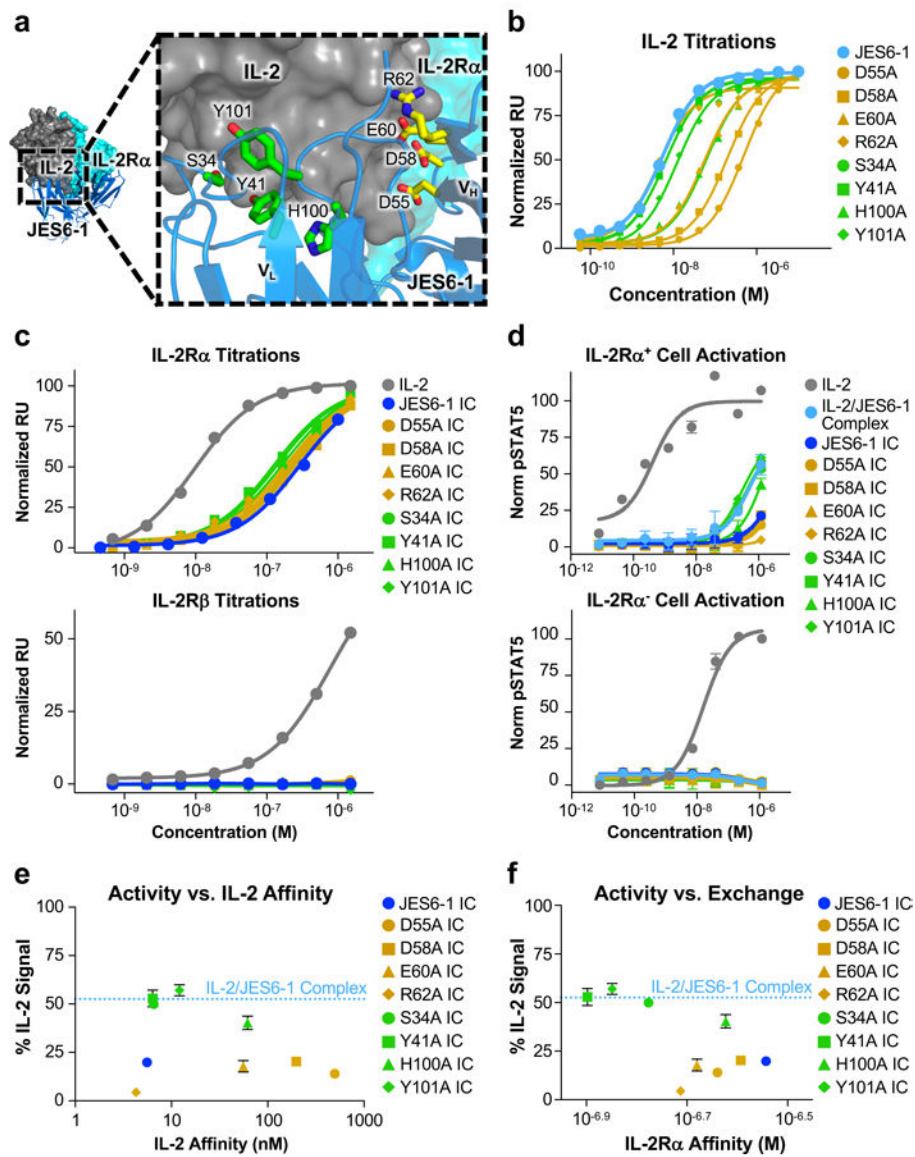
Figure 3. Disruption of antibody-cytokine affinity enhances immunocytokine activity on IL-2Rα⁺ cells.

(a) Crystallographic structure of the IL-2/JES6–1 interface (PDB ID 4YQX) (17) with interfacial antibody residues that were mutated to alanine highlighted in yellow (heavy chain) or green (light chain). Human IL-2Rα is overlaid from the IL-2 cytokine-receptor quaternary complex structure for reference (PDB ID 2B5I) (3). (b) Equilibrium surface plasmon resonance titrations of soluble IL-2 binding to immobilized JES6–1 or the indicated antibody variants. (c) Equilibrium surface plasmon resonance titrations of soluble IL-2, JES6–1 IC, or JES6–1 IC mutants binding to immobilized IL-2Rα (*top*) or IL-2Rβ (*bottom*). (d) STAT5 phosphorylation response of IL-2Rα⁺ (*top*) or IL-2Rα⁻ (*bottom*) YT-1 human NK cells treated with IL-2, JES6–1 IC, or JES6–1 IC mutants. Data represent mean ± s.d. (e) Comparison of the STAT5 phosphorylation activity of the indicated JES6–1 IC variants (% IL-2-induced signal at 1.2 μM concentration) versus IL-2 affinity of their corresponding antibodies. Activity of the IL-2/JES6–1 complex is indicated by the dashed

blue line. Data represent mean ± s.d. **(f)** Comparison of the STAT5 phosphorylation activity of the indicated JES6–1 IC variants (% IL-2-induced signal at 1.2 μM concentration) to their IL-2Rα affinities (representative of their exchanging propensities). Activity of the IL-2/JES6–1 complex is indicated by the dashed blue line. Data represent mean ± s.d. Heavy chain mutations are colored yellow and light chain mutations are colored green throughout the figure.

147
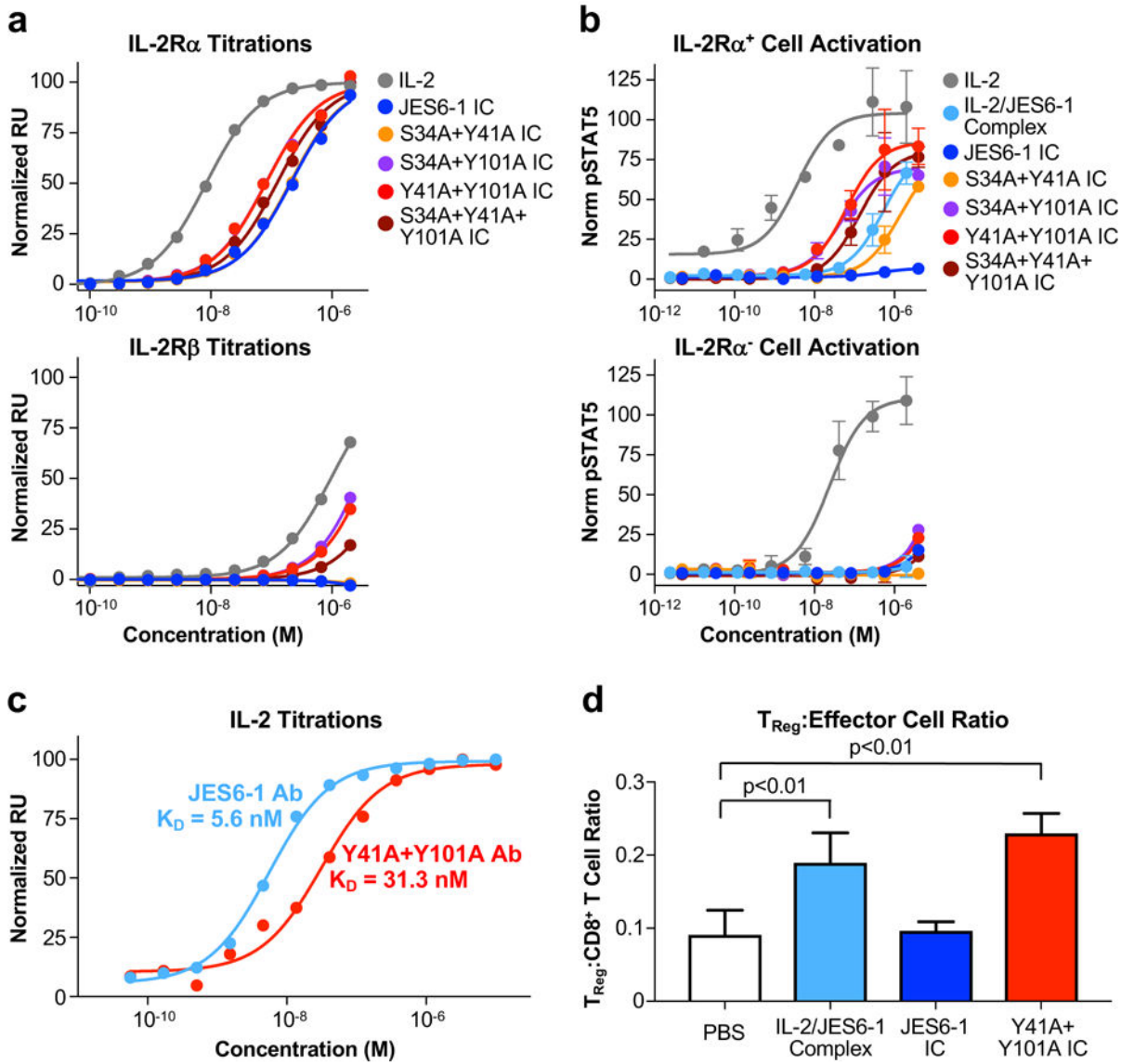
Figure 4. Engineered double mutant immunocytokine recovers T$_{Reg}$-biased activity of the IL-2/ JES6–1 complex.

(a) Equilibrium surface plasmon resonance titrations of soluble IL-2, JES6–1 IC, or double/ triple mutant JES6–1 IC mutants binding to immobilized IL-2Rα (*top*) or IL-2Rβ (*bottom*). (b) STAT5 phosphorylation response of IL-2Rα$^+$ (*top*) or IL-2Rα$^-$ (*bottom*) YT-1 human NK cells treated with IL-2, JES6–1 IC, or double/triple mutant JES6–1 IC mutants. Data represent mean ± s.d. (c) Equilibrium surface plasmon resonance titrations of soluble IL-2 binding immobilized JES6–1 antibody (light blue) or the JY3 antibody variant (red). (d) Ratio of T$_{Reg}$ to CD8$^+$ effector T cell abundance in spleens harvested from C57BL/6 mice (*n*=3 per cohort) treated with PBS, IL-2/JES6–1 complex, JES6–1 IC, or the Y41A+Y101A IC mutant for four consecutive days, as determined by flow cytometry analysis. Data represent mean ± s.d. Statistical significance was determined by two-tailed unpaired Student's *t*-test. The experiment was performed three times with similar results.
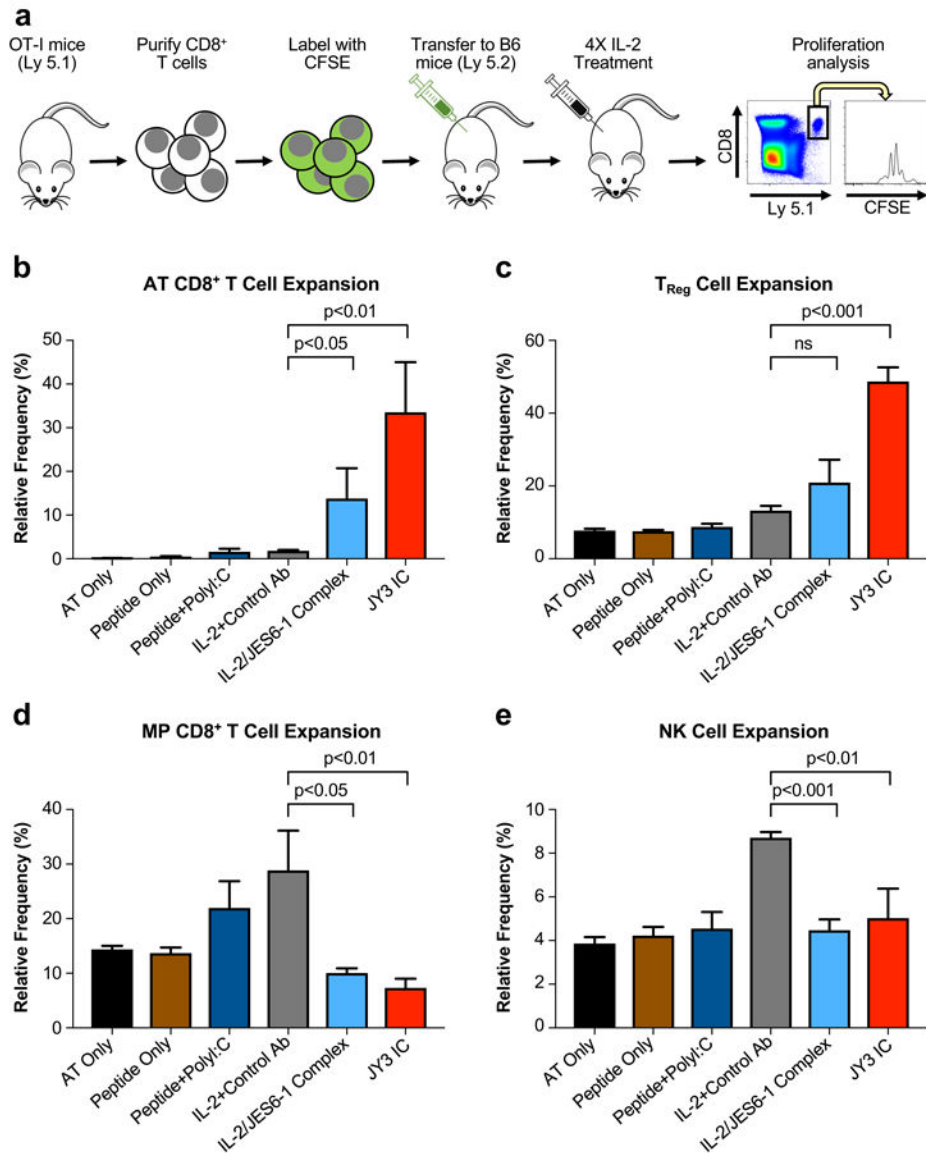
Figure 5. Engineered immunocytokine selectively potentiates the growth of activated adoptively transferred CD8$^+$ T cells while boosting immunosuppression in the recipient.
(a) Schematic of the adoptive transfer procedure. CD8$^+$ T cells were purified from OT-I/Ly 5.1 mice and adoptively transferred into C57BL/6 mice (Ly 5.2) (n=4 per cohort), which were then stimulated by SIINFEKL peptide and subjected to the indicated treatments for four consecutive days. Mice were sacrificed 48 hours after the final injection and relative expansion was quantified via flow cytometry for the adoptively transferred (AT) CD8$^+$ T cells (b) and the recipient T$_{Reg}$ cells (c), MP CD8$^+$ T cells (d), and NK cells (e). Data represent mean ± s.d. Statistical significance was determined by two-tailed unpaired Student's t-test. The experiment was performed three times with similar results.

a

BALB/c Mice

| | D0 | D1 | D2 | D3 | D4 | D5 | D6 | D7 | D8 | D9 | D10 | D11 | D12 | D13 | D14 | D15 | D16 |

Sacrifice mice; Analyze colons

IL-2 Treatment (i.p.)

Colitis induction (3% dextran sodium sulfate)

b Weight Loss

p<0.001
p<0.01

Weight loss (%)

PBS, IL-2+Control Ab, IL-2/JES6-1 Complex, JY3 IC

c Colon Length

p<0.01
NS

Length (cm)

PBS, IL-2+Control Ab, IL-2/JES6-1 Complex, JY3 IC

d Disease Activity Index

p<0.001
p<0.05

Activity Score

PBS, IL-2+Control Ab, IL-2/JES6-1 Complex, JY3 IC

Figure 6. Engineered immunocytokine reduces disease severity in a mouse model of colitis.
(a) Schematic of the mouse colitis study. BALB/c mice (n=6 per cohort) were treated once daily for 7 days with PBS, IL-2 plus a control antibody, IL-2/JES6–1 complex, or JY3 IC. Beginning on day 8, mice were subjected to 3% DSS in their drinking water to induce colitis. Weight loss (b) and disease activity index (c) were assessed on day 15. Mice were sacrificed on day 16 and colon length (d) was measured. Data represent mean ± s.d. Statistical significance by one-way ANOVA + Dunnett's multiple comparison post-test is indicated. The experiment was performed twice with similar results.

Table I.

Cytokine affinity and receptor exchange properties of engineered JES6–1 antibody and immunocytokine point mutants.

The JES6–1 antibody chains on which the mutations are located are indicated in parentheses.

Construct	K_D of IL-2/Antibody Complex (nM)	K_D of IL-2Rα/IC Complex (nM)
JES6–1	5.6	290
D55A (V_H)	500	230
D58A (V_H)	200	260
E60A (V_H)	56	210
R62A (V_H)	4.3	190
S34A (V_L)	6.5	170
Y41A (V_L)	6.4	130
H100A (V_L)	62	240
Y101A (V_L)	12	140

J Immunol. Author manuscript; available in PMC 2019 October 01.

151

Table II.

Receptor exchange properties of engineered JES6–1 antibody and immunocytokine multi-site mutants.

All mutations are located on the JES6–1 variable light chain.

Construct	K_D of IL-2Rα/IC Complex (nM)
JES6–1	220
S34A+Y41A	210
S34A+Y101A	82
Y41A+Y101A	82
S34A+Y41A+Y101A	130

J Immunol. Author manuscript; available in PMC 2019 October 01.

152
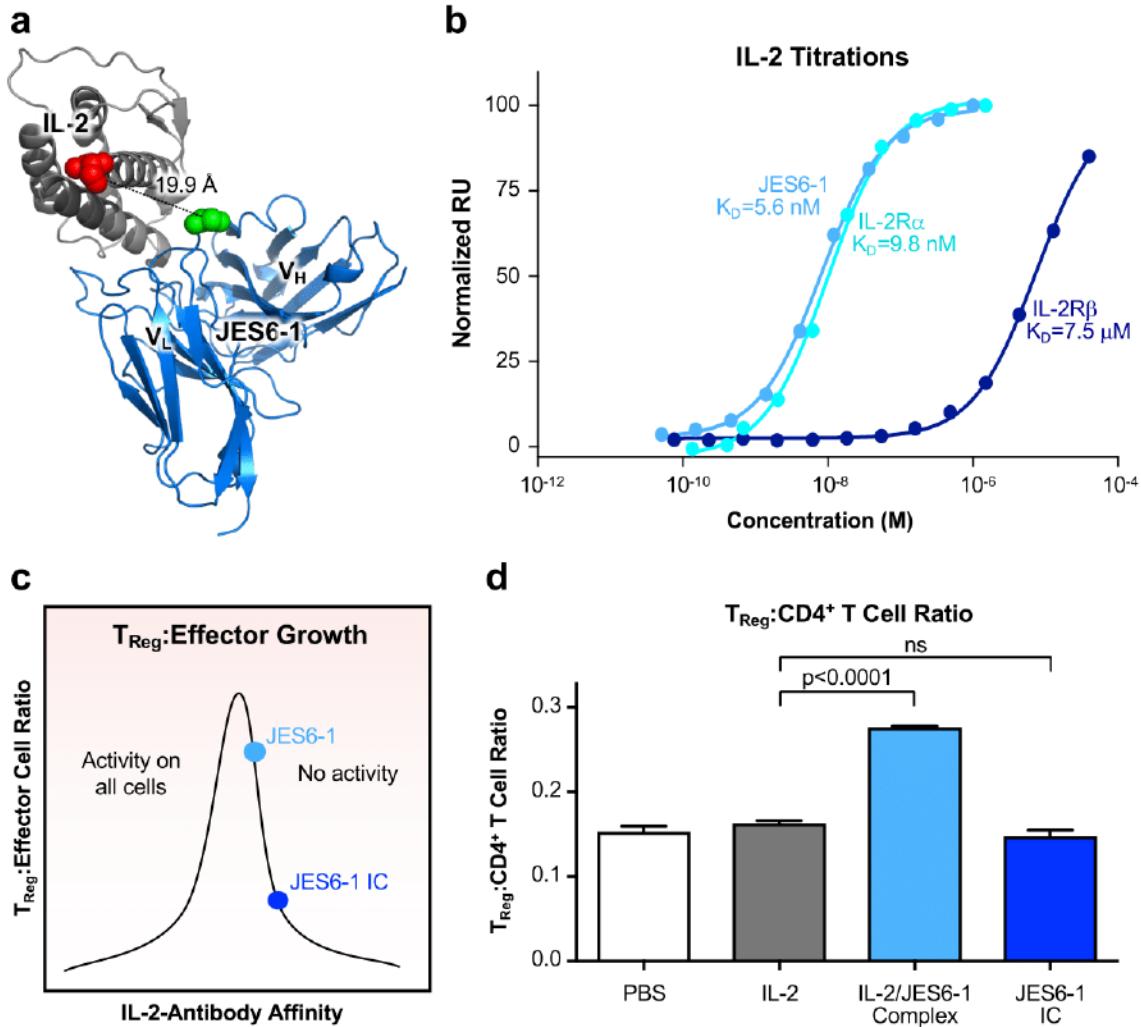
Supplemental Figure 1. *Design of a single-chain cytokine-antibody fusion linking IL-2 and JES6-1.* **(a)** Crystallographic structure of the IL-2/JES6-1 complex (PDB ID 4YQX) (17) with the distance annotated between the C-terminal residue of IL-2 (red) and the N-terminal residue of the JES6-1 V_L domain (green). The JES6-1 antibody is shown as a single-chain variable construct (scFv). **(b)** Equilibrium surface plasmon resonance titrations of soluble IL-2 binding to immobilized IL-2Rα (cyan), IL-2Rβ (navy), or JES6-1 (light blue). Fitted equilibrium dissociation constants (K_D) are indicated. **(c)** Hypothetical plot of the T_{Reg} to effector cell expansion ratio versus IL-2-antibody affinity in the framework of the JES6-1 allosteric exchange mechanism. If the cytokine-antibody affinity is very low, the cytokine will constitutively dissociate from the antibody, resulting in non-specific activation of both T_{Reg} and effector immune cells. However, if the cytokine-antibody affinity is very high, the antibody cannot be displaced by IL-2Rα, blocking IL-2 activity on both T_{Reg} and effector cells. The affinity of the JES6-1 antibody allows for receptor-antibody exchange to induce biased T_{Reg} expansion, whereas the increased affinity of JES6-1 IC precludes its stimulation of T_{Reg} proliferation. **(d)** Ratio of T_{Reg} to total CD4$^+$ T cell abundance in spleens harvested from non-obese diabetic (NOD) mice (*n*=4 per cohort) treated with PBS, IL-2, IL-2/JES6-1 complex, or JES6-1 IC for four consecutive days, as determined by flow cytometry analysis. Data represents mean ± s.d. Statistical significance was determined by two-tailed unpaired Student's *t*-test. The experiment was performed three times with similar results.
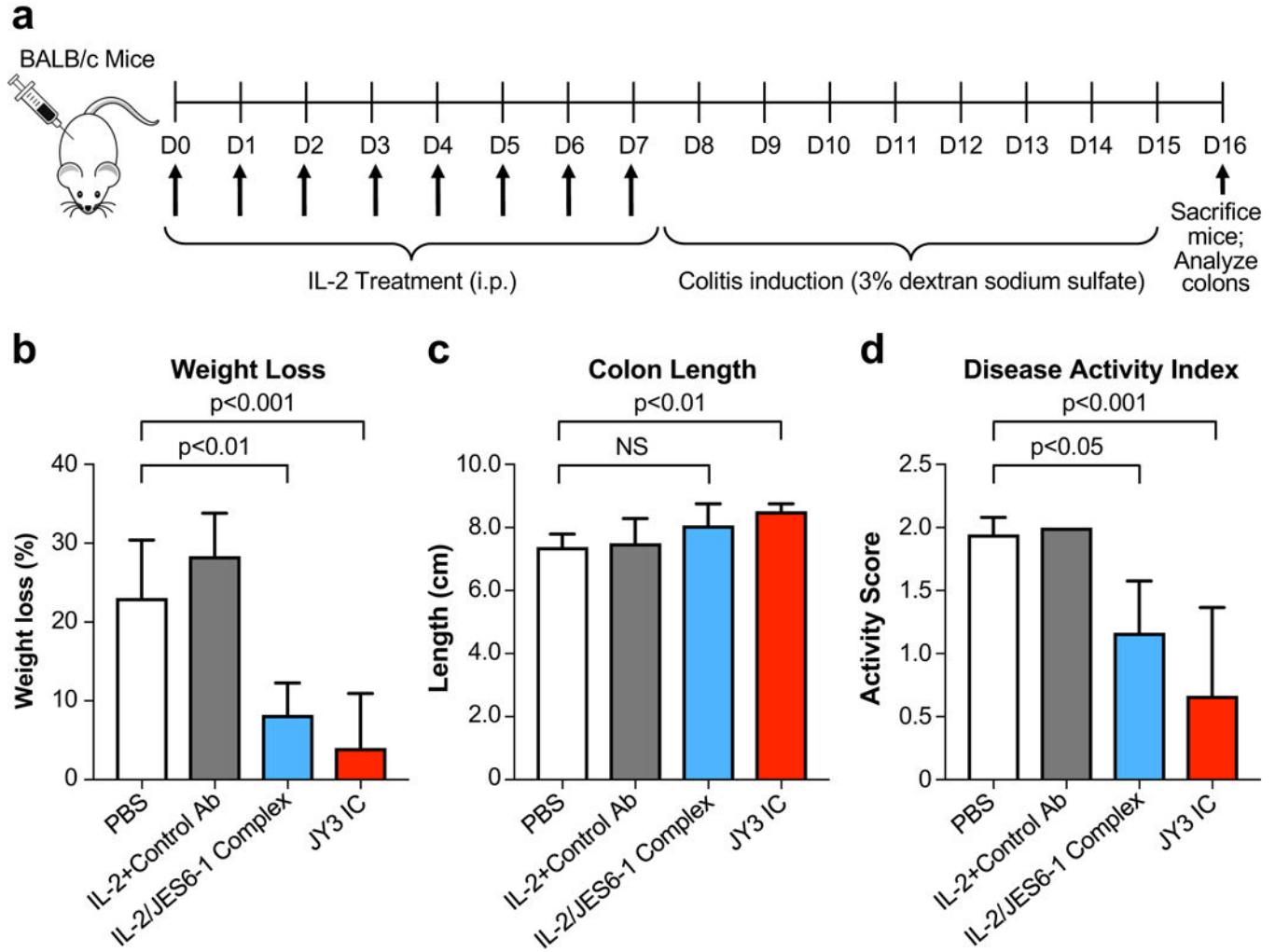
a IL-2 Titrations

JES6-1
K_D = 5.6 nM

S34A+Y101A IC
K_D = 10.6 nM

b T_{Reg}:Effector Cell Ratio

p<0.01

ns

c C57BL/6 T_{Reg}:Effector Cell Ratio

d C57BL/6 T_{Reg} Cell IL-2Rα Expression

e NOD T_{Reg}:Effector Cell Ratio

f NOD T_{Reg} Cell IL-2Rα Expression
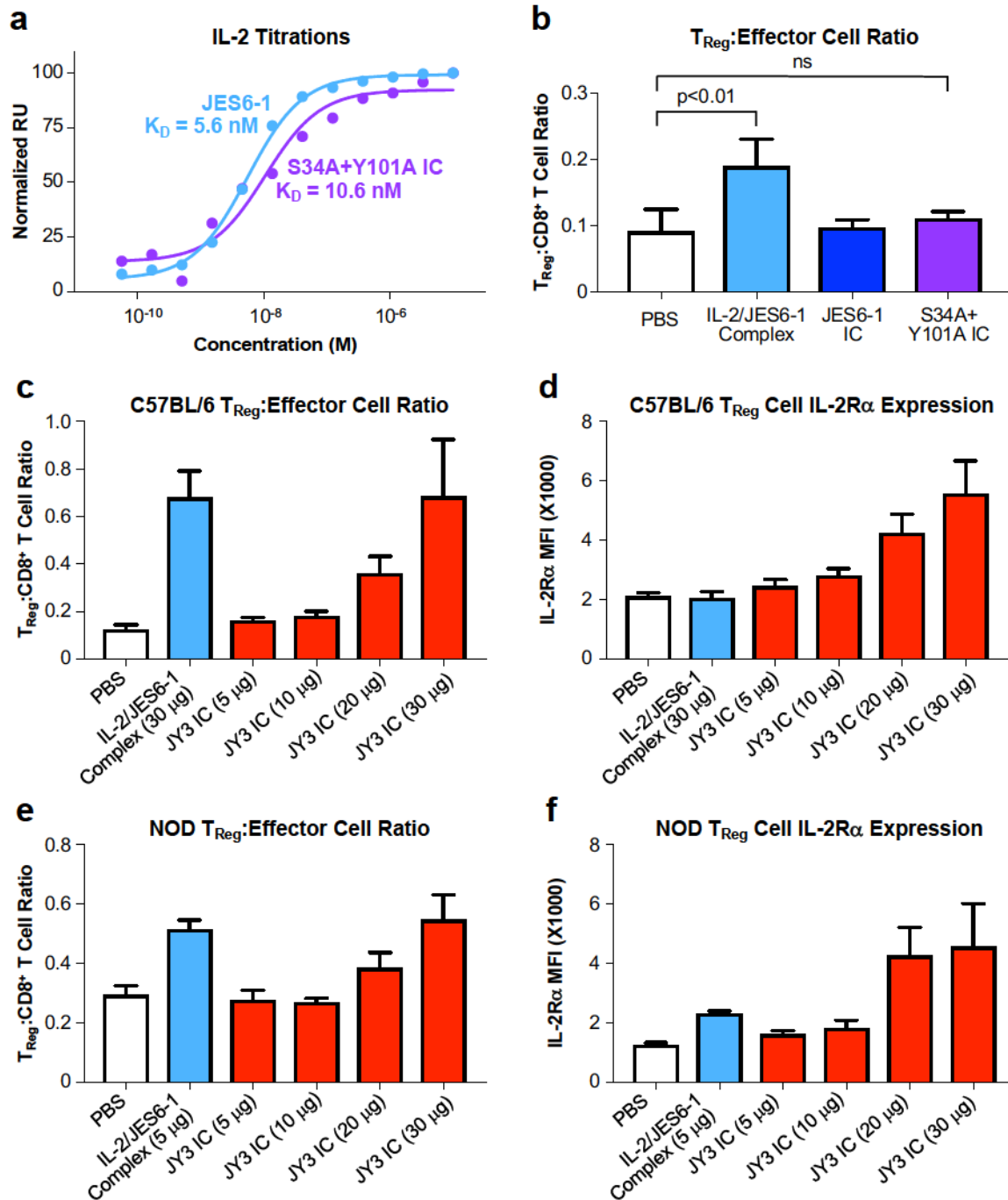
Supplemental Figure 2. *Engineered immunocytokines stimulate biased T_{Reg} potentiation and upregulate IL-2Rα expression in mice.* **(a)** Equilibrium surface plasmon resonance titrations of the soluble IL-2 interaction with immobilized JES6-1 antibody (light blue) or the S34A+Y101A antibody variant (purple). **(b)** Ratio of T_{Reg} to CD8^{+} effector T cell abundance in spleens harvested from C57BL/6 mice (*n*=3 per cohort) treated with PBS, IL-2/JES6-1 complex, JES6-1 IC, or the S34A+Y101A IC mutant, as determined by flow cytometry analysis. Data represent mean ± s.d. Statistical significance was determined by two-tailed unpaired Student's *t*-test. The experiment was performed three times with similar results. **(c)** - **(f)** The ratio of T_{Reg} cells to CD8^{+} effector T cells **(c)** and **(e)** and the mean fluorescence intensity (MFI) of IL-2Rα in T_{Reg} cells **(d)** and **(f)** harvested from the spleens of C57BL/6 **(c)** - **(d)** (*n*=3 per cohort) or non-obese diabetic (NOD) **(e)**

- **(f)** (*n*=4 per cohort) mice administered PBS or the indicated concentrations of IL-2/JES6-1 complex or JY3 IC for four consecutive days. Data represent mean ± s.d. Note that the IL-2/JES6-1 complex dose was restricted to 5 µg for NOD mice because 3/4 animals that were administered 30 µg of the IL-2/JES6-1 complex died during the course of the experiment. Experiments were performed three times with similar results.

a

T_Reg Cell Gating · CD4+ cells

CD8+ T Cell Gating · All cells

PBS — 4.76 — 10.0

IL-2/JES6-1 Complex — 14.3 — 9.16

JES6-1 IC — 5.90 — 10.9

Y41A+ Y101A IC — 14.7 — 10.6

S34A+ Y101A IC — 7.31 — 10.8

IL-2Rα / Foxp3 ; FSC-A / CD8

b

T_Reg:CD4+ T Cell Ratio

p<0.01

p<0.01

Groups: PBS, IL-2/JES6-1 Complex, JES6-1 IC, Y41A+ Y101A IC
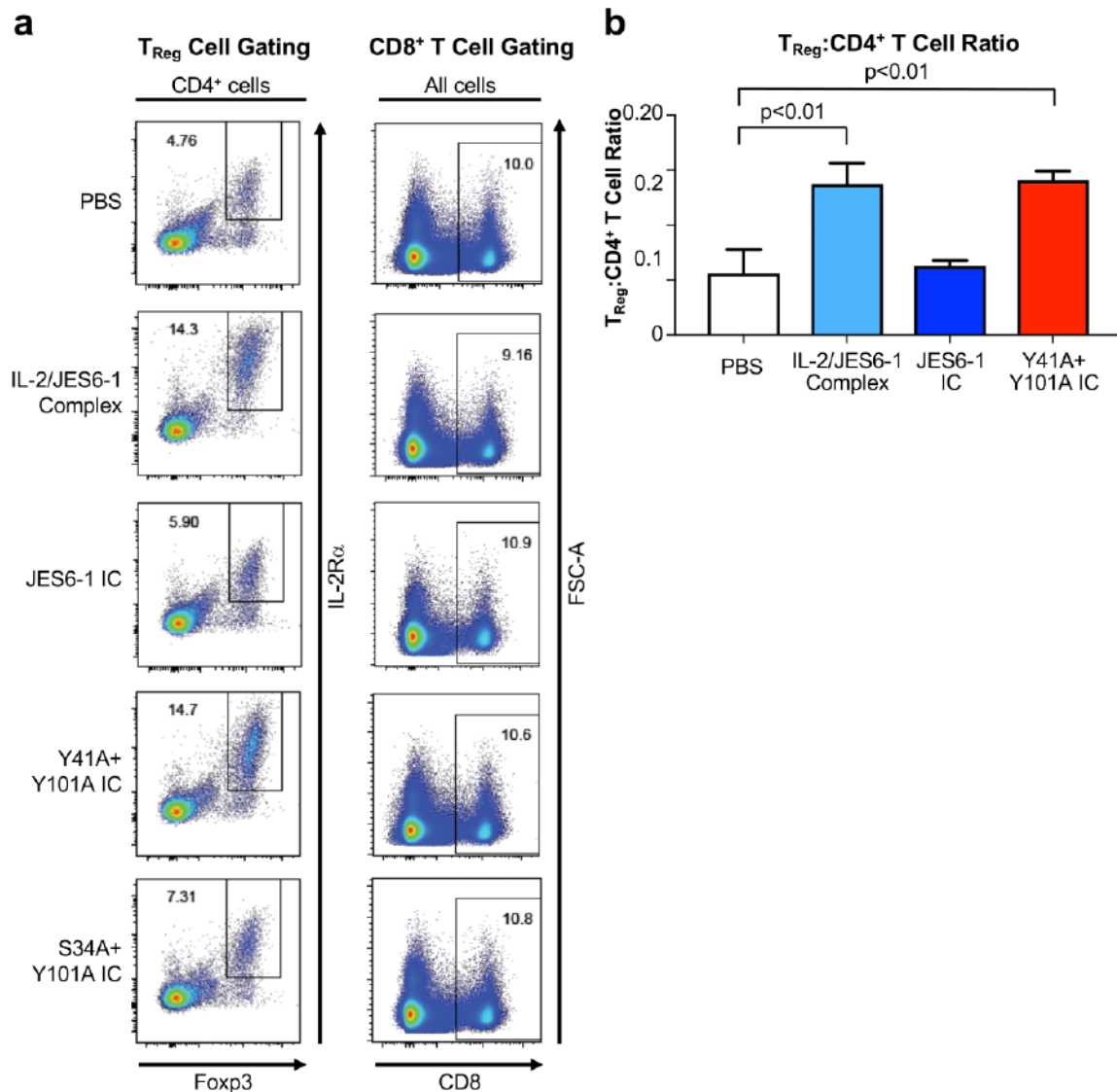
Supplemental Figure 3. *Immunocytokine selectively potentiates T_Reg cell over CD8+ T cell proliferation.* (**a**) Flow cytometry plots of IL-2Rα expression versus Foxp3 (*left*) on CD4+ cells and CD8 expression (*right*) in spleen cells harvested from C57BL/6 mice treated with PBS, IL-2/JES6-1 complex, JES6-1 IC, Y34A+Y101A IC, or S41A+Y101A IC for four consecutive days. One representative plot from three replicate mice per condition is shown. The experiment was performed three times with similar results. (**b**) Ratio of T_Reg to total CD4+ T cell abundance in spleens harvested from C57BL/6 mice (*n*=3 per cohort) treated with PBS, IL-2/JES6-1 complex, JES6-1 IC, or the Y41A+Y101A IC mutant for four consecutive days, as determined by flow cytometry analysis. Data represents mean ± s.d. Statistical significance was determined by two-tailed unpaired Student's *t*-test. The experiment was performed three times with similar results.
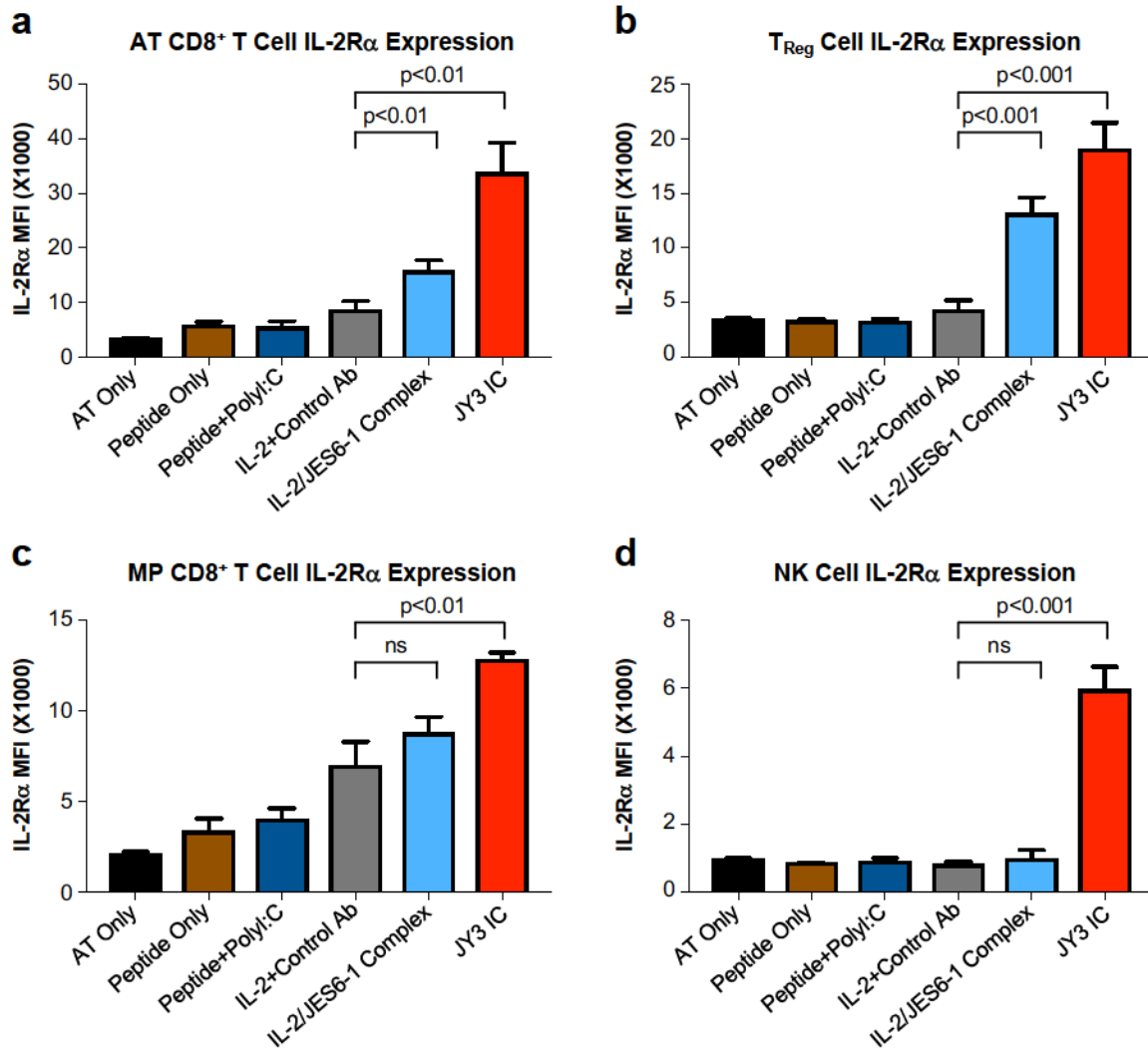
Supplemental Figure 4. *JY3 IC increases expression of IL-2Rα on immune cells in a model of adoptive CD8$^+$ T cell transfer.* CD8$^+$ T cells were purified from OT-I/Ly 5.1 mice and adoptively transferred into B6 mice (Ly 5.2) (n=3 per cohort), which were then stimulated by SIINFEKL peptide and subjected to the indicated treatments for four consecutive days. Mice were sacrificed 48 hours after the final injection and mean fluorescence intensity (MFI) of surface-expressed IL-2Rα was quantified via flow cytometry for the adoptively transferred (AT) CD8$^+$ T cells **(a)** and the recipient T$_{Reg}$ cells **(b)**, MP CD8$^+$ T cells **(c)**, and NK cells **(d)**. Data represent mean ± s.d. Statistical significance was determined by two-tailed unpaired Student's *t*-test. The experiment was performed three times with similar results.

IV.5 IL-2/JES6-1 mAb complexes dramatically increase sensitivity to LPS through IFN-γ production by CD25$^+$Foxp3$^-$ T cells

IL-2/JES6 complexes, highly selectively stimulating and expanding CD25$^+$ Treg cells, have shown considerable promise in the treatment of autoimmune diseases. However, our findings highlight a significant safety concern since IL-2/JES6 dramatically increases sensitivity to LPS-mediated shock in C57BL/6 mice. This increased susceptibility is linked to the production of IFN-γ by newly emerging populations of CD25$^+$Foxp3$^-$CD4$^+$ and CD25$^+$Foxp3$^-$CD8$^+$ T cells, particularly found in the liver. Importantly, increased sensitivity to LPS is absent in IFN-γ-deficient and nude mice, indicating a dependency on endogenous IFN-γ and T cells. Additionally, in the blood and spleen, IL-2/JES6 treatment elevates CD11b$^+$CD14$^+$ cells with induced CD25 expression and increased TNF-α production in response to LPS. These findings necessitate a reconsideration of the safety profiles of IL-2/JES6 and similar immunotherapeutic strategies, suggesting that while they hold therapeutic potential, a detailed investigation of their impact on immune function and inflammatory response is necessary. The insights from this study elucidate the complex immune modulation by IL-2/JES6 and show us an interesting connection between IL-2 stimulatory activity and sensitivity to LPS.

P. Weberová's contribution to this publication:

The majority of data used in this manuscript resulted from my work or the work of my colleague Jakub Tomala, including the execution of experiments, data analysis, and interpretation of results. I also contributed to the preparation of the manuscript. Overall contribution ~ 25 %.

IL-2/JES6-1 mAb complexes dramatically increase sensitivity to LPS through IFN-γ production by CD25⁺Foxp3⁻ T cells

Jakub Tomala[1], Petra Weberova[1], Barbora Tomalova[1],
Zuzana Jiraskova Zakostelska[2], Ladislav Sivak[1], Jirina Kovarova[1], Marek Kovar[1]*

[1]Laboratory of Tumor Immunology, Institute of Microbiology, Czech Academy of Sciences, Prague, Czech Republic; [2]Laboratory of Cellular and Molecular Immunology, Institute of Microbiology, Czech Academy of Sciences, Prague, Czech Republic

Abstract Complexes of IL-2 and JES6-1 mAb (IL-2/JES6) provide strong sustained IL-2 signal selective for CD25⁺ cells and thus they potently expand T_{reg} cells. IL-2/JES6 are effective in the treatment of autoimmune diseases and in protecting against rejection of pancreatic islet allografts. However, we found that IL-2/JES6 also dramatically increase sensitivity to LPS-mediated shock in C57BL/6 mice. We demonstrate here that this phenomenon is dependent on endogenous IFN-γ and T cells, as it is not manifested in IFN-γ deficient and nude mice, respectively. Administration of IL-2/JES6 leads to the emergence of CD25⁺Foxp3⁻CD4⁺ and CD25⁺Foxp3⁻CD8⁺ T cells producing IFN-γ in various organs, particularly in the liver. IL-2/JES6 also increase counts of CD11b⁺CD14⁺ cells in the blood and the spleen with higher sensitivity to LPS in terms of TNF-α production and induce expression of CD25 in these cells. These findings indicate safety issue for potential use of IL-2/JES6 or similar IL-2-like immunotherapeutics.

Editor's evaluation

Tomala et al., describes the ability of IL-2/JES6-1 mAb complexes to increase mouse sensitivity to LPS challenge. The authors present data to suggest this is due to IFN-γ production by CD25⁺Foxp3⁻ T cells. The manuscript has identified an interesting phenomenon as a result of IL-2/JES6-1 complex administration. These data may provide novel avenues for future therapeutic intervention in autoimmune disease.

*For correspondence:
makovar@biomed.cas.cz

Competing interest: The authors declare that no competing interests exist.

Introduction

IL-2 is a crucial cytokine for activation, expansion, and expression of effector functions of T and NK cells as well as for homeostasis of regulatory T (T_{reg}) cells (*Boyman and Sprent, 2012*; *Liao et al., 2013*; *Malek and Castro, 2010*). IL-2 exerts its biological activities through binding to either a dimeric receptor composed of IL-2Rβ (CD122) and common cytokine receptor gamma chain (γ$_c$, CD132) or to a trimeric receptor composed of a dimeric one with the addition of IL-2Rα (CD25) (*Minami et al., 1993*; *Waldmann, 1989*). CD25 is not involved in signal transduction, but increases the affinity of the trimeric receptor for IL-2 by about 100-fold (*Minami et al., 1993*; *Waldmann, 1989*). The dimeric receptor (K_d ~1 nM) is mostly found on memory CD8⁺ T and NK cells, whilst the trimeric receptor (K_d ~10 pM) is typically expressed at high levels by T_{reg} cells, recently activated T cells and ILC2s (*Boyman and Sprent, 2012*; *Roediger et al., 2013*; *Sakaguchi et al., 1995*).

IL-2 was the first immunotherapy approved for the treatment of metastatic renal cell carcinoma and malignant melanoma in the early 1990s (*Atkins et al., 1999*; *Klapper et al., 2008*), having induced

an overall response in 15–17% of patients with these cancers including 5–10% durable complete remissions (*Atkins et al., 1999*; *Klapper et al., 2008*). However, an extremely short half-life (*Donohue and Rosenberg, 1983*) and serious side toxicities associated with high-dose IL-2 treatment are the major drawbacks. Moreover, IL-2 treatment leads to expansion of T_{reg} cells which can dampen effector T cell activity against tumors (*Berendt and North, 1980*). Indeed, it has been shown that long-term, low-dose IL-2 therapy preferentially stimulates T_{reg} cells due to their constitutive high expression of trimeric IL-2R and can be used for treatment of autoimmune diseases and delaying allograft rejection (*Klatzmann and Abbas, 2015*; *Yu et al., 2009*). However, due to significant limitations of IL-2, strong attempts have been made to improve IL-2-based therapy. One of the most promising approaches is to employ complexes of IL-2 and certain anti-IL-2 mAbs. It has been demonstrated that these complexes not only markedly prolong the half-life of parenterally administered IL-2 (from minutes to hours) but they also exert selective stimulatory activity for different immune cell populations depending on the mAb used (*Boyman et al., 2006*; *Tomala et al., 2009*). Complexes of murine IL-2 and S4B6 mAb (IL-2/S4B6 henceforth) were shown to potently stimulate memory CD8^{+} T and NK cells, whilst complexes of murine IL-2 and JES6-1 mAb (IL-2/JES6 henceforth) highly selectively expand T_{reg} cells (*Boyman et al., 2006*; *Spangler et al., 2015*; *Tomala et al., 2009*). Selectivity of IL-2/JES6 for cells expressing the high-affinity IL-2R is governed by the fact that the binding site for JES6-1 mAb and CD122/CD132 in the IL-2 molecule, almost completely overlap. IL-2/JES6 is thus not able to bind to IL-2R and induce signaling per se. However, CD25 can engage IL-2 bound to JES6-1 mAb, particularly when expressed at high levels, and progressively 'peel off' the cytokine from the antibody in a zipper-like mechanism, ultimately leading to dissociation of JES6-1 mAb. Once JES6-1 mAb dissociates, the CD25-bound IL-2 is liberated to recruit CD122/CD132 to form the functional signaling complex (*Spangler et al., 2015*). Selectivity of IL-2/JES6 for CD25^{+} cells results in their high efficacy to expand T_{reg} cells in vivo and makes them an attractive immunotherapeutic. It has been shown that IL-2/JES6 could be used for treatment of various autoimmune diseases (*Izquierdo et al., 2018*; *Liu et al., 2011*; *Webster et al., 2009*; *Wilson et al., 2008*) and to facilitate long-term acceptance of allografts without the need for immunosuppression (*Webster et al., 2009*). A single-chain format of IL-2/JES6 was produced with a mutated JES6-1 mAb-binding site, termed JY3, which affected the affinity for IL-2. This proved to be effective in selective expansion of T_{reg} cells and in the model of autoimmune colitis (*Spangler et al., 2018*). Furthermore, there is a report describing the development of fully human mAb binding human IL-2 with the capacity to selectively expand T_{reg} cells in vivo when complexed with human IL-2 (*Trotta et al., 2018*).

It has been shown that T_{reg} cells expanded by IL-2/JES6 produce IL-10 and TGF-β (*Webster et al., 2009*). We therefore decided to explore the possibility that IL-2/JES6 are able to protect against LPS-induced toxicity. Interestingly, we found that short-term pre-treatment (three daily doses) with IL-2/JES6 dramatically increases sensitivity of C56BL/6 mice to LPS-induced shock and mortality. Thus, we decided to further investigate this phenomenon and to uncover the mechanism responsible for IL-2 signal-mediated LPS hyperreactivity.

Results
IL-2/JES6, but Not IL-2/S4B6, dramatically increase sensitivity to LPS

We asked whether selective expansion of T_{reg} cells via treatment with IL-2/JES6 could lead to protection from the toxic effect of LPS. To answer this we injected C56BL/6 mice with three daily doses of IL-2/JES6 (1.5 µg IL-2/dose) and challenged these mice with LPS 48 h after the last dose of IL-2/JES6 (*Figure 1A*). We titrated LPS dosing in previous experiments in order to determine the maximum non-lethal dose (MNLD), that is, the highest dose that causes significant toxic effect but no mortality. Since we found that toxicity of LPS varies from batch to batch even if ordered as identical product from the same commercial supplier, we isolated a large batch of LPS from *S. typhymurium* LT2, S-strain (see Materials and methods) and used it throughout the whole study. We determined that the MNLD of our LPS was ~200 µg/mice in C56BL/6 mice. Control C56BL/6 mice developed hypothermia starting about 4–6 h after LPS challenge (100% of MNLD) and peaking after approximately 24 h. However, all mice recovered over the next 2 d. Mice injected with a low dose of LPS (10% of MNLD) developed only negligible hypothermia 8 h after LPS injection and fully recovered within 24 h. Contrary to that, the same low dose of LPS induced extremely rapid onset of progressively worsening hypothermia
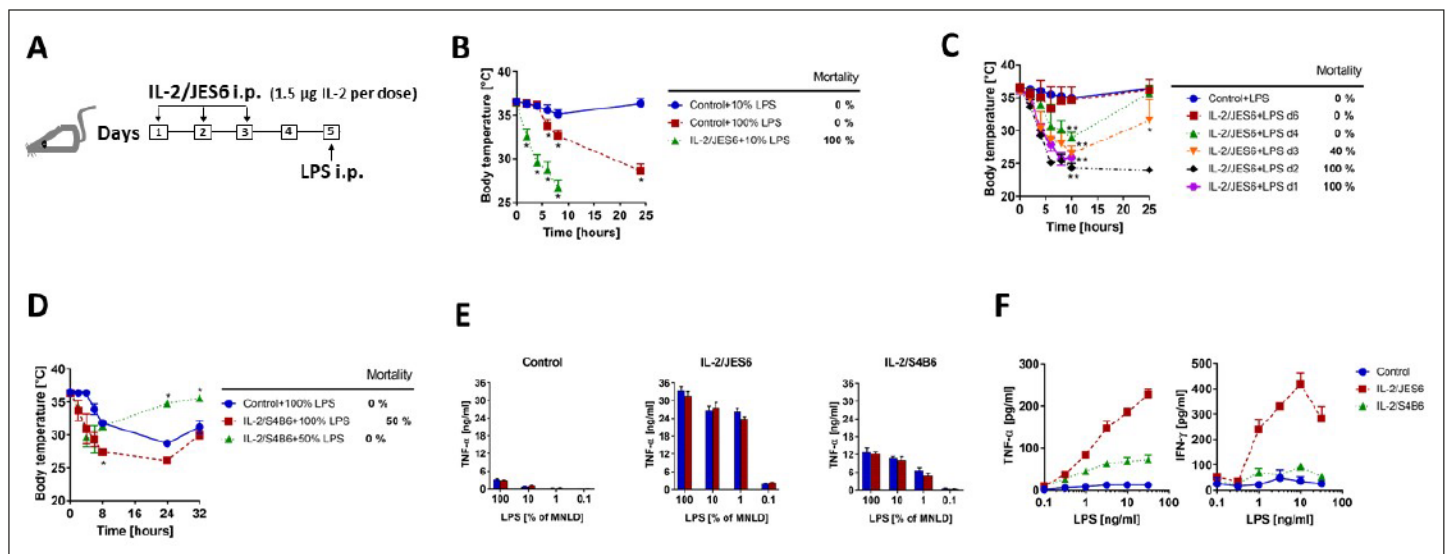
160

Figure 1. IL-2/JES6 dramatically increase sensitivity to LPS-induced shock and mortality. (**A**) Schedule of sensitization of mice to LPS through administration of IL-2/JES6 used throughout the study, unless stated otherwise. (**B**) C56BL/6 mice were treated with IL-2/JES6 as shown in A. Control mice were treated with sterile PBS. The dose of injected LPS is shown in % of maximum non-lethal dose, henceforth (MNLD; 100% ~ 200 μg LPS/mice). (**C**) C56BL/6 mice were treated with IL-2/JES6 and LPS (10% of MNLD) was injected 1–6 d after the last dose of IL-2/JES6. (**D**) C56BL/6 mice were treated with complexes of IL-2 and S4B6 mAb (IL-2/S4B6) followed by LPS challenge (100 or 50% of MNLD) using the same schedule as in A. (**E**) C56BL/6 mice were treated as in A with PBS (Control), IL-2/JES6 or IL-2/S4B6 complexes. Mice were euthanized 90 min post administration of titrated doses of LPS and their individual sera were collected. Concentration of TNF-α in the serum was determined by ELISA. Each bar represents one individual mouse± SD (n = 3 technical replicates). (**F**) C56BL/6 mice were treated as in A with PBS (Control), IL-2/JES6 or IL-2/S4B6 complexes, but not challenged with LPS. Mice were euthanized 2 d after the last dose of complexes and their spleen cells were cultivated in titrated concentrations of LPS for 16 h in vitro. Concentrations of TNF-α and IFN-γ in the supernatant were determined by ELISA. Each point represents pool of three individual mouse ± SD (n = 3 technical replicates). All experiments were done at least twice with similar results; n = 4–7 technical replicates (**B–D**). Data were analysed using an unpaired two-tailed Student's t-test. Significant differences to control are shown (* p ≤ 0.05; ** p ≤ 0.01).

The online version of this article includes the following source data and figure supplement(s) for figure 1:

Source data 1. Source data for *Figure 1*, panels B-F.

Figure supplement 1. Nitrite significantly reduces toxicity of LPS in mice pretreated with IL-2/JES6.

Figure supplement 1—source data 1. Source data for *Figure 1—figure supplement 1*.

Figure supplement 2. IL-2/JES6 induce more severe lung oedema in comparison to IL-2/S4B6.

Figure supplement 2—source data 1. Source data for *Figure 1—figure supplement 2*.

when mice were pretreated with IL-2/JES6 and the mice usually died within 8–24 h (*Figure 1B*). Next, we decided to determine the kinetics of sensitization to LPS by IL-2/JES6. Mice pretreated with IL-2/JES6 as in *Figure 1A* were challenged at different time points after IL-2/JES6 treatment with low dose of LPS (10% of MNLD). *Figure 1C* shows that LPS caused 100% mortality when injected up to 2 d post IL-2/JES6 treatment and 40% mortality when injected 3 d after that. Significant hypothermia, but no mortality was seen when LPS was injected 4 d post IL-2/JES6. No sensitization to LPS was found when LPS was injected 6 d post IL-2/JES6. These data shows that IL-2/JES6 dramatically increase sensitivity to LPS in C56BL/6 mice and that this increased sensitivity lasts about 4 d post IL-2/JES6 treatment.

We also wanted to know whether IL-2/S4B6 sensitize C56BL/6 mice to LPS. Mice pretreated with IL-2/S4B6 using the same schedule as in *Figure 1A*, showed only decent sensitization to LPS as challenge with relatively high dose of LPS (50% of MNLD) induced hypothermia but no mortality (*Figure 1D*). Thus, IL-2 complexes with selective stimulatory activity for CD25high cells, but not those which stimulate predominantly CD122high cell populations, dramatically increase sensitivity to LPS. Accordingly, TNF-α levels in sera of mice pretreated with IL-2/JES6 were significantly higher in comparison to sera from mice pretreated with IL-2/S4B6 after LPS challenge (*Figure 1E*). Furthermore, splenocytes from IL-2/JES6 pretreated mice produced much higher amounts of TNF-α and IFN-γ than those from IL-2/S4B6 pretreated mice when cultivated in the presence of LPS in vitro (*Figure 1F*).
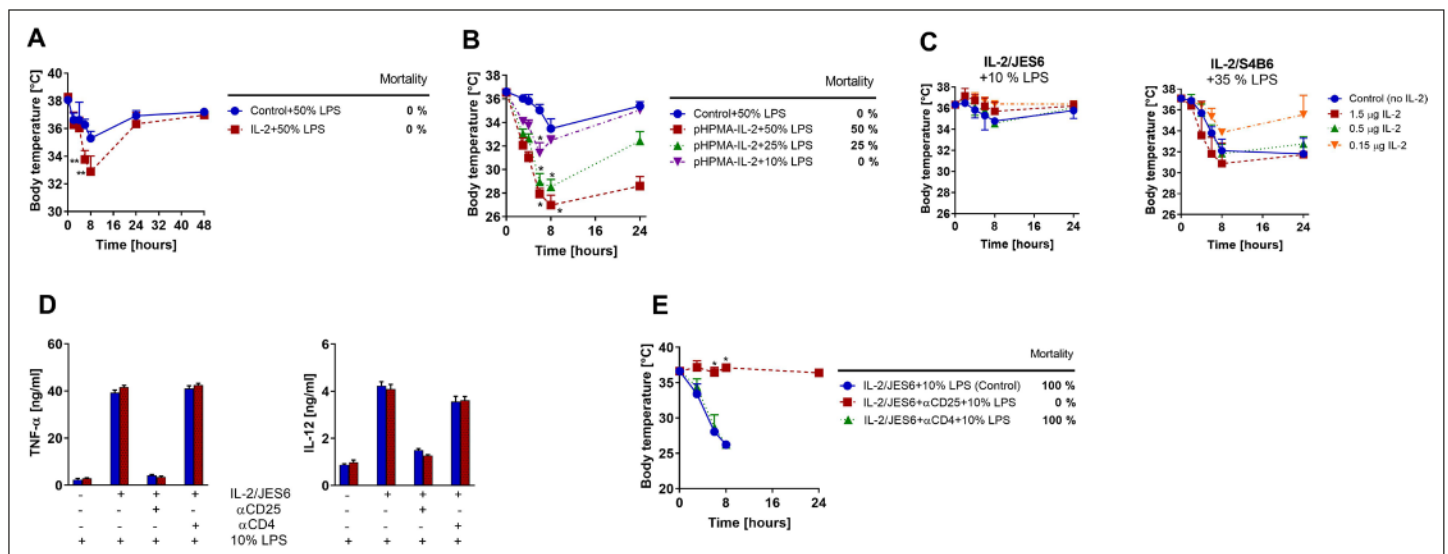
Figure 2. Strong sustained IL-2 signal and not solely IL-2/JES6, increases sensitivity to LPS; IL-2/JES6-mediated sensitivity to LPS could be completely blocked by αCD25 mAb. (**A**) C56BL/6 mice were treated with rmIL-2 (35 μg/dose) according to the schedule shown in *Figure 1A* and challenged with LPS (50% of MNLD). (**B**) C56BL/6 mice were treated with IL-2 covalently bound to the polymeric carrier based on poly(HPMA) using the same schedule as in *Figure 1A* and subsequently challenged with titrated doses of LPS. (**C**) C56BL/6 mice were injected simultaneously with LPS and either IL-2/JES6 or IL-2/S4B6 complexes (1.5 or 0.5 or 0.15 μg IL-2/dose) in one i.p. injection. Dosage of LPS is shown in % of MNLD above each graph. Control mice were injected with the same dose of LPS only. (**D**) C56BL/6 mice were injected with IL-2/JES6 and then challenged with LPS (10% of MNLD) as shown in *Figure 1A*. Some mice were also injected with either αCD25 or αCD4 mAb (250 μg/mouse i.p.) 4 h prior to the first injection of IL-2/JES6 as shown below in the graphs. Mice were euthanized 4 h after the LPS challenge and concentrations of TNF-α and IL-12 were determined by ELISA. Each bar represents one individual mouse± SD (n = 3 technical replicates). (**E**) C56BL/6 mice were treated with IL-2/JES6 and subsequently challenged with LPS as shown in *Figure 1A*. Some mice were also injected with either αCD25 or αCD4 mAb (250 μg per mouse i.p.) 4 h prior to the first injection of IL-2/JES6. All experiments were done at least twice with similar results; n = 4–6 technical replicates. Data were analysed using an unpaired two-tailed Student's t-test. Significant differences to control are shown (* p ≤ 0.05; ** p ≤ 0.01).

The online version of this article includes the following source data for figure 2:

Source data 1. Source data for *Figure 2*, panels A-E.

Both durability of IL-2 signal and its selectivity for CD25^{high} cells are necessary to induce high sensitivity to LPS

Next, we asked whether IL-2 alone is also able to measurably increase the sensitivity of C56BL/6 mice to LPS. We pretreated mice with high IL-2 dosage (35 μg/dose, i.e., more than 20-times higher compared to IL-2/JES6) and challenged them with LPS using the same schedule as in *Figure 1A*. We found that mice pretreated with IL-2 developed more profound hypothermia than controls, however, no mortality was recorded (*Figure 2A*). Thus, IL-2 alone can produce a slight increase in sensitivity to LPS when a high dosage is used. We decided to test whether IL-2 bound to a biocompatible polymeric carrier based on poly(*N*-(2-propyl)methacrylamide) would be more effective in sensitization to LPS. The rationale here is that IL-2 bound to this polymeric carrier has a significantly prolonged half-life in circulation (3–4 h, i.e., similar to IL-2 complexes) thus providing a more sustained IL-2 signal but with no selectivity for CD25^{high} cells (*Votavova et al., 2015*). Indeed, IL-2 bound to a polymeric carrier sensitized C56BL/6 mice to LPS substantially more effectively than IL-2. The LPS challenge with 50% of MNLD caused more severe hypothermia and 50% mortality (*Figure 2B*). These data demonstrate that durability of the IL-2 signal plays a remarkable role in sensitization to LPS via IL-2. However, sensitivity to LPS induced by IL-2 bound to the polymeric carrier is still much weaker in comparison to IL-2/JES6, showing that selectivity for CD25^{high} cells is also important. We injected LPS 48 h after the last dose of IL-2 complexes in our sensitization experiments. Therefore, it is highly unlikely that there was still a biologically active concentration of these complexes at the time of LPS administration since the half-life of IL-2 complexes was determined to be several hours. However, to exclude the possibility that increased sensitivity to LPS is caused by the presence of IL-2 complexes at the time of LPS injection, that is, that LPS and IL-2 complexes acts together at the same time, we injected C56BL/6 mice with

162

either IL-2/JES6 or IL-2/S4B6 and simultaneously challenged them with LPS (10% or 35% of MNLD, respectively). Simultaneous co-administration of IL-2 complexes and LPS did not increase toxicity of LPS, as seen in *Figure 2C*. These data show that it is important the IL-2/JES6 to be present before LPS administration rather than at the time of administration in order to induce LPS hyperreactivity. Thus, IL-2/JES6 either act on cells that are able to directly respond to LPS making them hyperresponsive, or they activate some immune cell subset(s), which in turn mediates LPS hyperreactivity, for example, via production of some effector molecule(s).

Since high expression of CD25 is a prerequisite for the ability to utilize IL-2/JES6, we decided to test whether blocking of CD25 abrogates sensitization to LPS by IL-2/JES6. Indeed, administration of anti-CD25 mAb completely diminished sensitization to LPS by IL-2/JES6 measured by both TNF-α or IL-12 serum levels (*Figure 2D*) and hypothermia plus mortality (*Figure 2E*). Notably, administration of anti-CD4 mAb had no effect, although CD25^{high} cells are mostly T$_{reg}$ cells in naïve unprimed mice (*Figure 2D and E*). This show that CD4$^+$ T cells, including T$_{reg}$ cells, do not play an irreplaceable role in the studied phenomenon.

IL-2/JES6 increase counts of CD11b$^+$CD14$^+$ cells and their responsiveness to LPS

Our next set of experiments aimed to deduce how IL-2/JES6 affect LPS-responding myeloid cells, particularly CD11b$^+$CD14$^+$ cells. We found that treatment of C56BL/6 mice with IL-2/JES6 (as in *Figure 1A*) increased relative counts of CD11b$^+$CD14$^+$ cells in the spleen and blood (*Figure 3A and B*) as well as absolute counts of these cells in the spleen (*Figure 3C*). We also found that treatment with IL-2/JES6 expands myeloid cells in general. IL-2/JES6 expanded significantly granulocytes, eosinophils and DCs and elevated, though not significantly, relative counts of monocytes and macrophages (*Figure 3—figure supplement 1*). Of note, treatment with IL-2/JES6 increased MHC II expression on monocytes and macrophages (*Figure 3—figure supplement 2*). The proliferation of myeloid cells driven by IL-2/JES6 was further confirmed by BrdU incorporation (*Figure 3—figure supplement 3*). IL-2/JES6 also remarkably increased responsiveness of CD11b$^+$CD14$^+$ cells from the spleen (*Figure 3D and E*) and blood (*Figure 3F and G*) to LPS in term of TNF-α production. Moreover, we found that IL-2/JES6 increased expression of CD25 in CD11b$^+$CD14$^+$ cells from the spleen and liver (*Figure 3H, I*) thus enabling these cells to effectively utilize IL-2/JES6. These data collectively show that treatment with IL-2/JES6 increases both the counts of LPS-responsive myeloid cells in various body compartments and their responsiveness to LPS. We asked a question whether this increased responsiveness of myeloid cells to LPS was due to the increased expression of TLR4. Thus, we analyzed *Tlr4* expression in spleen cells via quantitative RT-PCR and in various myeloid cell subsets via flow cytometry. Treatment with IL-2/JES6 did not affect the *Tlr4* expression in splenocytes on mRNA level (*Figure 3—figure supplement 4*). No statistically significant difference in TLR4 level upon IL-2/JES6 treatment in comparison to control was found in CD11b$^+$Ly6G$^-$Ly6C^{high} cells. Surprisingly, IL-2/JES6 treatment decently but statistically significantly decreased TLR4 levels in CD11b$^+$Ly6G$^+$ cells and CD11b$^+$Ly6G$^-$Ly6C^{low}cells (*Figure 3—figure supplement 5*). IL-2/JES6 thus did not increased the sensitivity to LPS via increased expression of TLR4.

T cells and IFN-γ are essential for sensitization to LPS by IL-2/JES6

IFN-γ is known to activate myeloid cells, particularly monocytes and macrophages, to more vigorously respond to TLR ligands including LPS. Thus, we decided to compare sensitization to LPS by IL-2/JES in C56BL/6 mice and BALB/c mice. C56BL/6 mice are described as a strand with sufficient IFN-γ production while BALB/c mice are poor producers. We determined levels of various cytokines in sera of C56BL/6 and BALB/c mice pretreated with IL-2/JES6 at different time points after LPS challenge. Levels of TNF-α, IFN-γ, IL-1β, IL-12, and IL-6 were much higher in sera of C56BL/6 mice pretreated with IL-2/JES6 in comparison with controls, despite the fact that control mice were challenged with 10-times higher doses of LPS. Contrary to this, levels of the above mentioned cytokines were comparable in sera of control and IL-2/JES6 pretreated BALB/c mice (*Figure 4A*). Furthermore, BALB/c mice pretreated with IL-2/JES6 showed much milder sensitization to LPS in term of hypothermia and mortality than C56BL/6 mice (*Figure 4B*). These data show that the endogenous production of IFN-γ upon IL-2/JES6 administration probably plays a crucial role in sensitization to LPS. To confirm a key role of IFN-γ directly, we injected C56BL/6 mice with anti-IFN-γ mAb prior to IL-2/JES6 pretreatment
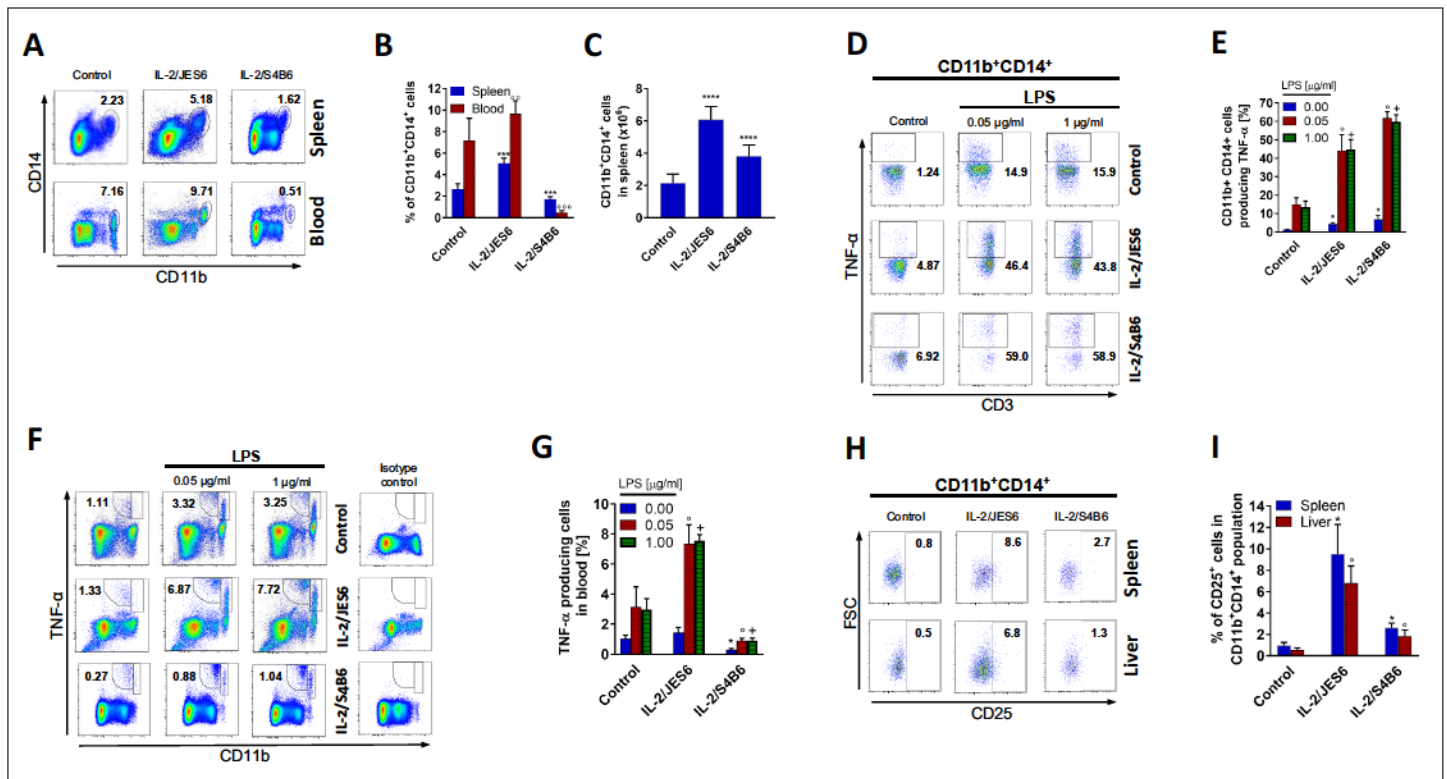
Figure 3. IL-2/JES6 increases counts of CD11b+CD14+ cells and their responsiveness to LPS in terms of TNF-α production. C56BL/6 mice were treated with IL-2/JES6 or IL-2/S4B6 as shown in *Figure 1A*. The relative number of CD11b+CD14+ cells was determined by flow cytometry in blood and spleen 2 d after the last dose of IL-2 complexes. Dot plots showing one representative mouse (**A**) and a bar graph showing the mean ± SD in the experimental groups (**B**) are shown. (**C**) Absolute numbers of CD11b+CD14+ cells in the spleen of mice from the same experiment as shown in A and B. C56BL/6 mice were treated with IL-2/JES6 or IL-2/S4B6 as shown in *Figure 1A*. Spleen cells were cultivated ex vivo with LPS for 2 h and TNF-α production in CD11b+CD14+ cells was determined by flow cytometry. Dot plots showing one representative mouse (**D**) and a bar graph showing the mean ± SD in experimental groups (**E**) are shown. A similar experiment to the one shown in D and E was done using the blood of C56BL/6 mice treated with IL-2/JES6 or IL-2/S4B6. TNF-α production in CD11b+ cells is shown in one representative mouse (**F**) and in a bar graph showing the mean ± SD in experimental groups (**G**). (**H**) C56BL/6 mice were treated with IL-2/JES6 or IL-2/S4B6 as shown in *Figure 1A*. Flow cytometry analysis of spleen and liver cells was used to evaluate CD25 expression in CD11b+CD14+ cells. Dot plots showing one representative mouse (**H**) and a bar graph showing mean ± SD in experimental groups (**I**) are presented. All experiments were done at least twice with similar results; n = 3–10 technical replicates. Data were analysed using an unpaired two-tailed Student's t-test. Significant differences to control are shown (*,°,+ p ≤ 0.05; °° p ≤ 0.01; ***, °°° p ≤ 0.001).

The online version of this article includes the following source data and figure supplement(s) for figure 3:

Source data 1. Source data for *Figure 3*, panels B, C, E, G, and I.

Figure supplement 1. IL-2/JES6 expands various subsets of myeloid cells in the spleen.

Figure supplement 1—source data 1. Source data for *Figure 3—figure supplement 1*, panels A-G.

Figure supplement 2. IL-2/JES6 increase MHC II expression in monocyte/macrophage population in the spleen.

Figure supplement 2—source data 1. Source data for *Figure 3—figure supplement 2*, panels A-D.

Figure supplement 3. IL-2/JES6 promote proliferation and expansion of myeloid cells in dose-dependent manner in the spleen.

Figure supplement 3—source data 1. Source data for *Figure 3—figure supplement 3*, panel A.

Figure supplement 4. The expression of TLR4 in splenocytes of C57BL/6 mice is not affected by the treatment with IL-2/JES6 or IL-2/S4B6.

Figure supplement 4—source data 1. Source data for *Figure 3—figure supplement 4*.

Figure supplement 5. IL-2/JES6 do not increase the level of TLR4 in myeloid cells in the spleen.

Figure supplement 5—source data 1. Source data for *Figure 3—figure supplement 5*, panels B, D and F.

Figure supplement 6. IL-2/JES6 increase counts of CD45+ and CD11b + CD14+ cells in the liver.

Figure supplement 6—source data 1. Source data for *Figure 3—figure supplement 6*, panels A-C.

Figure supplement 7. IL-2/JES6 increase counts of CD45+ and CD11b + CD14+ cells in the lungs.

Figure supplement 7—source data 1. Source data for *Figure 3—figure supplement 7*, panels A-C.
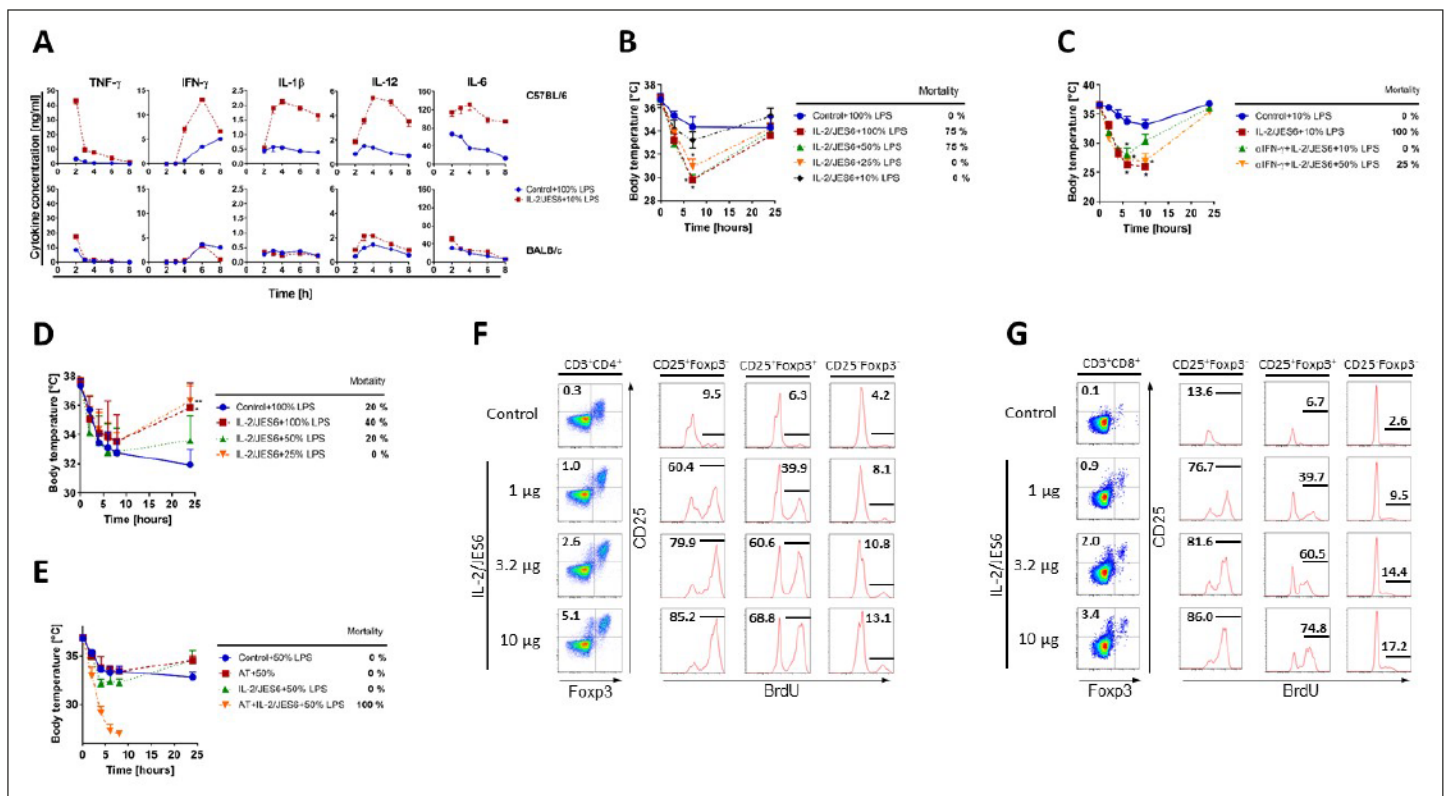
164

Figure 4. Sensitization to LPS via IL-2/JES6 requires endogenous IFN-γ production and is T cell-dependent. (**A**) C56BL/6 and BALB/c mice were treated with IL-2/JES6 and challenged with LPS (10% of MNLD) as shown in *Figure 1A*. Control mice were treated with PBS and challenged with LPS (100% of MNLD). Mice were euthanized at selected time points and their individual sera were collected. Concentrations of cytokines in the serum were determined by ELISA. Each experimental point represents the mean of two mice ± SD (n = 2 technical replicates). (**B**) BALB/c mice were treated with IL-2/JES6 and challenged with titrated doses of LPS as shown in *Figure 1A*. (**C**) C56BL/6 mice were treated with IL-2/JES6 and challenged with LPS (10 or 50% of MNLD) as shown in *Figure 1A*. Some mice were also injected with anti-IFN-γ mAb (αIFN-γ; 250 µg/mice i.p.) 4 h prior to the first injection of IL-2/JES6. (**D**) Nu/Nu mice were treated with IL-2/JES6 and challenged with titrated doses of LPS as shown in *Figure 1A*. (**E**) Two groups of Nu/Nu mice were adoptively transferred (AT) with 2 × 10^{6} CD4+CD25+ T cells from C56BL/6 mice pretreated with IL-2/JES6 as shown in *Figure 1A*. One group of AT mice and one group of normal Nu/Nu mice were treated with IL-2/JES6 as shown in *Figure 1A*. All groups including Nu/Nu mice without AT and IL-2/JES6 treatment (Control) were challenged with LPS (50% of MNLD). C56BL/6 mice were injected with one titrated dose of IL-2/JES6 or with PBS (Control). Mice were injected i.p. with BrdU 4 h after injection of IL-2/JES6 and put on drinking water with BrdU. Mice were euthanized 48 h after the injection of IL-2/JES6 and their CD4+ and CD8+ T cells (F and G, respectively) from the spleen were analysed by flow cytometry. One representative mouse out of two for each condition is shown. All experiments were done at least twice with similar results; n = 2–5 technical replicates (**B–G**). Data were analysed using an unpaired two-tailed Student's t-test. Significant differences to control are shown (* p ≤ 0.05; ** p ≤ 0.01).

The online version of this article includes the following source data and figure supplement(s) for figure 4:

Source data 1. Source data for *Figure 4*, panels A-E.

Figure supplement 1. TLR4 signalling in T cells is dispensable for inducing LPS hypersensitivity by IL-2/JES6.

Figure supplement 1—source data 1. Source data for *Figure 4—figure supplement 1*.

Figure supplement 2. Anti-IFN-γ mAb protects from sensitization to LPS more effectively when administered before treatment with IL-2/JES6.

Figure supplement 2—source data 1. Source data for *Figure 4—figure supplement 2*, panel B.

and LPS challenge. Indeed, anti-IFN-γ mAb markedly diminished sensitization to LPS by IL-2/JES6 (*Figure 4C*). Hence, we conclude that endogenous production of IFN-γ is a prerequisite for strong sensitization to LPS via IL-2/JES6.

Next, we asked which cells are key IFN-γ producers upon IL-2/JES6 administration. Since T cells are the most prominent IFN-γ producers, we decided to test sensitization to LPS by IL-2/JES6 in athymic Nu/Nu mice lacking T cells. We found that IL-2/JES6 almost do not sensitize Nu/Nu mice to LPS (*Figure 4D*). On the other hand, Nu/Nu mice with adoptively transferred CD4+CD25+ T cells from C56BL/6 mice injected with IL-2/JES6 showed very high sensitization to LPS upon IL-2/JES6 treatment (*Figure 4E*). These data show that IL-2/JES6 is able to induce IFN-γ production in T cells even in

the absence of TCR signal except that provided by self-MHC molecules. TLR4 expression on T cells seems to be irrelevant for their ability to sensitize the mice to LPS since $Rag1^{-/-}$ mice with adoptively transferred T cells from $Myd88^{-/-}$ mice, that is with severely impaired TLR4 downstream signaling, showed profound LPS sensitivity upon treatment with IL-2/JES6 (*Figure 4—figure supplement 1*). The key question is therefore, which T cell subset(s) produces IFN-γ upon IL-2/JES6 treatment? The ability to utilize IL-2/JES6 strictly requires CD25 expression and the only T cells expressing CD25 in naïve unprimed mice are T_{reg} cells. However, T_{reg} cells are considered as a T cell subset with no ability to produce IFN-γ under normal conditions. Nevertheless, we found that administration of IL-2/JES6 potently expanded CD25$^+$Foxp3$^-$ T cells in both CD4$^+$ and CD8$^+$ subsets and that these cells proliferate more vigorously in response to IL-2/JES6 than T_{reg} cells (*Figure 4F and G*).

IL-2/JES6 drive expansion of CD25$^+$Foxp3$^-$ T cells producing IFN-γ in lymphoid as well as non-lymphoid tissues

We focused on CD25$^+$Foxp3$^-$CD4$^+$ and CD8$^+$ T cells robustly expanded in the spleen of mice treated with IL-2/JES6. Since these cells resemble by their phenotype activated T cells, we presumed that these cells could be a key producers of IFN-γ in IL-2/JES6 treated mice causing the increased sensitivity to LPS. Thus, we decided to investigate whether these cells were expanded also in other organs except of spleen and whether they produced IFN-γ. Interestingly, we found that treatment of C56BL/6 mice with IL-2/JES6 led to the induction of these cells in both lymphoid tissues (spleen) as well as in non-lymphoid tissues (liver and lungs; *Figure 5A and B*). Relative counts of CD25$^+$Foxp3$^-$CD4$^+$ and CD8$^+$ T cells were particularly high in the liver where they typically represented about 6% and 10% of CD4$^+$ and CD8$^+$ T cells, respectively. We asked whether these CD25$^+$Foxp3$^-$CD4$^+$ and CD8$^+$ T cells are able to produce IFN-γ upon IL-2/JES6 administration in vivo. To answer this, C56BL/6 mice were treated with IL-2/JES6 as in *Figure 1A* and brefeldin A was injected 2 h after the last dose of IL-2/JES6 to enable the detection of IFN-γ production in various T cell subsets intracellularly. We proved that CD25$^+$Foxp3$^-$CD4$^+$ and CD8$^+$ T cells in spleen, liver, and lungs produced IFN-γ (*Figure 5C and D*). Again, relative counts of these cells producing IFN-γ were especially high in the liver and generally higher in the CD8$^+$ subset in comparison to the CD4$^+$ subset. Notably, T_{reg} cells in the liver of C56BL/6 mice treated with IL-2/JES6 also produced IFN-γ showing that T_{reg} cells may surprisingly participate in sensitization to LPS. IL-2/S4B6 almost did not induce CD25$^+$Foxp3$^-$CD4$^+$ and CD8$^+$ T cells in any tissue studied. This agrees with the previous finding that IL-2/S4B6 sensitize to LPS only very decently.

Production of IFN-γ by antigen-activated or IL-2/JES6-stimulated T cells drives LPS hyperreactivity

Previous experiments showed that IL-2/JES6 give rise to CD25$^+$Foxp3$^-$ T cells producing IFN-γ in various tissues which in turn leads to LPS hyperreactivity. We asked whether antigen-activated T cells, when present in sufficient numbers, were also able to induce LPS hyperreactivity since they also produce IFN-γ. Thus, we adoptively transferred CD8$^+$ OT-I and CD4$^+$ OT-II T cells into C56BL/6 mice and activated them with respective ovalbumin-derived peptides plus polyI:C. CD8$^+$ OT-I and CD4$^+$ OT-II T cells significantly expanded and altogether made up 12–13% of all T cells in the spleen on day 3 post priming (*Figure 6A and B*). C56BL/6 mice with primed adoptively transferred T cells showed significant sensitivity to LPS in comparison to C56BL/6 mice with unprimed adoptively transferred T cells (*Figure 6C*). Importantly, injection of anti-IFN-γ mAb abrogated sensitization to LPS in C56BL/6 mice with primed adoptively transferred T cells. C56BL/6 mice without adoptively transferred CD8$^+$ OT-I and CD4$^+$ OT-II T cells and immunized with OVA plus polyI:C showed no increased sensitivity to LPS (*Figure 6—figure supplement 1*).

Finally, we used IFN-γ deficient mice (IFN-γ$^{-/-}$) to prove that IFN-γ is the key factor mediating LPS hyperreactivity upon IL-2/JES6 administration. IFN-γ$^{-/-}$ mice pretreated with IL-2/JES6 showed sensitivity to LPS comparable to that of those not pretreated. IFN-γ sufficient C56BL/6 mice pretreated with IL-2/JES6 showed dramatically increased sensitivity to LPS (*Figure 6D and E*). Altogether, we conclude that IL-2/JES6 give rise to CD25$^+$Foxp3$^-$CD4$^+$ and CD8$^+$ T cells producing IFN-γ in various tissues, particularly in liver. IL-2/JES6 also expand LPS responsive CD11b$^+$CD14$^+$ myeloid cells and increase expression of CD25 in these cells. IFN-γ later acts on these myeloid cells and increases their responsiveness to LPS (*Figure 6F*).

166
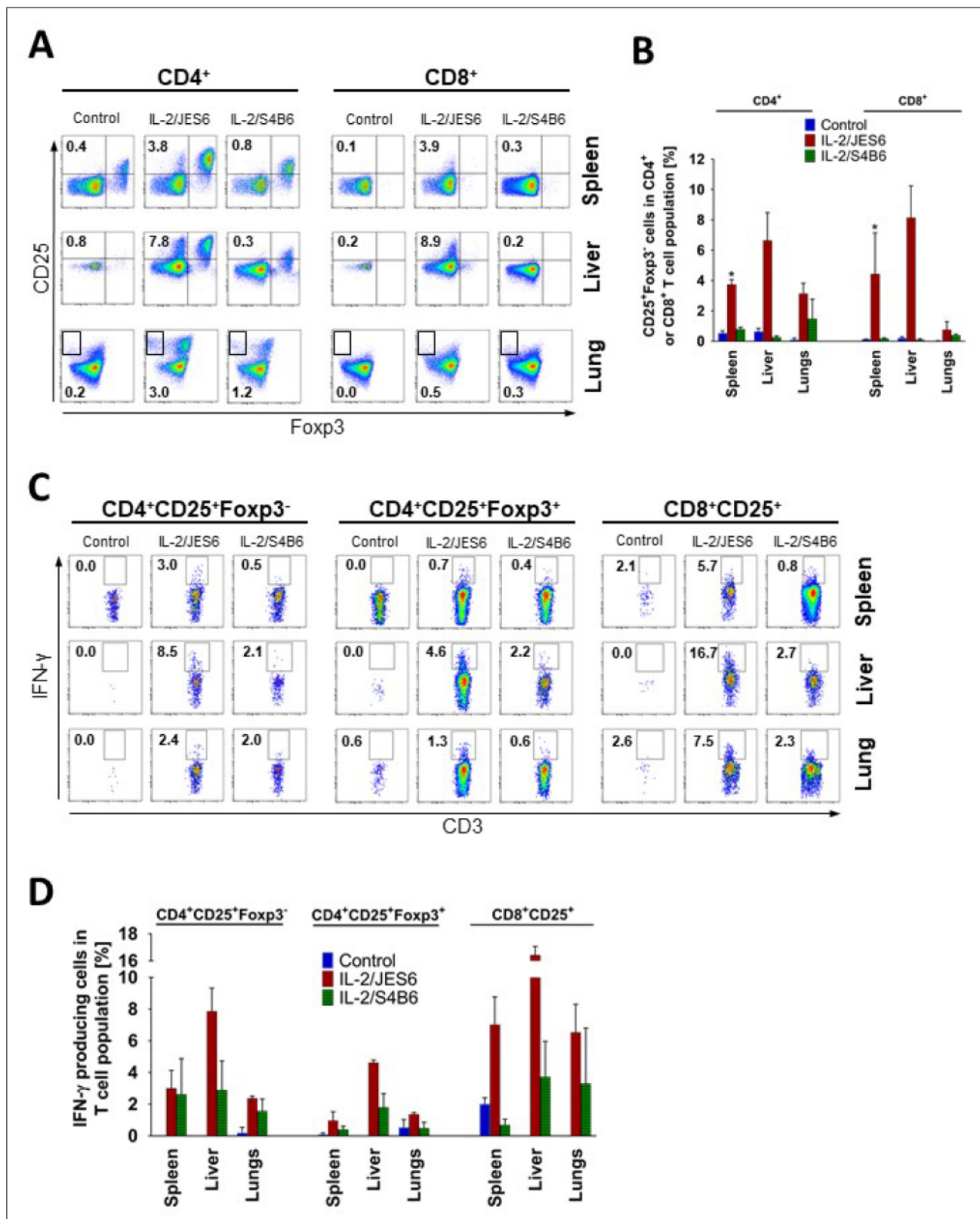
Figure 5. IL-2/JES6 expands CD25+Foxp3-T cells in both CD4+ and CD8+ subsets which produces IFN-γ in various tissues. (**A**) C56BL/6 mice were treated with IL-2/JES6 or IL-2/S4B6 as shown in *Figure 1A*. Mice were i.p. injected with 150 μg/mouse of brefeldin A 2 h after the last dose of IL-2/JES6 and euthanized 12 h after the injection of brefeldin A. CD4+ and CD8+ T cells from spleen, liver, and lung were analysed by flow cytometry for CD25 and Foxp3 expression. Dot plots showing one representative mouse (**A**) and a bar graph showing mean ± SD in experimental groups (**B**) are presented.

Figure 5 continued on next page

167

Intracellular production of IFN-γ in different subpopulations of T cells as shown in A, was determined. Dot plots showing one representative mouse (C) and a bar graph showing mean ± SD in experimental groups (D) are presented. Analysis of T cells from spleen and liver was carried out in the same experiment, but analysis of T cells from the lungs was done in a separate experiment. All experiments were done at least twice with similar results; n = 3 technical replicates. Data were analysed using an unpaired two-tailed Student's t-test. Significant differences to control are shown (* p ≤ 0.05).

The online version of this article includes the following source data for figure 5:

Source data 1. Source data for *Figure 5*, panels B and D.

Discussion

It has previously been shown that IL-2/JES6 immunocomplexes potently expand T_{reg} cells in vivo and that they can be used for treatment of various autoimmune diseases (*Liu et al., 2011*; *Webster et al., 2009*; *Wilson et al., 2008*). However, our results clearly demonstrate that these immunocomplexes also dramatically increase sensitivity to LPS. The key mechanism is the production of IFN-γ since administration of anti-IFN-γ mAb as well as the use of IFN-γ$^{-/-}$ mice abrogates the sensitization. This resembles the so-called Schwartzman-like shock reaction, an experimental model of lethal systemic inflammatory reaction induced by LPS injection. It is induced by two consecutive, rather low doses of LPS (preparatory and provocative ones) and occurrence of the reaction requires very exact dosage and careful timing (*Heremans et al., 1990*). The first LPS injection is given into the footpad, followed after 24 h by an i.v. dose. Administration of anti-IFN-γ mAb was found to completely prevent the reaction. Thus, a preparatory dose of LPS induces production of IFN-γ which consequently sensitizes immune cells to be hyperresponsive to a provocative dose of LPS. Contrary to the Schwartzman-like shock reaction, IL-2/JES6 is responsible for inducing the production of IFN-γ and for sensitization to LPS in our experimental system. Administration of anti-IFN-γ mAb before IL-2/JES6 treatment could, however, have two effects: it could prevent sensitization of immune cells to LPS or it could protect against the toxic effect of a massive production of IFN-γ upon LPS injection since IgG has a relatively long half-life (*Vieira and Rajewsky, 1988*). Thus, we compared the effect of anti-IFN-γ mAb administered either before pretreatment with IL-2/JES6 or after it, that is, shortly before LPS challenge (4 h). Anti-IFN-γ mAb had higher protective effect when injected before IL-2/JES6 pretreatment (*Figure 4—figure supplement 2*) further confirming the key role of IL-2/JES6-induced IFN-γ production for sensitization to LPS.

The key question was: which cells produce IFN-γ upon treatment with IL-2/JES6? IFN-γ is normally produced by effector T cells after their activation and expansion. It requires a TCR signal and is significantly augmented by the presence of IL-12 and IL-18 (*Berg et al., 2002*; *Li et al., 2005*; *Nakanishi, 2018*). However, IL-2 was shown to be also able to promote IFN-γ production, but usually in activated T cells, that is, upon TCR signaling (*Boyman and Sprent, 2012*; *Cousens et al., 1995*). Here, we show that a strong sustained IL-2 signal provided by IL-2/JES6 is able to induce production of IFN-γ in T cells in vivo even in the absence of a TCR signal, except that provided by self-MHC molecules. Contact with self-MHC class I and II molecules (low affinity interaction) is known to play an important role in homeostasis of naïve CD8$^+$ and CD4$^+$ T cells, respectively (*Kieper et al., 2004*; *Sprent and Surh, 2011*), but should not endow these cells with the capacity to express effector functions like IFN-γ production (*Kieper et al., 2004*). We saw the highest relative counts of IFN-γ-producing T cells in CD25$^+$Foxp$^-$CD4$^+$ and CD8$^+$ populations. Nevertheless, CD4$^+$CD25$^+$Foxp$^+$ T_{reg} cells also produced IFN-γ in IL-2/JES6-treated mice, particularly in liver (*Figure 5C and D*). One simple explanation could be that the strong sustained IL-2 signal provided by IL-2/JES6 also induces production of IFN-γ in T_{reg} cells. However, we speculate that the IFN-γ produced by CD25$^+$Foxp$^-$CD4$^+$ and CD8$^+$ cells may be a trigger for IFN-γ production in T_{reg} cells since it was shown previously that T_{reg} cells can be converted into IFN-γ-producing cells, especially in a strongly pro-inflammatory milieu (*Koenecke et al., 2012*) and/or in the presence of IFN-γ (*Wood and Sawitzki, 2006*). On the other hand, T_{reg} cells seems to be dispensable for sensitization to LPS via IL-2/JES6 as administration of anti-CD4 mAb had no effect (*Figure 2D*). This shows that CD8$^+$ T cells can substitute CD4$^+$ T cells in the process of sensitization, however, complete absence of T cells abolishes it (*Figure 4D*).

It has been shown that treatment with nitrite (NO$_2^-$), an important biological NO reservoir in vasculature and tissues, significantly attenuates hypothermia, tissue infarction and mortality in a mouse shock model induced by a lethal TNF-α or LPS challenge (*Cauwels et al., 2009*). We therefore asked
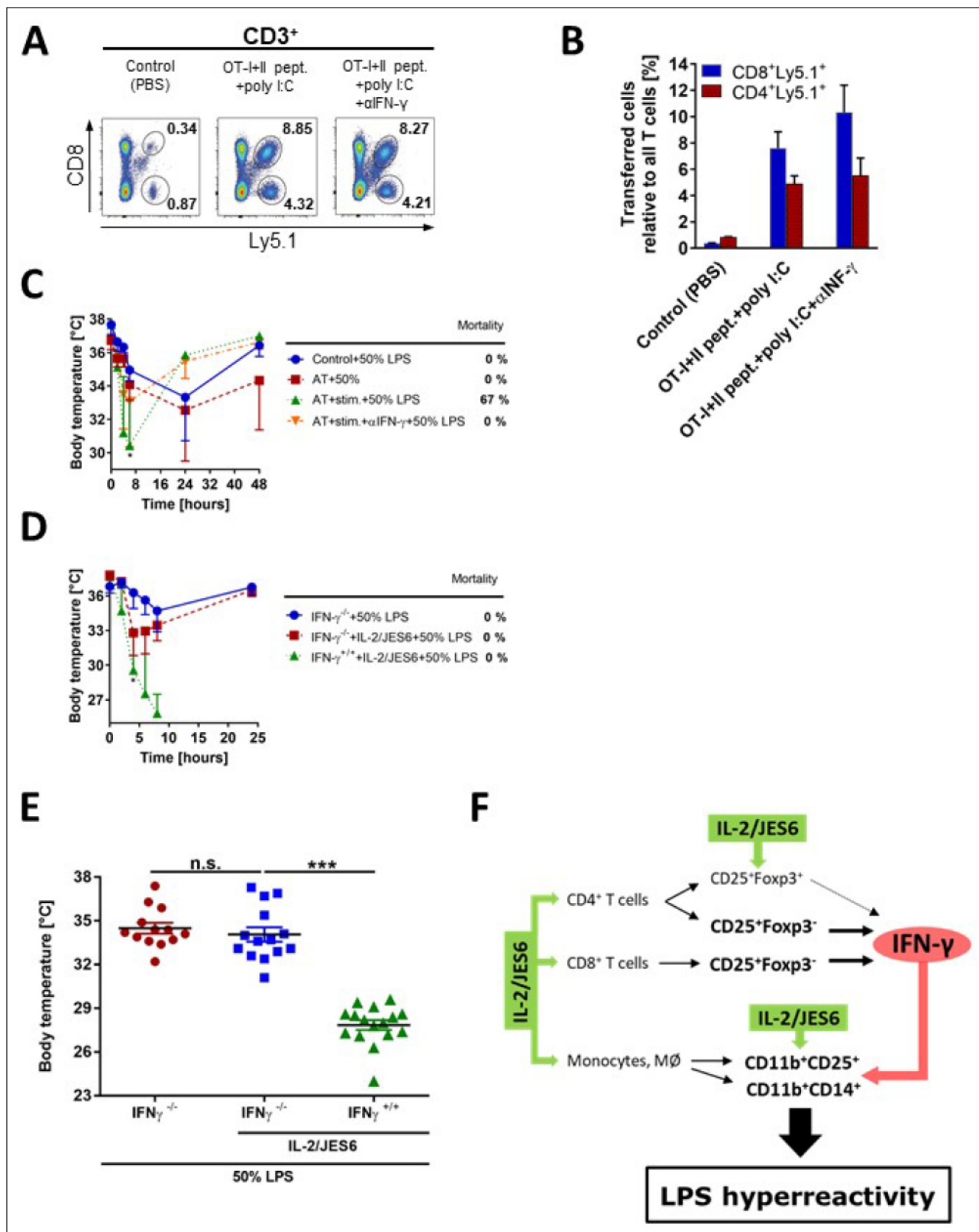
Figure 6. IFN-γ produced by activated antigen-specific T cells or by T cells stimulated with IL-2/JES6, is a crucial mediator of LPS hyperreactivity. Purified CD8⁺ and CD4⁺ T cells from OT-I/Ly5.1 and OT-II/Ly5.1 mice (2 and 4 × 10⁶ /mouse respectively), were adoptively transferred (AT) to C56BL/6 mice. One day later, mice were i.p. injected with PBS (Control), with both OT-I and OT-II specific peptides plus polyI:C (75 μg/mice) or with the latter plus αIFN-γ mAb (250 μg). Expansion of AT T cells was determined 3 d post stimulation by flow cytometry. Dot plots showing one representative

Figure 6 continued on next page

Figure 6 continued

mouse (**A**) out of two mice analysed by flow cytometry and a bar graph showing mean ± SD (**B**) are presented. (**C**) Three groups of C56BL/6 mice described above and one control group (no AT) were challenged with LPS (50% of MNLD). (**D**) IFN-γ$^{-/-}$ and normal C56BL/6 mice (IFN-γ$^{+/+}$) were treated with IL-2/JES6 and challenged with LPS (50% of MNLD) as shown in *Figure 1A*. IFN-γ$^{-/-}$ C56BL/6 mice challenged with the same dose of LPS were used as the control. (**E**) Data pooled from three independent experiments (n = 13–16 technical replicates) described in D showing body temperature of mice 8 h after LPS challenge. (**F**) Scheme showing the proposed mechanism of how IL-2/JES6 induces LPS hyperreactivity. Experiments A-D were done at least twice with similar results; n = 2–6 technical replicates. Data were analysed using unpaired two-tailed Student's t-test. Significant differences to control are shown (* $p \leq 0.05$; *** $p \leq 0.001$).

The online version of this article includes the following source data and figure supplement(s) for figure 6:

Source data 1. Source data for *Figure 6*, panels B-E.

Figure supplement 1. Immunization with ovalbumin plus poly I:C does not increase sensitivity to LPS.

Figure supplement 1—source data 1. Source data for *Figure 6—figure supplement 1*.

whether nitrite could protect, at least to some extent, IL-2/JES6 pretreated mice challenged with LPS, since we observed very high serum levels of TNF-α in these mice (*Figure 1E*). Indeed, nitrite was considerably effective in lowering hypothermia and mortality (*Figure 1—figure supplement 1*) showing that a massive production of TNF-α is a dominant pathogenic factor responsible for rapid onset of hypothermia in IL-2/JES6 sensitized mice challenged with LPS. Pathogenic effects that occur later on are mediated by other cytokines, particularly by IFN-γ. This is supported by the fact that serum levels of TNF-α peak very early (1–2 h) post LPS challenge while serum levels of IFN-γ peak around 6 h (*Figure 4A*).

Treatment with IL-2/JES6 not only affected T cell populations but to our surprise also affected some myeloid cell populations, particularly CD11b$^+$CD14$^+$ cells (monocytes/macrophages). Although IL-2 is a pleiotropic cytokine, it has stimulatory activity mostly for cells of lymphoid origin, especially for T$_{reg}$, recently activated T, memory CD8$^+$ T, and NK cells (*Boyman et al., 2010*; *Malek, 2008*; *Sharma and Das, 2018*; *Yu et al., 2000*). Increased counts of CD11b$^+$CD14$^+$ cells in response to IL-2/JES6 are thus intriguing. We tested the hypothesis that T cells upon stimulation with IL-2/JES6 do not produce GM-CSF but no production of this cytokine was found. However, there is a report showing that clonogenic common lymphoid progenitor (CLP), a bone marrow-resident cell that gives rise exclusively to lymphocytes, can be redirected to the myeloid lineage by stimulation through an exogenously expressed IL-2 receptor (*Kondo et al., 2000*). Authors suggest that CLPs and pro-T cells may have a latent granulocyte/monocyte lineage differentiation program that can be initiated by signaling through the reconstituted IL-2 receptor. We hypothesize that a strong IL-2 signal provided by IL-2/JES6 may lead to a similar effect. Nevertheless, this hypothesis requires that at least a fraction of CLPs express complete trimeric IL-2R at some stage of their development. Even low expression levels should be sufficient since it has been previously shown that IL-2/JES6 feeds back onto CD25 expression (*Spangler et al., 2015*).

An interesting feature of IL-2/JES6 treatment is the increased counts of CD45$^+$ cells (i.e. any haematopoietic cells, except erythrocytes) in the liver (*Figure 3—figure supplement 6*). This increase was found both in the T cell population (see later) as well as in CD11b$^+$CD14$^+$ cells (*Figure 3—figure supplement 6B* and C). A decent increase in counts of CD11b$^+$CD14$^+$ cells was also found in the lungs (*Figure 3—figure supplement 7*). We believe that accumulation of these cells in liver and lungs might significantly contribute to the pathological effects seen after LPS challenge in IL-2/JES6 pretreated mice, since these cells are likely to be sensitized to LPS via IFN-γ produced by CD25$^+$ T cells. This is not the case with IL-2/S4B6 pretreatment as there are much fewer IFN-γ-producing CD25$^+$ T cells (*Figure 5*). Further, treatment with IL-2/JES6 per se induces more severe lung oedema in comparison to treatment with IL-2/S4B6, which could contribute to the morbidity and mortality after LPS challenge to some extent (*Figure 1—figure supplement 2*).

We injected both IL-2/JES6 and LPS into mice via i.p. injections. There is a population of macrophages in the peritoneal cavity (*Cassado et al., 2015*) and therefore we asked whether these cells might contribute to the LPS sensitivity. However, adoptive transfer of peritoneal exudate cells from mice i.p. injected with IL-2/JES6 did not increase sensitivity to LPS in adoptively transferred mice. Moreover, i.v. administration of IL-2/JES6 leads to the same level of LPS sensitivity in comparison to i.p. administration. Therefore, we can rule out the idea that peritoneal macrophages play an important role.

We found significantly increased counts of T cells in the liver of mice treated with IL-2/JES6 or IL-2/S4B6 (*Figure 5A*). We do not know the mechanism of T cell accumulation in the liver upon treatment with either IL-2 complexes, however, we can speculate that IL-2 complexes (M_w ~190 kDa) are easily accessible in the liver interstitium due to the massive fenestration of capillaries in this organ (*DeLeve, 2015*). It seems that the liver and secondary lymphoid organs are the sites where increased numbers of CD11b⁺CD14⁺ and IFN-γ-producing T cells colocalize upon IL-2/JES6 treatment, and this feature governs LPS hyperresponsiveness.

Materials and methods

Key resources table

Reagent type (species) or resource	Designation	Source or reference	Identifiers	Additional information
Antibody	Anti-mouse CD3-eFluor 450 (clone: 17A2; rat monoclonal)	eBioscience	Cat#: 48-0032-82; RRID:AB_1272193	Flow Cytometry: (dilution 1:30)
Antibody	Anti-mouse CD8a-PerCP-Cyanine5.5 (clone: 53–6.7; rat monoclonal)	eBioscience	Cat#: 45-0081-82; RRID:AB_1107004	Flow Cytometry: (dilution 1:100)
Antibody	Anti-mouse CD11b-Alexa Fluor 700 (clone: M1/70; rat monoclonal)	eBioscience	Cat#: 56-0112-82; RRID:AB_1107004	Flow Cytometry: (dilution 1:300)
Antibody	Anti-mouse CD11b-eFluor450 (clone: M1/70; rat monoclonal)	eBioscience	Cat#: 48-0112-82; RRID:AB_1582236	Flow Cytometry: (dilution 1:500)
Antibody	Anti-mouse CD14-FITC (clone: Sa2-8; rat monoclonal)	eBioscience	Cat#: 11-0141-85; RRID:AB_464950	Flow Cytometry: (dilution 1:20)
Antibody	Anti-mouse CD25-APC (clone: PC61.5; rat monoclonal)	eBioscience	Cat#: 17-0251-82; RRID:AB_469366	Flow Cytometry: (dilution 1:500)
Antibody	Anti-mouse CD25-eFluor 450 (clone: PC61.5; rat monoclonal)	eBioscience	Cat#: 48-0251-82; RRID:AB_10671550	Flow Cytometry: (dilution 1:400)
Antibody	Anti-mouse CD45.1-APC (clone: A20; mouse monoclonal)	eBioscience	Cat#: 17-0453-82; RRID:AB_469398	Flow Cytometry: (dilution 1:200)
Antibody	Anti-mouse Ly-6C-APC-eFluor 780 (clone: HK1.4; rat monoclonal)	eBioscience	Cat#: 47-5932-82; RRID:AB_2573992	Flow Cytometry: (dilution 1:200)
Antibody	Anti-mouse MHC Class II (I-A/I-E)-FITC (clone: M5/114.15.2; rat monoclonal)	eBioscience	Cat#: 11-5321-82; RRID:AB_465232	Flow Cytometry: (dilution 1:300)
Antibody	Anti-mouse CD45.1-eFluor 450 (clone: A20; mouse monoclonal)	eBioscience	Cat#: 48-0453-82; RRID:AB_1272189	Flow Cytometry: (dilution 1:200)
Antibody	Anti-mouse CD45/B220-Horizon V500 (clone: RA3-6B2; rat monoclonal)	BD Biosciences	Cat#: 561226; RRID:AB_10563910	Flow Cytometry: (dilution 1:100)
Antibody	Anti-mouse CD3e-Horizon V500 (clone: 500A2; Syrian hamster monoclonal)	BD Biosciences	Cat#: 560771; RRID:AB_1937314	Flow Cytometry: (dilution 1:30)
Antibody	Anti-mouse CD4-Horizon V500 (clone: RM4.5; rat monoclonal)	BD Biosciences	Cat#: 560782; RRID:AB_1937327	Flow Cytometry: (dilution 1:400)
Antibody	Anti-mouse CD4-PerCP (clone: RM4-5; rat monoclonal)	BD Biosciences	Cat#: 553052; RRID:AB_394587	Flow Cytometry: (dilution 1:200)
Antibody	Anti-mouse CD8a-V500 (clone: 53–6.7; rat monoclonal)	BD Biosciences	Cat#: 560776; RRID:AB_1937317	Flow Cytometry: (dilution 1:80)

Continued on next page

Continued

Reagent type (species) or resource	Designation	Source or reference	Identifiers	Additional information
Antibody	Anti-mouse Ly-6G-Alexa Fluor 700 (clone: 1A8; rat monoclonal)	BD Biosciences	Cat#: 561236; RRID:AB_10611860	Flow Cytometry: (dilution 1:80)
Antibody	Anti-mouse Siglec-F-PE (clone: E50-2440; rat monoclonal)	BD Biosciences	Cat#: 562068; RRID:AB_394341	Flow Cytometry: (dilution 1:100)
Antibody	Anti-mouse TLR4-APC (clone: SA15-21; rat monoclonal)	BioLegend	Cat#: 145406; RRID:AB_2562503	Flow Cytometry: (dilution 1:300)
Antibody	Anti-mouse TNF alpha-PE (clone: MP6-XT22; rat monoclonal)	eBioscience	Cat#: 12-7321-82; RRID:AB_466199	Flow Cytometry: (dilution 0.35 μL/test)
Antibody	Anti-FOXP3-PE (clone: FJK/16 s; rat monoclonal)	eBioscience	Cat#: 12-5773-82; RRID:AB_465936	Flow Cytometry: (dilution 1 μL/test)
Antibody	Anti-mouse IFN gamma-PE (clone: XMG1.2; rat monoclonal)	eBioscience	Cat#: 12-7311-82; RRID:AB_466193	Flow Cytometry: (dilution 0.35 μL/test)
Antibody	Anti-mouse CD16/32 (clone: 03; rat monoclonal)	eBioscience	Cat#: 14-0161-86; RRID:AB_467135	Flow Cytometry: (dilution 0.5 μg/test)
Antibody	Anti-mouse IFN gamma (clone: XMG1.2; rat monoclonal)	BioXCell	Cat#: BE0055; RRID:AB_1107694	In vivo IFN gamma neutralization (dose: 250 μg/mouse)
Antibody	Anti-mouse IL-2 (clone: JES6-1A12; rat monoclonal)	BioXCell	Cat#: BE0043; RRID:AB_1107702	In vivo IL-2 receptor stimulation as a complex with IL-2 (dose: 1.5 μg /mouse)
Antibody	Anti-mouse IL-2 (clone: S4B6-1; rat monoclonal)	BioXCell	Cat#: BE0043-1; RRID:AB_1107705	In vivo IL-2 receptor stimulation as a complex with IL-2 (dose: 1.5 μg /mouse)
Antibody	Anti-mouse CD4 (clone: GK1.5; rat monoclonal)	BioXCell	Cat#: BE0003-1; RRID:AB_1107636	In vivo CD4+ T cell depletion (dose: 50 μg / mouse)
Antibody	Anti-mouse CD25 (clone: PC61.5; rat monoclonal)	BioXCell	Cat#: BE0012; RRID:AB_1107619	In vivo regulatory T cell depletion (dose: 50 μg /mouse)
Sequence-based Reagent	*Casc3for*	Sigma-Aldrich		5′-TTCGAGGTGTGCCTAACCA-3′
Sequence-based Reagent	*Casc3rev*	Sigma-Aldrich		5′-GCTTAGCTCGACCACTCTGG-3′
Sequence-based Reagent	*H6pdfor*	Sigma-Aldrich		5′-GGATTGTGTTTAAGAATCGGG-3′
Sequence-based Reagent	*H6pdrev*	Sigma-Aldrich		5′-AGTAGGCGTCTTGCTC-3′
Sequence-based Reagent	*Tlr4for*	Sigma-Aldrich		5′-GATCATGGCACTGTTCTTCTC-3′
Sequence-based Reagent	*Tlr4rev*	Sigma-Aldrich		5′-CACACCTGGATAAATCCAGC-3′
Strain, Strain Background (*Salmonella Typhymurium*)	LT2 (S-strain)	Gift from Dr. H. Nikaido (University of California, Berkeley)		LPS isolation
Strain, Strain Background (*Mus musculus*; Female)	BALB/c (*H-2d*)	Institute of Microbiology and Institute of Physiology of the Czech Academy of Sciences		

Continued on next page

172

Continued

Reagent type (species) or resource	Designation	Source or reference	Identifiers	Additional information
Strain, Strain Background (*Mus musculus*; Male)	C57BL/6 (*H-2b*)	Institute of Microbiology and Institute of Physiology of the Czech Academy of Sciences		
Strain, Strain Background (*Mus musculus*; Female)	CD1 nude mice (Nu/Nu)	Animal facility of Masaryk University, Czech Republic		
Strain, Strain Background (*Mus musculus*, C57BL/6 J)	Transgenic OVA-specific T cells (OT-I) mice	Institute of Microbiology of the Czech Academy of Sciences		
Strain, Strain Background (*Mus musculus*, C57BL/6 J)	Transgenic OVA-specific T cells (OT-II) mice	Institute of Microbiology of the Czech Academy of Sciences		
Strain, Strain Background (*Mus musculus*; C57BL/6 J)	IFN gamma deficient (*Ifng-/-*)	Institute of Microbiology of the Czech Academy of Sciences		
Strain, Strain Background (*Mus musculus*; C57BL/6 J)	MyD88 deficient (*Myd88-/-*)	Institute of Molecular Genetics of the Czech Academy of Sciences		
Strain, Strain Background (*Mus musculus*; C57BL/6 J)	Rag1 deficient (*Rag1-/-*)	Institute of Molecular Genetics of the Czech Academy of Sciences		
Strain, Strain Background (*Mus musculus*, C57BL/6 J)	B6.SJL (Ly5.1)	Institute of Microbiology of the Czech Academy of Sciences		
Peptide, Recombinant Protein	Recombinant Murine IL-2	PeproTech	Cat#: 212–12	Purified from *E. coli*
Commercial Assay or Kit	Mouse TNF-alpha DuoSet ELISA	R&D Systems	Cat#: DY410	
Commercial Assay or Kit	Mouse IFN-gamma DuoSet ELISA	R&D Systems	Cat#: DY485	
Commercial Assay or Kit	Mouse IL-1 beta/IL-1F2 DuoSet ELISA	R&D Systems	Cat#: DY401	
Commercial Assay or Kit	Mouse IL-12 p70 DuoSet ELISA	R&D Systems	Cat#: DY419	
Commercial Assay or Kit	Mouse IL-6 DuoSet ELISA	R&D Systems	Cat#: DY406	
Chemical Compound, Drug	Brefeldin A	Sigma-Aldrich	Cat#: B7651	150 µg/mouse
Software, Algorithm	FlowJo	Tree Star	RRID: SCR_008520	
Software, Algorithm	GraphPad Prism	GraphPad Software	RRID: SCR_002798	
Other	ACK Lysing Buffer	Thermo Fisher Scientific	Cat#: A1049201	Red blood cell lysis
Other	Collagenase D	Sigma-Aldrich (Roche)	Cat#: 11088858001	1 mg/mL

Continued on next page

173

Continued

Reagent type (species) or resource	Designation	Source or reference	Identifiers	Additional information
Other	Foxp3/ Transcription Factor Fixation/Permeabilization Concentrate and Diluent	eBioscience	Cat#: 00-5521-00	
Other	Polyinosinic-polycytidylic acid potassium salt (Poly I:C)	Sigma-Aldrich	Cat#: P9582	75 μg/mouse
Other	5-Bromo-2'-deoxyuridine (BrdU)	Sigma-Aldrich (Roche)	Cat#: 10280879001	0.5 μg/mouse i.p., 0.8 mg/mL p.o.
Other	TRIzol Reagent	Thermo Fisher Scientific (Invitrogen)	Cat#: 15596026	
Other	TURBO DNase	Thermo Fisher Scientific	Cat#: AM2238	
Other	SuperScript IV Reverse Transcriptase	Thermo Fisher Scientific	Cat#: 18090010	

Mice

BALB/c (*H-2d*) and C57BL/6 (*H-2b*) mice were obtained from a breeding colony at the Institute of Microbiology or Institute of Physiology of the Czech Academy of Sciences (Prague, Czech Republic). Athymic CD1 nude mice (Nu/Nu) were acquired from the animal facility of Masaryk University (Brno, Czech Republic). Transgenic OT-I and OT-II mice, *Ifng*^{-/-}, *Myd88*^{-/-} and *Rag1*^{-/-} mice and B6.SJL (Ly5.1) mice were bred and kept at mouse facilities at the Institute of Molecular Genetics or the Institute of Microbiology of the Czech Academy of Sciences (Prague, Czech Republic). Mice were used at 9–15 weeks of age.

Monoclonal antibodies (MAbs)

The following anti-mouse mAbs were used for surface staining during flow cytometry: CD3-eFluor 450, CD8-PerCP-Cy5.5, CD11b-AlexaFluor 700, CD11b-eFluor 450, CD14-FITC, CD25-APC, CD25-eFluor 450, CD45.1-APC, Ly6C-APC-eFluor 780, I-A/E-FITC (eBioscience, San Diego, CA, USA), CD45.1-eFluor 450, CD45R-Horizont V500, CD3-Horizont V500, CD4-Horizont V500, CD4-PerCP, CD8-Horizont V500, Ly6G-AlexaFluor 700, Siglec F-PE (BD Biosciences, San Jose, California, USA) and TLR4-APC (BioLegend, San Diego, Ca, USA). For intracellular staining, the following anti-mouse mAbs were used: TNFα-PE, Foxp3- and IFNγ-PE (eBioscience; San Diego, California, USA). Fc-block (anti-CD16/CD32 mAbs; eBioscience, San Diego, California, USA) was used both in surface and intracellular staining. For ELISA, matched anti-mouse capture mAb and biotinylated detection mAb against TNF-α, IFN-γ, IL-1β, IL-12 and IL-6 were used (R&D System, Minneapolis, Minnesota, USA). Blocking anti-mouse CD25 (PC61.5), CD4 (GK1.5) and anti-IFN-γ (XMG1.2) mAbs, as well as anti-mIL-2 mAbs for preparing IL-2 complexes (S4B6, JES6-1A12), were obtained from BioXcell (Lebanon, New Hampshire, USA).

IL-2/JES6-1 and IL-2/S4B6 complexes

Complexes were prepared by mixing recombinant mouse IL-2 (Peprotech, Cranbury, New Jersey, USA) with anti-IL-2 mAb S4B6 or JES6-1A12 (both reagents were in PBS) at molar ratio 2:1. After 15 min (min) incubation at room temperature, the complexes were diluted with PBS to the desired concentration before application.

Isolation of LPS

Bacterial culture (*S. typhymurium* LT2, S-strain; a kind gift from Dr. H. Nikaido, University of California, Berkeley, USA) was first cultivated on agar (Nutrient agar nr.2, HiMedia Laboratories, Mumbai, India) in a petri dish and then transferred to an Erlenmayer flask with liquid media (150 ml, MRS Broth, Oxoid, Hampshire, UK). The bacterial culture was cultivated at 37 °C for up to 24 h (h) in order to reach the exponential growth phase according to measured OD (~ 5×10^8/ml bacteria). Next, it was transferred to the solid substrate (12 g Nutrient agar nr.2, 3.5 g agar, 15 g glucose, 300 ml water) in 2 l glass

cultivation bottles by Roux (4 ml inoculum/bottle). Bottles were cultured for 24 h at 37 °C. Bottles were washed with PBS and bacteria were removed from the surface of the substrate with a glass rod. The acquired suspension was filtered through the gauze, and bacteria were killed with 2% phenol (Sigma-Aldrich, St. Louis, Missouri, USA) in ethanol (96%; Lachner, Neratovice, Czech Republic) and deionized water at room temperature. Viability of the bacteria was tested by plating on a new agar petri dish (Nutrient agar nr.2, HiMedia Laboratories, Mumbai, India). Bacteria were sequentially centrifuged at 4600 and 16,000 rpm (room temperature, 20 min). They were washed once with PBS followed by a triple wash with deionized water to remove salts and phenol before they underwent lyophilization in order to get dry matter. Crude LPS was acquired from dry matter by fractionation. This was achieved by the addition of preheated phenol and deionized water at 68 °C (water bath) for 15 min while stirring constantly (20 g of dry matter + 350 ml deionized water and 350 ml 90% phenol). After incubation, the sample was cooled down to 4 °C and sequentially centrifuged at 4600 rpm and 16,000 rpm (4 °C, 20 min). The water phase (top part) was removed and stored whilst the pellet was subjected to a second round of fractionation. Water phases from both separations were pooled, shaken with diethylether (600 ml; Lachner, Neratovice, Czech Republic) and left overnight at 4 °C, followed by repeated dialysis of the water phase for 3–5 days (d) in a huge excess of deionized water. The whole process of crude LPS isolation was finalized by lyophilization. To achieve this, 0.76 g of crude LPS was dissolved in 50 ml of deionized water and cooled down to 4 °C. Next, 150 ml of ice-cold methanol (Lachner, Neratovice, Czech Republic) and 1.5 ml 20% $MgCl_2$ (Sigma-Aldrich, St. Louis, Missouri, USA) were added and it was left stirring overnight. The following day, the solution was centrifuged at 5000 rpm (4 °C, 20 min) and the pellet was resuspended again in 50 ml of deionized water and cooled down to 4 °C. After this, 150 ml of ice-cold methanol was added and it was left stirring overnight. On the following day, the same procedure was repeated and the pellet was resuspended in 20 ml of deionized water. Pure LPS was finally lyophilized.

LPS challenge in vivo

Mice were treated i.p. with IL-2/JES6-1 or IL-2/S4B6 complexes daily for 3 d (1.5 µg IL-2/mouse in 250 µl) as shown in *Figure 1A*, unless stated otherwise. After 48 h, mice were i.p. injected with LPS. Control mice were injected with the same volume of sterile PBS (250 µl). The dose of injected LPS is shown in % of maximum non-lethal dose (MNLD; 100% MNLD ~ 200, 35 and 35 µg LPS in C57BL/6, BALB/c and Nu/Nu mice, respectively), that is the highest possible dose which causes significant toxic effect, but no mortality. Body temperature (measured by stylus in the throat) and survival of mice were recorded.

Preparation of single-cell suspension for flow cytometry

For spleen cells, animals were sacrificed by cervical dislocation and spleens were harvested and homogenized by GentleMACS Dissociator (Miltenyi Biotec, Bergisch Gladbach, North Rhine-Westphalia, Germany). After red blood cell lysis (ACK lysing buffer, Gibco, Gaithersburg, Maryland, USA), cells were strained twice to remove clumps (70 µm BD Falcon strainer, Corning, New York, New York, USA, followed by 30 µm CellTrics strainer, Sysmex, Norderstedt, Germany) and resuspended in FACS buffer (PBS, 2% FCS, 2 mmol EDTA). For peripheral blood cells, mice were exsanguinated via carotid excision into the heparinized Eppendorf tubes. Whole blood was lysed twice with ACK Lysing buffer, strained once (30 µm, Sysmex Norderstedt, Germany) and resuspended in FACS buffer. Lungs and livers were injected with Colagenase D solution (1 mg/ml, Roche, Basel, Switzerland), incubated for 30 min at 37 °C, homogenized by GentleMACS Dissociator and further processed like the spleen cells.

Staining for surface markers

Cells were blocked by 10% mouse serum and/or Fc block for 30 min on ice and stained with fluorochrome-labelled mAbs recognizing selected surface markers for 30 min on ice in the dark. After each step, cells were washed twice in FACS buffer and fixed with Foxp3 Fixation/Permeabilization buffer (eBiosciences, San Diego, California, USA) for 30 min on ice in the dark before analysis. Flow cytometric analysis was performed on LSRII (BD Biosciences, San Jose, California, USA) and data were analysed using FlowJo X software (Tree Star, Inc, Ashland, Oregon, USA).

175

Staining for intracellular markers

After staining of surface antigens, fluorochrome-labelled mAbs recognizing intracellular markers were added and cells were incubated for 30 min on ice in the dark. Washing was performed twice with Fixation/Permeabilization buffer (eBiosciences, San Diego, California, USA). Cells were resuspended in FACS buffer before analysis. Analysis was performed as described above.

RT-qPCR analysis

RNA from splenocytes was isolated using TRIzol reagent (Invitrogen, USA) regarding to the manufacturer's protocol. One µg RNA treated with DNAse I (Turbo DNAse; Thermo Fisher Scientific, USA) was reverse-transcribed using the Oligo(dT)12–18 primer and Superscript IV Reverse Transcriptase (Life Technologies, Carlsbad, CA, USA). To select suitable housekeeping genes, the gene expression stability was assessed using RefFinder (https://www.heartcure.com.au/reffinder/). Evaluation of amplification efficiency was performed by dilution series of cDNA. qPCR (CFX96 TouchTM, Bio-Rad) was performed to determine the changes in the mRNA levels of TLR4. The cycling parameters were as follows: 4 min at 94 °C, 35 cycles of 10 s at 94 °C, 25 s at 58 °C, and a final extension for 7 min at 72 °C. Gene expression changes were calculated according to the $2-\Delta\Delta CT$ (Livak) method. Two reference genes (*Casc3, H6pd*) were selected as the most stable internal controls for the normalization of the *Tlr4* gene expression. The fold change in the mRNA level was related to the change in the settled controls. All parameters were determined in duplicates. Primers used:

Name	Sequence (5'- 3')	Target
*Casc3*for	TTCGAGGTGTGCCTAACCA	
*Casc3*rev	GCTTAGCTCGACCACTCTGG	*Casc3*
*H6pd*for	GGATTGTGTTTAAGAATCGGG	
*H6pd*rev	AGTAGGCGTCTTGCTC	*H6pd*
*Tlr4*for	GATCATGGCACTGTTCTTCTC	
*Tlr4*rev	CACACCTGGATAAATCCAGC	*Tlr4*

Casc3: cancer susceptibility candidate gene 3; *H6pd*: Hexose-6-phosphate dehydrogenase; *Tlr4*: Toll-like receptor 4.

Adoptive transfer of OT-I CD8^{+} T cells, OT-II CD4^{+} T cells, CD4^{+}CD25^{+} T cells and CD3^{+} T cells

MACS-separated (negative selection, AutoMACS, Miltenyi Biotec, Bergisch Gladbach, North Rhine-Westphalia, Germany) OT-I CD8^{+} T and OT-II CD4^{+} cells (both Ly5.1^{+}) were injected i.v. into C57BL/6 (Ly5.2^{+}) mice via tail vein. C57BL/6 mice were injected i.p. with PBS, OT-I plus OT-II peptides (10 and 50 µg/mouse, respectively; MBL International, Woburn, Massachusetts, USA; or Genscript, Piscataway, New Jersey, USA, respectively) plus polyI:C (75 µg/mouse; Sigma-Aldrich, St. Louis, Missouri, USA) or with the latter plus αIFN-γ mAb (250 µg/mouse; XMG1.2; BioXcell, Lebanon, New Hampshire, USA). Mice were either sacrificed 3 days post priming and spleen cells were analyzed by flow cytometry for expansion of adoptively transferred cells or challenged with LPS. CD4^{+}CD25^{+} T cells were purified by MACS (negative selection for CD4^{+} T cells and positive selection for CD25^{+} cells) from C56BL/6 mice treated with IL-2/JES6 as shown in *Figure 1A* (2 days after the last dose of IL-2/JES6). CD4^{+}CD25^{+} T cells were injected i.v. into Nu/Nu mice via tail vein. Next, Nu/Nu mice were treated with IL-2/JES6 and challenged with LPS as in *Figure 1A*. CD3^{+} T cells were purified by MACS (negative selection) from MyD88^{-/-} mice treated with IL-2/JES6 as shown in *Figure 1A* (2 days after the last dose of IL-2/JES6). CD3^{+} T cells were injected i.v. into Rag1^{-/-} mice via tail vein. Next, Rag1^{-/-} mice were treated with IL-2/JES6 and challenged with LPS as in *Figure 1A*.

Immunization with ovalbumin

C57BL/6 mice were i.p. injected with ovalbumin (OVA, 0.5 mg/mouse, Warthington, New Jersey, USA) plus polyI:C (75 µg/mouse) on day 0. Mice were i.p. challenged with LPS on day 4.

BrdU incorporation assay in vivo

C57BL/6 mice were i.p. injected with titrated doses of IL-2/JES6 or with PBS. After 4 h, mice were injected i.p. with 0.5 µg of BrdU (Sigma-Aldrich, St. Louis, Missouri, USA) in 50 µl PBS. At the same time, mice were given 0.8 mg/ml BrdU in their drinking water. BrdU solution was prepared in sterile water, protected from light exposure and changed daily. Mice were sacrificed 48 h later and spleens were harvested. Single cell suspensions were prepared as described above. BrdU staining was performed in similar fashion to staining of intracellular antigens with two additional steps following fixation with Fixation/Permeabilization buffer (eBiosciences, San Diego, California, USA). First, cells were treated with BD Cytofix/Cytoperm Plus buffer (BD Biosciences, San Jose, California, USA) for 10 min on ice. Second, cells were treated with DNAse (BD Biosciences, San Jose, California, USA) for 1 h at 37 °C. Fluorochrome-labelled mAbs were added together with anti-BrdU mAb (BD Biosciences, San Jose, California, USA) and cells were incubated for 30 min on ice in the dark. Washing, resuspending of cells and subsequent analysis was performed as described above.

Detection of IFN-γ production in vivo

C57BL/6 mice were i.p. injected with IL-2/JES6-1, IL-2/S4B6 or PBS (Control) as in *Figure 1A*. Each mouse was i.p. injected with 150 µg of brefeldin A (Sigma-Aldrich, St. Louis, Missouri, USA) 2 h after the last dose. Mice were sacrificed 12 h after injection of brefeldin A. Spleens, livers, and lungs were harvested for subsequent flow cytometry analysis performed as described above.

Detection of cytokines in serum

C57BL/6 and BALB/c mice were treated with IL-2/JES6 and challenged with LPS (10% of MNLD) as shown in *Figure 1A*. Control mice were treated with sterile PBS and challenged with LPS (100% of MNLD). Mice were euthanized by exsanguination via carotid excision at 2, 3, 4, 6, and 8 h after the LPS challenge and their sera were collected. Levels of TNF-α, IL-1β, IL-12, and IL-6 (R&D System, Minneapolis, Minnesota, USA) following manufacturer's protocol.

Determination of vascular leak syndrome (VLS) in the lungs

C57BL/6 mice were treated with IL-2/JES6, IL-2/S4B6 or PBS (Control) as shown in the *Figure 1A*. Mice were euthanized 1 day after the last dose and their lungs were harvested. Pulmonary wet weight was determined by weighting lungs before and after lyophilization overnight at 58 °C under vacuum.

Statistical analysis

All experiments were done at least twice with similar results; n = 2–16 technical replicates. Statistical analysis was performed using GraphPad Prism (GraphPad Software, San Diego, California, USA). The difference between groups was analysed by unpaired two-tailed Student's t-test. The confidence level was 95%. Differences with *,°,+ $p \leq 0.05$; **, °° $p \leq 0.01$; ***, °°° $p \leq 0.001$ were considered as statistically significant.

177

Additional information

Author contributions

Jakub Tomala, Data curation, Investigation, Methodology, Validation, Writing - original draft; Petra Weberova, Investigation, Methodology, Validation; Barbora Tomalova, Data curation, Formal analysis, Investigation, Methodology, Validation, Visualization, Writing - original draft, Writing - review and editing; Zuzana Jiraskova Zakostelska, Data curation, Investigation, Methodology; Ladislav Sivak, Data curation, Formal analysis, Investigation, Visualization; Jirina Kovarova, Investigation, Methodology; Marek Kovar, Conceptualization, Data curation, Formal analysis, Funding acquisition, Investigation, Project administration, Supervision, Visualization, Writing - original draft, Writing - review and editing

Author ORCIDs

Jakub Tomala ⓘ http://orcid.org/0000-0002-6315-2832
Ladislav Sivak ⓘ http://orcid.org/0000-0003-2623-8458
Marek Kovar ⓘ http://orcid.org/0000-0002-6602-1678

Ethics

All experiments were approved by the Animal Welfare Committee at the Institute of Microbiology of the Czech Academy of Sciences (Prague, Czech Republic) and performed in strict accordance with the recommendations of local and European guidelines. Every effort was made to minimize animal suffering. This work was approved by protocol number 112/2012. Accreditation number of the animal facility where the research was conducted: 51205/2018-MZE-17214.

Decision letter and Author response

Decision letter https://doi.org/10.7554/eLife.62432.sa1
Author response https://doi.org/10.7554/eLife.62432.sa2

Additional files

Supplementary files
• Transparent reporting form

Data availability

All data generated or analysed during this study are included in the manuscript and supporting files. Source data files have been provided for Figures 1-6 and all figure supplements (12 in total).

References

Atkins MB, Lotze MT, Dutcher JP, Fisher RI, Weiss G, Margolin K, Abrams J, Sznol M, Parkinson D, Hawkins M, Paradise C, Kunkel L, Rosenberg SA. 1999. High-dose recombinant interleukin 2 therapy for patients with metastatic melanoma: analysis of 270 patients treated between 1985 and 1993. *Journal of Clinical Oncology* **17**:2105–2116. DOI: https://doi.org/10.1200/JCO.1999.17.7.2105, PMID: 10561265

Berendt MJ, North RJ. 1980. T-cell-mediated suppression of anti-tumor immunity An explanation for progressive growth of an immunogenic tumor. *The Journal of Experimental Medicine* **151**:69–80. DOI: https://doi.org/10.1084/jem.151.1.69, PMID: 6444236

Berg RE, Cordes CJ, Forman J. 2002. Contribution of CD8+ T cells to innate immunity: IFN-gamma secretion induced by IL-12 and IL-18. *European Journal of Immunology* **32**:2807–2816. DOI: https://doi.org/10.1002/1521-4141(2002010)32:10<2807::AID-IMMU2807>3.0.CO;2-0, PMID: 12355433

Boyman O, Kovar M, Rubinstein MP, Surh CD, Sprent J. 2006. Selective stimulation of T cell subsets with antibody-cytokine immune complexes. *Science* **311**:1924–1927. DOI: https://doi.org/10.1126/science.1122927, PMID: 16484453

Boyman O, Cho JH, Sprent J. 2010. The role of interleukin-2 in memory CD8 cell differentiation. *Advances in Experimental Medicine and Biology* **684**:28–41. DOI: https://doi.org/10.1007/978-1-4419-6451-9_3, PMID: 20795538

Boyman O, Sprent J. 2012. The role of interleukin-2 during homeostasis and activation of the immune system. *Nature Reviews. Immunology* **12**:180–190. DOI: https://doi.org/10.1038/nri3156, PMID: 22343569

Cassado ADA, D'Império Lima MR, Bortoluci KR. 2015. Revisiting mouse peritoneal macrophages: heterogeneity, development, and function. *Frontiers in Immunology* **6**:225. DOI: https://doi.org/10.3389/fimmu.2015.00225, PMID: 26042120

Cauwels A, Buys ES, Thoonen R, Geary L, Delanghe J, Shiva S, Brouckaert P. 2009. Nitrite protects against morbidity and mortality associated with TNF- or LPS-induced shock in a soluble guanylate cyclase-dependent manner. *The Journal of Experimental Medicine* **206**:2915–2924. DOI: https://doi.org/10.1084/jem.20091236, PMID: 19934018

Cousens LP, Orange JS, Biron CA. 1995. Endogenous IL-2 contributes to T cell expansion and IFN-gamma production during lymphocytic choriomeningitis virus infection. *Journal of Immunology* **155**:5690–5699 PMID: 7499855.,

DeLeve LD. 2015. Liver sinusoidal endothelial cells in hepatic fibrosis. *Hepatology* **61**:1740–1746. DOI: https://doi.org/10.1002/hep.27376, PMID: 25131509

Donohue JH, Rosenberg SA. 1983. The fate of interleukin-2 after in vivo administration. *Journal of Immunology* **130**:2203–2208 PMID: 6601147.,

Heremans H, Van Damme J, Dillen C, Dijkmans R, Billiau A. 1990. Interferon gamma, a mediator of lethal lipopolysaccharide-induced Shwartzman-like shock reactions in mice. *The Journal of Experimental Medicine* **171**:1853–1869. DOI: https://doi.org/10.1084/jem.171.6.1853, PMID: 2112583

Izquierdo C, Ortiz AZ, Presa M, Malo S, Montoya A, Garabatos N, Mora C, Verdaguer J, Stratmann T. 2018. Treatment of T1D via optimized expansion of antigen-specific Tregs induced by IL-2/anti-IL-2 monoclonal antibody complexes and peptide/MHC tetramers. *Scientific Reports* **8**:8106. DOI: https://doi.org/10.1038/s41598-018-26161-6, PMID: 29802270

Kieper WC, Burghardt JT, Surh CD. 2004. A role for TCR affinity in regulating naive T cell homeostasis. *Journal of Immunology* **172**:40–44. DOI: https://doi.org/10.4049/jimmunol.172.1.40, PMID: 14688307

Klapper JA, Downey SG, Smith FO, Yang JC, Hughes MS, Kammula US, Sherry RM, Royal RE, Steinberg SM, Rosenberg S. 2008. High-dose interleukin-2 for the treatment of metastatic renal cell carcinoma : a retrospective analysis of response and survival in patients treated in the surgery branch at the National Cancer Institute between 1986 and 2006. *Cancer* **113**:293–301. DOI: https://doi.org/10.1002/cncr.23552, PMID: 18457330

Klatzmann D, Abbas AK. 2015. The promise of low-dose interleukin-2 therapy for autoimmune and inflammatory diseases. *Nature Reviews. Immunology* **15**:283–294. DOI: https://doi.org/10.1038/nri3823, PMID: 25882245

Koenecke C, Lee C-W, Thamm K, Föhse L, Schafferus M, Mittrücker H-W, Floess S, Huehn J, Ganser A, Förster R, Prinz I. 2012. IFN-γ production by allogeneic Foxp3+ regulatory T cells is essential for preventing experimental graft-versus-host disease. *Journal of Immunology* **189**:2890–2896. DOI: https://doi.org/10.4049/jimmunol.1200413, PMID: 22869903

Kondo M, Scherer DC, Miyamoto T, King AG, Akashi K, Sugamura K, Weissman IL. 2000. Cell-fate conversion of lymphoid-committed progenitors by instructive actions of cytokines. *Nature* **407**:383–386. DOI: https://doi.org/10.1038/35030112, PMID: 11014194

Li Q, Carr AL, Donald EJ, Skitzki JJ, Okuyama R, Stoolman LM, Chang AE. 2005. Synergistic effects of IL-12 and IL-18 in skewing tumor-reactive T-cell responses towards a type 1 pattern. *Cancer Research* **65**:1063–1070 PMID: 15705908.,

Liao W, Lin JX, Leonard WJ. 2013. Interleukin-2 at the crossroads of effector responses, tolerance, and immunotherapy. *Immunity* **38**:13–25. DOI: https://doi.org/10.1016/j.immuni.2013.01.004, PMID: 23352221

Liu CL, Ye P, Yen BC, Miao CH. 2011. In vivo expansion of regulatory T cells with IL-2/IL-2 mAb complexes prevents anti-factor VIII immune responses in hemophilia A mice treated with factor VIII plasmid-mediated gene therapy. *Molecular Therapy* 19:1511–1520. DOI: https://doi.org/10.1038/mt.2011.61, PMID: 21468007

Malek TR. 2008. The biology of interleukin-2. *Annual Review of Immunology* 26:453–479. DOI: https://doi.org/10.1146/annurev.immunol.26.021607.090357, PMID: 18062768

Malek TR, Castro I. 2010. Interleukin-2 receptor signaling: at the interface between tolerance and immunity. *Immunity* 33:153–165. DOI: https://doi.org/10.1016/j.immuni.2010.08.004, PMID: 20732639

Minami Y, Kono T, Miyazaki T, Taniguchi T. 1993. The IL-2 receptor complex: its structure, function, and target genes. *Annual Review of Immunology* 11:245–268. DOI: https://doi.org/10.1146/annurev.iy.11.040193.001333, PMID: 8476561

Nakanishi K. 2018. Unique Action of Interleukin-18 on T Cells and Other Immune Cells. *Frontiers in Immunology* 9:763. DOI: https://doi.org/10.3389/fimmu.2018.00763, PMID: 29731751

Roediger B, Kyle R, Yip KH, Sumaria N, Guy TV, Kim BS, Mitchell AJ, Tay SS, Jain R, Forbes-Blom E, Chen X, Tong PL, Bolton HA, Artis D, Paul WE, Fazekas de St Groth B, Grimbaldeston MA, Le Gros G, Weninger W. 2013. Cutaneous immunosurveillance and regulation of inflammation by group 2 innate lymphoid cells. *Nature Immunology* 14:564–573. DOI: https://doi.org/10.1038/ni.2584, PMID: 23603794

Sakaguchi S, Sakaguchi N, Asano M, Itoh M, Toda M. 1995. Immunologic self-tolerance maintained by activated T cells expressing IL-2 receptor alpha-chains (CD25). Breakdown of a single mechanism of self-tolerance causes various autoimmune diseases. *Journal of Immunology* 155:1151–1164.

Sharma R, Das A. 2018. IL-2 mediates NK cell proliferation but not hyperactivity. *Immunologic Research* 66:151–157. DOI: https://doi.org/10.1007/s12026-017-8982-3, PMID: 29256180

Spangler JB, Tomala J, Luca VC, Jude KM, Dong S, Ring AM, Votavova P, Pepper M, Kovar M, Garcia KC. 2015. Antibodies to Interleukin-2 Elicit Selective T Cell Subset Potentiation through Distinct Conformational Mechanisms. *Immunity* 42:815–825. DOI: https://doi.org/10.1016/j.immuni.2015.04.015, PMID: 25992858

Spangler JB, Trotta E, Tomala J, Peck A, Young TA, Savvides CS, Silveria S, Votavova P, Salafsky J, Pande VS, Kovar M, Bluestone JA, Garcia KC. 2018. Engineering a Single-Agent Cytokine/Antibody Fusion That Selectively Expands Regulatory T Cells for Autoimmune Disease Therapy. *Journal of Immunology* 201:2094–2106. DOI: https://doi.org/10.4049/jimmunol.1800578, PMID: 30104245

Sprent J, Surh CD. 2011. Normal T cell homeostasis: the conversion of naive cells into memory-phenotype cells. *Nature Immunology* 12:478–484. DOI: https://doi.org/10.1038/ni.2018, PMID: 21739670

Tomala J, Chmelova H, Mrkvan T, Rihova B, Kovar M. 2009. In vivo expansion of activated naive CD8+ T cells and NK cells driven by complexes of IL-2 and anti-IL-2 monoclonal antibody as novel approach of cancer immunotherapy. *Journal of Immunology* 183:4904–4912. DOI: https://doi.org/10.4049/jimmunol.0900284, PMID: 19801515

Trotta E, Bessette PH, Silveria SL, Ely LK, Jude KM, Le DT, Holst CR, Coyle A, Potempa M, Lanier LL, Garcia KC, Crellin NK, Rondon IJ, Bluestone JA. 2018. A human anti-IL-2 antibody that potentiates regulatory T cells by a structure-based mechanism. *Nature Medicine* 24:1005–1014. DOI: https://doi.org/10.1038/s41591-018-0070-2, PMID: 29942088

Vieira P, Rajewsky K. 1988. The half-lives of serum immunoglobulins in adult mice. *European Journal of Immunology* 18:313–316. DOI: https://doi.org/10.1002/eji.1830180221, PMID: 3350037

Votavova P, Tomala J, Subr V, Strohalm J, Ulbrich K, Rihova B, Kovar M. 2015. Novel IL-2-Poly(HPMA) Nanoconjugate Based Immunotherapy. *Journal of Biomedical Nanotechnology* 11:1662–1673. DOI: https://doi.org/10.1166/jbn.2015.2114, PMID: 26485935

Waldmann TA. 1989. The multi-subunit interleukin-2 receptor. *Annual Review of Biochemistry* 58:875–911. DOI: https://doi.org/10.1146/annurev.bi.58.070189.004303, PMID: 2673025

Webster KE, Walters S, Kohler RE, Mrkvan T, Boyman O, Surh CD, Grey ST, Sprent J. 2009. In vivo expansion of T reg cells with IL-2-mAb complexes: induction of resistance to EAE and long-term acceptance of islet allografts without immunosuppression. *The Journal of Experimental Medicine* 206:751–760. DOI: https://doi.org/10.1084/jem.20082824, PMID: 19332874

Wilson MS, Pesce JT, Ramalingam TR, Thompson RW, Cheever A, Wynn TA. 2008. Suppression of murine allergic airway disease by IL-2:anti-IL-2 monoclonal antibody-induced regulatory T cells. *Journal of Immunology* 181:6942–6954. DOI: https://doi.org/10.4049/jimmunol.181.10.6942, PMID: 18981114

Wood KJ, Sawitzki B. 2006. Interferon gamma: a crucial role in the function of induced regulatory T cells in vivo. *Trends in Immunology* 27:183–187. DOI: https://doi.org/10.1016/j.it.2006.02.008, PMID: 16527542

Yu TK, Caudell EG, Smid C, Grimm EA. 2000. IL-2 activation of NK cells: involvement of MKK1/2/ERK but not p38 kinase pathway. *Journal of Immunology* 164:6244–6251. DOI: https://doi.org/10.4049/jimmunol.164.12.6244, PMID: 10843677

Yu A, Zhu L, Altman NH, Malek TR. 2009. A low interleukin-2 receptor signaling threshold supports the development and homeostasis of T regulatory cells. *Immunity* 30:204–217. DOI: https://doi.org/10.1016/j.immuni.2008.11.014, PMID: 19185518

180
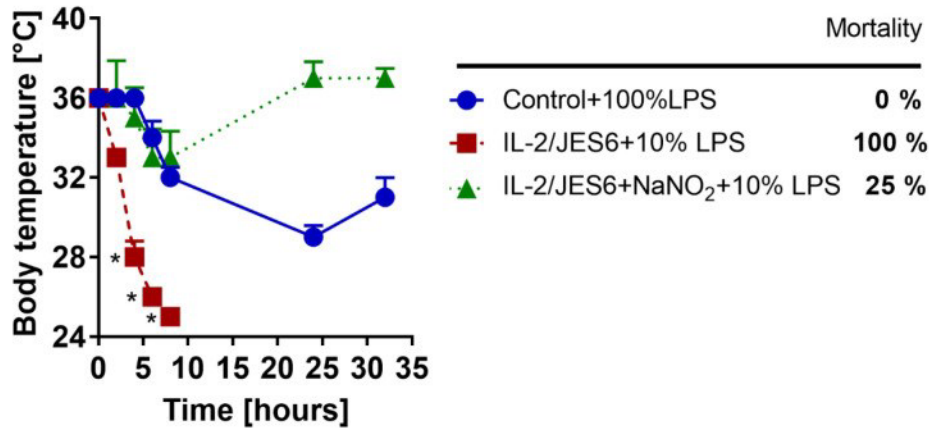
Figure 1 - Figure Supplement 1. Nitrite significantly reduces the toxicity of LPS in mice pretreated with IL-2/JES6.

C56BL/6 mice were treated with IL-2/JES6 and challenged with LPS (10% of MNLD) as shown in Figure 1A. One group of mice was i.p. injected with sodium nitrate (NaNO2; 1.5 mg/kg in 250 µl) 1 h before the LPS challenge. Control mice were challenged with LPS (100% of MNLD) only. Four mice per group were used. Data were analyzed using an unpaired two-tailed Student's t-test. Significant differences to control are shown (* $p \leq 0.05$).
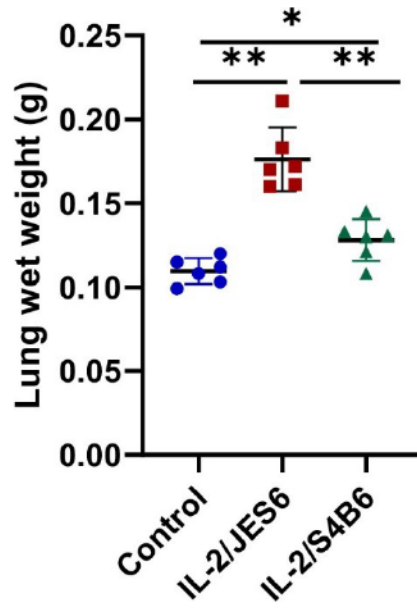
Figure 1 - Figure Supplement 2. IL-2/JES6 induces more severe lung edema in comparison to IL-2/S4B6.

C56BL/6 mice were treated with IL-2/JES6 or IL-2/S4B6 as shown in Figure 1A. Mice were euthanized 1 d after the last dose of IL-2 complexes and their lungs were harvested. Pulmonary wet weight was determined by weighing lungs before and after lyophilization overnight at 58 °C under vacuum. Six mice per group were used. Data were analyzed using an unpaired two-tailed Student's t-test. Significant differences to control are shown (* $p \leq 0.05$; ** $p \leq 0.01$).
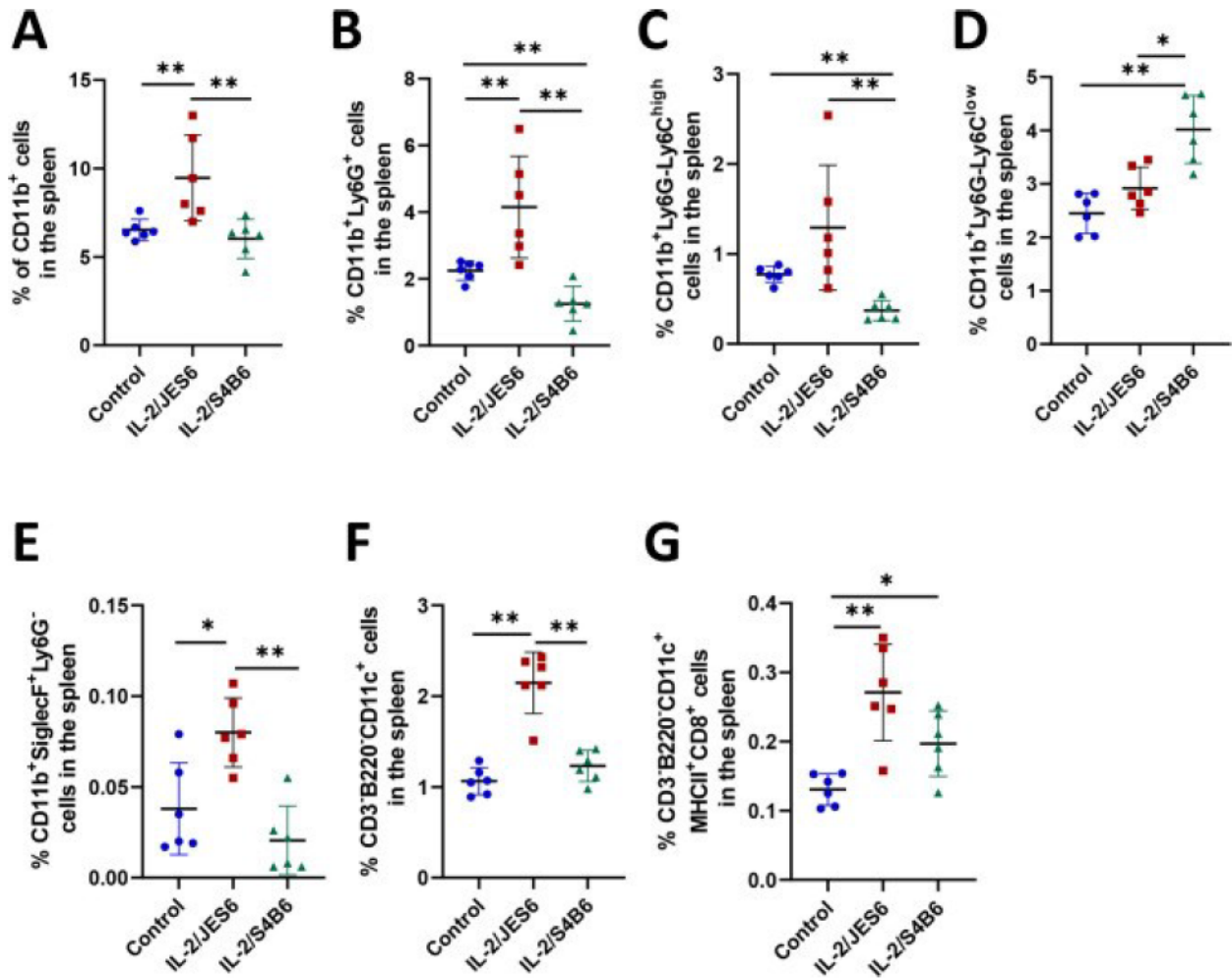
Figure 3 - Figure Supplement 1. IL-2/JES6 expands various subsets of myeloid cells in the spleen.

C56BL/6 mice were treated with IL-2/JES6 or IL-2/S4B6 as shown in Figure 1A. Mice were euthanized 2 d after the last dose of IL-2 complexes and their spleens were harvested and analyzed by flow cytometry. Relative counts of myeloid cells in general (A), granulocytes (B), monocytes/macrophages (C, D), eosinophils (E), and dendritic cells (F, G) are shown. Six mice per group were used. Data were analyzed using an unpaired two-tailed Student's t-test. Significant differences are shown (* $p \leq 0.05$; ** $p \leq 0.01$; *** $p \leq 0.001$).

Figure 3 - Figure Supplement 2. IL-2/JES6 increases MHC II expression in the monocyte/macrophage population in the spleen.

C56BL/6 mice were treated with IL-2/JES6 or IL-2/S4B6 as shown in Figure 1A. Mice were euthanized 2 d after the last dose of IL-2 complexes and their spleens were harvested and analyzed by flow cytometry. The percentage of MHC II positive cells (A, B) and relative MHC II expression level (C, D) are shown. Six mice per group were used. Data were analyzed using an unpaired two-tailed Student's t-test. Significant differences are shown (* $p \leq 0.05$; ** $p \leq 0.01$; *** $p \leq 0.001$).

Figure 3 - Figure Supplement 3. IL-2/JES6 promotes the proliferation and expansion of myeloid cells in a dose-dependent manner in the spleen.

C56BL/6 mice were treated with a titrated single dose of IL-2/JES6. Mice were i.p. injected with BrdU 4 h after administration of IL-2/JES and put on drinking water with BrdU. Mice were euthanized 2 d after administration of IL-2/JES6 and their spleens were harvested and analyzed by flow cytometry. Relative counts (A) and BrdU incorporation (B) of F4/80 positive and negative myeloid cells are shown. Two mice per group were used. Data were analyzed using one-way analysis of variance (ANOVA) with Tukey's multiple comparison test. Significant differences are shown (* $p \leq 0.05$; ** $p \leq 0.01$; *** $p \leq 0.001$).
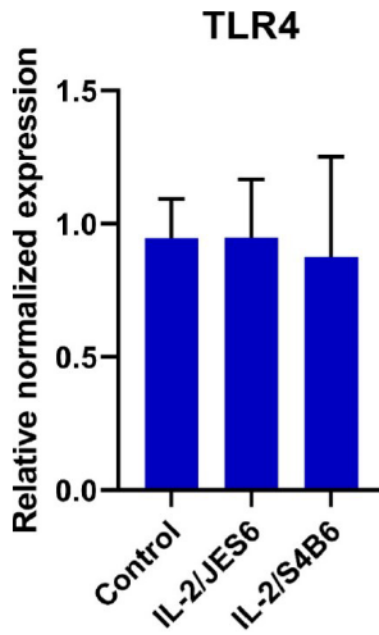
Figure 3 - Figure Supplement 4. The expression of TLR4 in splenocytes of C57BL/6 mice is not affected by the treatment with IL-2/JES6 or IL-2/S4B6.

C56BL/6 mice were treated with IL-2/JES6 or IL-2/S4B6 as shown in Figure 1A. Mice were euthanized on day five and mRNA was isolated from harvested spleen cells. Relative expression of Tlr4 was normalized to two reference genes (Casc3, H6pd). Data were analyzed using an unpaired two-tailed Student's t-test. Data is presented as mean ± SD of six mice per group.
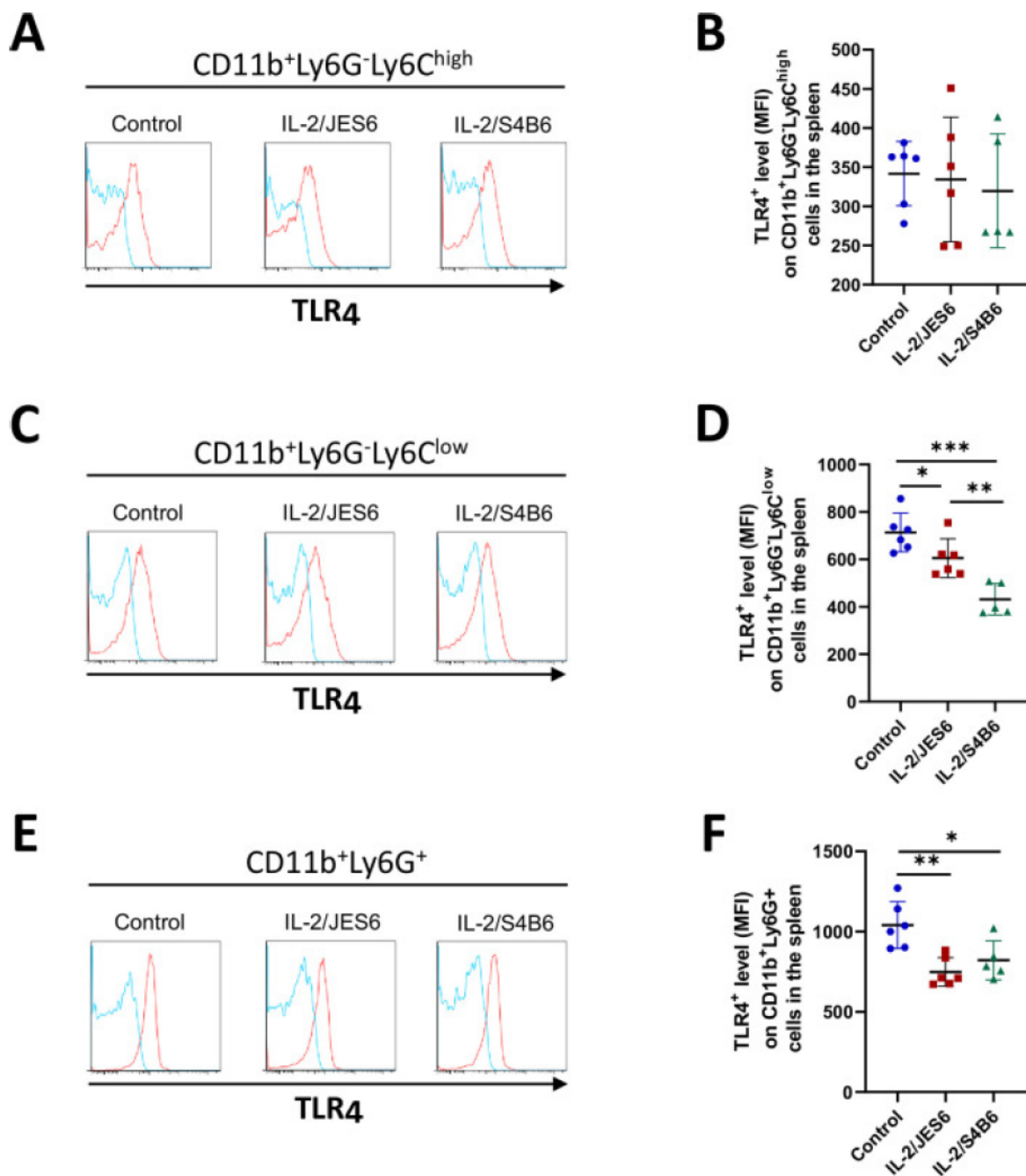
Figure 3—Figure Supplement 5. IL-2/JES6 does not increase the level of TLR4 in myeloid cells in the spleen.

C56BL/6 mice were treated with IL-2/JES6 or IL-2/S4B6 as shown in Figure 1A. Mice were euthanized 2 d after the last dose of IL-2 complexes and their spleens were harvested. Spleen cells were stained for surface markers (including TLR4), fixed, permeabilized, stained again for TLR4, and analyzed by flow cytometry. Histograms showing one representative mouse (A, C, and E; blue line: isotype control mAb, red line: anti-TLR4 mAb) and graphs showing average ± SD in experimental groups (B, D, and F) are presented. Six (control, IL-2/JES6) or five (IL-2/S4B6) mice per group were used. Data were analyzed using an unpaired two-tailed Student's t-test. Significant differences are shown (* $p \leq 0.05$; ** $p \leq 0.01$; *** $p \leq 0.001$).
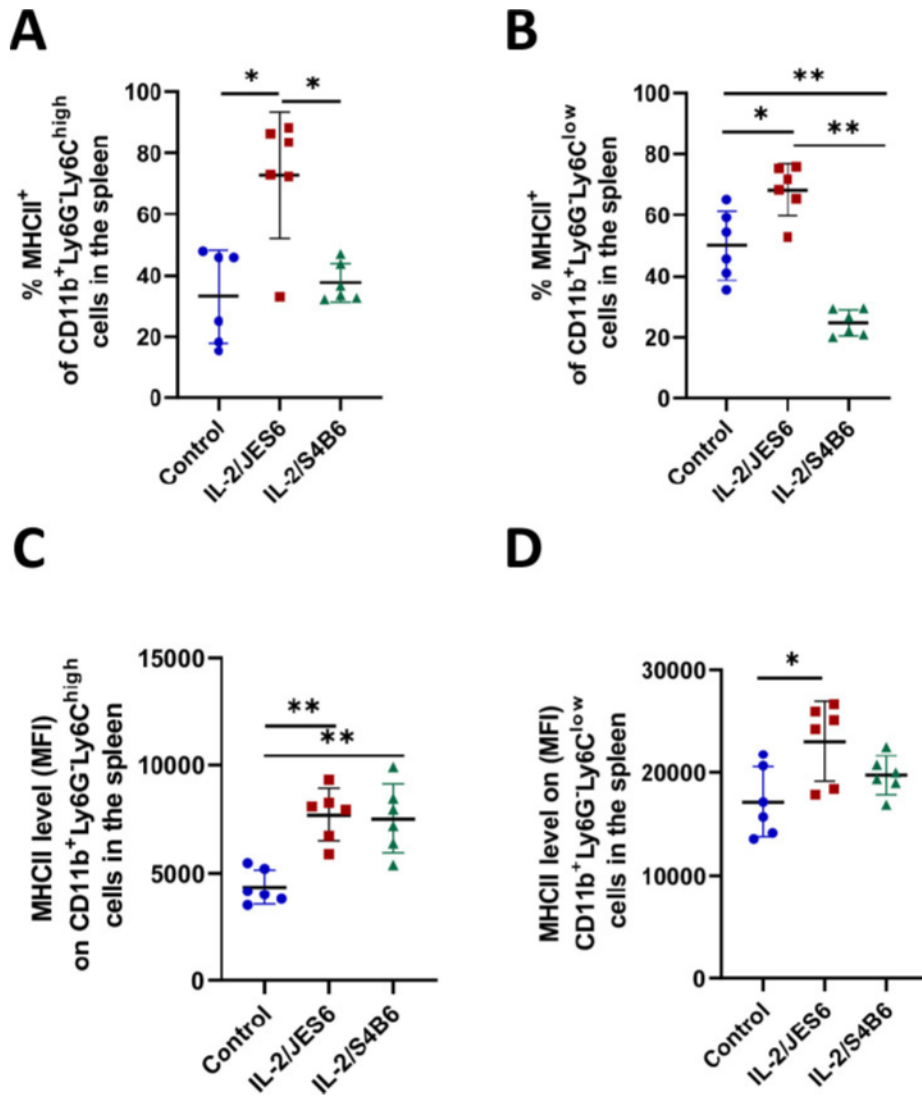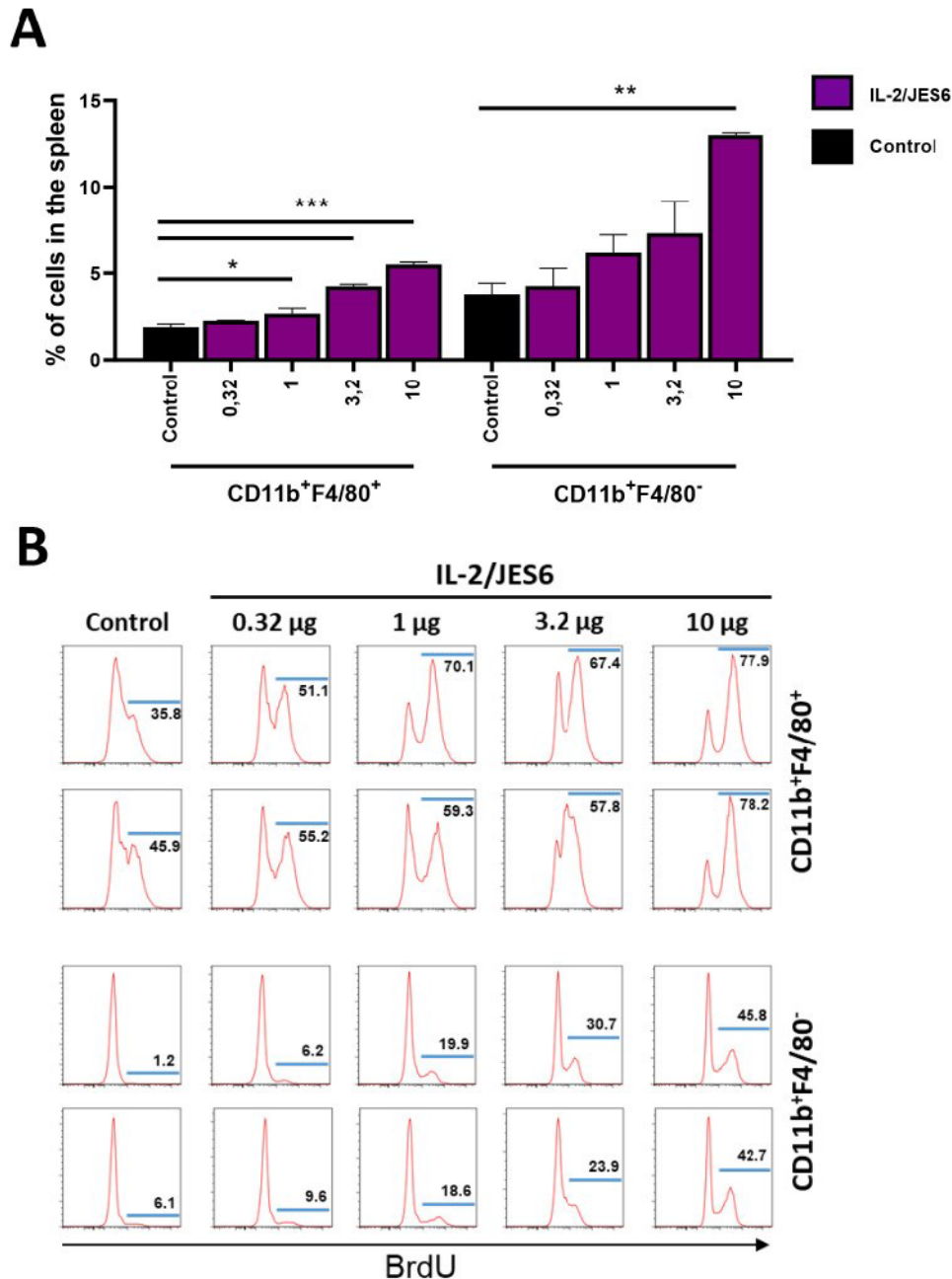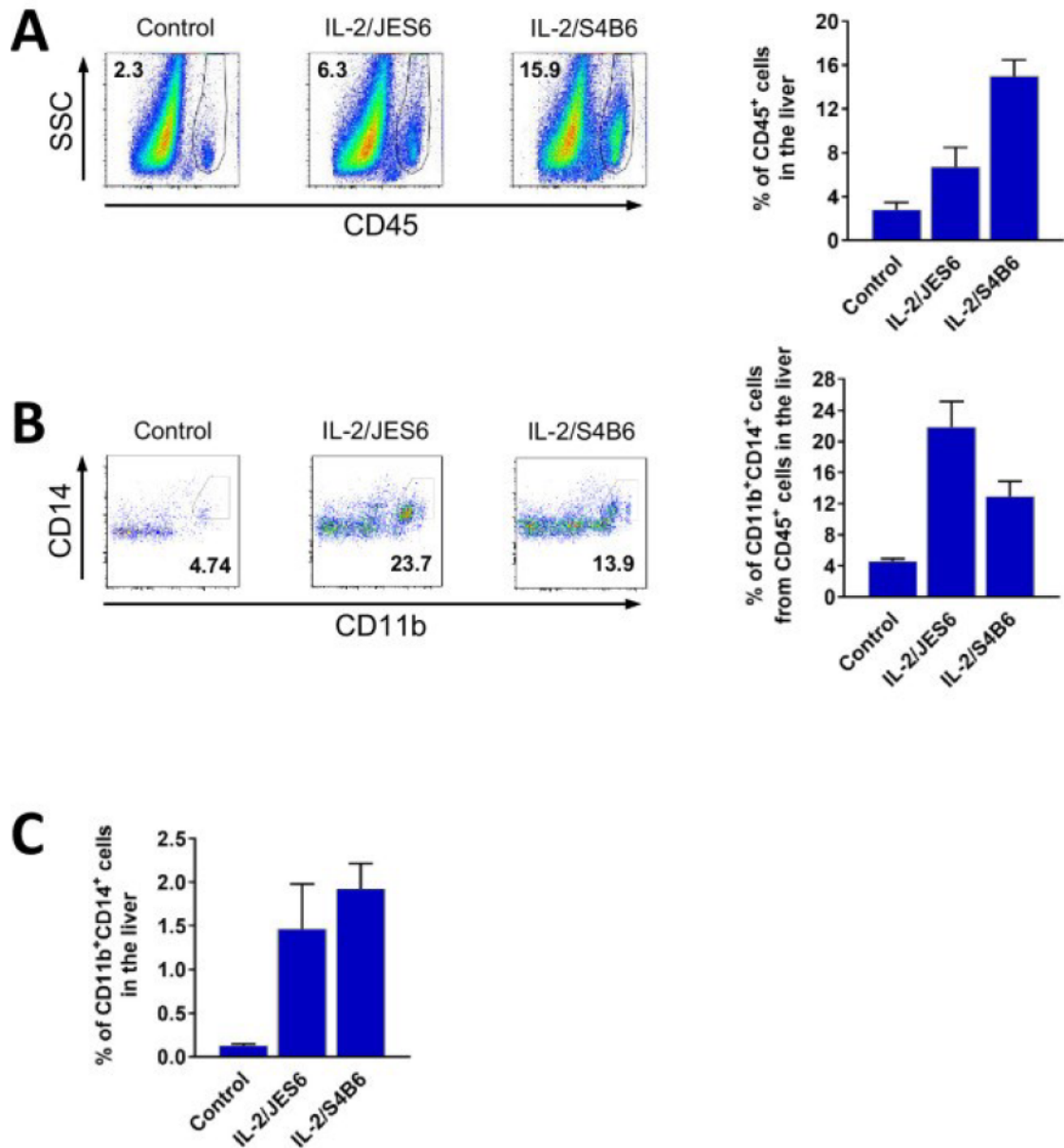
Figure 3 - Figure Supplement 6. IL-2/JES6 increases the counts of CD45$^+$ and CD11b$^+$ CD14$^+$ cells in the liver.

C56BL/6 mice were treated with IL-2/JES6 or IL-2/S4B6 as shown in Figure 1A. Mice were euthanized 2 d after the last dose of IL-2 complexes and their livers were harvested. The relative number of CD45+ cells in the liver (A), CD11b+ CD14+ cells within CD45+ cells in the liver (B), and CD11b+ CD14+ cells in the liver (C) were determined by flow cytometry. Dot plots showing one representative mouse (A and B) and a bar graph showing average ± SD in experimental groups (B–C) are presented. Three mice per group were used.
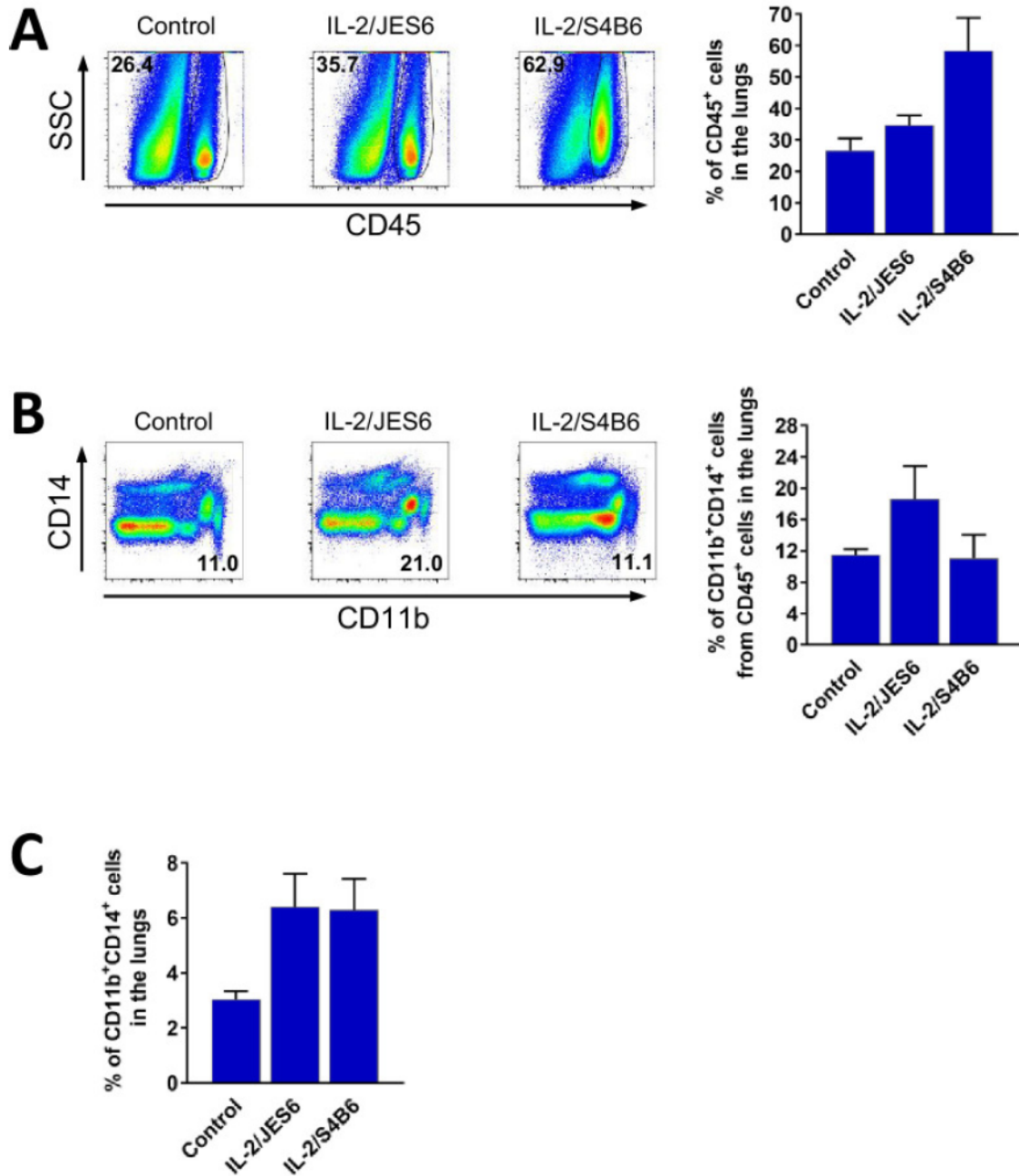
Figure 3 - Figure Supplement 7. IL-2/JES6 increases the counts of CD45$^+$ and CD11b$^+$ CD14$^+$ cells in the lungs.

C56BL/6 mice were treated with IL-2/JES6 or IL-2/S4B6 as shown in Figure 1A. Mice were euthanized 2 d after the last dose of IL-2 complexes and their lungs were harvested. The relative number of CD45+ cells in the lungs (A), CD11b+ CD14+ cells within CD45+ cells in the lungs (B), and CD11b+ CD14+ cells in the lungs (C) were determined by flow cytometry. Dot plots showing one representative mouse (A and B) and a bar graph showing average ± SD in experimental groups (B–C) are presented. Three mice per group were used.
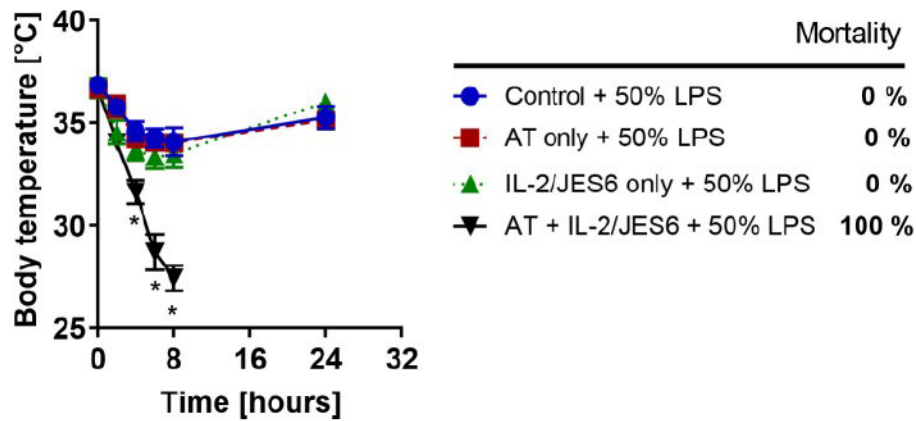
Figure 4 - Figure Supplement 1. TLR4 signaling in T cells is dispensable for inducing LPS hypersensitivity by IL-2/JES6.

Two groups of Rag1-/- mice were adoptively transferred (AT) with 5.6×106 T cells (CD3+ cells sorted by MACS using negative selection) from MyD88-/- mice pretreated with IL-2/JES6 as shown in Figure 1A. One group of AT mice and one group of normal Rag1-/- mice were treated with IL-2/JES6 as shown in Figure 1A. All experimental groups including Rag1-/- mice without AT and IL-2/JES6 treatment (Control) were challenged with LPS (50% of MNLD). Four mice per group were used. Data were analyzed using an unpaired two-tailed Student's t-test. Significant differences to control are shown (* $p \leq 0.05$).
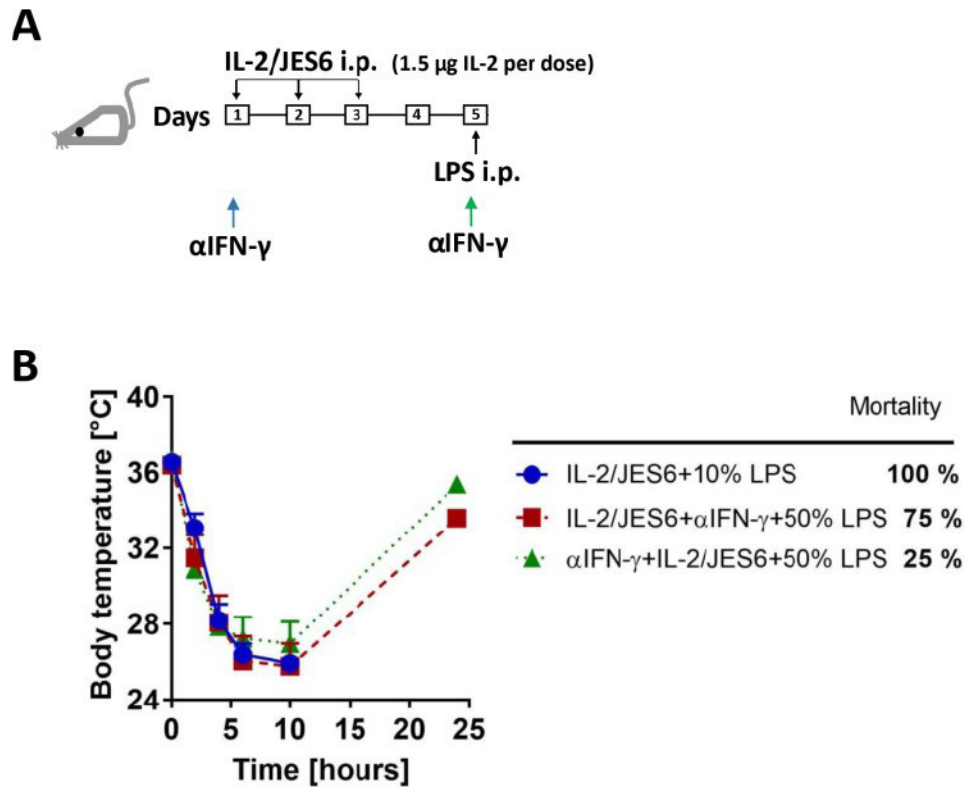
Figure 4 - Figure Supplement 2. Anti-IFN-γ mAb protects from sensitization to LPS more effectively when administered before treatment with IL-2/JES6.

(A) Schedule of sensitization of mice to LPS by IL-2/JES6 and administration of anti-IFN-γ mAb (αIFN-γ; 250 μg/mice i.p.). Anti-IFN-γ mAb was injected either 4 h before the first dose of IL-2/JES6 (blue arrow) or 4 h before the LPS challenge (green arrow). (B) C56BL/6 mice were treated with IL-2/JES6 and challenged with LPS (10% and 50% of MNLD for control and mice injected with anti-IFN-γ mAb, respectively) as shown in A. Four mice per group were used. Data were analyzed using an unpaired two-tailed Student's t-test.
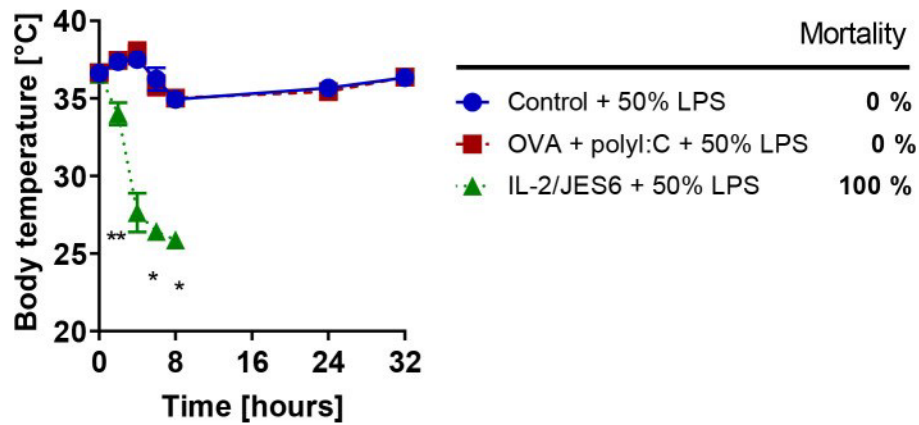
Figure 6 - Figure Supplement 1. Immunization with ovalbumin plus poly I:C does not increase sensitivity to LPS.

C56BL/6 mice were treated with IL-2/JES6 and challenged with LPS (50% of MNLD) as shown in Figure 1A. Another group of C56BL/6 mice was immunized with ovalbumin (OVA; 0.5 mg/mice i.p) plus poly I:C (75 µg/mice i.p.) on day one and challenged with LPS (50% of MNLD) on day 5. The control group was challenged with the same dose of LPS only. Five mice per group were used. Data were analyzed using an unpaired two-tailed Student's t-test. Significant differences to control are shown (* $p \leq 0.05$; ** $p \leq 0.01$).

V. Discussion

IL-2 is a fundamental cytokine in T cell biology, having a profound role in the development, proliferation, and survival of various T cell subsets. Its capacity to support the proliferation and survival of activated T cells and their differentiation into effector T cells while maintaining regulatory T cell numbers and their suppressive activity highlights its dual role in immune regulation. These immunostimulatory and immunosuppressive actions make IL-2 a promising target for treating immune-related diseases, including cancer and autoimmune disorders. The success of IL-2-based immunotherapies crucially depends on finely tuning this balance to harness its therapeutic potential effectively.

One of the primary challenges with IL-2 therapy is its rapid renal clearance, due to its small molecular size [204, 476, 477], which results in a short half-life and low bioavailability of this parenterally administered recombinant protein [478]. High-dose administrations, intended to overcome this limitation, often lead to severe toxicities, such as vascular leak syndrome and severe pulmonary edema, caused by direct activation of CD25$^+$ endothelial cells [94, 208, 479, 480]. Moreover, IL-2 stimulates Treg cells which may dampen the antitumor immunity. These challenges have necessitated the development of modified IL-2 variants and novel delivery systems to optimize therapeutic outcomes while minimizing adverse effects. For instance, IL-2 muteins with reduced CD25 binding favor the expansion of effector T cells and NK cells, making them promising candidates for cancer immunotherapy.

To address some of these issues, strategies to increase the molecular size of IL-2, thereby reducing renal clearance and prolonging its circulation time in the bloodstream, have been explored [424, 481]. A notable approach involves polymer modification, specifically PEGylation. Initial studies confirmed the antitumor activity of IL-2-PEG conjugate in various cancers [422, 424, 482-486]. However, subsequent comparisons to native IL-2 revealed no significant advantages [426, 427, 487, 488], and adverse reactions to PEG or its byproducts, including hypersensitivity, have been noted [489-494]. Our laboratory has pursued an alternative strategy using poly(HPMA), a synthetic, non-immunogenic polymer [495, 496]. The design, architecture, and structural properties of poly(HPMA) make it a versatile system for the synthesis of polymeric conjugates for biomedical applications. We also took advantage of the fact that poly(HPMA)-modified proteins exhibit lower immunogenicity and better biocompatibility when compared to their PEGylated counterparts [497, 498]. Therefore, our research [472] has pioneered the development of IL-2 modified with several chains of poly(HPMA). The resulting IL-2-poly(HPMA) conjugate demonstrated significantly increased biological activity *in vivo*. Moreover, compared to IL-2-PEG, IL-2-poly(HPMA) conjugate showed more biased activity towards CD122^{high} cells, as the modification of IL-2 with poly(HPMA) chains decreased the ability of IL-2 to interact with CD25. Remarkably, IL-2-poly(HPMA) conjugate demonstrated a significantly enhanced ability to stimulate IL-2 responsive immune cells over free IL-2 *in vivo*. Moreover, this conjugate has shown potential for various immunological applications beyond cancer therapy, such as vaccination and immune system reconstitution after bone marrow transplantation. However, our study was not focused on developing a new form of IL-2 for tumor immunotherapy, but rather broadly to generally increase the biological activity and improve pharmacological features of IL-2 *in vivo* and thus potentially enable the use of this cytokine and, theoretically, also other cytokines in various

biomedical applications. Nevertheless, our development predated NKTR-214, a related IL-2-PEG prodrug designed to enhance $CD8^+$ T cell and NK cell activation while minimizing Treg cell expansion [428]. Despite initial promise, NKTR-214 faced challenges in clinical trials due to its toxicity profile and rather unimpressive efficacy, leading to its eventual discontinuation [432, 433]. Although research suggests that poly(HPMA) could be a promising alternative for PEG in biomedical applications [499-503], we can only speculate that modification of IL-2 with poly(HPMA) will result in any advantage over unmodified IL-2 in cancer therapy. Although numerous HPMA-drug conjugates have reached Phase I and/or Phase II clinical evaluations, no product has yet been successfully brought to the market. Thus, further research is required to develop poly(HPMA)-drug conjugates as successful cancer therapeutics [504, 505].

The development of anti-IL-2 mAbs represents a significant breakthrough in immunotherapy, with profound implications for the treatment of cancer and autoimmune diseases. Originally developed to neutralize endogenous IL-2 and inhibit its activity, these mAbs were soon found to form immunocomplexes with IL-2 that substantially potentiate the stimulatory activity of IL-2 *in vivo*. Moreover, IL-2co exhibits unique biological activities based on the specificity of the given clone of anti-IL-2 mAb [74]. These IL-2co alter the selectivity of IL-2, enabling more specific activation of particular T-cell subsets. For instance, CD25-biased IL-2co skew IL-2 activity towards the expansion of Treg cells, which can be beneficial for treating autoimmune diseases. Conversely, CD122-biased IL-2co preferentially promotes effector T and NK cell expansion, which have been harnessed to enhance anti-tumor responses.

Two studies have provided further insight into the molecular interactions of mIL-2 with anti-IL-2 mAbs, specifically S4B6, JES6-5H4 [506], and JES6-1A12 [507]. The first study [506] identified key epitopes involved in the binding of mIL-2 to its respective anti-IL-2 mAbs, S4B6 and JES6-5H4. Data analysis using the phage-display method showed that S4B6 and JES6-5H4 mAbs share a significant overlap in critical residues in the IL-2 molecule to which they bind, resulting in similar biological effects of respective IL-2co [74]. This overlap occurs at the CD25/IL-2 interface thus providing an explanation of previous functional studies on the molecular level [463]. Our study [508] provided a novel tool for IL-2-based immunotherapy by introducing so far undescribed protein chimera scIL-2/S4B6, i.e., a new IC structure, where IL-2 was covalently linked to a light chain of S4B6 anti-IL-2 mAb via a flexible oligopeptide $(Gly_4Ser)_3$ spacer. This design addressed concerns associated with the potential use of IL-2co in human medicine, namely stoichiometry and stability. Thus, through this novel class of ICs, we provided a general principle on designing an IL-2-based immunotherapeutics that mimics the IL-2co structurally and functionally but without the most significant drawbacks. This study also offers a structural basis for understanding the mechanism of IL-2co, together with other published data collectively suggesting that S4B6 and JES6-5H4 mAbs impede the binding of IL-2 to CD25.

Rojas *et al.* [507] identified a unique cluster of residues in the IL-2 molecule recognized by JES6-1A12 mAb, distinct from those recognized by S4B6 or JES6-5H4 mAbs. Our report [509] provided X-ray crystallography data showing that S4B6 mAb completely blocks IL-2/CD25 interaction due to the overlap of the epitopes in the IL-2 molecule responsible for binding to CD25 and S4B6 mAb. Moreover, the binding of S4B6 mAb to IL-2 also induces a conformational change in the IL-2 molecule thereby increasing its affinity to CD122. This unique feature further increases the selectivity of IL-2/S4B6 to stimulate CD122^{high} cells, such

as memory CD8$^+$ T and NK cells. Interestingly, this S4B6 mAb-induced structural shift mimics the effect of CD25. It is a very unique situation where the binding of artificial protein (S4B6 mAb) to IL-2 results in the same change of the IL-2 conformation as the binding of the natural receptor (CD25). Overlaying the epitopes responsible for the binding of IL-2R subunits with S4B6 mAb-bound IL-2 clearly illustrated the direct occlusion of CD25 binding by the S4B6 mAb. The comparison also highlights a striking similarity between the interfaces of hIL-2/hCD25 and mIL-2/S4B6 mAb.

JES6-1A12 mAb recognizes an epitope in mIL-2 that is involved in the interaction with both IL-2Rβ and γ$_c$. Thus, IL-2 bound to this mAb is not able to interact with signaling IL-2R subunits. Moreover, this mAb also allosterically impedes the IL-2/CD25 interaction. However, the interaction between IL-2 and JES6-1A12 mAb could be replaced by CD25 through a so-called "trigger exchange" mechanism, favoring CD25^{high} cells such as Treg cells or activated T cells as they express sufficiently high levels of CD25 to displace the mAb [509]. Activation of the IL-2 signaling pathway in CD25^{high} cells further upregulates CD25 expression to create a positive feedback loop that favors CD25^{high} cell expansion [509] through the IL-2/JES6 complex, further highlighting superior selectivity of this IL-2co for CD25^{high} cells such as Treg cell population. In summary, we elucidated here the mechanism of how IL-2co formed by JES6-1A12 and S4B6 mAbs interact with IL-2R and differentially stimulate various IL-2 responsive immune cell subsets based on their IL-2 receptor surface expression profiles. Moreover, this biased stimulation is further enhanced by transcriptional feedback in the case of IL-2/JES6. This work further enabled structure-based engineering of a single agent fusion of the IL-2 and JES6-1A12 mAb (JY3 IC, described in our next paper [510]). This IC preserves the CD25-antibody exchange mechanism of IL-2 delivery despite IL-2 being covalently linked to the antibody. JY3 IC "shields" a cytokine from non-specifically engaging immune cells and instead targets it preferentially to Treg cells based on their high surface CD25 expression levels. This offers a more sophisticated mode of selective IL-2 delivery than direct mutagenesis of the cytokine reducing its receptor affinity [403, 434], which may also alter functional activity and raise concerns about immunogenicity. Moreover, this approach overcomes logistical challenges in drug formulation such as the instability of the cytokine/antibody complex. ICs based on muteins derived from JES6-1A12 mAb with different affinities for IL-2 selectively target IL-2 activity to CD25^{high} immune cell subsets. In turn, such ICs significantly upregulate CD25 on activated CD8$^+$ T cells and Tregs, creating an amplification loop and resulting in the superior expansion of these subsets compared to that induced by IL-2/JES6 complex. Moreover, pretreatment with JY3 IC prevents the development of autoimmune disease in a dextran sodium sulfate (DSS)-induced colitis model with a higher efficacy than the IL-2/JES6 complex. Although JY3 IC induces CD25 upregulation on MP CD8$^+$ T cells and surprisingly on NK cells, it did not affect the expansion of these populations. Human CD56^{hi} NK cells express low levels of CD25 yet show good pSTAT5 responses to lower IL-2 concentrations, albeit responses that are not as robust as those by Tregs [511]. Although not tested, we can only speculate, that significantly increased CD25 levels on NK cells will render these cells more responsive to JY3 IC, which could subsequently enhance their cytotoxicity and effector cytokine production [182, 511, 512], thus making them potentially harmful [513-515]. However, given that Treg cells restrain NK cell cytotoxicity by limiting the availability of IL-2 [516] and that JY3 IC-induced

Treg cells express much higher amounts of CD25 than NK cells, the concerns are probably not justified if relevant therapeutic doses of JY3 IC are used to expand Treg cells.

Despite significant progress in optimizing IL-2 therapy for cancer treatment, the current data is almost entirely from preclinical models. While there is a consensus that IL-2 or its delivery methods must be modified for successful clinical use, opinions differ on the best approach. Until recently, the goal of IL-2 cancer immunotherapy has been to reduce its toxic effects by directing signaling to the intermediate-affinity IL-2R$\beta\gamma_c$, thereby selectively stimulating effector CD8$^+$ T cells and NK cells but not CD25$^+$ Tregs or endothelial cells. This has been achieved by reducing IL-2 interaction with CD25 through various methods, including complexing with CD122-biased mAbs, fusion to soluble CD25, selective polymer modifications, or engineering muteins with low or no CD25 binding activity. These approaches have been successful in mouse models, leading to selective expansion of effector CD8$^+$ T cells with minimal Treg cell stimulation, resulting in effective anti-tumor responses and limited toxicity.

Numerous preclinical studies have demonstrated the efficacy of CD122-biased IL-2co in multiple murine cancer models including B16F10 melanoma [94, 469, 517, 518], pancreatic cancer model [519], BCL1 leukemia [469, 518], TRAMP-C1 sarcoma [520], LM8 mouse osteosarcoma [521], and orthotopic bladder cancer [522]. However, these studies also indicate that the antitumor activity of CD122-biased IL-2co can be significantly improved in combination therapies.

In clinical settings, the antitumor effects of HD IL-2 therapy have been surpassed by more effective immune checkpoint inhibitors (ICIs), particularly those targeting the PD-1/PD-L1 pathway. While blockade of PD-1 and CTLA-4 with ICIs has shown responses in up to 60% of patients [523], there is still a need to understand the mechanisms driving resistance to these agents. Recent studies have highlighted the importance of CD8$^+$ T cell stemness in chronic viral infection and cancer [456, 524-528]. These antigen-experienced stem-like CD8$^+$ T cells express both the TCF-1 transcription factor and the checkpoint receptor PD-1 and have self-renewal capacity in response to viral or tumor antigens. The PD-1$^+$TCF-1$^+$ CD8$^+$ T cells act as a reservoir that can continually produce TCF-1$^-$ effector T cells exhibiting cytotoxic functions. The expansion and differentiation of these PD-1$^+$TCF-1$^+$ stem-like CD8$^+$ T cells into effector T cells is critical for the success of immunotherapies based on PD-1 blockade [524, 526, 529, 530]. Interestingly, PD-1 blockade alone acts on stem-like T cells to expand a population of transitory effector cells, but it eventually leads to the accumulation of Tex [456, 531]. Tex cells developed in response to chronic antigen exposure in tumors, infections, and autoimmune diseases [532, 533] tend to lose their proliferative capacity and effector functions and eventually die via apoptosis. Despite that these cells develop to prevent harmful immune responses [534] they pose significant challenges for disease therapy. Tex cells exhibit unique characteristics, notably the co-expression of multiple inhibitory receptors (e.g. PD1, CTLA-4, LAG3, TIM-3, BTLA, TIGIT) and functional impairment [535-540]. Their exhaustion stages include the early loss of IL-2 production [329], intermediate loss of TNF-α, and advanced loss of IFN-γ and granzyme B expression [541].

Interestingly, combining IL-2 with PD-1 blockade triggers an alternative differentiation pathway from stem-like cells to a distinct subset of highly proliferative and cytotoxic CD8$^+$ T cells, or "better effectors" [347, 348, 456]. This unique subset of cytotoxic T cells is

characterized by increased expression of genes encoding cytotoxic molecules (Granzyme A and B), adhesion molecules, receptors for proinflammatory cytokines and chemokines (IL-18R, IFNGR, and CCR5), transcription factors (TBET/Tbx21), interferon-response genes, NK receptors (NKG2D), and proinflammatory S100 proteins [542]. Better effectors induced by the combination of IL-2 plus PD-1 blockade in murine intratumoral and splenic CD8$^+$ T cells possess superior antitumor and antiviral cytotoxic capacity [348, 456, 459]. IL-2 binding to CD25 is essential for triggering this alternative differentiation pathway and expanding better effectors with distinct transcriptional and epigenetic profiles [348]. Collectively, these data provide a clue as to why NKTR-214, engineered to have reduced or masked ability to engage with CD25 failed in large, well-controlled clinical trials. It is noteworthy that the ability of both the IL-2/S4B6 or the scIL-2-S4B6 chimera to stimulate CD25$^+$ cells is rather limited due to their previously described characteristics.

In light of these recent findings, interest in IL-2 therapy is now shifting to methods that mildly reduce, rather than abolish, strong signaling in activated and effector CD8$^+$ T cells, i.e., by preserving IL-2 binding to CD25 but reducing interaction with CD122 [543] or γ_c [528]. Surprisingly, better immune responses occurred with a partial IL-2 agonist, H9T, which has increased binding affinity for CD122 and reduced binding to γ_c, leading to decreased STAT5 phosphorylation but not ERK [528]. H9T-expanded T cells showed markedly reduced expression of exhaustion markers (including PD-1 and TIM-3), and reduced levels of perforin, granzyme B, and IFN-γ when compared to those stimulated by native IL-2 or "super-2". In addition, H9T treatment sustained the expression of TCF-1 and promoted mitochondrial fitness, thereby facilitating the maintenance of a stem-cell-like state. The authors provided data showing that in H9T-expanded CD8$^+$ T cells, glycolysis was reduced compared with those expanded by IL-2 or "super-2", as evidenced by reduced glucose uptake, lower levels of acetate and a lower rate of basal extracellular acidification. Moreover, inhibiting glycolysis increased the expression of CD62L and TCF-1, consistent with the notion that restricting glycolysis promotes T cell stemness and T cell memory generation. The expression of a constitutively active form of STAT5 in T cells enhanced glycolysis, promoted T cell exhaustion, and suppressed T cell stemness, thus highlighting that STAT5 signaling contributes to the functional differences between IL-2 and the IL-2 variant H9T. Importantly, TCR-transgenic and CAR-modified CD8$^+$ T cells that were expanded with H9T induced robust anti-tumor activity *in vivo* in mouse models of melanoma and acute lymphoblastic leukemia [528].

The importance of IL-2/CD25 interaction for effective IL-2 antitumor activity is further highlighted by studies showing that both wild-type IL-2 and IL-2R$\beta\gamma_c$-attenuated agonists with intact CD25 binding can effectively expand tumor-specific CD8$^+$ T cells (TSTs) and exhibit better antitumor efficacy and safety than their "non-CD25" counterparts [543]. This study further shows that at least a part of TSTs from mice and human tumors co-express elevated CD25 and PD-1. Therefore, these TSTs are susceptible to stimulation by CD25-biased IL-2 agonists, especially in combination with PD-1 blockade. Moreover, CD25-biased IL-2 agonists elevate the CD8$^+$ Teff cell-to-Treg cell ratio in tumors, but not in the periphery, to promote antitumor efficacy. In multiple mouse models, CD25-biased, but not non-CD25 agonists, restore the IL-2 signature and synergize with PD-1 blockade to eradicate large established tumors. Notably, this study also shows that the antitumor efficacy of PD-1 blockade is highly dependent on the activation of PD-1$^+$CD25$^+$CD8$^+$ TILs through autocrine IL-2-CD25 signaling.

The proposed model of autocrine IL-2-CD25 signaling in mediating the antitumor activity of PD-1 blockade is that it stimulates PD-1$^+$ TST cells to secrete IL-2, which activates the autocrine IL-2-STAT5 signaling pathway via high-affinity receptors. This leads to the secretion of effector molecules, such as IFN-γ, TNF-α, and GZMB, which may kill tumor cells [543]. Another study confirms that robust IL-2-dependent antitumor immunotherapy requires targeting the high-affinity IL-2R on tumor-specific CD8$^+$ T cells [544]. Collectively, these data underscore the highly important function of CD25 in IL-2-based immunotherapy and provide rationales for evaluating CD25-biased agonists in cancer immunotherapy.

These findings raise the question of whether under PD-1 blockade these PD-1$^+$CD25$^+$CD8$^+$ TILs can be expanded with CD25-biased IL-2co, i.e., in parallel with Tregs. This approach may fail, because the CD25^{high} Tregs also utilize IL-2co, thus lower IL-2co availability for PD-1$^+$CD25$^+$CD8$^+$ TILs. Moreover, Treg cell activity can impede effector T cell expansion. However, our recent (unpublished) data show that CD25-biased IL-2co synergizes with immune checkpoint blockade in cancer immunotherapy despite robust Treg cell expansion. Proper timing is crucial, as IL-2/JES6 administered after immune checkpoint blockade, but not vice versa, leads to profound antitumor effects. Mechanistically, CD25-biased IL-2co potently and selectively stimulates the expansion of CD8$^+$ TST cells and enhances their effector functions in a CD25-dependent manner, overcoming Treg cell-mediated suppression. These findings therefore support the use of CD25-biased IL-2/JES6 in combination with ICIs for cancer immunotherapy.

Of note, in a model of chronic LCMV infection, the transcriptional profiles of CD8$^+$ T cells induced by IL-2 alone or in combination with anti-PD-1 antibody are largely similar, which suggests that the differentiation of CD8$^+$ T cells into better effectors is induced by the IL-2 signal rather than by PD-1 blockade [348]. Additionally, CD25-biased IL-2co increases the frequency of GZMB$^+$NGK2D$^+$ cells (corresponding to the better effector T cells) among splenic and tumor-infiltrating CD8$^+$ T cells, however only after immunogenic chemotherapy [545], suggesting that only antigen-stimulated CD8$^+$ T cells form better effectors. Collectively, these reports explain why high-dose treatment with unmodified IL-2 has the significant advantage of eliciting potent effector CD8$^+$ T cell responses [543], despite also causing dangerous toxicity.

Additionally, a new approach using PD1-IL2v fusion protein for IL-2 therapy shows great promise. Here, IL-2 mutein, which is not able to interact with CD25, is fused to anti-PD-1 mAb to present IL-2 to IL-Rβγ$_c$ on PD-1$^+$ T cells in *cis*. Interestingly, binding of the PD1-IL2v to PD-1 and IL-2Rβγ$_c$ on the same cell leads to an alternative differentiation of PD-1$^+$TCF-1$^+$ stem-like CD8$^+$ T cells into better effectors, rather than exhausted T cells in models of both chronic infection and cancer and provides superior therapeutic efficacy [456, 459]. By contrast, PD-1- or PD-L1-blocking mAbs alone, or their combination with clinically relevant doses of IL-2v with abolished CD25 binding, do not induce this unique subset of better effector T cells and instead lead to the accumulation of terminally differentiated exhausted T cells [456]. This implies that strong binding of IL-2 to its receptor, mediated either through the intact IL-2:CD25 interaction or through the anchoring of IL-2v to PD-1 in *cis*, is required for generating better effectors. Therefore, it once again supports the hypothesis that cancer treatment using a combination of CD122-biased IL-2co and the PD1-PD-L1 pathway blockade would likely be less effective.

These findings provide the basis for developing a new generation of PD-1-targeted IL-2 agonists that strongly activate IL-2 signaling exclusively in PD-1$^+$ T cells in *cis*, offering enhanced therapeutic potential for treating cancer and chronic infections. Through selective stimulation of PD-1$^+$ T cells, i.e. antigen-experienced T cells, this method could also potentiate the anti-tumor activity of other γ_c cytokines, notably IL-15. Indeed, impressive results have recently been reported for fusion proteins consisting of anti-PD-1 mAb and IL-15 [546, 547]. A key advantage of tethering cytokines to T cells via anti-PD-1 mAb for cancer immunotherapy is that the cytokines might be effective in very low concentrations, thereby avoiding toxicity.

It is becoming apparent that there is a fundamental functional difference between the targeted delivery of engineered IL-2 to antigen-experienced cells that are PD-1$^+$ and just engineering IL-2 with modified affinity for its receptor subunits on all cells. The former approach increases selectivity for antigen-experienced T cell populations, while the latter increases signaling potency on many cells irrespective of their antigen experience and is only regulated by the expression profile of IL-2R and general responsiveness of various lymphocytes to IL-2 signal. In addition to biological design, optimizing the dose and duration of exposure for a particular IL-2 variant may be necessary for clinical success.

Another interesting option is an engineered orthogonal (ortho) pair IL-2:IL2Rβ, where cytokine and receptor interact specifically with each other but not with their natural counterparts [548]. This approach enables selective targeting of engineered CAR T cells in *vitro* and *in vivo*, with limited off-target effects and negligible toxicity. OrthoIL-2 pairs were effective in preclinical mouse cancer models of CAR T cell therapy and may represent a synthetic approach to enhancing the antitumor efficacy of engineered cells [549, 550]. In a broader context, these data highlight the potential of combining an orthogonal cytokine approach with T cell-based immunotherapies to augment the antitumor efficacy of engineered T cells.

It seems that the above discussed results diminish the importance of CD122-biased IL-2co in cancer therapy. However, these IL-2co, which potently expand NK cells, could be applied to treat MHC I low or negative tumors where CD8$^+$ T cells are inefficient [551]. Moreover, CD122-biased IL-2co or ICs could also expand existing recently activated antigen-specific T cells to control chronic infection or malignant cells. Although the capacity of IL-2/S4B6 or other CD122-biased ICs to expand activated CD8 T cells is somewhat lower in comparison to CD25-biased IL-co or ICS after antigen encounter, i.e., at a stage when the cells are CD25^{hi}, it improves at later stages when the cells downregulate CD25 along with upregulation of CD122 [552]. Central memory populations, which express higher levels of CD122 than naïve or activated T cells, preferentially expand following IL-2/S4B6 treatment, unlike effector memory T cell populations that expand less vigorously. Recent observations have indicated that central memory T cells generally provide better antitumor and antiviral immunity, due to a much more dramatic expansion in the absolute number of cytotoxic T cells following adoptive transfer [553-555]. The timing and understanding of the responding T cell populations will be critical for the successful application of CD122-biased IL-2co therapy. We hypothesize that CD122-biased IL-2co or ICs may be beneficial for immunotherapy particularly when applied in later stages of T cell response if at least some memory-phenotype CD122^{high} CD8$^+$ T cells are formed.

A deeper understanding of the mechanisms regulating T cell exhaustion and the underlying molecular pathways can improve the current T cell-based immunotherapies in

people with cancer. Studies pointed out NFAT, XBP1, and TOX being the three main transcription factors regulating T cell exhaustion [556-560]. Recent findings suggest that the molecular mechanisms regulating the exhaustion of T cells, which were thought to be common in infection and cancer despite obvious differences in their microenvironments, actually differ. Tillé *et al.* [561] demonstrated that NFAT5, highly expressed in exhausted CD8$^+$ T cells in chronic infections and tumors, is selectively activated in the hyperosmolar tumor microenvironment, promoting T cell exhaustion. In contrast, this group showed that NFAT5 does not induce exhaustion during chronic infections. Moreover, a report by Liu *et al.* [562] demonstrated that IL-2 is critical for the generation of Tex cells in many types of tumors in mice and humans, identifying IL-2 as a novel inducer of T-cell exhaustion. Interestingly, at the early stage of tumor growth, CD8$^+$ T cells were activated by autocrine IL-2 and inhibited tumor growth. However, as tumors became larger, CD8$^+$ T cells produced less IL-2 and became exhausted by the CD4$^+$ T cell-produced IL-2. At present, it is unknown why IL-2 production is shifted from CD8$^+$ to CD4$^+$ T cells during tumor progression. Sustained intratumoral CD4$^+$ T cell production of IL-2 led to the persistent activation of STAT5 in CD8$^+$ T cells, which in turn induced strong expression of tryptophan hydroxylase 1, thus catalyzing the conversion to tryptophan to 5-hydroxytryptophan (5-HTP). 5-HTP subsequently activated AhR nuclear translocation, causing a coordinated upregulation of inhibitory receptors and downregulation of cytokine and effector-molecule expression, thereby rendering T cells dysfunctional in the tumor microenvironment. Together with the fact that IL-2R signaling also increases the mTORC1 mediated glycolysis in effector CD8$^+$ T cells rather than memory CD8$^+$ T cells [33], and that enhanced glycolysis promotes T cell exhaustion and suppresses T cell stemness [528], this pieces of evidence collectively demonstrate a double-edged role of IL-2 in regulating tumor-specific CD8$^+$ T cells. Correspondingly, another report showed that signaling via IL-2Rβ, a receptor chain shared by IL-2 and IL-15, drives the differentiation of CD8$^+$ Tex rather than memory CD8$^+$ T cells during chronic infection, further emphasizing that IL-2 determines T cell fate in a context-dependent fashion [563].

In clinical settings, the efficacy of IL-2-based therapies may depend on multiple factors, including tumor size, microenvironment, tumor mutation burden [564], presence of tertiary lymphoid structures in the tumor [565], the differentiation state of TILs [566], and timing of IL-2 administration. The actual clinical significance of IL-2-mediated effects on Tregs seems not to be as important since the specific IL-2 variants sufficiently expand tumor-specific CD8$^+$ T cells and/or restore the functionality of the exhausted tumor-specific CD8$^+$ T cell pool, particularly within the tumor microenvironment. However, an intense and more detailed investigation is necessary to clarify this important issue. Despite the paucity of clinical data, recent progress with IL-2-based therapy to augment checkpoint blockade therapeutic efficacy is impressive, and many clinical trials are underway. The toxicity of IL-2 therapy remains a challenge, but new techniques to focus IL-2 selectively on PD-1$^+$ T cells may mitigate this issue. There are many opportunities to be explored in the clinic that go beyond a combination of the novel IL-2-based molecules with immune checkpoint inhibitors, for example, combinations with other cytokines, cell therapies, and bispecific CD3 or NK cell engagers.

As described earlier, LD IL-2 therapy selectively stimulating the high-affinity IL-2R expressing Treg cells has shown promise for the treatment of autoimmune diseases in numerous clinical trials. However, the effects of LD IL-2 therapy can significantly vary depending on the

type of autoimmune disease (e.g., organ-specific versus systemic autoimmunity), the number of elicited Tregs, and the immunocompetent state of the patient. Additionally, the selectivity of LD IL-2 for Tregs compared to effector T cells may be also highly dependent on the disease or organ system involved.

An important question is how many Treg cells should be elicited by LD IL-2 treatment to avoid severe immunosuppression in patients with autoimmunity. The paradox here is that while the goal is to control excessive immunity in autoimmune patients, therapies that induce immunosuppression might increase the risk of opportunistic infections or malignancies, posing significant risks for these patients. IL-2 supports the cytotoxic function of CD8^{+} T and NK cells against infections or cancer, and LD IL-2 therapy might maintain this capacity to induce immune tolerance without severe immunosuppression, potentially outcompeting other CD25-biased IL-2 variants in treating autoimmune patients. However, new data suggests that although LD IL-2 therapy can induce competent immunity towards infections when treating autoimmunity, this balance has to be cautiously monitored as IL-2 treatment might exacerbate immunopathology mediated by strongly activated CD8^{+} T cells [381]. This evidence suggests that though rare in clinical practice, extra caution is needed when administrating LD IL-2 therapy to those susceptible to systemic or severe infection. This is particularly important during global pandemics like COVID-19, where autoimmune patients might have a higher risk of severe infection.

An increasing number of studies focus on novel IL-2-based therapies across a wide range of diseases, contributing to the rapid expansion in the field of immunotherapy. The development of new molecules aims to improve ease of administration, tolerability, and the differential induction of Tregs without activating autoreactive effector T cells. However, drawing a general conclusion about the ideal form of modified IL-2 for treating autoimmunity, graft rejection, or GvHD is currently challenging. NKTR-358 has shown promising efficacy and safety in clinical trials, as described in detail earlier. However, CD25-biased IL-2co and ICs represent a superior way of IL-2 delivery selectively to Tregs due to their exclusive mechanisms of action, translating to higher efficacy over LD IL-2 in many preclinical models.

Toxicity following IL-2 administration is at least by significant part attributed to the direct action of IL-2 on CD25^{+} endothelial cells in the lungs, brain, and liver [93, 94, 567]. Depletion of T cell subsets during HD IL-2 treatment reduces the toxicity of IL-2 therapy in the immune system of a humanized mouse model, highlighting the central role of T cells. Moreover, inflammation elicited by HD IL-2 administration may cause Treg dysfunction [568], leading to generalized T cell activation and bystander damage to the gut. Interestingly, IL-2 toxicity is also induced by selective depletion or inhibition of Treg cell functions after LD IL-2 therapy and it is ameliorated in HD IL-2-treated humanized mice receiving the PIM-1 kinase inhibitor, which preserves Treg suppressive function [568]. These findings collectively show that Treg cells play a significant role in controlling IL-2 toxicity.

Considering these findings, avoiding toxicity during IL-2 therapy may depend on preserving significant Treg function. IL-2 muteins with reduced CD25-binding activity generally have some capacity to expand Tregs in addition to effector CD8^{+} T cells. Therefore, it will be interesting to see whether variants of IL-2 with residual Treg-stimulating function show limited toxicity in clinical trials. Krieg et al. demonstrated that high doses of CD25-biased IL-2/JES6 induce toxicity despite increased Treg numbers [94], suggesting a threshold amount

of IL-2 or IL-2-activated effector cells that Tregs can control and thus limit the toxicity. Moreover, a comparison of CD122-biased and CD25-biased IL-2co at the same IL-2 dose showed that CD122-biased IL-2co dramatically boosted NK and CD8$^+$ cell numbers and induced relatively mild pulmonary edema, while CD25-biased IL-2co caused minimal expansion of these cells but induced more severe pulmonary edema and significant pulmonary changes on histological examination, along with a significant drop in hemoglobin oxygen saturation [94].

While the impacts of systemic IL-2co administration are well-defined in the spleen, lungs, and peripheral lymph nodes, the response of immune cells in the gut and gut-associated lymphoid tissues (GALT) to IL-2co is not well characterized. This is particularly important, given that one of the well-known side effects of HD IL-2 treatment in cancer patients is severe gastrointestinal symptoms [479]. Therefore, understanding how IL-2 signaling affects leukocyte populations in the gut and GALT under steady-state conditions is crucial. A recent report describes that CD122-biased IL-2co causes an acute decrease in Peyer's Patches (PP) cellularity due to selective apoptosis of multiple B-cell subsets. However, PP B cells recover within two weeks after cessation of IL-2co administration, indicating that the treatment does not permanently disrupt PP B cell homeostasis or the supporting PP architecture [569]. These results should be considered when interpreting results from mouse models using CD122-biased IL-2co or ICs.

Surprisingly, data from our laboratory show that CD122-biased IL-2co is much more toxic than CD25-biased IL-2co. The toxicity of CD122-biased IL-2co likely reflects its lower selectivity, leading to the stimulation of a broader spectrum of immune cells, namely various subsets of T and NK cells, resulting in massive effector cytokine production ("cytokine storm") [469]. We repeatedly observe that mice suffer from toxicity and die earlier from IL-2/S4B6-induced overactivation of immune cells than from IL-2/JES6-induced vascular syndrome and associated pulmonary edema. This discrepancy might result from the fact that our parameters for assessing toxicity only include weight loss, mortality, and pulmonary edema, which is probably insufficient and should be improved.

Since CD25-biased IL-2co is highly selective for Treg and activated T cells, a significant obstacle in treating autoimmune diseases is that activated pathogenic CD25$^+$ T cells may respond to the complex, ultimately enhancing disease activity. Several studies support this notion. In NOD mice, diabetes onset is preceded by circulating autoreactive T cells, some of which express CD25. A one-week treatment of pre-diabetic NOD mice with IL-2/JES6 led to a marked increase in CD25 expression on Treg cells and both CD4$^+$ and CD8$^+$ T cells. Additionally, a substantial expansion of NK cells was observed in lymph nodes, spleen, and within islet infiltrate. Unfortunately, this regimen accelerated diabetes and death in pre-diabetic mice. Conversely, treatment with IL-2/JES6 at a much lower (~ 10-times) dosage promoted Treg survival and protected mice from diabetes with minimal effects on non-Treg cells [351], suggesting that low-dose IL-2/JES6 should be used to stimulate and expand Treg cells selectively. In a mouse multiple sclerosis model, IL-2/JES6 administration after EAE onset resulted in accelerated EAE progression [352]. Similarly, in virus-induced joint inflammation models, IL-2/JES6 administration led to a massive expansion of virus-specific effector T cells, which aggravated joint pathology [570]. This suggests that active virus infection can alter the response pattern of IL-2/JES6 complexes, promoting pro-inflammatory rather than anti-

202

inflammatory T cells, further cautioning its use as a therapeutic agent. The therapeutic use of CD25-biased IL-2co and ICs in clinics will likely require combination therapy with immunosuppressive drugs such as rapamycin, which blocks IL-2-mediated stimulation of activated T cells but not Tregs [571].

Our study raised another safety concern with CD25-biased IL-2co [572]. We found that short-term pretreatment with IL-2/JES6 dramatically increases sensitivity to LPS-induced shock and mortality. IL-2/JES6 administration led to the emergence of CD25$^+$Foxp3$^-$ T cells producing IFN-γ, particularly in the liver, with higher relative counts in the CD8$^+$ T cell subset. Additionally, IL-2/JES6 expanded LPS-responsive CD11b$^+$CD14$^+$ myeloid cells and increased their CD25 expression. IFN-γ then acted on these myeloid cells further increasing their responsiveness to LPS. A fraction of liver-resident Treg cells also produced IFN-γ after IL-2/JES6 treatment, indicating that Treg cells may participate in sensitization to LPS. This aligns with a recent report showing that liver resident Treg cells display increased expression of genes associated with effector T cell phenotype (*IFNG, IL1B*) compared to splenic Foxp3$^+$ Tregs [573]. This data indicates that strong sustained CD25-biased IL-2 signal provided by IL-2/JES6 (and potentially CD25-biased ICs) can induce CD25 expression on T cells and IFN-γ production in those CD25$^+$ T cells, even without a TCR signal other than that provided by self-MHC molecules. This has significant implications for safety issues of immunotherapy through CD25-biased IL-2-based immunotherapeutics.

Yu *et al.* [574] demonstrated that although *in vitro* activated T cells express substantially higher levels of CD25, and CD122 subunits than Tregs, their IL-2-dependent pSTAT5 response requires higher IL-2 levels than Tregs. Therefore, because activated T cells are intrinsically less responsive to low doses of IL-2, other factors besides IL-2R levels probably contribute to unique Treg responsiveness to low-dose IL-2. Three conditions that selectively support the activation and function of human Tregs to limited IL-2 amounts include enhanced pSTAT5 activation, decreased negative signaling (likely mediated by PP2A), and integration of proximal IL-2R signals to amplify CD25 expression [574]. These conditions ensure that human Tregs selectively and effectively respond to low IL-2 concentrations. We can speculate that affinity mutants of JY3 IC could be an interesting option to overcome the abovementioned issues related to IL-2/JES6 therapy, but this remains to be investigated.

VI. Conclusions

Aim 1: Design and develop novel IL-2 formulations

- o **IL-2-poly(HPMA) conjugate:** The development of the IL-2-poly(HPMA) conjugate successfully addressed the limitations of native IL-2, primarily by significantly improving its pharmacokinetic properties. The conjugate exhibited a considerably prolonged half-life in circulation (~ 4 h compared to less than 10 min for free IL-2), which, together with its more biased activity towards CD122^{high} cells, enhanced its biological activity *in vivo*.

- o **Immunocytokines:**
  - **scIL-2/S4B6 IC:** The scIL-2/S4B6 IC mimicked the IL-2/S4B6 mAb immunocomplexes both structurally and functionally. The single-chain molecular design overcame the inherent limitations of IL-2co and we confirmed that the intramolecular interaction between IL-2 and the S4B6 mAb binding site was preserved.
  - **JY3 IC:** The JY3 IC maintained the unique IL-2/JES6 IL-2co mechanism of action while addressing its limitations, such as stoichiometry and potential dissociation. However, to enable CD25-mediated triggered exchange of IL-2, it was necessary to lower the affinity of JES6-1A12 mAb to IL-2 by approximately sixfold through mutations introduced into the binding site of the antibody's V_L domain.

Aim 2: Evaluate biological activity and therapeutic efficacy

- o The IL-2-poly(HPMA) conjugate exhibited reduced biological activity compared to IL-2 *in vitro*. However, it expanded recently activated and memory CD8$^+$ T, NK, NKT, $\gamma\delta$ T, and Treg cells much more potently than IL-2 *in vivo*. This conjugate also effectively potentiated T cell response to peptide-based vaccination, thereby supporting its potential as an effective immunotherapeutic agent.

- o The scIL-2/S4B6 IC showed comparable *in vitro* activity and superior *in vivo* stimulatory activity compared to IL-2/S4B6 IL-2co, promoting the expansion of activated CD8$^+$ T cells more effectively than the IL-2/S4B6.

- o The JY3 IC induced STAT5 signaling to a similar extent as IL-2/JES6 IL-2co *in vitro*. However, JY3 IC selectively stimulated Treg cell expansion *in vivo*, demonstrating superior disease control compared to the IL-2/JES6 in a murine model of colitis. This highlights its potential for treating autoimmune diseases.

Aim 3: Provide mechanistic insights

- o We found that S4B6 mAb completely blocks IL-2/CD25 interaction and increases the affinity of IL-2 for CD122, thus further increasing selective stimulatory activity for CD122^{high} cells such as memory CD8$^+$ T and NK cells. Compared to that, JES6-1A12 mAb prevents IL-2 from interacting with CD122 and CD132 while allowing CD25 to displace the mAb, selectively stimulating CD25^{high} cells like Treg and activated T cells and creating a positive feedback loop for their expansion.

Aim 4: Address safety concerns of CD25-biased IL-2co

- o Our study highlighted a significant safety concern with the IL-2/JES6 IL-2co that dramatically increased sensitivity to LPS-mediated shock and mortality. This was linked to IFN-γ production by CD25$^+$Foxp3$^-$ T cells, particularly in the liver and lungs, and increased TNF-α production in an expanded population of CD11b$^+$CD14$^+$ cells in the blood and spleen upon LPS stimulation. These findings underscore the need for a detailed investigation into the immune modulation and inflammatory responses induced by CD25-biased IL-2co and similar immunotherapeutic strategies.

This thesis achieved its aims by developing novel IL-2 formulations, demonstrating their enhanced pharmacokinetic and therapeutic profiles, and providing mechanistic insights into their biological activities. The research also addressed critical safety concerns, providing a comprehensive evaluation of these innovative IL-2-based immunotherapeutics for the treatment of cancer and autoimmune diseases. These findings significantly contribute to the field of IL-2-based immunotherapy, providing a foundation for future clinical applications and the development of safer and more effective immunotherapeutic agents.

VII. References

1. Paliard, X., et al., *Simultaneous production of IL-2, IL-4, and IFN-gamma by activated human CD4+ and CD8+ T cell clones.* J Immunol, 1988. **141**(3): p. 849-55.
2. Lagoo, A., C.K. Tseng, and S. Sell, *Interleukin 2 produced by activated B lymphocytes acts as an autocrine proliferation-inducing lymphokine.* Cytokine, 1990. **2**(4): p. 272-9.
3. Yui, M.A., L.L. Sharp, W.L. Havran, and E.V. Rothenberg, *Preferential activation of an IL-2 regulatory sequence transgene in TCR gamma delta and NKT cells: subset-specific differences in IL-2 regulation.* J Immunol, 2004. **172**(8): p. 4691-9.
4. De Sanctis, J.B., I. Blanca, and N.E. Bianco, *Secretion of cytokines by natural killer cells primed with interleukin-2 and stimulated with different lipoproteins.* Immunology, 1997. **90**(4): p. 526-33.
5. Zhou, L., et al., *Innate lymphoid cells support regulatory T cells in the intestine through interleukin-2.* Nature, 2019. **568**(7752): p. 405-409.
6. Roediger B, K.R., Tay SS, Mitchell AJ, Bolton HA, Guy TV, Tan SY, Forbes-Blom E, Tong PL, Köller Y, Shklovskaya E, Iwashima M, McCoy KD, Le Gros G and W.W. Fazekas de St Groth B, *IL-2 is a critical regulator of group 2 innate lymphoid cell function during pulmonary inflammation.* J Allergy Clin Immunol., 2015. **Dec;136**(6): p. 1653-1663.e7.
7. Granucci, F., et al., *Inducible IL-2 production by dendritic cells revealed by global gene expression analysis.* Nat Immunol, 2001. **2**(9): p. 882-8.
8. Granucci, F., I. Zanoni, S. Feau, and P. Ricciardi-Castagnoli, *Dendritic cell regulation of immune responses: a new role for interleukin 2 at the intersection of innate and adaptive immunity.* EMBO J, 2003. **22**(11): p. 2546-51.
9. Zelante, T., J. Fric, A.Y. Wong, and P. Ricciardi-Castagnoli, *Interleukin-2 production by dendritic cells and its immuno-regulatory functions.* Front Immunol, 2012. **3**: p. 161.
10. Hershko, A.Y., et al., *Mast cell interleukin-2 production contributes to suppression of chronic allergic dermatitis.* Immunity, 2011. **35**(4): p. 562-71.
11. Feau, S., et al., *Dendritic cell-derived IL-2 production is regulated by IL-15 in humans and in mice.* Blood, 2005. **105**(2): p. 697-702.
12. Ono, M., et al., *Foxp3 controls regulatory T-cell function by interacting with AML1/Runx1.* Nature, 2007. **446**(7136): p. 685-9.
13. Wu, Y., et al., *FOXP3 controls regulatory T cell function through cooperation with NFAT.* Cell, 2006. **126**(2): p. 375-87.
14. Granucci, F., et al., *Early IL-2 production by mouse dendritic cells is the result of microbial-induced priming.* J Immunol, 2003. **170**(10): p. 5075-81.
15. Boyman, O. and J. Sprent, *The role of interleukin-2 during homeostasis and activation of the immune system.* Nat Rev Immunol, 2012. **12**(3): p. 180-90.
16. Malek, T.R. and I. Castro, *Interleukin-2 receptor signaling: at the interface between tolerance and immunity.* Immunity, 2010. **33**(2): p. 153-65.
17. Pol, J.G., et al., *Effects of interleukin-2 in immunostimulation and immunosuppression.* J Exp Med, 2020. **217**(1).
18. Gorentla, B.K. and X.P. Zhong, *T cell Receptor Signal Transduction in T lymphocytes.* J Clin Cell Immunol, 2012. **2012**(Suppl 12): p. 5.
19. Serfling, E., A. Avots, and M. Neumann, *The architecture of the interleukin-2 promoter: a reflection of T lymphocyte activation.* Biochim Biophys Acta, 1995. **1263**(3): p. 181-200.
20. Jain, J., C. Loh, and A. Rao, *Transcriptional regulation of the IL-2 gene.* Curr Opin Immunol, 1995. **7**(3): p. 333-42.

21. Pei, Y., et al., *Nuclear export of NF90 to stabilize IL-2 mRNA is mediated by AKT-dependent phosphorylation at Ser647 in response to CD28 costimulation.* J Immunol, 2008. **180**(1): p. 222-9.

22. Ogilvie, R.L., et al., *Tristetraprolin down-regulates IL-2 gene expression through AU-rich element-mediated mRNA decay.* J Immunol, 2005. **174**(2): p. 953-61.

23. Yang, C., S. Huang, X. Wang, and Y. Gu, *Emerging Roles of CCCH-Type Zinc Finger Proteins in Destabilizing mRNA Encoding Inflammatory Factors and Regulating Immune Responses.* Crit Rev Eukaryot Gene Expr, 2015. **25**(1): p. 77-89.

24. Gong, D. and T.R. Malek, *Cytokine-dependent Blimp-1 expression in activated T cells inhibits IL-2 production.* J Immunol, 2007. **178**(1): p. 242-52.

25. Hwang, E.S., J.H. Hong, and L.H. Glimcher, *IL-2 production in developing Th1 cells is regulated by heterodimerization of RelA and T-bet and requires T-bet serine residue 508.* J Exp Med, 2005. **202**(9): p. 1289-300.

26. Martins, G.A., et al., *Blimp-1 directly represses Il2 and the Il2 activator Fos, attenuating T cell proliferation and survival.* J Exp Med, 2008. **205**(9): p. 1959-65.

27. Kallies, A., et al., *Transcriptional repressor Blimp-1 is essential for T cell homeostasis and self-tolerance.* Nat Immunol, 2006. **7**(5): p. 466-74.

28. Martins, G.A., et al., *Transcriptional repressor Blimp-1 regulates T cell homeostasis and function.* Nat Immunol, 2006. **7**(5): p. 457-65.

29. Shin, H., et al., *A role for the transcriptional repressor Blimp-1 in CD8(+) T cell exhaustion during chronic viral infection.* Immunity, 2009. **31**(2): p. 309-20.

30. Mosmann, T.R., et al., *Species-specificity of T cell stimulating activities of IL 2 and BSF-1 (IL 4): comparison of normal and recombinant, mouse and human IL 2 and BSF-1 (IL 4).* J Immunol, 1987. **138**(6): p. 1813-6.

31. Matesanz, F., A. Alcina, and A. Pellicer, *Existence of at least five interleukin-2 molecules in different mouse strains.* Immunogenetics, 1993. **38**(4): p. 300-3.

32. Nakamura, Y., et al., *Heterodimerization of the IL-2 receptor beta- and gamma-chain cytoplasmic domains is required for signalling.* Nature, 1994. **369**(6478): p. 330-3.

33. Zhou, P., *Emerging mechanisms and applications of low-dose IL-2 therapy in autoimmunity.* Cytokine Growth Factor Rev, 2022. **67**: p. 80-88.

34. Sugamura, K., et al., *The interleukin-2 receptor gamma chain: its role in the multiple cytokine receptor complexes and T cell development in XSCID.* Annu Rev Immunol, 1996. **14**: p. 179-205.

35. Holter, W., et al., *Expression of functional IL 2 receptors by lipopolysaccharide and interferon-gamma stimulated human monocytes.* J Immunol, 1987. **138**(9): p. 2917-22.

36. Honda, M., et al., *Identification of a soluble IL-2 receptor beta-chain from human lymphoid cell line cells.* J Immunol, 1990. **145**(12): p. 4131-5.

37. Waickman, A.T., J.Y. Park, and J.H. Park, *The common gamma-chain cytokine receptor: tricks-and-treats for T cells.* Cell Mol Life Sci, 2016. **73**(2): p. 253-69.

38. Won, H.Y., et al., *The Timing and Abundance of IL-2Rbeta (CD122) Expression Control Thymic iNKT Cell Generation and NKT1 Subset Differentiation.* Front Immunol, 2021. **12**: p. 642856.

39. Mathews, D.V., et al., *CD122 signaling in CD8+ memory T cells drives costimulation-independent rejection.* J Clin Invest, 2018. **128**(10): p. 4557-4572.

40. Reya, T., J.A. Yang-Snyder, E.V. Rothenberg, and S.R. Carding, *Regulated expression and function of CD122 (interleukin-2/interleukin-15R-beta) during lymphoid development.* Blood, 1996. **87**(1): p. 190-201.

41. Kmieciak, M., et al., *Human T cells express CD25 and Foxp3 upon activation and exhibit effector/memory phenotypes without any regulatory/suppressor function.* J Transl Med, 2009. **7**: p. 89.

42. Flynn, M.J. and J.A. Hartley, *The emerging role of anti-CD25 directed therapies as both immune modulators and targeted agents in cancer.* Br J Haematol, 2017. **179**(1): p. 20-35.

43. Waldmann, T.A., *The multi-subunit interleukin-2 receptor.* Annu Rev Biochem, 1989. **58**: p. 875-911.

44. Willerford, D.M., et al., *Interleukin-2 receptor alpha chain regulates the size and content of the peripheral lymphoid compartment.* Immunity, 1995. **3**(4): p. 521-30.

45. Almeida, A.R., N. Legrand, M. Papiernik, and A.A. Freitas, *Homeostasis of peripheral CD4+ T cells: IL-2R alpha and IL-2 shape a population of regulatory cells that controls CD4+ T cell numbers.* J Immunol, 2002. **169**(9): p. 4850-60.

46. O'Gorman, W.E., et al., *The initial phase of an immune response functions to activate regulatory T cells.* J Immunol, 2009. **183**(1): p. 332-9.

47. Crowley, M., K. Inaba, M. Witmer-Pack, and R.M. Steinman, *The cell surface of mouse dendritic cells: FACS analyses of dendritic cells from different tissues including thymus.* Cell Immunol, 1989. **118**(1): p. 108-25.

48. Freudenthal, P.S. and R.M. Steinman, *The distinct surface of human blood dendritic cells, as observed after an improved isolation method.* Proc Natl Acad Sci U S A, 1990. **87**(19): p. 7698-702.

49. Steiner, G., et al., *Interleukin 2 receptors on cultured murine epidermal Langerhans cells.* J Immunol, 1986. **137**(1): p. 155-9.

50. von Bergwelt-Baildon, M.S., et al., *CD25 and indoleamine 2,3-dioxygenase are up-regulated by prostaglandin E2 and expressed by tumor-associated dendritic cells in vivo: additional mechanisms of T-cell inhibition.* Blood, 2006. **108**(1): p. 228-37.

51. Smith, K.A., *Interleukin-2: inception, impact, and implications.* Science, 1988. **240**(4856): p. 1169-76.

52. Nelson, B.H. and D.M. Willerford, *Biology of the interleukin-2 receptor.* Adv Immunol, 1998. **70**: p. 1-81.

53. Ma, A., R. Koka, and P. Burkett, *Diverse functions of IL-2, IL-15, and IL-7 in lymphoid homeostasis.* Annu Rev Immunol, 2006. **24**: p. 657-79.

54. Bergmann, C.A., D.L. Gould, and D.R. Kaplan, *Cytometrically detected specific binding of interleukin 2 to cells.* Cytokine, 1992. **4**(3): p. 192-200.

55. Fallon, E.M., et al., *Increased endosomal sorting of ligand to recycling enhances potency of an interleukin-2 analog.* J Biol Chem, 2000. **275**(10): p. 6790-7.

56. Rao, B.M., I. Driver, D.A. Lauffenburger, and K.D. Wittrup, *Interleukin 2 (IL-2) variants engineered for increased IL-2 receptor alpha-subunit affinity exhibit increased potency arising from a cell surface ligand reservoir effect.* Mol Pharmacol, 2004. **66**(4): p. 864-9.

57. Su, E.W., et al., *IL-2Rα mediates temporal regulation of IL-2 signaling and enhances immunotherapy.* Sci Transl Med, 2015. **7**(311): p. 311ra170.

58. Obar, J.J., et al., *CD4+ T cell regulation of CD25 expression controls development of short-lived effector CD8+ T cells in primary and secondary responses.* Proc Natl Acad Sci U S A, 2010. **107**(1): p. 193-8.

59. Cousens, L.P., J.S. Orange, and C.A. Biron, *Endogenous IL-2 contributes to T cell expansion and IFN-gamma production during lymphocytic choriomeningitis virus infection.* J Immunol, 1995. **155**(12): p. 5690-9.

60. Rubin, L.A., et al., *Soluble interleukin 2 receptors are released from activated human lymphoid cells in vitro.* J Immunol, 1985. **135**(5): p. 3172-7.

61. Baran, D., M. Korner, and J. Theze, *Characterization of the soluble murine IL-2R and estimation of its affinity for IL-2.* J Immunol, 1988. **141**(2): p. 539-46.

62. Gooding, R., et al., *Increased soluble interleukin-2 receptor concentration in plasma predicts a decreased cellular response to IL-2.* Br J Cancer, 1995. **72**(2): p. 452-5.

63. Cabrera, R., et al., *Influence of serum and soluble CD25 (sCD25) on regulatory and effector T-cell function in hepatocellular carcinoma.* Scand J Immunol, 2010. **72**(4): p. 293-301.

64. Hannani, D., et al., *Anticancer immunotherapy by CTLA-4 blockade: obligatory contribution of IL-2 receptors and negative prognostic impact of soluble CD25.* Cell Res, 2015. **25**(2): p. 208-24.

65. Li, J., E. Lu, T. Yi, and J.G. Cyster, *EBI2 augments Tfh cell fate by promoting interaction with IL-2-quenching dendritic cells.* Nature, 2016. **533**(7601): p. 110-4.

66. Tokano, Y., et al., *Relation between soluble interleukin 2 receptor and clinical findings in patients with systemic lupus erythematosus.* Ann Rheum Dis, 1989. **48**(10): p. 803-9.

67. Sawada, S., et al., *Increased soluble IL-2 receptor in serum of patients with systemic lupus erythematosus.* Clin Rheumatol, 1993. **12**(2): p. 204-9.

68. Ward, M.M., M.A. Dooley, V.D. Christenson, and D.S. Pisetsky, *The relationship between soluble interleukin 2 receptor levels and antidouble stranded DNA antibody levels in patients with systemic lupus erythematosus.* J Rheumatol, 1991. **18**(2): p. 235-40.

69. ter Borg, E.J., G. Horst, P.C. Limburg, and C.G. Kallenberg, *Changes in plasma levels of interleukin-2 receptor in relation to disease exacerbations and levels of anti-dsDNA and complement in systemic lupus erythematosus.* Clin Exp Immunol, 1990. **82**(1): p. 21-6.

70. Maier, L.M., et al., *IL2RA genetic heterogeneity in multiple sclerosis and type 1 diabetes susceptibility and soluble interleukin-2 receptor production.* PLoS Genet, 2009. **5**(1): p. e1000322.

71. Maier, L.M., et al., *Soluble IL-2RA levels in multiple sclerosis subjects and the effect of soluble IL-2RA on immune responses.* J Immunol, 2009. **182**(3): p. 1541-7.

72. Bien, E. and A. Balcerska, *Serum soluble interleukin 2 receptor alpha in human cancer of adults and children: a review.* Biomarkers, 2008. **13**(1): p. 1-26.

73. Russell, S.E., A.C. Moore, P.G. Fallon, and P.T. Walsh, *Soluble IL-2Rα (sCD25) exacerbates autoimmunity and enhances the development of Th17 responses in mice.* PLoS One, 2012. 7(10): p. e47748.

74. Boyman, O., et al., *Selective stimulation of T cell subsets with antibody-cytokine immune complexes.* Science, 2006. **311**(5769): p. 1924-7.

75. Cantrell, D.A. and K.A. Smith, *Transient expression of interleukin 2 receptors. Consequences for T cell growth.* J Exp Med, 1983. **158**(6): p. 1895-911.

76. Gullberg, M. and K.A. Smith, *Regulation of T cell autocrine growth. T4+ cells become refractory to interleukin 2.* J Exp Med, 1986. **163**(2): p. 270-84.

77. Sakaguchi, S., et al., *Immunologic self-tolerance maintained by activated T cells expressing IL-2 receptor alpha-chains (CD25). Breakdown of a single mechanism of self-tolerance causes various autoimmune diseases.* J Immunol, 1995. **155**(3): p. 1151-64.

78. Roediger, B., et al., *Cutaneous immunosurveillance and regulation of inflammation by group 2 innate lymphoid cells.* Nat Immunol, 2013. **14**(6): p. 564-73.

79. Overwijk, W.W., M.A. Tagliaferri, and J. Zalevsky, *Engineering IL-2 to Give New Life to T Cell Immunotherapy.* Annu Rev Med, 2021. **72**: p. 281-311.

80. Bosco, M.C., et al., *IL-2 signaling in human monocytes involves the phosphorylation and activation of p59hck.* J Immunol, 2000. **164**(9): p. 4575-85.

81. Herr, F., et al., *IL-2 phosphorylates STAT5 to drive IFN-gamma production and activation of human dendritic cells.* J Immunol, 2014. **192**(12): p. 5660-70.

82. Kitashima, D.Y., et al., *Langerhans Cells Prevent Autoimmunity via Expansion of Keratinocyte Antigen-Specific Regulatory T Cells.* EBioMedicine, 2018. **27**: p. 293-303.

83. Eicher, D.M. and T.A. Waldmann, *IL-2R alpha on one cell can present IL-2 to IL-2R beta/gamma(c) on another cell to augment IL-2 signaling.* J Immunol, 1998. **161**(10): p. 5430-7.

84. Fukao, T. and S. Koyasu, *Expression of functional IL-2 receptors on mature splenic dendritic cells.* Eur J Immunol, 2000. **30**(5): p. 1453-7.

85. Wuest, S.C., et al., *A role for interleukin-2 trans-presentation in dendritic cell-mediated T cell activation in humans, as revealed by daclizumab therapy.* Nat Med, 2011. **17**(5): p. 604-9.

86. Sabatos, C.A., et al., *A synaptic basis for paracrine interleukin-2 signaling during homotypic T cell interaction.* Immunity, 2008. **29**(2): p. 238-48.

87. Huse, M., et al., *T cells use two directionally distinct pathways for cytokine secretion.* Nat Immunol, 2006. **7**(3): p. 247-55.

88. Kulhankova, K., T. Rouse, M.E. Nasr, and E.H. Field, *Dendritic cells control CD4+CD25+ Treg cell suppressor function in vitro through juxtacrine delivery of IL-2.* PLoS One, 2012. **7**(9): p. e43609.

89. Cohan, S.L., E.B. Lucassen, M.C. Romba, and S.N. Linch, *Daclizumab: Mechanisms of Action, Therapeutic Efficacy, Adverse Events and Its Uncovering the Potential Role of Innate Immune System Recruitment as a Treatment Strategy for Relapsing Multiple Sclerosis.* Biomedicines, 2019. **7**(1).

90. Reinecker, H.C. and D.K. Podolsky, *Human intestinal epithelial cells express functional cytokine receptors sharing the common gamma c chain of the interleukin 2 receptor.* Proc Natl Acad Sci U S A, 1995. **92**(18): p. 8353-7.

91. Ciacci, C., et al., *Functional interleukin-2 receptors on intestinal epithelial cells.* J Clin Invest, 1993. **92**(1): p. 527-32.

92. Corrigall, V.M., et al., *Functional IL-2 receptor beta (CD122) and gamma (CD132) chains are expressed by fibroblast-like synoviocytes: activation by IL-2 stimulates monocyte chemoattractant protein-1 production.* J Immunol, 2001. **166**(6): p. 4141-7.

93. Wylezinski, L.S. and J. Hawiger, *Interleukin 2 Activates Brain Microvascular Endothelial Cells Resulting in Destabilization of Adherens Junctions.* J Biol Chem, 2016. **291**(44): p. 22913-22923.

94. Krieg, C., S. Letourneau, G. Pantaleo, and O. Boyman, *Improved IL-2 immunotherapy by selective stimulation of IL-2 receptors on lymphocytes and endothelial cells.* Proc Natl Acad Sci U S A, 2010. **107**(26): p. 11906-11.

95. Arumugam, P., et al., *Expression of a Functional IL-2 Receptor in Vascular Smooth Muscle Cells.* J Immunol, 2019. **202**(3): p. 694-703.

96. Gerritsma, J.S., et al., *Expression of the IL-2 receptor on human renal proximal tubular epithelial cells.* J Am Soc Nephrol, 1997. **8**(10): p. 1510-6.

97. Gruss, H.J., et al., *Human fibroblasts express functional IL-2 receptors formed by the IL-2R alpha- and beta-chain subunits: association of IL-2 binding with secretion of the monocyte chemoattractant protein-1.* J Immunol, 1996. **157**(2): p. 851-7.

98. Ozawa, A., et al., *Expression of IL-2 receptor beta and gamma chains by human gingival fibroblasts and up-regulation of adhesion to neutrophils in response to IL-2.* J Leukoc Biol, 2003. **74**(3): p. 352-9.

99. Valle-Mendiola, A., et al., *Pleiotropic Effects of IL-2 on Cancer: Its Role in Cervical Cancer.* Mediators Inflamm, 2016. **2016**: p. 2849523.

100. Cho, J.H., H.O. Kim, C.D. Surh, and J. Sprent, *T cell receptor-dependent regulation of lipid rafts controls naive CD8+ T cell homeostasis.* Immunity, 2010. **32**(2): p. 214-26.

101. Vámosi, G., et al., *IL-2 and IL-15 receptor alpha-subunits are coexpressed in a supramolecular receptor cluster in lipid rafts of T cells.* Proc Natl Acad Sci U S A, 2004. **101**(30): p. 11082-7.

102. Wang, X., M. Rickert, and K.C. Garcia, *Structure of the quaternary complex of interleukin-2 with its alpha, beta, and gammac receptors.* Science, 2005. **310**(5751): p. 1159-63.

103. Stauber, D.J., et al., *Crystal structure of the IL-2 signaling complex: paradigm for a heterotrimeric cytokine receptor.* Proc Natl Acad Sci U S A, 2006. **103**(8): p. 2788-93.

104. Yu, A., F. Olosz, C.Y. Choi, and T.R. Malek, *Efficient internalization of IL-2 depends on the distal portion of the cytoplasmic tail of the IL-2R common gamma-chain and a lymphoid cell environment.* J Immunol, 2000. **165**(5): p. 2556-62.

105. Duprez, V., M. Ferrer, and A. Dautry-Varsat, *High-affinity interleukin 2 receptor alpha and beta chains are internalized and remain associated inside the cells after interleukin 2 endocytosis.* J Biol Chem, 1992. **267**(26): p. 18639-43.

106. Lowenthal, J.W., H.R. MacDonald, and B.J. Iacopetta, *Intracellular pathway of interleukin 2 following receptor-mediated endocytosis.* Eur J Immunol, 1986. **16**(11): p. 1461-3.

107. Weissman, A.M., et al., *Only high-affinity receptors for interleukin 2 mediate internalization of ligand.* Proc Natl Acad Sci U S A, 1986. **83**(5): p. 1463-6.

108. Hémar, A., et al., *Endocytosis of interleukin 2 receptors in human T lymphocytes: distinct intracellular localization and fate of the receptor alpha, beta, and gamma chains.* J Cell Biol, 1995. **129**(1): p. 55-64.

109. Malek, T.R., *The biology of interleukin-2.* Annu Rev Immunol, 2008. **26**: p. 453-79.

110. Abbas, A.K., et al., *Revisiting IL-2: Biology and therapeutic prospects.* Sci Immunol, 2018. **3**(25).

111. Nelson, B.H., J.D. Lord, and P.D. Greenberg, *Cytoplasmic domains of the interleukin-2 receptor beta and gamma chains mediate the signal for T-cell proliferation.* Nature, 1994. **369**(6478): p. 333-6.

112. Miyazaki, T., et al., *Functional activation of Jak1 and Jak3 by selective association with IL-2 receptor subunits.* Science, 1994. **266**(5187): p. 1045-7.

113. Liu, K.D., S.L. Gaffen, M.A. Goldsmith, and W.C. Greene, *Janus kinases in interleukin-2-mediated signaling: JAK1 and JAK3 are differentially regulated by tyrosine phosphorylation.* Curr Biol, 1997. **7**(11): p. 817-26.

114. Witthuhn, B.A., M.D. Williams, H. Kerawalla, and F.M. Uckun, *Differential substrate recognition capabilities of Janus family protein tyrosine kinases within the interleukin 2 receptor (IL2R) system: Jak3 as a potential molecular target for treatment of leukemias with a hyperactive Jak-Stat signaling machinery.* Leuk Lymphoma, 1999. **32**(3-4): p. 289-97.

115. Kirken, R.A., et al., *Activation of JAK3, but not JAK1, is critical for IL-2-induced proliferation and STAT5 recruitment by a COOH-terminal region of the IL-2 receptor beta-chain.* Cytokine, 1995. **7**(7): p. 689-700.

116. Thèze, J., P.M. Alzari, and J. Bertoglio, *Interleukin 2 and its receptors: recent advances and new immunological functions.* Immunol Today, 1996. **17**(10): p. 481-6.

117. Kovanen, P.E. and W.J. Leonard, *Cytokines and immunodeficiency diseases: critical roles of the gamma(c)-dependent cytokines interleukins 2, 4, 7, 9, 15, and 21, and their signaling pathways.* Immunol Rev, 2004. **202**: p. 67-83.

118. Waldmann, T.A., *The shared and contrasting roles of IL2 and IL15 in the life and death of normal and neoplastic lymphocytes: implications for cancer therapy.* Cancer Immunol Res, 2015. **3**(3): p. 219-27.

119. Boyman, O., J.F. Purton, C.D. Surh, and J. Sprent, *Cytokines and T-cell homeostasis.* Curr Opin Immunol, 2007. **19**(3): p. 320-6.

120. Liao, W., J.-X. Lin, and W.J. Leonard, *Interleukin-2 at the Crossroads of Effector Responses, Tolerance, and Immunotherapy.* Immunity, 2013. **38**(1): p. 13-25.

121. Cheng, G., A. Yu, and T.R. Malek, *T-cell tolerance and the multi-functional role of IL-2R signaling in T-regulatory cells.* Immunol Rev, 2011. **241**(1): p. 63-76.

122. Walsh, P.T., et al., *PTEN inhibits IL-2 receptor-mediated expansion of CD4+ CD25+ Tregs.* J Clin Invest, 2006. **116**(9): p. 2521-31.

123. Bensinger, S.J., et al., *Distinct IL-2 receptor signaling pattern in CD4+CD25+ regulatory T cells.* J Immunol, 2004. **172**(9): p. 5287-96.

124. Kovanen, P.E., et al., *Global analysis of IL-2 target genes: identification of chromosomal clusters of expressed genes.* Int Immunol, 2005. **17**(8): p. 1009-21.

125. Grange, M., et al., *Active STAT5 regulates T-bet and eomesodermin expression in CD8 T cells and imprints a T-bet-dependent Tc1 program with repressed IL-6/TGF-beta1 signaling.* J Immunol, 2013. **191**(7): p. 3712-24.

126. Knosp, C.A., et al., *Regulation of Foxp3+ inducible regulatory T cell stability by SOCS2.* J Immunol, 2013. **190**(7): p. 3235-45.

127. Kanai, T., et al., *Identification of STAT5A and STAT5B target genes in human T cells.* PLoS One, 2014. **9**(1): p. e86790.

128. Ross, S.H. and D.A. Cantrell, *Signaling and Function of Interleukin-2 in T Lymphocytes.* Annu Rev Immunol, 2018. **36**: p. 411-433.

129. Kim, H.P., J. Kelly, and W.J. Leonard, *The basis for IL-2-induced IL-2 receptor alpha chain gene regulation: importance of two widely separated IL-2 response elements.* Immunity, 2001. **15**(1): p. 159-72.

130. Bodnár, A., et al., *A biophysical approach to IL-2 and IL-15 receptor function: localization, conformation and interactions.* Immunol Lett, 2008. **116**(2): p. 117-25.

131. Mishra, A., L. Sullivan, and M.A. Caligiuri, *Molecular pathways: interleukin-15 signaling in health and in cancer.* Clin Cancer Res, 2014. **20**(8): p. 2044-50.

132. Grabstein, K.H., et al., *Cloning of a T cell growth factor that interacts with the beta chain of the interleukin-2 receptor.* Science, 1994. **264**(5161): p. 965-8.

133. Waldmann, T.A. and Y. Tagaya, *The multifaceted regulation of interleukin-15 expression and the role of this cytokine in NK cell differentiation and host response to intracellular pathogens.* Annu Rev Immunol, 1999. **17**: p. 19-49.

134. Armitage, R.J., et al., *IL-15 has stimulatory activity for the induction of B cell proliferation and differentiation.* J Immunol, 1995. **154**(2): p. 483-90.

135. Giri, J.G., et al., *IL-15, a novel T cell growth factor that shares activities and receptor components with IL-2.* J Leukoc Biol, 1995. **57**(5): p. 763-6.

136. Tagaya, Y., R.N. Bamford, A.P. DeFilippis, and T.A. Waldmann, *IL-15: a pleiotropic cytokine with diverse receptor/signaling pathways whose expression is controlled at multiple levels.* Immunity, 1996. **4**(4): p. 329-36.

137. Ring, A.M., et al., *Mechanistic and structural insight into the functional dichotomy between IL-2 and IL-15.* Nat Immunol, 2012. **13**(12): p. 1187-95.

138. Morgan, D.A., F.W. Ruscetti, and R. Gallo, *Selective in vitro growth of T lymphocytes from normal human bone marrows.* Science, 1976. **193**(4257): p. 1007-8.

139. Refaeli, Y., et al., *Biochemical mechanisms of IL-2-regulated Fas-mediated T cell apoptosis.* Immunity, 1998. **8**(5): p. 615-23.

140. Boyman, O., J.H. Cho, and J. Sprent, *The role of interleukin-2 in memory CD8 cell differentiation.* Adv Exp Med Biol, 2010. **684**: p. 28-41.

141. Kalia, V., et al., *Prolonged interleukin-2Ralpha expression on virus-specific CD8+ T cells favors terminal-effector differentiation in vivo.* Immunity, 2010. **32**(1): p. 91-103.

142. Feau, S., R. Arens, S. Togher, and S.P. Schoenberger, *Autocrine IL-2 is required for secondary population expansion of CD8(+) memory T cells.* Nat Immunol, 2011. **12**(9): p. 908-13.

143. Chin, S.S., et al., *T cell receptor and IL-2 signaling strength control memory CD8(+) T cell functional fitness via chromatin remodeling.* Nat Commun, 2022. **13**(1): p. 2240.

144. Pipkin, M.E., et al., *Interleukin-2 and inflammation induce distinct transcriptional programs that promote the differentiation of effector cytolytic T cells.* Immunity, 2010. **32**(1): p. 79-90.

145. Araki, K., et al., *mTOR regulates memory CD8 T-cell differentiation.* Nature, 2009. **460**(7251): p. 108-12.

146. Mitchell, D.M., E.V. Ravkov, and M.A. Williams, *Distinct roles for IL-2 and IL-15 in the differentiation and survival of CD8+ effector and memory T cells.* J Immunol, 2010. **184**(12): p. 6719-30.

147. Rutishauser, R.L., et al., *Transcriptional repressor Blimp-1 promotes CD8(+) T cell terminal differentiation and represses the acquisition of central memory T cell properties.* Immunity, 2009. **31**(2): p. 296-308.

148. Kursar, M., et al., *Regulatory CD4+CD25+ T cells restrict memory CD8+ T cell responses.* J Exp Med, 2002. **196**(12): p. 1585-92.

149. Murakami, M., et al., *CD25+CD4+ T cells contribute to the control of memory CD8+ T cells.* Proc Natl Acad Sci U S A, 2002. **99**(13): p. 8832-7.

150. Chinen, T., et al., *An essential role for the IL-2 receptor in T(reg) cell function.* Nat Immunol, 2016. **17**(11): p. 1322-1333.

151. Constant, S., et al., *Extent of T cell receptor ligation can determine the functional differentiation of naive CD4+ T cells.* J Exp Med, 1995. **182**(5): p. 1591-6.

152. Fazilleau, N., L.J. McHeyzer-Williams, H. Rosen, and M.G. McHeyzer-Williams, *The function of follicular helper T cells is regulated by the strength of T cell antigen receptor binding.* Nat Immunol, 2009. **10**(4): p. 375-84.

153. Tubo, N.J., et al., *Single naive CD4+ T cells from a diverse repertoire produce different effector cell types during infection.* Cell, 2013. **153**(4): p. 785-96.

154. Snook, J.P., C. Kim, and M.A. Williams, *TCR signal strength controls the differentiation of CD4(+) effector and memory T cells.* Sci Immunol, 2018. **3**(25).

155. DiToro, D., et al., *Differential IL-2 expression defines developmental fates of follicular versus nonfollicular helper T cells.* Science, 2018. **361**(6407).

156. Liao, W., et al., *Modulation of cytokine receptors by IL-2 broadly regulates differentiation into helper T cell lineages.* Nat Immunol, 2011. **12**(6): p. 551-9.

157. Oestreich, K.J., et al., *Bcl-6 directly represses the gene program of the glycolysis pathway.* Nat Immunol, 2014. **15**(10): p. 957-64.

158. Ray, J.P., et al., *The Interleukin-2-mTORc1 Kinase Axis Defines the Signaling, Differentiation, and Metabolism of T Helper 1 and Follicular B Helper T Cells.* Immunity, 2015. **43**(4): p. 690-702.

159. Zhu, J., H. Yamane, and W.E. Paul, *Differentiation of effector CD4 T cell populations (*).* Annu Rev Immunol, 2010. **28**: p. 445-89.

160. Zhu, J., J. Cote-Sierra, L. Guo, and W.E. Paul, *Stat5 activation plays a critical role in Th2 differentiation.* Immunity, 2003. **19**(5): p. 739-48.

161. Liao, W., et al., *Priming for T helper type 2 differentiation by interleukin 2-mediated induction of interleukin 4 receptor alpha-chain expression.* Nat Immunol, 2008. **9**(11): p. 1288-96.

162. Cote-Sierra, J., et al., *Interleukin 2 plays a central role in Th2 differentiation.* Proc Natl Acad Sci U S A, 2004. **101**(11): p. 3880-5.

163. Hondowicz, B.D., et al., *Interleukin-2-Dependent Allergen-Specific Tissue-Resident Memory Cells Drive Asthma.* Immunity, 2016. **44**(1): p. 155-166.

164. Papillion, A., et al., *Inhibition of IL-2 responsiveness by IL-6 is required for the generation of GC-T(FH) cells.* Sci Immunol, 2019. **4**(39).

165. Zhou, P., K. Liang, and D. Yu, *Germinal center T(FH) cells: T(w)o be or not t(w)o be, IL-6 is the answer.* Sci Immunol, 2019. **4**(39).

166. Fontenot, J.D., J.P. Rasmussen, M.A. Gavin, and A.Y. Rudensky, *A function for interleukin 2 in Foxp3-expressing regulatory T cells.* Nat Immunol, 2005. **6**(11): p. 1142-51.

167. Goldstein, J.D., et al., *Role of cytokines in thymus- versus peripherally derived-regulatory T cell differentiation and function.* Front Immunol, 2013. **4**: p. 155.

168. Hemmers, S., et al., *IL-2 production by self-reactive CD4 thymocytes scales regulatory T cell generation in the thymus.* J Exp Med, 2019. **216**(11): p. 2466-2478.

169. Furtado, G.C., M.A. Curotto de Lafaille, N. Kutchukhidze, and J.J. Lafaille, *Interleukin 2 signaling is required for CD4(+) regulatory T cell function.* J Exp Med, 2002. **196**(6): p. 851-7.

170. Yao, Z., et al., *Nonredundant roles for Stat5a/b in directly regulating Foxp3.* Blood, 2007. **109**(10): p. 4368-75.

171. Malek, T.R. and A.L. Bayer, *Tolerance, not immunity, crucially depends on IL-2.* Nat Rev Immunol, 2004. **4**(9): p. 665-74.

172. Yu, A., L. Zhu, N.H. Altman, and T.R. Malek, *A low interleukin-2 receptor signaling threshold supports the development and homeostasis of T regulatory cells.* Immunity, 2009. **30**(2): p. 204-17.

173. Barron, L., et al., *Cutting edge: mechanisms of IL-2-dependent maintenance of functional regulatory T cells.* J Immunol, 2010. **185**(11): p. 6426-30.

174. Izcue, A., J.L. Coombes, and F. Powrie, *Regulatory lymphocytes and intestinal inflammation.* Annu Rev Immunol, 2009. **27**: p. 313-38.

175. Schallenberg, S., P.Y. Tsai, J. Riewaldt, and K. Kretschmer, *Identification of an immediate Foxp3(-) precursor to Foxp3(+) regulatory T cells in peripheral lymphoid organs of nonmanipulated mice.* J Exp Med, 2010. **207**(7): p. 1393-407.

176. Chen, Q., et al., *IL-2 controls the stability of Foxp3 expression in TGF-beta-induced Foxp3+ T cells in vivo.* J Immunol, 2011. **186**(11): p. 6329-37.

177. Mencarelli, A., et al., *Calcineurin-mediated IL-2 production by CD11c(high)MHCII(+) myeloid cells is crucial for intestinal immune homeostasis.* Nat Commun, 2018. **9**(1): p. 1102.

178. Schnell, A., D.R. Littman, and V.K. Kuchroo, *T(H)17 cell heterogeneity and its role in tissue inflammation.* Nat Immunol, 2023. **24**(1): p. 19-29.

179. Littman, D.R. and A.Y. Rudensky, *Th17 and regulatory T cells in mediating and restraining inflammation.* Cell, 2010. **140**(6): p. 845-58.

180. Pandiyan, P., et al., *CD4(+)CD25(+)Foxp3(+) regulatory T cells promote Th17 cells in vitro and enhance host resistance in mouse Candida albicans Th17 cell infection model.* Immunity, 2011. **34**(3): p. 422-34.

181. Chen, Y., et al., *Foxp3(+) regulatory T cells promote T helper 17 cell development in vivo through regulation of interleukin-2.* Immunity, 2011. **34**(3): p. 409-21.

182. Wang, K.S., J. Ritz, and D.A. Frank, *IL-2 induces STAT4 activation in primary NK cells and NK cell lines, but not in T cells.* J Immunol, 1999. **162**(1): p. 299-304.

183. Bonnema, J.D., et al., *Cytokine-enhanced NK cell-mediated cytotoxicity. Positive modulatory effects of IL-2 and IL-12 on stimulus-dependent granule exocytosis.* J Immunol, 1994. **152**(5): p. 2098-104.

184. Wang, K.S., D.A. Frank, and J. Ritz, *Interleukin-2 enhances the response of natural killer cells to interleukin-12 through up-regulation of the interleukin-12 receptor and STAT4.* Blood, 2000. **95**(10): p. 3183-90.

185. Naranjo-Gomez, M., et al., *Expression and function of the IL-2 receptor in activated human plasmacytoid dendritic cells.* Eur J Immunol, 2007. **37**(7): p. 1764-72.

186. Raeber, M.E., et al., *Interleukin-2 signals converge in a lymphoid-dendritic cell pathway that promotes anticancer immunity.* Sci Transl Med, 2020. **12**(561).

187. Mingari, M.C., et al., *Human interleukin-2 promotes proliferation of activated B cells via surface receptors similar to those of activated T cells.* Nature, 1984. **312**(5995): p. 641-3.

188. Hipp, N., et al., *IL-2 imprints human naive B cell fate towards plasma cell through ERK/ELK1-mediated BACH2 repression.* Nat Commun, 2017. **8**(1): p. 1443.

189. Schultz, M., et al., *Disrupted B-lymphocyte development and survival in interleukin-2-deficient mice.* Immunology, 2001. **104**(2): p. 127-34.

190. Miller, J.D., et al., *Interleukin-2 is present in human blood vessels and released in biologically active form by heparanase.* Immunol. Cell Biol., 2012. **90**: p. 159–167.

191. Raeber, M.E., D. Sahin, and O. Boyman, *Interleukin-2-based therapies in cancer.* Sci Transl Med, 2022. **14**(670): p. eabo5409.

192. Rosenberg, S.A., et al., *Observations on the systemic administration of autologous lymphokine-activated killer cells and recombinant interleukin-2 to patients with metastatic cancer.* N Engl J Med, 1985. **313**(23): p. 1485-92.

193. Bright, R., B.J. Coventry, N. Eardley-Harris, and N. Briggs, *Clinical Response Rates From Interleukin-2 Therapy for Metastatic Melanoma Over 30 Years' Experience: A Meta-Analysis of 3312 Patients.* J Immunother, 2017. **40**(1): p. 21-30.

194. Rosenberg, S.A., J.C. Yang, D.E. White, and S.M. Steinberg, *Durability of complete responses in patients with metastatic cancer treated with high-dose interleukin-2: identification of the antigens mediating response.* Ann Surg, 1998. **228**(3): p. 307-19.

195. Fisher, R.I., S.A. Rosenberg, and G. Fyfe, *Long-term survival update for high-dose recombinant interleukin-2 in patients with renal cell carcinoma.* Cancer J Sci Am, 2000. **6 Suppl 1**: p. S55-7.

196. Atkins, M.B., L. Kunkel, M. Sznol, and S.A. Rosenberg, *High-dose recombinant interleukin-2 therapy in patients with metastatic melanoma: long-term survival update.* Cancer J Sci Am, 2000. **6 Suppl 1**: p. S11-4.

197. Portillas, R., et al., *High-Dose Interleukin-2: Evaluation of a Standardized Order Set for Biotherapy in an Intensive Care Unit.* Clin J Oncol Nurs, 2017. **21**(2): p. E49-e53.

198. Rosenberg, S.A., *IL-2: the first effective immunotherapy for human cancer.* J Immunol, 2014. **192**(12): p. 5451-8.

199. Hernandez, R., J. Poder, K.M. LaPorte, and T.R. Malek, *Engineering IL-2 for immunotherapy of autoimmunity and cancer.* Nat Rev Immunol, 2022. **22**(10): p. 614-628.

200. Rosenberg, S.A., et al., *Treatment of 283 consecutive patients with metastatic melanoma or renal cell cancer using high-dose bolus interleukin 2.* Jama, 1994. **271**(12): p. 907-13.

201. Yang, J.C., et al., *Randomized study of high-dose and low-dose interleukin-2 in patients with metastatic renal cancer.* J Clin Oncol, 2003. **21**(16): p. 3127-32.

202. Weber, J.S., et al., *The use of interleukin-2 and lymphokine-activated killer cells for the treatment of patients with non-Hodgkin's lymphoma.* J Clin Oncol, 1992. **10**(1): p. 33-40.

203. Konrad, M.W., et al., *Pharmacokinetics of recombinant interleukin 2 in humans.* Cancer Res, 1990. **50**(7): p. 2009-17.

204. Donohue, J.H. and S.A. Rosenberg, *The fate of interleukin-2 after in vivo administration.* J Immunol, 1983. **130**(5): p. 2203-8.

205. Dutcher, J.P., et al., *High dose interleukin-2 (Aldesleukin) - expert consensus on best management practices-2014.* J Immunother Cancer, 2014. **2**(1): p. 26.

206. Lotze, M.T., et al., *Lysis of fresh and cultured autologous tumor by human lymphocytes cultured in T-cell growth factor.* Cancer Res, 1981. **41**(11 Pt 1): p. 4420-5.

207. Rosenstein, M., S.E. Ettinghausen, and S.A. Rosenberg, *Extravasation of intravascular fluid mediated by the systemic administration of recombinant interleukin 2.* J Immunol, 1986. **137**(5): p. 1735-42.

208. Kammula, U.S., D.E. White, and S.A. Rosenberg, *Trends in the safety of high dose bolus interleukin-2 administration in patients with metastatic cancer.* Cancer, 1998. **83**(4): p. 797-805.

209. Dutcher, J., et al., *Kidney cancer: the Cytokine Working Group experience (1986-2001): part II. Management of IL-2 toxicity and studies with other cytokines.* Med Oncol, 2001. **18**(3): p. 209-19.

210. Schwartzentruber, D.J., *Guidelines for the safe administration of high-dose interleukin-2.* J Immunother, 2001. **24**(4): p. 287-93.

211. Panelli, M.C., et al., *Forecasting the cytokine storm following systemic interleukin (IL)-2 administration.* J Transl Med, 2004. **2**(1): p. 17.

212. Saxon, R.R., et al., *Pathogenesis of pulmonary edema during interleukin-2 therapy: correlation of chest radiographic and clinical findings in 54 patients.* AJR Am J Roentgenol, 1991. **156**(2): p. 281-5.

213. McKinstry, K.K., et al., *Memory CD4 T cell-derived IL-2 synergizes with viral infection to exacerbate lung inflammation.* PLoS Pathog, 2019. **15**(8): p. e1007989.

214. Baluna, R. and E.S. Vitetta, *Vascular leak syndrome: a side effect of immunotherapy.* Immunopharmacology, 1997. **37**(2-3): p. 117-32.

215. Nishikawa, H. and S. Sakaguchi, *Regulatory T cells in cancer immunotherapy.* Curr Opin Immunol, 2014. **27**: p. 1-7.

216. Shevach, E.M. and A.M. Thornton, *tTregs, pTregs, and iTregs: similarities and differences.* Immunol Rev, 2014. **259**(1): p. 88-102.

217. Yuan, X., G. Cheng, and T.R. Malek, *The importance of regulatory T-cell heterogeneity in maintaining self-tolerance.* Immunol Rev, 2014. **259**(1): p. 103-14.

218. Zhang, H., et al., *Lymphopenia and interleukin-2 therapy alter homeostasis of CD4+CD25+ regulatory T cells.* Nat Med, 2005. **11**(11): p. 1238-43.

219. Abès, R., E. Gélizé, W.H. Fridman, and J.L. Teillaud, *Long-lasting antitumor protection by anti-CD20 antibody through cellular immune response.* Blood, 2010. **116**(6): p. 926-34.

220. Yao, Z., et al., *Effect of albumin fusion on the biodistribution of interleukin-2.* Cancer Immunol Immunother, 2004. **53**(5): p. 404-10.

221. Clark, J.W., et al., *Interleukin 2 and lymphokine-activated killer cell therapy: analysis of a bolus interleukin 2 and a continuous infusion interleukin 2 regimen.* Cancer Research, 1990. **50**(22): p. 7343-50.

222. Weiss, G.R., et al., *A randomized phase II trial of continuous infusion interleukin-2 or bolus injection interleukin-2 plus lymphokine-activated killer cells for advanced renal cell carcinoma.* Journal of Clinical Oncology, 1992. **10**(2): p. 275-281.

223. Cascinelli, N., et al., *A phase II study of the administration of recombinant interleukin 2 (rIL-2) plus lymphokine activated killer (LAK) cells in stage IV melanoma patients.* Tumori, 1989. **75**(3): p. 233-44.

224. Grimm, E.A., A. Mazumder, H.Z. Zhang, and S.A. Rosenberg, *Lymphokine-activated killer cell phenomenon. Lysis of natural killer-resistant fresh solid tumor cells by*

interleukin 2-activated autologous human peripheral blood lymphocytes. J Exp Med, 1982. **155**(6): p. 1823-41.

225. Rosenberg, S.A., et al., *Experience with the use of high-dose interleukin-2 in the treatment of 652 cancer patients.* Ann Surg, 1989. **210**(4): p. 474-84; discussion 484-5.

226. Rosenberg, S.A., et al., *Prospective randomized trial of high-dose interleukin-2 alone or in conjunction with lymphokine-activated killer cells for the treatment of patients with advanced cancer.* J Natl Cancer Inst, 1993. **85**(8): p. 622-32.

227. Rosenberg, S.A., *Cell transfer immunotherapy for metastatic solid cancer--what clinicians need to know.* Nat Rev Clin Oncol, 2011. **8**(10): p. 577-85.

228. Muul, L.M., P.J. Spiess, E.P. Director, and S.A. Rosenberg, *Identification of specific cytolytic immune responses against autologous tumor in humans bearing malignant melanoma.* J Immunol, 1987. **138**(3): p. 989-95.

229. Rosenberg, S.A., P. Spiess, and R. Lafreniere, *A new approach to the adoptive immunotherapy of cancer with tumor-infiltrating lymphocytes.* Science, 1986. **233**(4770): p. 1318-21.

230. Topalian, S.L., L.M. Muul, D. Solomon, and S.A. Rosenberg, *Expansion of human tumor infiltrating lymphocytes for use in immunotherapy trials.* J Immunol Methods, 1987. **102**(1): p. 127-41.

231. Topalian, S.L., et al., *Immunotherapy of patients with advanced cancer using tumor-infiltrating lymphocytes and recombinant interleukin-2: a pilot study.* J Clin Oncol, 1988. **6**(5): p. 839-53.

232. Rosenberg, S.A., et al., *Use of tumor-infiltrating lymphocytes and interleukin-2 in the immunotherapy of patients with metastatic melanoma. A preliminary report.* N Engl J Med, 1988. **319**(25): p. 1676-80.

233. Rohaan, M.W., S. Wilgenhof, and J. Haanen, *Adoptive cellular therapies: the current landscape.* Virchows Arch, 2019. **474**(4): p. 449-461.

234. Restifo, N.P., M.E. Dudley, and S.A. Rosenberg, *Adoptive immunotherapy for cancer: harnessing the T cell response.* Nat Rev Immunol, 2012. **12**(4): p. 269-81.

235. Rosenberg, S.A., et al., *Adoptive cell transfer: a clinical path to effective cancer immunotherapy.* Nat Rev Cancer, 2008. **8**(4): p. 299-308.

236. Vogelstein, B., et al., *Cancer genome landscapes.* Science, 2013. **339**(6127): p. 1546-58.

237. Dudley, M.E., et al., *Adoptive transfer of cloned melanoma-reactive T lymphocytes for the treatment of patients with metastatic melanoma.* J Immunother, 2001. **24**(4): p. 363-73.

238. Dudley, M.E., et al., *A phase I study of nonmyeloablative chemotherapy and adoptive transfer of autologous tumor antigen-specific T lymphocytes in patients with metastatic melanoma.* J Immunother, 2002. **25**(3): p. 243-51.

239. Gattinoni, L., D.J. Powell, Jr., S.A. Rosenberg, and N.P. Restifo, *Adoptive immunotherapy for cancer: building on success.* Nat Rev Immunol, 2006. **6**(5): p. 383-93.

240. Schluns, K.S., W.C. Kieper, S.C. Jameson, and L. Lefrançois, *Interleukin-7 mediates the homeostasis of naïve and memory CD8 T cells in vivo.* Nat Immunol, 2000. **1**(5): p. 426-32.

241. Tan, J.T., et al., *Interleukin (IL)-15 and IL-7 jointly regulate homeostatic proliferation of memory phenotype CD8+ cells but are not required for memory phenotype CD4+ cells.* J Exp Med, 2002. **195**(12): p. 1523-32.

242. Goldrath, A.W., et al., *Cytokine requirements for acute and Basal homeostatic proliferation of naive and memory CD8+ T cells.* J Exp Med, 2002. **195**(12): p. 1515-22.

243. Gattinoni, L., et al., *Removal of homeostatic cytokine sinks by lymphodepletion enhances the efficacy of adoptively transferred tumor-specific CD8+ T cells*. J Exp Med, 2005. **202**(7): p. 907-12.

244. Johnson, C.B., et al., *Effector CD8+ T-cell Engraftment and Antitumor Immunity in Lymphodepleted Hosts Is IL7Rα Dependent*. Cancer Immunol Res, 2015. **3**(12): p. 1364-74.

245. Martin, C.E., et al., *Interleukin-7 Availability Is Maintained by a Hematopoietic Cytokine Sink Comprising Innate Lymphoid Cells and T Cells*. Immunity, 2017. **47**(1): p. 171-182.e4.

246. Yao, X., et al., *Levels of peripheral CD4(+)FoxP3(+) regulatory T cells are negatively associated with clinical response to adoptive immunotherapy of human cancer*. Blood, 2012. **119**(24): p. 5688-96.

247. Bolotin, E., G. Annett, R. Parkman, and K. Weinberg, *Serum levels of IL-7 in bone marrow transplant recipients: relationship to clinical characteristics and lymphocyte count*. Bone Marrow Transplant, 1999. **23**(8): p. 783-8.

248. Fry, T.J., et al., *A potential role for interleukin-7 in T-cell homeostasis*. Blood, 2001. **97**(10): p. 2983-90.

249. Napolitano, L.A., et al., *Increased production of IL-7 accompanies HIV-1-mediated T-cell depletion: implications for T-cell homeostasis*. Nat Med, 2001. **7**(1): p. 73-9.

250. Miller, J.S., et al., *Successful adoptive transfer and in vivo expansion of human haploidentical NK cells in patients with cancer*. Blood, 2005. **105**(8): p. 3051-7.

251. Dudley, M.E., et al., *Adoptive cell therapy for patients with metastatic melanoma: evaluation of intensive myeloablative chemoradiation preparative regimens*. J Clin Oncol, 2008. **26**(32): p. 5233-9.

252. Guimond, M., et al., *Interleukin 7 signaling in dendritic cells regulates the homeostatic proliferation and niche size of CD4+ T cells*. Nat Immunol, 2009. **10**(2): p. 149-57.

253. Bergamaschi, C., et al., *Circulating IL-15 exists as heterodimeric complex with soluble IL-15Rα in human and mouse serum*. Blood, 2012. **120**(1): p. e1-8.

254. Hill, G.R., et al., *Total body irradiation and acute graft-versus-host disease: the role of gastrointestinal damage and inflammatory cytokines*. Blood, 1997. **90**(8): p. 3204-13.

255. Zhang, Y., et al., *Preterminal host dendritic cells in irradiated mice prime CD8+ T cell-mediated acute graft-versus-host disease*. J Clin Invest, 2002. **109**(10): p. 1335-44.

256. Klebanoff, C.A., et al., *Sinks, suppressors and antigen presenters: how lymphodepletion enhances T cell-mediated tumor immunotherapy*. Trends Immunol, 2005. **26**(2): p. 111-7.

257. Paulos, C.M., et al., *Microbial translocation augments the function of adoptively transferred self/tumor-specific CD8+ T cells via TLR4 signaling*. J Clin Invest, 2007. **117**(8): p. 2197-204.

258. Salem, M.L., et al., *Recovery from cyclophosphamide-induced lymphopenia results in expansion of immature dendritic cells which can mediate enhanced prime-boost vaccination antitumor responses in vivo when stimulated with the TLR3 agonist poly(I:C)*. J Immunol, 2009. **182**(4): p. 2030-40.

259. Dudley, M.E., et al., *Cancer regression and autoimmunity in patients after clonal repopulation with antitumor lymphocytes*. Science, 2002. **298**(5594): p. 850-4.

260. Goff, S.L., et al., *Randomized, Prospective Evaluation Comparing Intensity of Lymphodepletion Before Adoptive Transfer of Tumor-Infiltrating Lymphocytes for Patients With Metastatic Melanoma*. J Clin Oncol, 2016. **34**(20): p. 2389-97.

261. Li, Y., et al., *MART-1-specific melanoma tumor-infiltrating lymphocytes maintaining CD28 expression have improved survival and expansion capability following antigenic restimulation in vitro*. J Immunol, 2010. **184**(1): p. 452-65.

262. Gross, G., G. Gorochov, T. Waks, and Z. Eshhar, *Generation of effector T cells expressing chimeric T cell receptor with antibody type-specificity.* Transplant Proc, 1989. **21**(1 Pt 1): p. 127-30.

263. Cole, D.J., et al., *Characterization of the functional specificity of a cloned T-cell receptor heterodimer recognizing the MART-1 melanoma antigen.* Cancer Res, 1995. **55**(4): p. 748-52.

264. Kaplan, B.L., D.C. Yu, T.M. Clay, and M.I. Nishimura, *Redirecting T lymphocyte specificity using T cell receptor genes.* Int Rev Immunol, 2003. **22**(3-4): p. 229-53.

265. Kochenderfer, J.N. and S.A. Rosenberg, *Treating B-cell cancer with T cells expressing anti-CD19 chimeric antigen receptors.* Nat Rev Clin Oncol, 2013. **10**(5): p. 267-76.

266. Barrett, D.M., et al., *Chimeric antigen receptor therapy for cancer.* Annu Rev Med, 2014. **65**: p. 333-47.

267. Jensen, M.C. and S.R. Riddell, *Design and implementation of adoptive therapy with chimeric antigen receptor-modified T cells.* Immunol Rev, 2014. **257**(1): p. 127-44.

268. Kenderian, S.S., M. Ruella, S. Gill, and M. Kalos, *Chimeric antigen receptor T-cell therapy to target hematologic malignancies.* Cancer Res, 2014. **74**(22): p. 6383-9.

269. Stromnes, I.M., et al., *Re-adapting T cells for cancer therapy: from mouse models to clinical trials.* Immunol Rev, 2014. **257**(1): p. 145-64.

270. Nelson, M.H. and C.M. Paulos, *Novel immunotherapies for hematologic malignances.* Immunol Rev, 2015. **263**(1): p. 90-105.

271. Debets, R., E. Donnadieu, S. Chouaib, and G. Coukos, *TCR-engineered T cells to treat tumors: Seeing but not touching?* Semin Immunol, 2016. **28**(1): p. 10-21.

272. Spear, T.T., K. Nagato, and M.I. Nishimura, *Strategies to genetically engineer T cells for cancer immunotherapy.* Cancer Immunol Immunother, 2016. **65**(6): p. 631-49.

273. Turtle, C.J., S.R. Riddell, and D.G. Maloney, *CD19-Targeted chimeric antigen receptor-modified T-cell immunotherapy for B-cell malignancies.* Clin Pharmacol Ther, 2016. **100**(3): p. 252-8.

274. Lim, W.A. and C.H. June, *The Principles of Engineering Immune Cells to Treat Cancer.* Cell, 2017. **168**(4): p. 724-740.

275. Wang, R.F. and H.Y. Wang, *Immune targets and neoantigens for cancer immunotherapy and precision medicine.* Cell Res, 2017. **27**(1): p. 11-37.

276. Johnson, L.A., et al., *Gene therapy with human and mouse T-cell receptors mediates cancer regression and targets normal tissues expressing cognate antigen.* Blood, 2009. **114**(3): p. 535-46.

277. Parkhurst, M.R., et al., *T cells targeting carcinoembryonic antigen can mediate regression of metastatic colorectal cancer but induce severe transient colitis.* Mol Ther, 2011. **19**(3): p. 620-6.

278. Robbins, P.F., et al., *A pilot trial using lymphocytes genetically engineered with an NY-ESO-1-reactive T-cell receptor: long-term follow-up and correlates with response.* Clin Cancer Res, 2015. **21**(5): p. 1019-27.

279. Robbins, P.F., et al., *Tumor regression in patients with metastatic synovial cell sarcoma and melanoma using genetically engineered lymphocytes reactive with NY-ESO-1.* J Clin Oncol, 2011. **29**(7): p. 917-24.

280. Morgan, R.A., et al., *Cancer regression and neurological toxicity following anti-MAGE-A3 TCR gene therapy.* J Immunother, 2013. **36**(2): p. 133-51.

281. Chodon, T., et al., *Adoptive transfer of MART-1 T-cell receptor transgenic lymphocytes and dendritic cell vaccination in patients with metastatic melanoma.* Clin Cancer Res, 2014. **20**(9): p. 2457-65.

282. Kageyama, S., et al., *Adoptive Transfer of MAGE-A4 T-cell Receptor Gene-Transduced Lymphocytes in Patients with Recurrent Esophageal Cancer.* Clin Cancer Res, 2015. **21**(10): p. 2268-77.

283. Rapoport, A.P., et al., *NY-ESO-1-specific TCR-engineered T cells mediate sustained antigen-specific antitumor effects in myeloma.* Nat Med, 2015. **21**(8): p. 914-921.

284. Atkins, M.B., *Cytokine-based therapy and biochemotherapy for advanced melanoma.* Clin Cancer Res, 2006. **12**(7 Pt 2): p. 2353s-2358s.

285. Keilholz, U., et al., *Dacarbazine, cisplatin, and interferon-alfa-2b with or without interleukin-2 in metastatic melanoma: a randomized phase III trial (18951) of the European Organisation for Research and Treatment of Cancer Melanoma Group.* J Clin Oncol, 2005. **23**(27): p. 6747-55.

286. Ridolfi, R., et al., *Cisplatin, dacarbazine with or without subcutaneous interleukin-2, and interferon alpha-2b in advanced melanoma outpatients: results from an Italian multicenter phase III randomized clinical trial.* J Clin Oncol, 2002. **20**(6): p. 1600-7.

287. Bajetta, E., et al., *Multicenter phase III randomized trial of polychemotherapy (CVD regimen) versus the same chemotherapy (CT) plus subcutaneous interleukin-2 and interferon-alpha2b in metastatic melanoma.* Ann Oncol, 2006. **17**(4): p. 571-7.

288. Atkins, M.B., et al., *Phase III trial comparing concurrent biochemotherapy with cisplatin, vinblastine, dacarbazine, interleukin-2, and interferon alfa-2b with cisplatin, vinblastine, and dacarbazine alone in patients with metastatic malignant melanoma (E3695): a trial coordinated by the Eastern Cooperative Oncology Group.* J Clin Oncol, 2008. **26**(35): p. 5748-54.

289. Keilholz, U., et al., *Interferon alfa-2a and interleukin-2 with or without cisplatin in metastatic melanoma: a randomized trial of the European Organization for Research and Treatment of Cancer Melanoma Cooperative Group.* J Clin Oncol, 1997. **15**(7): p. 2579-88.

290. Eton, O., et al., *Sequential biochemotherapy versus chemotherapy for metastatic melanoma: results from a phase III randomized trial.* J Clin Oncol, 2002. **20**(8): p. 2045-52.

291. Rosenberg, S.A., et al., *Prospective randomized trial of the treatment of patients with metastatic melanoma using chemotherapy with cisplatin, dacarbazine, and tamoxifen alone or in combination with interleukin-2 and interferon alfa-2b.* J Clin Oncol, 1999. **17**(3): p. 968-75.

292. Sasse, A.D., et al., *Chemoimmunotherapy versus chemotherapy for metastatic malignant melanoma.* Cochrane Database Syst Rev, 2007(1): p. Cd005413.

293. Ives, N.J., R.L. Stowe, P. Lorigan, and K. Wheatley, *Chemotherapy compared with biochemotherapy for the treatment of metastatic melanoma: a meta-analysis of 18 trials involving 2,621 patients.* J Clin Oncol, 2007. **25**(34): p. 5426-34.

294. Redmond, K.L., A. Papafili, M. Lawler, and S. Van Schaeybroeck, *Overcoming Resistance to Targeted Therapies in Cancer.* Semin Oncol, 2015. **42**(6): p. 896-908.

295. Jänne, P.A., et al., *AZD9291 in EGFR inhibitor-resistant non-small-cell lung cancer.* N Engl J Med, 2015. **372**(18): p. 1689-99.

296. Tan, C.S., D. Gilligan, and S. Pacey, *Treatment approaches for EGFR-inhibitor-resistant patients with non-small-cell lung cancer.* Lancet Oncol, 2015. **16**(9): p. e447-e459.

297. De Vita, F., et al., *Analysis of interleukin-2/interleukin-2 receptor system in advanced non-small-cell lung cancer.* Tumori, 1998. **84**(1): p. 33-8.

298. Chen, Y.M., et al., *Restoration of the immunocompetence by IL-2 activation and TCR-CD3 engagement of the in vivo anergized tumor-specific CTL from lung cancer patients.* J Immunother, 1997. **20**(5): p. 354-64.

299. Umekawa, K., et al., *Plasma RANTES, IL-10, and IL-8 levels in non-small-cell lung cancer patients treated with EGFR-TKIs.* BMC Res Notes, 2013. **6**: p. 139.

300. Yamamoto, N., M. Honma, and H. Suzuki, *Off-target serine/threonine kinase 10 inhibition by erlotinib enhances lymphocytic activity leading to severe skin disorders.* Mol Pharmacol, 2011. **80**(3): p. 466-75.

301. Bersanelli, M., et al., *Gefitinib plus interleukin-2 in advanced non-small cell lung cancer patients previously treated with chemotherapy.* Cancers (Basel), 2014. **6**(4): p. 2035-48.

302. Lam, E.T., et al., *Retrospective analysis of the safety and efficacy of high-dose interleukin-2 after prior tyrosine kinase inhibitor therapy in patients with advanced renal cell carcinoma.* J Immunother, 2014. **37**(7): p. 360-5.

303. Overwijk, W.W., M.R. Theoret, and N.P. Restifo, *The future of interleukin-2: enhancing therapeutic anticancer vaccines.* Cancer J Sci Am, 2000. **6 Suppl 1**(Suppl 1): p. S76-80.

304. Smith, F.O., et al., *Treatment of metastatic melanoma using interleukin-2 alone or in conjunction with vaccines.* Clin Cancer Res, 2008. **14**(17): p. 5610-8.

305. Schwartzentruber, D.J., et al., *gp100 peptide vaccine and interleukin-2 in patients with advanced melanoma.* N Engl J Med, 2011. **364**(22): p. 2119-27.

306. Chen, L. and D.B. Flies, *Molecular mechanisms of T cell co-stimulation and co-inhibition.* Nat Rev Immunol, 2013. **13**(4): p. 227-42.

307. Das, M., C. Zhu, and V.K. Kuchroo, *Tim-3 and its role in regulating anti-tumor immunity.* Immunol Rev, 2017. **276**(1): p. 97-111.

308. Derré, L., et al., *BTLA mediates inhibition of human tumor-specific CD8+ T cells that can be partially reversed by vaccination.* J Clin Invest, 2010. **120**(1): p. 157-67.

309. Wang, X., F. Teng, L. Kong, and J. Yu, *PD-L1 expression in human cancers and its association with clinical outcomes.* Onco Targets Ther, 2016. **9**: p. 5023-39.

310. Linsley, P.S., et al., *Intracellular trafficking of CTLA-4 and focal localization towards sites of TCR engagement.* Immunity, 1996. **4**(6): p. 535-43.

311. Egen, J.G. and J.P. Allison, *Cytotoxic T lymphocyte antigen-4 accumulation in the immunological synapse is regulated by TCR signal strength.* Immunity, 2002. **16**(1): p. 23-35.

312. Yokosuka, T., et al., *Spatiotemporal basis of CTLA-4 costimulatory molecule-mediated negative regulation of T cell activation.* Immunity, 2010. **33**(3): p. 326-39.

313. Chambers, C.A., M.S. Kuhns, J.G. Egen, and J.P. Allison, *CTLA-4-mediated inhibition in regulation of T cell responses: mechanisms and manipulation in tumor immunotherapy.* Annu Rev Immunol, 2001. **19**: p. 565-94.

314. Teft, W.A., M.G. Kirchhof, and J. Madrenas, *A molecular perspective of CTLA-4 function.* Annu Rev Immunol, 2006. **24**: p. 65-97.

315. Fraser, J.H., M. Rincón, K.D. McCoy, and G. Le Gros, *CTLA4 ligation attenuates AP-1, NFAT and NF-kappaB activity in activated T cells.* Eur J Immunol, 1999. **29**(3): p. 838-44.

316. Olsson, C., K. Riesbeck, M. Dohlsten, and E. Michaëlsson, *CTLA-4 ligation suppresses CD28-induced NF-kappaB and AP-1 activity in mouse T cell blasts.* J Biol Chem, 1999. **274**(20): p. 14400-5.

317. Takahashi, T., et al., *Immunologic self-tolerance maintained by CD25(+)CD4(+) regulatory T cells constitutively expressing cytotoxic T lymphocyte-associated antigen 4.* J Exp Med, 2000. **192**(2): p. 303-10.

318. Wing, K., et al., *CTLA-4 control over Foxp3+ regulatory T cell function.* Science, 2008. **322**(5899): p. 271-5.

319. Qureshi, O.S., et al., *Trans-endocytosis of CD80 and CD86: a molecular basis for the cell-extrinsic function of CTLA-4.* Science, 2011. **332**(6029): p. 600-3.

320. Li, R., et al., *Enhanced engagement of CTLA-4 induces antigen-specific CD4+CD25+Foxp3+ and CD4+CD25- TGF-beta 1+ adaptive regulatory T cells.* J Immunol, 2007. **179**(8): p. 5191-203.

321. Tivol, E.A., et al., *Loss of CTLA-4 leads to massive lymphoproliferation and fatal multiorgan tissue destruction, revealing a critical negative regulatory role of CTLA-4.* Immunity, 1995. **3**(5): p. 541-7.

322. Mohr, P., et al., *Real-world treatment patterns and outcomes among metastatic cutaneous melanoma patients treated with ipilimumab.* J Eur Acad Dermatol Venereol, 2018. **32**(6): p. 962-971.

323. Kohlhapp, F.J., et al., *NK cells and CD8+ T cells cooperate to improve therapeutic responses in melanoma treated with interleukin-2 (IL-2) and CTLA-4 blockade.* J Immunother Cancer, 2015. **3**: p. 18.

324. Maker, A.V., et al., *Tumor regression and autoimmunity in patients treated with cytotoxic T lymphocyte-associated antigen 4 blockade and interleukin 2: a phase I/II study.* Ann Surg Oncol, 2005. **12**(12): p. 1005-16.

325. Ray, A., et al., *A phase I study of intratumoral ipilimumab and interleukin-2 in patients with advanced melanoma.* Oncotarget, 2016. **7**(39): p. 64390-64399.

326. Keir, M.E., M.J. Butte, G.J. Freeman, and A.H. Sharpe, *PD-1 and its ligands in tolerance and immunity.* Annu Rev Immunol, 2008. **26**: p. 677-704.

327. Yao, S. and L. Chen, *PD-1 as an immune modulatory receptor.* Cancer J, 2014. **20**(4): p. 262-4.

328. Ishida, Y., Y. Agata, K. Shibahara, and T. Honjo, *Induced expression of PD-1, a novel member of the immunoglobulin gene superfamily, upon programmed cell death.* Embo j, 1992. **11**(11): p. 3887-95.

329. Wherry, E.J., *T cell exhaustion.* Nat Immunol, 2011. **12**(6): p. 492-9.

330. Ahmadzadeh, M., et al., *Tumor antigen-specific CD8 T cells infiltrating the tumor express high levels of PD-1 and are functionally impaired.* Blood, 2009. **114**(8): p. 1537-44.

331. Gehring, A.J., et al., *Profile of tumor antigen-specific CD8 T cells in patients with hepatitis B virus-related hepatocellular carcinoma.* Gastroenterology, 2009. **137**(2): p. 682-90.

332. Saito, H., et al., *Increased PD-1 expression on CD4+ and CD8+ T cells is involved in immune evasion in gastric cancer.* J Surg Oncol, 2013. **107**(5): p. 517-22.

333. Yamamoto, R., et al., *PD-1-PD-1 ligand interaction contributes to immunosuppressive microenvironment of Hodgkin lymphoma.* Blood, 2008. **111**(6): p. 3220-4.

334. Fourcade, J., et al., *PD-1 is a regulator of NY-ESO-1-specific CD8+ T cell expansion in melanoma patients.* J Immunol, 2009. **182**(9): p. 5240-9.

335. Iwai, Y., et al., *Involvement of PD-L1 on tumor cells in the escape from host immune system and tumor immunotherapy by PD-L1 blockade.* Proc Natl Acad Sci U S A, 2002. **99**(19): p. 12293-7.

336. Blank, C., et al., *PD-L1/B7H-1 inhibits the effector phase of tumor rejection by T cell receptor (TCR) transgenic CD8+ T cells.* Cancer Res, 2004. **64**(3): p. 1140-5.

337. Postow, M.A., M.K. Callahan, and J.D. Wolchok, *Immune Checkpoint Blockade in Cancer Therapy.* J Clin Oncol, 2015. **33**(17): p. 1974-82.

338. Weber, J.S., et al., *Nivolumab versus chemotherapy in patients with advanced melanoma who progressed after anti-CTLA-4 treatment (CheckMate 037): a randomised, controlled, open-label, phase 3 trial.* Lancet Oncol, 2015. **16**(4): p. 375-84.

339. Duraiswamy, J., K.M. Kaluza, G.J. Freeman, and G. Coukos, *Dual blockade of PD-1 and CTLA-4 combined with tumor vaccine effectively restores T-cell rejection function in tumors.* Cancer Res, 2013. **73**(12): p. 3591-603.

340. Syn, N.L., M.W.L. Teng, T.S.K. Mok, and R.A. Soo, *De-novo and acquired resistance to immune checkpoint targeting.* Lancet Oncol, 2017. **18**(12): p. e731-e741.

341. Herbst, R.S., et al., *Predictive correlates of response to the anti-PD-L1 antibody MPDL3280A in cancer patients.* Nature, 2014. **515**(7528): p. 563-7.

342. Snyder, A., et al., *Genetic basis for clinical response to CTLA-4 blockade in melanoma.* N Engl J Med, 2014. **371**(23): p. 2189-2199.

343. Buchbinder, E.I. and A. Desai, *CTLA-4 and PD-1 Pathways: Similarities, Differences, and Implications of Their Inhibition.* Am J Clin Oncol, 2016. **39**(1): p. 98-106.

344. Rotte, A., *Combination of CTLA-4 and PD-1 blockers for treatment of cancer.* J Exp Clin Cancer Res, 2019. **38**(1): p. 255.

345. Hodi, F.S., et al., *Improved survival with ipilimumab in patients with metastatic melanoma.* N Engl J Med, 2010. **363**(8): p. 711-23.

346. Lo, B.C., et al., *Microbiota-dependent activation of CD4(+) T cells induces CTLA-4 blockade-associated colitis via Fcγ receptors.* Science, 2024. **383**(6678): p. 62-70.

347. West, E.E., et al., *PD-L1 blockade synergizes with IL-2 therapy in reinvigorating exhausted T cells.* J Clin Invest, 2013. **123**(6): p. 2604-15.

348. Hashimoto, M., et al., *PD-1 combination therapy with IL-2 modifies CD8(+) T cell exhaustion program.* Nature, 2022. **610**(7930): p. 173-181.

349. Suzuki, H., et al., *Deregulated T cell activation and autoimmunity in mice lacking interleukin-2 receptor beta.* Science, 1995. **268**(5216): p. 1472-6.

350. Zorn, E., et al., *IL-2 regulates FOXP3 expression in human CD4+CD25+ regulatory T cells through a STAT-dependent mechanism and induces the expansion of these cells in vivo.* Blood, 2006. **108**(5): p. 1571-9.

351. Tang, Q., et al., *Central role of defective interleukin-2 production in the triggering of islet autoimmune destruction.* Immunity, 2008. **28**(5): p. 687-97.

352. Webster, K.E., et al., *In vivo expansion of T reg cells with IL-2-mAb complexes: induction of resistance to EAE and long-term acceptance of islet allografts without immunosuppression.* J Exp Med, 2009. **206**(4): p. 751-60.

353. Grinberg-Bleyer, Y., et al., *IL-2 reverses established type 1 diabetes in NOD mice by a local effect on pancreatic regulatory T cells.* J Exp Med, 2010. **207**(9): p. 1871-8.

354. Baeyens, A., et al., *Limitations of IL-2 and rapamycin in immunotherapy of type 1 diabetes.* Diabetes, 2013. **62**(9): p. 3120-31.

355. Dansokho, C., et al., *Regulatory T cells delay disease progression in Alzheimer-like pathology.* Brain, 2016. **139**(Pt 4): p. 1237-51.

356. González, F.B., et al., *Immunoendocrine dysbalance during uncontrolled T. cruzi infection is associated with the acquisition of a Th-1-like phenotype by Foxp3(+) T cells.* Brain Behav Immun, 2015. **45**: p. 219-32.

357. Pérol, L. and E. Piaggio, *New Molecular and Cellular Mechanisms of Tolerance: Tolerogenic Actions of IL-2.* Methods Mol Biol, 2016. **1371**: p. 11-28.

358. Humrich, J.Y., et al., *Rapid induction of clinical remission by low-dose interleukin-2 in a patient with refractory SLE.* Ann Rheum Dis, 2015. **74**(4): p. 791-2.

359. Grasshoff, H., et al., *Low-Dose IL-2 Therapy in Autoimmune and Rheumatic Diseases.* Front Immunol, 2021. **12**: p. 648408.

360. Klatzmann, D. and A.K. Abbas, *The promise of low-dose interleukin-2 therapy for autoimmune and inflammatory diseases.* Nat Rev Immunol, 2015. **15**(5): p. 283-94.

361. Koreth, J., et al., *Interleukin-2 and regulatory T cells in graft-versus-host disease.* N Engl J Med, 2011. **365**(22): p. 2055-66.

362. Saadoun, D., et al., *Regulatory T-cell responses to low-dose interleukin-2 in HCV-induced vasculitis.* N Engl J Med, 2011. **365**(22): p. 2067-77.

363. Koreth, J., et al., *Efficacy, durability, and response predictors of low-dose interleukin-2 therapy for chronic graft-versus-host disease.* Blood, 2016. **128**(1): p. 130-7.

364. Matsuoka, K., et al., *Low-dose interleukin-2 therapy restores regulatory T cell homeostasis in patients with chronic graft-versus-host disease.* Sci Transl Med, 2013. **5**(179): p. 179ra43.

365. Kennedy-Nasser, A.A., et al., *Ultra low-dose IL-2 for GVHD prophylaxis after allogeneic hematopoietic stem cell transplantation mediates expansion of regulatory T cells without diminishing antiviral and antileukemic activity.* Clin Cancer Res, 2014. **20**(8): p. 2215-25.

366. Long, S.A., et al., *Rapamycin/IL-2 combination therapy in patients with type 1 diabetes augments Tregs yet transiently impairs β-cell function.* Diabetes, 2012. **61**(9): p. 2340-8.

367. Hartemann, A., et al., *Low-dose interleukin 2 in patients with type 1 diabetes: a phase 1/2 randomised, double-blind, placebo-controlled trial.* Lancet Diabetes Endocrinol, 2013. **1**(4): p. 295-305.

368. Todd, J.A., et al., *Regulatory T Cell Responses in Participants with Type 1 Diabetes after a Single Dose of Interleukin-2: A Non-Randomised, Open Label, Adaptive Dose-Finding Trial.* PLoS Med, 2016. **13**(10): p. e1002139.

369. Castela, E., et al., *Effects of low-dose recombinant interleukin 2 to promote T-regulatory cells in alopecia areata.* JAMA Dermatol, 2014. **150**(7): p. 748-51.

370. He, J., et al., *Low-dose interleukin-2 treatment selectively modulates CD4(+) T cell subsets in patients with systemic lupus erythematosus.* Nat Med, 2016. **22**(9): p. 991-3.

371. Humrich, J.Y. and G. Riemekasten, *Restoring regulation - IL-2 therapy in systemic lupus erythematosus.* Expert Rev Clin Immunol, 2016. **12**(11): p. 1153-1160.

372. He, J., et al., *Efficacy and safety of low-dose IL-2 in the treatment of systemic lupus erythematosus: a randomised, double-blind, placebo-controlled trial.* Ann Rheum Dis, 2020. **79**(1): p. 141-149.

373. von Spee-Mayer, C., et al., *Low-dose interleukin-2 selectively corrects regulatory T cell defects in patients with systemic lupus erythematosus.* Ann Rheum Dis, 2016. **75**(7): p. 1407-15.

374. Rosenzwajg, M., et al., *Immunological and clinical effects of low-dose interleukin-2 across 11 autoimmune diseases in a single, open clinical trial.* Ann Rheum Dis, 2019. **78**(2): p. 209-217.

375. Humrich, J.Y., et al., *Low-dose interleukin-2 therapy in refractory systemic lupus erythematosus: an investigator-initiated, single-centre phase 1 and 2a clinical trial.* Lancet Rheumatol, 2019. **1**(1): p. e44-e54.

376. Miao, M., et al., *Therapeutic potential of targeting Tfr/Tfh cell balance by low-dose-IL-2 in active SLE: a post hoc analysis from a double-blind RCT study.* Arthritis Res Ther, 2021. **23**(1): p. 167.

377. Fardet, L., I. Petersen, and I. Nazareth, *Common Infections in Patients Prescribed Systemic Glucocorticoids in Primary Care: A Population-Based Cohort Study.* PLoS Med, 2016. **13**(5): p. e1002024.

378. Dixon, W.G., A. Kezouh, S. Bernatsky, and S. Suissa, *The influence of systemic glucocorticoid therapy upon the risk of non-serious infection in older patients with rheumatoid arthritis: a nested case-control study.* Ann Rheum Dis, 2011. **70**(6): p. 956-60.

379. Zandman-Goddard, G. and Y. Shoenfeld, *Infections and SLE.* Autoimmunity, 2005. **38**(7): p. 473-85.

380. Doria, A., et al., *Infections as triggers and complications of systemic lupus erythematosus.* Autoimmun Rev, 2008. **8**(1): p. 24-8.

381. Zhou, P., et al., *Low-dose IL-2 therapy invigorates CD8+ T cells for viral control in systemic lupus erythematosus.* PLoS Pathog, 2021. **17**(10): p. e1009858.

382. Miao, M., et al., *Short-term and low-dose IL-2 therapy restores the Th17/Treg balance in the peripheral blood of patients with primary Sjögren's syndrome.* Ann Rheum Dis, 2018. **77**(12): p. 1838-1840.

383. Luo, J., et al., *IL-2 Inhibition of Th17 Generation Rather Than Induction of Treg Cells Is Impaired in Primary Sjögren's Syndrome Patients.* Front Immunol, 2018. **9**: p. 1755.

384. Zhang, S.X., et al., *Low-dose IL-2 therapy limits the reduction in absolute numbers of circulating regulatory T cells in rheumatoid arthritis.* Ther Adv Musculoskelet Dis, 2021. **13**: p. 1759720x211011370.

385. Zhang, S.X., et al., *Circulating regulatory T cells were absolutely decreased in dermatomyositis/polymyositis patients and restored by low-dose IL-2.* Ann Rheum Dis, 2021. **80**(8): p. e130.

386. Miao, M., et al., *Treatment of Active Idiopathic Inflammatory Myopathies by Low-Dose Interleukin-2: A Prospective Cohort Pilot Study.* Rheumatol Ther, 2021. **8**(2): p. 835-847.

387. Buitrago-Molina, L.E., et al., *Treg-specific IL-2 therapy can reestablish intrahepatic immune regulation in autoimmune hepatitis.* J Autoimmun, 2021. **117**: p. 102591.

388. Lim, T.Y., et al., *Low-Dose Interleukin-2 for Refractory Autoimmune Hepatitis.* Hepatology, 2018. **68**(4): p. 1649-1652.

389. Zhao, T.X., et al., *Low-dose interleukin-2 in patients with stable ischaemic heart disease and acute coronary syndromes (LILACS): protocol and study rationale for a randomised, double-blind, placebo-controlled, phase I/II clinical trial.* BMJ Open, 2018. **8**(9): p. e022452.

390. Zhao, T.X., et al., *Regulatory T-Cell Response to Low-Dose Interleukin-2 in Ischemic Heart Disease.* NEJM Evid, 2022. **1**(1): p. EVIDoa2100009.

391. Goettel, J.A., et al., *Low-Dose Interleukin-2 Ameliorates Colitis in a Preclinical Humanized Mouse Model.* Cell Mol Gastroenterol Hepatol, 2019. **8**(2): p. 193-195.

392. Dong, G., et al., *Low-Dose IL-2 Treatment Affords Protection against Subarachnoid Hemorrhage Injury by Expanding Peripheral Regulatory T Cells.* ACS Chem Neurosci, 2021. **12**(3): p. 430-440.

393. Le Duff, F., et al., *Low-Dose IL-2 for Treating Moderate to Severe Alopecia Areata: A 52-Week Multicenter Prospective Placebo-Controlled Study Assessing its Impact on T Regulatory Cell and NK Cell Populations.* J Invest Dermatol, 2021. **141**(4): p. 933-936.e6.

394. Corfmat, M., et al., *Low dose IL-2 in patients with steroid-dependent dysimmune manifestations associated with myelodysplastic syndromes: a three-case report.* Rheumatology (Oxford), 2021. **60**(7): p. 3404-3408.

395. Kromer, G., et al., *Analysis of lymphocytes infiltrating the thyroid gland of Obese strain chickens.* J Immunol, 1985. **135**(4): p. 2452-7.

396. Raeber, M.E., D. Sahin, U. Karakus, and O. Boyman, *A systematic review of interleukin-2-based immunotherapies in clinical trials for cancer and autoimmune diseases.* EBioMedicine, 2023. **90**: p. 104539.

397. Levin, A.M., et al., *Exploiting a natural conformational switch to engineer an interleukin-2 'superkine'.* Nature, 2012. **484**(7395): p. 529-33.

398. Lopes, J.E., et al., *ALKS 4230: a novel engineered IL-2 fusion protein with an improved cellular selectivity profile for cancer immunotherapy.* J Immunother Cancer, 2020. **8**(1).

399. Pan, Y., et al., *Nemvaleukin alfa, a novel engineered IL-2 fusion protein, drives antitumor immunity and inhibits tumor growth in small cell lung cancer.* J Immunother Cancer, 2022. **10**(9).

400. Herzog, T.J., et al., *ARTISTRY-7: phase III trial of nemvaleukin alfa plus pembrolizumab vs chemotherapy for platinum-resistant ovarian cancer.* Future Oncol, 2023. **19**(23): p. 1577-1591.

401. Gastman, B., et al., *432 Nemvaleukin alfa, a novel engineered IL-2 cytokine, in combination with the anti-PD-1 antibody pembrolizumab in patients with recurrent/metastatic head and neck squamous cell carcinoma (ION-01 study).* Journal for ImmunoTherapy of Cancer, 2021. **9**(Suppl 2): p. A462-A462.

402. Vaishampayan, U.N., et al., *Nemvaleukin alfa monotherapy and in combination with pembrolizumab in patients (pts) with advanced solid tumors: ARTISTRY-1.* Journal of Clinical Oncology, 2022. **40**(16_suppl): p. 2500-2500.

403. Shanafelt, A.B., et al., *A T-cell-selective interleukin 2 mutein exhibits potent antitumor activity and is well tolerated in vivo.* Nat Biotechnol, 2000. **18**(11): p. 1197-202.

404. Steppan, S., et al., *Reduced secondary cytokine induction by BAY 50-4798, a high-affinity receptor-specific interleukin-2 analog.* J Interferon Cytokine Res, 2006. **26**(3): p. 171-8.

405. Matthews, L., et al., *BAY 50-4798, a novel, high-affinity receptor-specific recombinant interleukin-2 analog, induces dose-dependent increases in CD25 expression and proliferation among unstimulated, human peripheral blood mononuclear cells in vitro.* Clin Immunol, 2004. **113**(3): p. 248-55.

406. Weishaupt, A., et al., *The T cell-selective IL-2 mutant AIC284 mediates protection in a rat model of Multiple Sclerosis.* J Neuroimmunol, 2015. **282**: p. 63-72.

407. Margolin, K., et al., *Phase I trial of BAY 50-4798, an interleukin-2-specific agonist in advanced melanoma and renal cancer.* Clin Cancer Res, 2007. **13**(11): p. 3312-9.

408. Rao, B.M., et al., *Interleukin-2 mutants with enhanced alpha-receptor subunit binding affinity.* Protein Eng, 2003. **16**(12): p. 1081-7.

409. Rao, B.M., I. Driver, D.A. Lauffenburger, and K.D. Wittrup, *High-affinity CD25-binding IL-2 mutants potently stimulate persistent T cell growth.* Biochemistry, 2005. **44**(31): p. 10696-701.

410. Dubois, S., J. Mariner, T.A. Waldmann, and Y. Tagaya, *IL-15Ralpha recycles and presents IL-15 In trans to neighboring cells.* Immunity, 2002. **17**(5): p. 537-47.

411. Liu, D.V., L.M. Maier, D.A. Hafler, and K.D. Wittrup, *Engineered interleukin-2 antagonists for the inhibition of regulatory T cells.* J Immunother, 2009. **32**(9): p. 887-94.

412. Mitra, S., et al., *Interleukin-2 activity can be fine tuned with engineered receptor signaling clamps.* Immunity, 2015. **42**(5): p. 826-38.

413. Tsytsikov, V.N., et al., *Identification and characterization of two alternative splice variants of human interleukin-2.* J Biol Chem, 1996. **271**(38): p. 23055-60.

414. Zheng, X.X., et al., *IL-2 receptor-targeted cytolytic IL-2/Fc fusion protein treatment blocks diabetogenic autoimmunity in nonobese diabetic mice.* J Immunol, 1999. **163**(7): p. 4041-8.

415. Melder, R.J., et al., *Pharmacokinetics and in vitro and in vivo anti-tumor response of an interleukin-2-human serum albumin fusion protein in mice.* Cancer Immunol Immunother, 2005. **54**(6): p. 535-47.

416. Peterson, L.B., et al., *A long-lived IL-2 mutein that selectively activates and expands regulatory T cells as a therapy for autoimmune disease.* J Autoimmun, 2018. **95**: p. 1-14.

417. Merchant, R., et al., *Fine-tuned long-acting interleukin-2 superkine potentiates durable immune responses in mice and non-human primate.* J Immunother Cancer, 2022. **10**(1).

418. Pasut, G. and F.M. Veronese, *PEGylation for improving the effectiveness of therapeutic biomolecules.* Drugs Today (Barc), 2009. **45**(9): p. 687-95.

419. Milla, P., F. Dosio, and L. Cattel, *PEGylation of proteins and liposomes: a powerful and flexible strategy to improve the drug delivery.* Curr Drug Metab, 2012. **13**(1): p. 105-19.

420. Turecek, P.L., M.J. Bossard, F. Schoetens, and I.A. Ivens, *PEGylation of Biopharmaceuticals: A Review of Chemistry and Nonclinical Safety Information of Approved Drugs.* J Pharm Sci, 2016. **105**(2): p. 460-475.

421. Katre, N.V., *Immunogenicity of recombinant IL-2 modified by covalent attachment of polyethylene glycol.* J Immunol, 1990. **144**(1): p. 209-13.

422. Yang, J.C., S.L. Schwarz, D.M. Perry-Lalley, and S.A. Rosenberg, *Murine studies using polyethylene glycol-modified recombinant human interleukin 2 (PEG-IL-2): antitumor effects of PEG-IL2 alone and in combination with adoptive cellular transfer.* Lymphokine Cytokine Res, 1991. **10**(6): p. 475-80.

423. Charych, D.H., et al., *NKTR-214, an Engineered Cytokine with Biased IL2 Receptor Binding, Increased Tumor Exposure, and Marked Efficacy in Mouse Tumor Models.* Clin Cancer Res, 2016. **22**(3): p. 680-90.

424. Katre, N.V., M.J. Knauf, and W.J. Laird, *Chemical modification of recombinant interleukin 2 by polyethylene glycol increases its potency in the murine Meth A sarcoma model.* Proc Natl Acad Sci U S A, 1987. **84**(6): p. 1487-91.

425. Knauf, M.J., et al., *Relationship of effective molecular size to systemic clearance in rats of recombinant interleukin-2 chemically modified with water-soluble polymers.* J Biol Chem, 1988. **263**(29): p. 15064-70.

426. Zimmerman, R.J., et al., *Schedule dependency of the antitumor activity and toxicity of polyethylene glycol-modified interleukin 2 in murine tumor models.* Cancer Res, 1989. **49**(23): p. 6521-8.

427. Yang, J.C., et al., *The use of polyethylene glycol-modified interleukin-2 (PEG-IL-2) in the treatment of patients with metastatic renal cell carcinoma and melanoma. A phase I study and a randomized prospective study comparing IL-2 alone versus IL-2 combined with PEG-IL-2.* Cancer, 1995. **76**(4): p. 687-94.

428. Charych, D., et al., *Modeling the receptor pharmacology, pharmacokinetics, and pharmacodynamics of NKTR-214, a kinetically-controlled interleukin-2 (IL2) receptor agonist for cancer immunotherapy.* PLoS One, 2017. **12**(7): p. e0179431.

429. Sharma, M., et al., *Bempegaldesleukin selectively depletes intratumoral Tregs and potentiates T cell-mediated cancer therapy.* Nat Commun, 2020. **11**(1): p. 661.

430. Bentebibel, S.E., et al., *A First-in-Human Study and Biomarker Analysis of NKTR-214, a Novel IL2Rβγ-Biased Cytokine, in Patients with Advanced or Metastatic Solid Tumors.* Cancer Discov, 2019. **9**(6): p. 711-721.

431. Eggermont, A.M., et al., *PIVOT-12: a phase III study of adjuvant bempegaldesleukin plus nivolumab in resected stage III/IV melanoma at high risk for recurrence.* Future Oncol, 2022. **18**(8): p. 903-913.

432. *Bristol Myers Squibb and Nektar Therapeutics announce update on phase 3 PIVOT IO-001 trial evaluating Bempegaldesleukin (BEMPEG) in combination with Opdivo (Nivolumab) in previously untreated unresectable or metastatic melanoma.* Press release published on Business Wire, 2022.

433. *Nektar Therapeutics and Bristol Myers Squibb announce update on clinical development program for Bempegaldesleukin (BEMPEG) in combination with Opdivo (Nivolumab) Press release published on Cision PR Newswire. . Press release published on Cision PR Newswire, 2022.*

434.	Dixit, N., et al., *NKTR-358: A novel regulatory T-cell stimulator that selectively stimulates expansion and suppressive function of regulatory T cells for the treatment of autoimmune and inflammatory diseases.* J Transl Autoimmun, 2021. **4**: p. 100103.

435.	Fanton, C., et al., *Selective expansion of regulatory T cells by NKTR-358 in healthy volunteers and patients with systemic lupus erythematosus.* J Transl Autoimmun, 2022. **5**: p. 100152.

436.	Du, Y.J., et al., *Stability of the recombinant anti-erbB2 scFv-Fc-interleukin-2 fusion protein and its inhibition of HER2-overexpressing tumor cells.* Int J Oncol, 2013. **42**(2): p. 507-16.

437.	Gillies, S.D., et al., *A low-toxicity IL-2-based immunocytokine retains antitumor activity despite its high degree of IL-2 receptor selectivity.* Clin Cancer Res, 2011. **17**(11): p. 3673-85.

438.	Gutbrodt, K.L., et al., *Antibody-based delivery of interleukin-2 to neovasculature has potent activity against acute myeloid leukemia.* Sci Transl Med, 2013. **5**(201): p. 201ra118.

439.	Gutbrodt, K.L., G. Casi, and D. Neri, *Antibody-based delivery of IL2 and cytotoxics eradicates tumors in immunocompetent mice.* Mol Cancer Ther, 2014. **13**(7): p. 1772-6.

440.	Becker, J.C., et al., *An antibody-interleukin 2 fusion protein overcomes tumor heterogeneity by induction of a cellular immune response.* Proc Natl Acad Sci U S A, 1996. **93**(15): p. 7826-31.

441.	Yang, R.K., et al., *Intratumoral treatment of smaller mouse neuroblastoma tumors with a recombinant protein consisting of IL-2 linked to the hu14.18 antibody increases intratumoral CD8+ T and NK cells and improves survival.* Cancer Immunol Immunother, 2013. **62**(8): p. 1303-13.

442.	Klein, C., et al., *Cergutuzumab amunaleukin (CEA-IL2v), a CEA-targeted IL-2 variant-based immunocytokine for combination cancer immunotherapy: Overcoming limitations of aldesleukin and conventional IL-2-based immunocytokines.* Oncoimmunology, 2017. **6**(3): p. e1277306.

443.	Mortara, L., et al., *Anti-cancer Therapies Employing IL-2 Cytokine Tumor Targeting: Contribution of Innate, Adaptive and Immunosuppressive Cells in the Anti-tumor Efficacy.* Front Immunol, 2018. **9**: p. 2905.

444.	Penichet, M.L., J.S. Dela Cruz, S.U. Shin, and S.L. Morrison, *A recombinant IgG3-(IL-2) fusion protein for the treatment of human HER2/neu expressing tumors.* Hum Antibodies, 2001. **10**(1): p. 43-9.

445.	Saif, A., et al., *Efficacy of Neoadjuvant Intratumoral Darleukin/Fibromun (L19IL2 + L19TNF) in Patients with Clinical Stage IIIB/C Melanoma (Neo-DREAM).* Ann Surg Oncol, 2022. **29**(6): p. 3377-3378.

446.	Lieverse, R.I.Y., et al., *Stereotactic ablative body radiotherapy (SABR) combined with immunotherapy (L19-IL2) versus standard of care in stage IV NSCLC patients, ImmunoSABR: a multicentre, randomised controlled open-label phase II trial.* BMC Cancer, 2020. **20**(1): p. 557.

447.	Card, K.F., et al., *A soluble single-chain T-cell receptor IL-2 fusion protein retains MHC-restricted peptide specificity and IL-2 bioactivity.* Cancer Immunol Immunother, 2004. **53**(4): p. 345-57.

448.	Fishman, M.N., et al., *Phase I trial of ALT-801, an interleukin-2/T-cell receptor fusion protein targeting p53 (aa264-272)/HLA-A*0201 complex, in patients with advanced malignancies.* Clin Cancer Res, 2011. **17**(24): p. 7765-75.

449.   Hank, J.A., et al., *Activation of human effector cells by a tumor reactive recombinant anti-ganglioside GD2 interleukin-2 fusion protein (ch14.18-IL2)*. Clin Cancer Res, 1996. **2**(12): p. 1951-9.

450.   Shusterman, S., et al., *Antitumor activity of hu14.18-IL2 in patients with relapsed/refractory neuroblastoma: a Children's Oncology Group (COG) phase II study*. J Clin Oncol, 2010. **28**(33): p. 4969-75.

451.   Osenga, K.L., et al., *A phase I clinical trial of the hu14.18-IL2 (EMD 273063) as a treatment for children with refractory or recurrent neuroblastoma and melanoma: a study of the Children's Oncology Group*. Clin Cancer Res, 2006. **12**(6): p. 1750-9.

452.   Gillies, S.D., et al., *An anti-CD20-IL-2 immunocytokine is highly efficacious in a SCID mouse model of established human B lymphoma*. Blood, 2005. **105**(10): p. 3972-8.

453.   Tzeng, A., et al., *Antigen specificity can be irrelevant to immunocytokine efficacy and biodistribution*. Proc Natl Acad Sci U S A, 2015. **112**(11): p. 3320-5.

454.   Zhu, E.F., et al., *Synergistic innate and adaptive immune response to combination immunotherapy with anti-tumor antigen antibodies and extended serum half-life IL-2*. Cancer Cell, 2015. **27**(4): p. 489-501.

455.   Moynihan, K.D., et al., *IL-2 targeted to CD8+ T cells promotes robust effector T cell responses and potent antitumor immunity*. Cancer Discov, 2024.

456.   Codarri Deak, L., et al., *PD-1-cis IL-2R agonism yields better effectors from stem-like CD8(+) T cells*. Nature, 2022. **610**(7930): p. 161-172.

457.   Andreata, F., et al., *CD8 cis-targeted IL-2 drives potent antiviral activity against hepatitis B virus*. Sci Transl Med, 2024. **16**(729): p. eadi1572.

458.   Piper, M., et al., *Simultaneous targeting of PD-1 and IL-2Rβγ with radiation therapy inhibits pancreatic cancer growth and metastasis*. Cancer Cell, 2023. **41**(5): p. 950-969.e6.

459.   Tichet, M., et al., *Bispecific PD1-IL2v and anti-PD-L1 break tumor immunity resistance by enhancing stem-like tumor-reactive CD8(+) T cells and reprogramming macrophages*. Immunity, 2023. **56**(1): p. 162-179.e6.

460.   Boyman, O., C.D. Surh, and J. Sprent, *Potential use of IL-2/anti-IL-2 antibody immune complexes for the treatment of cancer and autoimmune disease*. Expert Opin Biol Ther, 2006. **6**(12): p. 1323-31.

461.   Kamimura, D., et al., *IL-2 in vivo activities and antitumor efficacy enhanced by an anti-IL-2 mAb*. J Immunol, 2006. **177**(1): p. 306-14.

462.   Caudana, P., et al., *IL2/Anti-IL2 Complex Combined with CTLA-4, But Not PD-1, Blockade Rescues Antitumor NK Cell Function by Regulatory T-cell Modulation*. Cancer Immunol Res, 2019. **7**(3): p. 443-457.

463.   Létourneau, S., et al., *IL-2/anti-IL-2 antibody complexes show strong biological activity by avoiding interaction with IL-2 receptor alpha subunit CD25*. Proc Natl Acad Sci U S A, 2010. **107**(5): p. 2171-6.

464.   Kupz, A., et al., *Treatment of mice with S4B6 IL-2 complex prevents lethal toxoplasmosis via IL-12- and IL-18-dependent interferon-gamma production by non-CD4 immune cells*. Sci Rep, 2020. **10**(1): p. 13115.

465.   Molloy, M.J., W. Zhang, and E.J. Usherwood, *Cutting edge: IL-2 immune complexes as a therapy for persistent virus infection*. J Immunol, 2009. **182**(8): p. 4512-5.

466.   Arenas-Ramirez, N., et al., *Improved cancer immunotherapy by a CD25-mimobody conferring selectivity to human interleukin-2*. Sci Transl Med, 2016. **8**(367): p. 367ra166.

467.   Sahin, D., et al., *An IL-2-grafted antibody immunotherapy with potent efficacy against metastatic cancer*. Nat Commun, 2020. **11**(1): p. 6440.

468.	Liu, R., et al., *Expansion of regulatory T cells via IL-2/anti-IL-2 mAb complexes suppresses experimental myasthenia.* Eur J Immunol, 2010. **40**(6): p. 1577-89.

469.	Tomala, J., et al., *In vivo expansion of activated naive CD8+ T cells and NK cells driven by complexes of IL-2 and anti-IL-2 monoclonal antibody as novel approach of cancer immunotherapy.* J Immunol, 2009. **183**(8): p. 4904-12.

470.	Roopenian, D.C., et al., *The MHC class I-like IgG receptor controls perinatal IgG transport, IgG homeostasis, and fate of IgG-Fc-coupled drugs.* J Immunol, 2003. **170**(7): p. 3528-33.

471.	Smaldini, P.L., et al., *Systemic IL-2/anti-IL-2Ab complex combined with sublingual immunotherapy suppresses experimental food allergy in mice through induction of mucosal regulatory T cells.* Allergy, 2018. **73**(4): p. 885-895.

472.	Lee, S.Y., et al., *Interleukin-2/anti-interleukin-2 monoclonal antibody immune complex suppresses collagen-induced arthritis in mice by fortifying interleukin-2/STAT5 signalling pathways.* Immunology, 2012. **137**(4): p. 305-16.

473.	Dinh, T.N., et al., *Cytokine therapy with interleukin-2/anti-interleukin-2 monoclonal antibody complexes expands CD4+CD25+Foxp3+ regulatory T cells and attenuates development and progression of atherosclerosis.* Circulation, 2012. **126**(10): p. 1256-66.

474.	Diaz-de-Durana, Y., et al., *IL-2 immunotherapy reveals potential for innate beta cell regeneration in the non-obese diabetic mouse model of autoimmune diabetes.* PLoS One, 2013. **8**(10): p. e78483.

475.	Trotta, E., et al., *A human anti-IL-2 antibody that potentiates regulatory T cells by a structure-based mechanism.* Nat Med, 2018. **24**(7): p. 1005-1014.

476.	Ohnishi, H., et al., *Role of the kidney in metabolic change of interleukin-2.* Tumour Biol, 1989. **10**(4): p. 202-14.

477.	Gibbons, J.A., et al., *Quantitation of the renal clearance of interleukin-2 using nephrectomized and ureter-ligated rats.* J Pharmacol Exp Ther, 1995. **272**(1): p. 119-25.

478.	Anderson, P.M. and M.A. Sorenson, *Effects of route and formulation on clinical pharmacokinetics of interleukin-2.* Clin Pharmacokinet, 1994. **27**(1): p. 19-31.

479.	Schwartz, R.N., L. Stover, and J.P. Dutcher, *Managing toxicities of high-dose interleukin-2.* Oncology (Williston Park), 2002. **16**(11 Suppl 13): p. 11-20.

480.	Conlon, K.C., M.D. Miljkovic, and T.A. Waldmann, *Cytokines in the Treatment of Cancer.* J Interferon Cytokine Res, 2019. **39**(1): p. 6-21.

481.	Lei, J., et al., *Expression, purification and characterization of recombinant human interleukin-2-serum albumin (rhIL-2-HSA) fusion protein in Pichia pastoris.* Protein Expr Purif, 2012. **84**(1): p. 154-60.

482.	Mattijssen, V., L.T. Balemans, P.A. Steerenberg, and P.H. De Mulder, *Polyethylene-glycol-modified interleukin-2 is superior to interleukin-2 in locoregional immunotherapy of established guinea-pig tumors.* Int J Cancer, 1992. **51**(5): p. 812-7.

483.	Feng, X.S., *[In vivo antitumor activities of polyethylene glycol modified recombinant interleukin 2 (PEG-rIL-2) against murine hepatoma].* Zhonghua Zhong Liu Za Zhi, 1993. **15**(4): p. 256-8.

484.	Wang, L., Y. Wu, and Y. Zhang, *[In vivo antitumor effects of polyethylene glycol--modified recombinant human interleukin-2 on mouse uterine cervical carcinoma].* Zhonghua Zhong Liu Za Zhi, 1996. **18**(4): p. 253-5.

485.	Meyers, F.J., et al., *A phase I study including pharmacokinetics of polyethylene glycol conjugated interleukin-2.* Clin Pharmacol Ther, 1991. **49**(3): p. 307-13.

486.	Menzel, T., et al., *Clinical and preclinical evaluation of recombinant PEG-IL-2 in human.* Cancer Biother, 1993. **8**(3): p. 199-212.

487. Bukowski, R.M., et al., *Polyethylene glycol conjugated interleukin-2: clinical and immunologic effects in patients with advanced renal cell carcinoma.* Invest New Drugs, 1993. **11**(2-3): p. 211-7.

488. Bernsen, M.R., H.F. Dullens, W. Den Otter, and P.M. Heintz, *Reevaluation of the superiority of polyethylene glycol-modified interleukin-2 over regular recombinant interleukin-2.* J Interferon Cytokine Res, 1995. **15**(7): p. 641-5.

489. Richter, A.W. and E. Akerblom, *Antibodies against polyethylene glycol produced in animals by immunization with monomethoxy polyethylene glycol modified proteins.* Int Arch Allergy Appl Immunol, 1983. **70**(2): p. 124-31.

490. Chanan-Khan, A., et al., *Complement activation following first exposure to pegylated liposomal doxorubicin (Doxil): possible role in hypersensitivity reactions.* Ann Oncol, 2003. **14**(9): p. 1430-7.

491. Szebeni, J., *Complement activation-related pseudoallergy: a new class of drug-induced acute immune toxicity.* Toxicology, 2005. **216**(2-3): p. 106-21.

492. Dewachter, P. and C. Mouton-Faivre, *Anaphylaxis to macrogol 4000 after a parenteral corticoid injection.* Allergy, 2005. **60**(5): p. 705-6.

493. Ganson, N.J., et al., *Control of hyperuricemia in subjects with refractory gout, and induction of antibody against poly(ethylene glycol) (PEG), in a phase I trial of subcutaneous PEGylated urate oxidase.* Arthritis Res Ther, 2006. **8**(1): p. R12.

494. Knop, K., R. Hoogenboom, D. Fischer, and U.S. Schubert, *Poly(ethylene glycol) in drug delivery: pros and cons as well as potential alternatives.* Angew Chem Int Ed Engl, 2010. **49**(36): p. 6288-308.

495. Sprincl, L., J. Exner, O. Stěrba, and J. Kopecek, *New types of synthetic infusion solutions. III. Elimination and retention of poly-[N-(2-hydroxypropyl)methacrylamide] in a test organism.* J Biomed Mater Res, 1976. **10**(6): p. 953-63.

496. Rihová, B., et al., *Effect of the chemical structure of N-(2-hydroxypropyl)methacrylamide copolymers on their ability to induce antibody formation in inbred strains of mice.* Biomaterials, 1984. **5**(3): p. 143-8.

497. Ríhová, B. and M. Kovár, *Immunogenicity and immunomodulatory properties of HPMA-based polymers.* Adv Drug Deliv Rev, 2010. **62**(2): p. 184-91.

498. Ríhová, B., *Immunomodulating activities of soluble synthetic polymer-bound drugs.* Adv Drug Deliv Rev, 2002. **54**(5): p. 653-74.

499. Duncan, R., *Designing polymer conjugates as lysosomotropic nanomedicines.* Biochem Soc Trans, 2007. **35**(Pt 1): p. 56-60.

500. Duncan, R., *Development of HPMA copolymer-anticancer conjugates: clinical experience and lessons learnt.* Adv Drug Deliv Rev, 2009. **61**(13): p. 1131-48.

501. Zamani, M.R., et al., *Polymer-based antibody mimetics (iBodies) target human PD-L1 and function as a potent immune checkpoint blocker.* J Biol Chem, 2024: p. 107325.

502. Duncan, R. and M.J. Vicent, *Do HPMA copolymer conjugates have a future as clinically useful nanomedicines? A critical overview of current status and future opportunities.* Adv Drug Deliv Rev, 2010. **62**(2): p. 272-82.

503. Li, L., M. Zhou, and Y. Huang, *Synergistic enhancement of anticancer therapeutic efficacy of HPMA copolymer doxorubicin conjugates via combination of ligand modification and stimuli-response srategies.* Int J Pharm, 2018. **536**(1): p. 450-458.

504. Rani, S. and U. Gupta, *HPMA-based polymeric conjugates in anticancer therapeutics.* Drug Discov Today, 2020. **25**(6): p. 997-1012.

505. Yang, J. and J. Kopeček, *The Light at the End of the Tunnel-Second Generation HPMA Conjugates for Cancer Treatment.* Curr Opin Colloid Interface Sci, 2017. **31**: p. 30-42.

506. Rojas, G., et al., *Deciphering the molecular bases of the biological effects of antibodies against Interleukin-2: a versatile platform for fine epitope mapping.* Immunobiology, 2013. **218**(1): p. 105-13.

507. Rojas, G., Y. Cabrera Infante, A. Pupo, and T. Carmenate, *Fine epitope specificity of antibodies against interleukin-2 explains their paradoxical immunomodulatory effects.* MAbs, 2014. **6**(1): p. 273-85.

508. Tomala, J., et al., *Chimera of IL-2 linked to light chain of anti-IL-2 mAb mimics IL-2/anti-IL-2 mAb complexes both structurally and functionally.* ACS Chem Biol, 2013. **8**(5): p. 871-6.

509. Spangler, J.B., et al., *Antibodies to Interleukin-2 Elicit Selective T Cell Subset Potentiation through Distinct Conformational Mechanisms.* Immunity, 2015. **42**(5): p. 815-25.

510. Spangler, J.B., et al., *Engineering a Single-Agent Cytokine/Antibody Fusion That Selectively Expands Regulatory T Cells for Autoimmune Disease Therapy.* J Immunol, 2018. **201**(7): p. 2094-2106.

511. Cooper, M.A., T.A. Fehniger, and M.A. Caligiuri, *The biology of human natural killer-cell subsets.* Trends Immunol, 2001. **22**(11): p. 633-40.

512. Nagler, A., L.L. Lanier, S. Cwirla, and J.H. Phillips, *Comparative studies of human FcRIII-positive and negative natural killer cells.* J Immunol, 1989. **143**(10): p. 3183-91.

513. Hudspeth, K., et al., *The role of natural killer cells in autoimmune liver disease: a comprehensive review.* J Autoimmun, 2013. **46**: p. 55-65.

514. Liu, M., S. Liang, and C. Zhang, *NK Cells in Autoimmune Diseases: Protective or Pathogenic?* Front Immunol, 2021. **12**: p. 624687.

515. Rudnicka, K., A. Matusiak, and M. Chmiela, *CD25 (IL-2R) expression correlates with the target cell induced cytotoxic activity and cytokine secretion in human natural killer cells.* Acta Biochim Pol, 2015. **62**(4): p. 885-94.

516. Liu, R., et al., *Autoreactive T cells mediate NK cell degeneration in autoimmune disease.* J Immunol, 2006. **176**(9): p. 5247-54.

517. Jin, G.H., T. Hirano, and M. Murakami, *Combination treatment with IL-2 and anti-IL-2 mAbs reduces tumor metastasis via NK cell activation.* Int Immunol, 2008. **20**(6): p. 783-9.

518. Tomala, J., et al., *Antitumor activity of IL-2/anti-IL-2 mAb immunocomplexes exerts synergism with that of N-(2-hydroxypropyl)methacrylamide copolymer-bound doxorubicin conjugate due to its low immunosuppressive activity.* Int J Cancer, 2011. **129**(8): p. 2002-12.

519. Verdeil, G., K. Marquardt, C.D. Surh, and L.A. Sherman, *Adjuvants targeting innate and adaptive immunity synergize to enhance tumor immunotherapy.* Proc Natl Acad Sci U S A, 2008. **105**(43): p. 16683-8.

520. Redmond, W.L., T. Triplett, K. Floyd, and A.D. Weinberg, *Dual anti-OX40/IL-2 therapy augments tumor immunotherapy via IL-2R-mediated regulation of OX40 expression.* PLoS One, 2012. **7**(4): p. e34467.

521. Takahashi, Y., et al., *Radiation Enhances the Efficacy of Antitumor Immunotherapy with an Immunocomplex of Interleukin-2 and Its Monoclonal Antibody.* Anticancer Res, 2017. **37**(12): p. 6799-6806.

522. Reyes, R.M., et al., *CD122-directed interleukin-2 treatment mechanisms in bladder cancer differ from αPD-L1 and include tissue-selective γδ T cell activation.* J Immunother Cancer, 2021. **9**(4).

523. Das, S. and D.B. Johnson, *Immune-related adverse events and anti-tumor efficacy of immune checkpoint inhibitors.* J Immunother Cancer, 2019. **7**(1): p. 306.

524. Siddiqui, I., et al., *Intratumoral Tcf1(+)PD-1(+)CD8(+) T Cells with Stem-like Properties Promote Tumor Control in Response to Vaccination and Checkpoint Blockade Immunotherapy.* Immunity, 2019. **50**(1): p. 195-211.e10.

525. Di Pilato, M., et al., *CXCR6 positions cytotoxic T cells to receive critical survival signals in the tumor microenvironment.* Cell, 2021. **184**(17): p. 4512-4530.e22.

526. Hudson, W.H., et al., *Proliferating Transitory T Cells with an Effector-like Transcriptional Signature Emerge from PD-1(+) Stem-like CD8(+) T Cells during Chronic Infection.* Immunity, 2019. **51**(6): p. 1043-1058.e4.

527. Sade-Feldman, M., et al., *Defining T Cell States Associated with Response to Checkpoint Immunotherapy in Melanoma.* Cell, 2018. **175**(4): p. 998-1013.e20.

528. Mo, F., et al., *An engineered IL-2 partial agonist promotes CD8(+) T cell stemness.* Nature, 2021. **597**(7877): p. 544-548.

529. Jansen, C.S., et al., *An intra-tumoral niche maintains and differentiates stem-like CD8 T cells.* Nature, 2019. **576**(7787): p. 465-470.

530. Miller, B.C., et al., *Subsets of exhausted CD8(+) T cells differentially mediate tumor control and respond to checkpoint blockade.* Nat Immunol, 2019. **20**(3): p. 326-336.

531. Wu, T., et al., *The TCF1-Bcl6 axis counteracts type I interferon to repress exhaustion and maintain T cell stemness.* Sci Immunol, 2016. **1**(6).

532. McLane, L.M., M.S. Abdel-Hakeem, and E.J. Wherry, *CD8 T Cell Exhaustion During Chronic Viral Infection and Cancer.* Annu Rev Immunol, 2019. **37**: p. 457-495.

533. Blank, C.U., et al., *Defining 'T cell exhaustion'.* Nat Rev Immunol, 2019. **19**(11): p. 665-674.

534. Medzhitov, R., *Origin and physiological roles of inflammation.* Nature, 2008. **454**(7203): p. 428-35.

535. Blackburn, S.D., et al., *Coregulation of CD8+ T cell exhaustion by multiple inhibitory receptors during chronic viral infection.* Nat Immunol, 2009. **10**(1): p. 29-37.

536. Fourcade, J., et al., *CD8(+) T cells specific for tumor antigens can be rendered dysfunctional by the tumor microenvironment through upregulation of the inhibitory receptors BTLA and PD-1.* Cancer Res, 2012. **72**(4): p. 887-96.

537. Joller, N., et al., *Cutting edge: TIGIT has T cell-intrinsic inhibitory functions.* J Immunol, 2011. **186**(3): p. 1338-42.

538. Barber, D.L., et al., *Restoring function in exhausted CD8 T cells during chronic viral infection.* Nature, 2006. **439**(7077): p. 682-7.

539. Jin, H.T., et al., *Cooperation of Tim-3 and PD-1 in CD8 T-cell exhaustion during chronic viral infection.* Proc Natl Acad Sci U S A, 2010. **107**(33): p. 14733-8.

540. Crawford, A. and E.J. Wherry, *The diversity of costimulatory and inhibitory receptor pathways and the regulation of antiviral T cell responses.* Curr Opin Immunol, 2009. **21**(2): p. 179-86.

541. Wherry, E.J., et al., *Viral persistence alters CD8 T-cell immunodominance and tissue distribution and results in distinct stages of functional impairment.* J Virol, 2003. **77**(8): p. 4911-27.

542. Niederlova, V., O. Tsyklauri, M. Kovar, and O. Stepanek, *IL-2-driven CD8(+) T cell phenotypes: implications for immunotherapy.* Trends Immunol, 2023. **44**(11): p. 890-901.

543. Wu, W., et al., *IL-2Rα-biased agonist enhances antitumor immunity by invigorating tumor-infiltrating CD25(+)CD8(+) T cells.* Nat Cancer, 2023. **4**(9): p. 1309-1325.

544. LaPorte, K.M., R. Hernandez, A. Santos Savio, and T.R. Malek, *Robust IL-2-dependent antitumor immunotherapy requires targeting the high-affinity IL-2R on tumor-specific CD8(+) T cells.* J Immunother Cancer, 2023. **11**(6).

545. Tsyklauri, O., et al., *Regulatory T cells suppress the formation of potent KLRK1 and IL-7R expressing effector CD8 T cells by limiting IL-2*. Elife, 2023. **12**.

546. Xu, Y., et al., *An Engineered IL15 Cytokine Mutein Fused to an Anti-PD1 Improves Intratumoral T-cell Function and Antitumor Immunity*. Cancer Immunol Res, 2021. **9**(10): p. 1141-1157.

547. Shi, W., et al., *Next-generation anti-PD-L1/IL-15 immunocytokine elicits superior antitumor immunity in cold tumors with minimal toxicity*. Cell Rep Med, 2024: p. 101531.

548. Sockolosky, J.T., et al., *Selective targeting of engineered T cells using orthogonal IL-2 cytokine-receptor complexes*. Science, 2018. **359**(6379): p. 1037-1042.

549. Zhang, Q., et al., *A human orthogonal IL-2 and IL-2Rß system enhances CAR T cell expansion and antitumor activity in a murine model of leukemia*. Sci Transl Med, 2021. **13**(625): p. eabg6986.

550. Aspuria, P.J., et al., *An orthogonal IL-2 and IL-2Rß system drives persistence and activation of CAR T cells and clearance of bulky lymphoma*. Sci Transl Med, 2021. **13**(625): p. eabg7565.

551. Guillaume, J., A. Perzolli, and M. Boes, *Strategies to overcome low MHC-I expression in paediatric and adult tumours*. Immunother Adv, 2024. **4**(1): p. ltad028.

552. Smith, C., M. Martinez, J. Peet, and R. Khanna, *Differential outcome of IL-2/anti-IL-2 complex therapy on effector and memory CD8+ T cells following vaccination with an adenoviral vector encoding EBV epitopes*. J Immunol, 2011. **186**(10): p. 5784-90.

553. Wherry, E.J., et al., *Lineage relationship and protective immunity of memory CD8 T cell subsets*. Nat Immunol, 2003. **4**(3): p. 225-34.

554. Gattinoni, L., et al., *Acquisition of full effector function in vitro paradoxically impairs the in vivo antitumor efficacy of adoptively transferred CD8+ T cells*. J Clin Invest, 2005. **115**(6): p. 1616-26.

555. Klebanoff, C.A., et al., *Central memory self/tumor-reactive CD8+ T cells confer superior antitumor immunity compared with effector memory T cells*. Proc Natl Acad Sci U S A, 2005. **102**(27): p. 9571-6.

556. Ma, X., et al., *Cholesterol Induces CD8(+) T Cell Exhaustion in the Tumor Microenvironment*. Cell Metab, 2019. **30**(1): p. 143-156.e5.

557. Scott, A.C., et al., *TOX is a critical regulator of tumour-specific T cell differentiation*. Nature, 2019. **571**(7764): p. 270-274.

558. Alfei, F., et al., *TOX reinforces the phenotype and longevity of exhausted T cells in chronic viral infection*. Nature, 2019. **571**(7764): p. 265-269.

559. Martinez, G.J., et al., *The transcription factor NFAT promotes exhaustion of activated CD8+ T cells*. Immunity, 2015. **42**(2): p. 265-278.

560. Khan, O., et al., *TOX transcriptionally and epigenetically programs CD8(+) T cell exhaustion*. Nature, 2019. **571**(7764): p. 211-218.

561. Tillé, L., et al., *Activation of the transcription factor NFAT5 in the tumor microenvironment enforces CD8(+) T cell exhaustion*. Nat Immunol, 2023. **24**(10): p. 1645-1653.

562. Liu, Y., et al., *IL-2 regulates tumor-reactive CD8(+) T cell exhaustion by activating the aryl hydrocarbon receptor*. Nat Immunol, 2021. **22**(3): p. 358-369.

563. Beltra, J.C., et al., *IL2Rß-dependent signals drive terminal exhaustion and suppress memory development during chronic viral infection*. Proc Natl Acad Sci U S A, 2016. **113**(37): p. E5444-53.

564. Chalmers, Z.R., et al., *Analysis of 100,000 human cancer genomes reveals the landscape of tumor mutational burden*. Genome Med, 2017. **9**(1): p. 34.

565. Kasikova, L., et al., *Tertiary lymphoid structures and B cells determine clinically relevant T cell phenotypes in ovarian cancer.* Nat Commun, 2024. **15**(1): p. 2528.

566. Qayoom, H., S. Sofi, and M.A. Mir, *Targeting tumor microenvironment using tumor-infiltrating lymphocytes as therapeutics against tumorigenesis.* Immunol Res, 2023. **71**(4): p. 588-599.

567. Nakagawa, K., et al., *Mechanisms of interleukin-2-induced hepatic toxicity.* Cancer Res, 1996. **56**(3): p. 507-10.

568. Li, Y., et al., *Regulatory T cells control toxicity in a humanized model of IL-2 therapy.* Nat Commun, 2017. **8**(1): p. 1762.

569. Singh, A., et al., *CD122-targetted IL-2 signals cause acute and selective apoptosis of B cells in Peyer's Patches.* Sci Rep, 2020. **10**(1): p. 12668.

570. Lee, W.W., et al., *Virus infection drives IL-2 antibody complexes into pro-inflammatory agonists in mice.* Sci Rep, 2016. **6**: p. 37603.

571. Basu, S., et al., *Cutting edge: Foxp3-mediated induction of pim 2 allows human T regulatory cells to preferentially expand in rapamycin.* J Immunol, 2008. **180**(9): p. 5794-8.

572. Tomala, J., et al., *IL-2/JES6-1 mAb complexes dramatically increase sensitivity to LPS through IFN-γ production by CD25(+)Foxp3(-) T cells.* Elife, 2021. **10**.

573. Kurt, A.S., et al., *IL-2 availability regulates the tissue specific phenotype of murine intra-hepatic Tregs.* Front Immunol, 2022. **13**: p. 1040031.

574. Yu, A., et al., *Selective IL-2 responsiveness of regulatory T cells through multiple intrinsic mechanisms supports the use of low-dose IL-2 therapy in type 1 diabetes.* Diabetes, 2015. **64**(6): p. 2172-83.